Studies on the Role of Two Proteins in Breast Cancer – Histone Deacetylase 11 in Estrogen Receptor Positive Breast Cancer and the Redox Protein Memo in Metastasis and Tumorigenesis

Inauguraldissertation

zur

Erlangung der Würde eines Doktors der Philosophie

vorgelegt der

Philosophisch-Naturwissenschaftlichen Fakultät

der Universität Basel

von

Anna Frei

aus Zürich

Basel, 2015

Genehmigt von der Philosophisch-Naturwissenschaftlichen Fakultät auf Antrag von

Prof. Dr. Nancy E. Hynes

Prof. Dr. Gerhard Christofori

Basel, den 15.09.2015

Prof. Dr. Jörg Schibler

Dekan

Namensnennung-Keine kommerzielle Nutzung-Keine Bearbeitung 3.0 Schweiz
(CC BY-NC-ND 3.0 CH)

Sie dürfen: **Teilen** — den Inhalt kopieren, verbreiten und zugänglich machen

Unter den folgenden Bedingungen:

Namensnennung — Sie müssen den Namen des Autors/Rechteinhabers in der von ihm festgelegten Weise nennen.

Keine kommerzielle Nutzung — Sie dürfen diesen Inhalt nicht für kommerzielle Zwecke nutzen.

Keine Bearbeitung erlaubt — Sie dürfen diesen Inhalt nicht bearbeiten, abwandeln oder in anderer Weise verändern.

Wobei gilt:

- **Verzichtserklärung —** Jede der vorgenannten Bedingungen kann **aufgehoben** werden, sofern Sie die ausdrückliche Einwilligung des Rechteinhabers dazu erhalten.
- **Public Domain (gemeinfreie oder nicht-schützbare Inhalte) —** Soweit das Werk, der Inhalt oder irgendein Teil davon zur Public Domain der jeweiligen Rechtsordnung gehört, wird dieser Status von der Lizenz in keiner Weise berührt.
- **Sonstige Rechte —** Die Lizenz hat keinerlei Einfluss auf die folgenden Rechte:
    - Die Rechte, die jedermann wegen der Schranken des Urheberrechts oder aufgrund gesetzlicher Erlaubnisse zustehen (in einigen Ländern als grundsätzliche Doktrin des **fair use** bekannt);
    - Die **Persönlichkeitsrechte** des Urhebers;
    - Rechte anderer Personen, entweder am Lizenzgegenstand selber oder bezüglich seiner Verwendung, zum Beispiel für **Werbung** oder Privatsphärenschutz.
- **Hinweis —** Bei jeder Nutzung oder Verbreitung müssen Sie anderen alle Lizenzbedingungen mitteilen, die für diesen Inhalt gelten. Am einfachsten ist es, an entsprechender Stelle einen Link auf diese Seite einzubinden.

Quelle: http://creativecommons.org/licenses/by-nc-nd/3.0/ch/ Datum: 12.11.2013

Table of Contents

1. Summary

Breast cancer is the most diagnosed cancer type in women worldwide. It is a heterogeneous disease that can progress and metastasize into distant organs. After lung cancer, breast cancer is the second leading cause of cancer death among women in developed countries. However, death rates are declining since 1990, mainly due to earlier detection and improved therapies. The development of therapies specifically targeting known oncogenes have improved patient survival. For example the estrogen receptor (ER), a hormone receptor expressed in 70% of breast cancer and the receptor tyrosine kinase ErbB2, which is expressed in 20% of breast cancer, are treated by endocrine therapies and targeted antibodies or kinase inhibitors, respectively. Despite many successes, not all patients respond to these treatments or they develop resistance leading to cancer recurrence. The treatment of metastases remains the biggest challenge. Therefore, new therapies are required and this demands a better understanding of disease development and progression. With the two studies presented here, we aimed to gain more insight in the role of histone deacetylase 11 (HDAC11) in breast cancer, and in the function of Memo (Mediator of ErbB2-driven cell motility), in tumorigenesis and metastasis.

Results from several preclinical studies suggest that the inhibition of HDACs is a promising approach to target cancer. However, the role of individual HDACs in breast cancer is largely unknown. In our study, we aimed to find HDACs with an oncogenic role in breast cancer. By screening available online databases, we discovered HDAC11 to be overexpressed in breast cancer compared to normal breast. Furthermore, we found a correlation between HDAC11 expression and ER levels in breast cancer, and could show that HDAC11 expression is induced by estrogen-signaling. Moreover, a knockdown (KD) approach revealed that HDAC11 promotes proliferation in the ER-positive breast cancer cell lines T47D and MCF7, but does not significantly alter proliferation of the ER-negative breast cancer cell lines MDA-MB-231 and SUM159. KD of HDAC11 in the ER-positive murine breast cancer cell line J110 decreased tumor growth *in vivo*. In addition, RNA sequencing combined with gene set enrichment analyses (GSEA) revealed that HDAC11 controls part of the estrogen responsive transcriptional program,

especially genes that are normally downregulated upon estrogen induced signaling. This suggests that HDAC11 is an estrogen induced repressor of gene transcription. Furthermore, Kaplan-Meier analysis revealed that HDAC11 has prognostic value for patients who received endocrine therapy, as the probability of recurrence-free survival (RFS) and distant metastasis-free survival (DMFS) decreased significantly for patients having tumors with high levels of HDAC11. In summary, we show that HDAC11 has oncogenic potential in ER-positive breast cancer and therefore might be a new target for therapy.

Memo was initially found through its interaction with ErbB2. Several studies have demonstrated that Memo is required for breast cancer cell migration in response to ligands activating receptor tyrosine kinases (RTKs). In this study we aimed to investigate if Memo is involved in breast cancer metastasis and tumorigenesis. Recently, we discovered that Memo is a copper-dependent redox enzyme, which promotes spontaneous metastasis from a xenograft breast cancer model. By tissue microarray analysis of primary human breast tumors we found Memo to be overexpressed in 40% of breast cancer, while expressed at low levels in the normal human breast. Moreover, high cytoplasmic Memo localization has prognostic value for early distant metastasis and death. However, primary tumor growth was not affected by Memo, neither in a xenograft model using the triple-negative human breast cancer cell line MDA-MB-231, nor in a constitutively active ErbB2 (NeuNT)-driven murine spontaneous breast cancer model. Immunohistochemistry of normal murine mammary glands revealed that Memo is expressed throughout all stages of development, specifically in the luminal cell compartment. To study the role of Memo in tumorigenesis, we generated a spontaneous NeuNT-driven murine breast cancer cell model, in which Memo excision and NeuNT expression should be achieved at the same time. Mice from all strains developed tumors with the same frequency. However, they were all positive for Memo expression, suggesting that either Memo-depleted mammary epithelial cells were outcompeted by Memo expressing cells and/or only Memo-positive cells can give rise to tumors, or that Cre-recombinase mediated excision of Memo was not functional. In summary, this study revealed that Memo is a copper-dependent redox enzyme that promotes breast cancer metastasis.

2. Introduction

2.1 Breast cancer

Breast cancer is the most diagnosed cancer in women worldwide. In 2012, 1.7 million new cases were reported with over 500'000 deaths, rendering it the major cause of cancer death among women. Although the incidence of breast cancer is rising, death rates are declining, due to better screening methods and therefore earlier detection, as well as improvements in cancer treatment (Torre et al., 2015). Several risk factors for the development of breast cancer are known, and include menopausal hormones (Saxena et al., 2010), a long menstrual history, overweight, and a family history of breast cancer (Tamimi et al., 2012). Factors associated with decreased risk are a younger age at first pregnancy and breastfeeding (Clavel-Chapelon et al., 2002).

Breast cancer arises from epithelial cells lining the ducts and the lobules of the mammary gland. The epithelium consists of two layers, an inner layer of secretory luminal cells facing the lumen of the ducts, and the outer layer of basal, or myoepithelial, cells (Macias and Hinck, 2012). As breast cancer can arise from either of these two cell lineages, and can be caused by various genetic and epigenetic alterations, breast tumors from different patients can have vastly different phenotypic properties. Depending on the expression of specific oncogenes, mutations and epigenetic modifications, breast tumors can vary in their proliferation rate, metastatic potential, invasiveness, and response to anti-cancer therapies (Skibinski and Kuperwasser, 2015). This inter-tumor heterogeneity represents a significant challenge for the treatment of patients with breast cancer.

2.1.1 Characterization of Breast Cancer Subtypes

In order to better predict breast cancer outcome and response to therapy, breast cancers have been classified based on their clinical parameters, such as histopathological type, grade of differentiation, lymph node status, and stage of the tumor as well as on their expression of the estrogen receptor (ER), progesterone receptor (PR) and the receptor-tyrosine kinase ErbB2 (Di

Cosimo and Baselga, 2010). In the last decade, gene expression profiling of breast cancer samples has been used to characterize the disease. In the original studies, five molecular subtypes were found including luminal A, luminal B, normal-like, ErbB2-enriched and basal-like (Perou et al., 2000; Sørlie et al., 2001). Further studies comparing gene expression profiles from human and murine breast tumors revealed an additional subtype, comprising tumors which are claudin-low that are similar to the normal-like group (Herschkowitz et al., 2007; Prat et al., 2010). These six breast cancer subtypes have distinctive prognoses for tumor progression, the potential to metastasize and to treatment response, and are now being used in the clinic to predict sensitivity to specific therapeutic regimes.

The normal breast-like subtype shares characteristics with normal breast cells (Sørlie et al., 2001) and is associated with good prognosis (Liu et al., 2014). However, the significance of this subtype is under debate as studies suggest that this subtype results from a high percentage of normal cells in the tumor (Parker et al., 2009). Luminal A and B subtypes are ER-positive and express luminal markers, distinguishing them from the other subtypes (Perou et al., 2000; Sørlie et al., 2001). In addition to the expression of ER, luminal A tumors tend to be PR-positive. Conversely, luminal B tumors usually have low or no PR expression, in addition to lower ER levels, and a reduced reliance on the estrogen pathway (Inic et al., 2014; Osborne, 1998). Compared to luminal A tumors, luminal B tumors are associated with a worse prognosis, and generally have a higher tumor grade, higher expression of proliferation-related genes, activation of alternative signaling pathways, and are less responsive to hormonal therapy (Creighton, 2012; Sørlie et al., 2001). The ErbB2-enriched subtype is characterized by the amplification of the *ERBB2* gene and is associated with aggressive disease and decreased survival (Slamon et al., 1987). The basal like subtype is characterized by the expression of markers of basal-cellular origin, like cytokeratins, and by the lack of ErbB2, ER and PR expression (triple-negative). This subtype is associated with aggressive behavior and poor prognosis (Perou et al., 2000; Sørlie et al., 2001). The claudin-low tumors are also triple-negative, have low or absent expression of luminal differentiation markers, and are enriched for epithelial to mesenchymal transition (EMT) markers, as well as immune response genes (Prat et al., 2010). In

summary, luminal A tumors tend to have the best outcome, whereas luminal B, ErbB2-enriched, basal-like and claudin-low tumors have worse prognosis (Figure 2.1) (Prat and Perou, 2011).

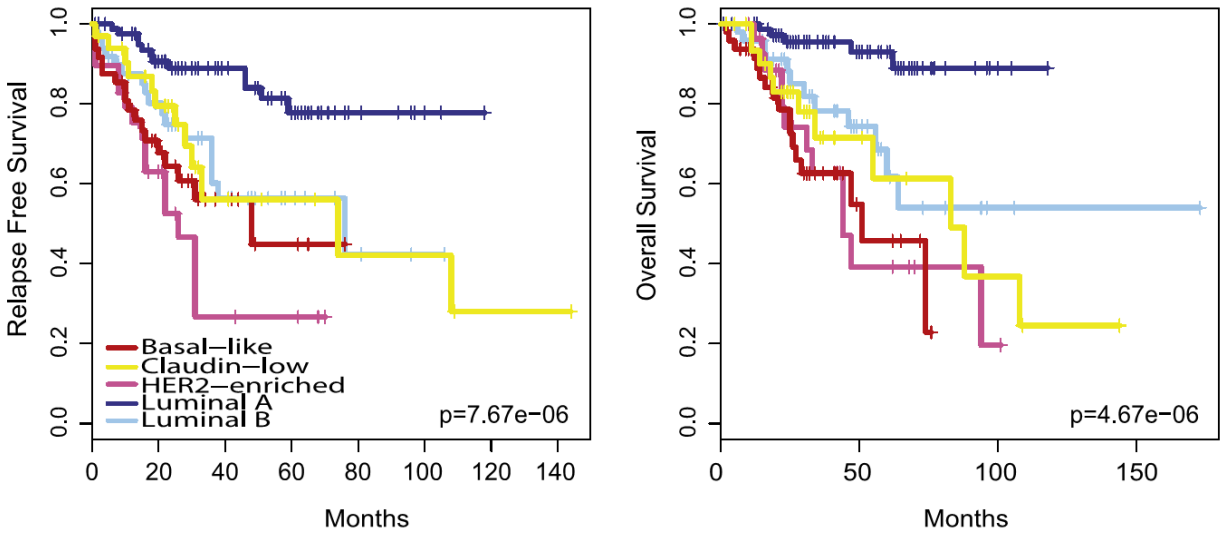

Figure 2.1 Prognosis of different molecular breast cancer subtypes. Kaplan-Meier curves for probability of Relapse Free Survival and Overall Survival (Prat and Perou, 2011).

With the improvements in sequencing methods, several further studies have proposed alternative tumor subclasses. For example, an analysis of copy number and gene expression in 2000 breast tumors revealed 10 new subgroups within the subgroups described above, with distinct clinical prognoses (Curtis et al., 2012). In another study, hundreds of primary breast cancers were analyzed for DNA copy numbers, methylation, messenger RNAs (mRNA), microRNAs (miR) and protein expression, which revealed the existence of four main breast cancer classes that correlated well with previously published mRNA subtypes (luminal A, luminal B, ErbB2-enriched and basal-like). Interestingly, this study demonstrated that different genetic and epigenetic alterations can lead to similar phenotypes, and that these all converge into four main breast cancer classes. However, these classes also display a lot of heterogeneity (The Cancer Genome Atlas Network, 2012).

2.1.2 Intra-Tumor Heterogeneity and its Implications

Although the classification of tumors into different subtypes can help to predict tumor response to cancer therapeutics, a big obstacle in cancer therapy is the presence of spatial and temporal intra-tumor heterogeneity. Spatial heterogeneity describes differences observed within the primary tumor (Patani et al., 2011), between metastasis and the primary tumor, or between individual metastases (Wu et al., 2008), which could reflect different subclones. The term temporal heterogeneity refers to the differences occurring over time in local or distant tumor recurrence (Kuukasjärvi et al., 1997). Depending on the genetic or epigenetic alterations present in different areas of a particular tumor and/or metastases, cancer cells can have different drug sensitivities. Thus, cancer therapies might not be effective against all subclones or all metastases. Furthermore, through the selective pressure applied by anticancer therapeutics, as well as through the host immune response, subclones can be selected for and give rise to therapeutic resistance (Balko et al., 2014). Thus, the phenomenon of intra-tumor heterogeneity renders the successful treatment of patients challenging. New strategies that take inter- and intra-tumor heterogeneity into account will probably help to improve breast cancer treatment. Such strategies might include the sampling and sequencing of biopsies and blood throughout tumor progression, which could allow adjustment of the applied cancer therapies to the emerging alterations. Such an approach is currently being performed by the AURORA initiative for metastatic breast cancer (Zardavas et al., 2014).

2.1.3 The Metastatic Process

Mortality due to breast cancer is rarely a result of the primary tumor, which is usually surgically removed, but results from the metastatic dissemination of cancer cells from the primary tumor that spread into distant organs, which give rise to new tumors. Common sites of metastasis for breast cancer patients are lung, liver, brain and bone. The metastatic process involves several steps including intravasation into blood and/or lymphatic vessels, survival in the circulation,

extravasation into distant sites, and survival and proliferation in the foreign microenvironment (Figure 2.2) (Nguyen et al., 2009).

During each step of the metastatic cascade tumor cells are exposed to immune cells that can recognize and destroy them. It has been demonstrated that depletion of $CD8^+$ T cells and natural killer (NK) cells increases breast cancer metastasis without altering primary tumor growth (Bidwell et al., 2012). To overcome anti-tumor immune responses, tumor cells recruit immunosuppressive cells and modulate their expansion and function. Secretion of various cytokines and chemokines by the tumor attracts macrophages that infiltrate the tumor. These so called tumor-associated macrophages were shown to suppress infiltration of $CD8^+$ T cells and anti-tumor immunity in primary tumors (DeNardo et al., 2011). Furthermore, myeloid derived suppressor cells (MDSCs) can suppress cytokine production and proliferation of T cells (Abe et al., 2010; Gallina et al., 2006). Recruitment of regulatory T cells (T_{Reg} cells), immunosuppressive cells that normally prevent over-reaction of the immune system to avoid self-destruction, also suppresses anti-tumor responses (Karavitis et al., 2012). Thus, tumor cells can avoid detection and destruction by the immune system by altering the recruitment, expansion and function of immune cells, which allows them to disseminate to distant organs.

In order to metastasize, tumor cells need to overcome physical and biological barriers. As a first step, cells need to acquire the ability to migrate and to leave the primary tumor. The traditional view is that individual cells gain the ability to migrate and leave the primary tumor by activation of an epithelial to mesenchymal transition (EMT), a crucial embryogenic developmental program that leads to loss of intercellular adhesion, increase of mesenchymal markers and polarization of tumor cells (Bill and Christofori, 2015; Tiwari et al., 2013). In addition to individually migrating cells, collective tumor migration as a group of cells with intact cell-cell interactions, has been observed in breast cancer tumors, suggesting that several modes of tumor cell migration might exist (Giampieri et al., 2009). Furthermore, other models propose that tumor clumps might break off from primary tumors into the blood circulation, where they get blocked in small capillaries and grow into distant tumors (Aceto et al., 2014). However, most tumors are surrounded by the basal membrane and an extracellular matrix (ECM) that tumor cells need to overcome in order to intravasate into blood vessels. This can be achieved by the

secretion of matrix metalloproteases (MMPs) by tumor as well as stromal cells, which can degrade the ECM and basement membrane (Kessenbrock et al., 2010). Tumor cells can reach the tumor associated vessels by squeezing through existing gaps in the ECM that is facilitated by the leakiness of vessels often observed in tumors (Hashizume et al., 2000; Kitamura et al., 2015).

Once the cells are in the circulation, they need to find ways to survive the harsh environment and to extravasate into distant organs. Platelets support this process by the formation of fibrin clots that protects tumor cells in the circulation from NK cells (Camerer et al., 2004; Palumbo et al., 2005), and by the recruitment of tumor-associated macrophages that transmit pro-survival signals to the tumor cells (Gil-Bernabé et al., 2012). In the distant organ tumor cells need to be able to survive in an environment different than the original tumor. Interestingly, it has been described that tumors can create metastasis-promoting environments at the future metastatic sites through the production of systemic factors that attract myeloid cells (Kaplan et al., 2005). As myeloid cells can suppress immune responses, it is likely that these cells prepare an immunosuppressive niche that favors the extravasation and survival of tumor cells and thus the formation of metastases. Once in the distant organ, the tumor cells need to proliferate in order to form macrometastases. To achieve this, the mesenchymal tumor cells, which are thought to be slowly proliferating cells, need to undergo mesenchymal to epithelial transition (MET). Thus EMT is likely to be a transient and reversible transition (Brabletz, 2012). Tumor cells, referred to as micrometastases, can remain quiescent for long periods of time and only start to form macrometastases many years after removal of the primary tumor. The switch from a dormant to a proliferating state might be caused by changes in the microenvironment that suddenly allow the cells to activate proliferative programs and form a new tumor (Wan et al., 2013).

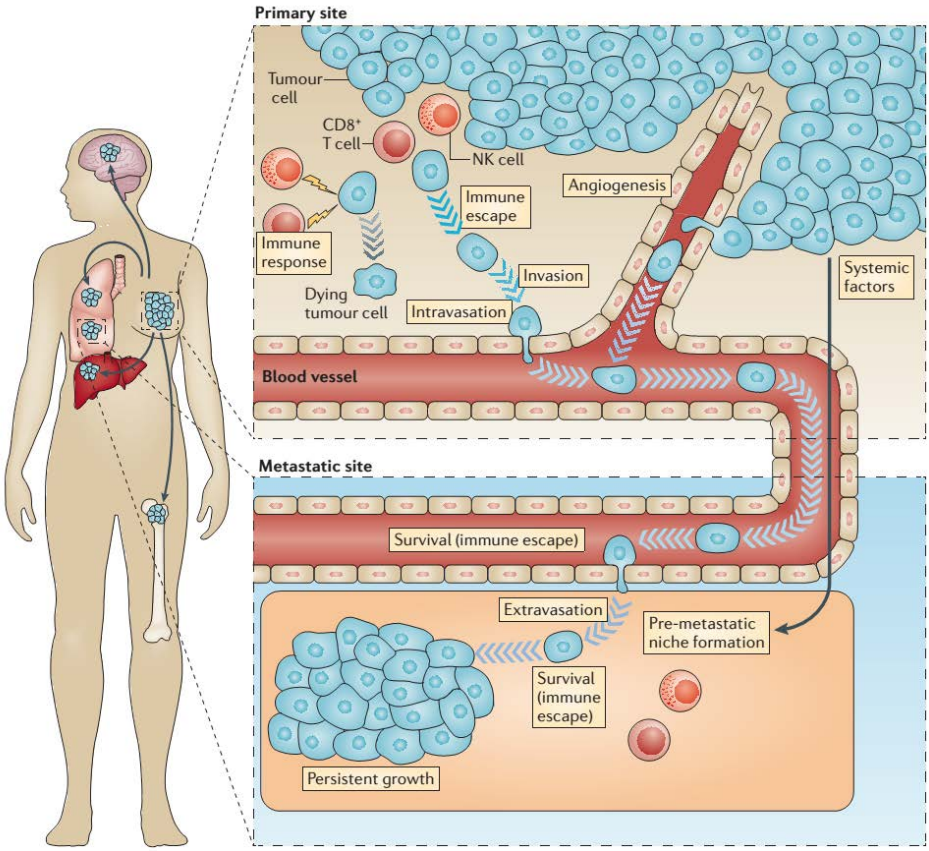

Figure 2.2 The metastatic process. Several steps are required for the formation of metastases in distant organs such as brain, lung, liver and bone. First, the tumor cells need to escape from anti-tumor immune responses mediated by T-cells and natural killer (NK) cells. Furthermore, they secrete systemic factors to prepare the pre-metastatic niche and have to acquire the ability to migrate to enter blood vessels (intravasation). The circulating tumor cells that survive in the circulation escape from the blood vessel (extravasation) and have to be able to survive in the new environment in order to from a secondary tumor (Kitamura et al., 2015).

Treating patients with metastatic cancer is the biggest challenge in breast cancer therapy and until now there has been limited success. After an initial response, metastases often become resistant to targeted therapies which might be due to heterogeneity between the primary tumor on which the targeted therapy was based, and the metastatic lesions, as well as between secondary lesions. One strategy for the treatment of patients with metastases has arisen from the many studies that describe the involvement of immune cells in the different steps of metastasis. It is thought that targeting these cell populations may be beneficial for the treatment of metastases (Wan et al., 2013). Furthermore, recent work has shown that metastasis

can emerge from cell clusters that escaped the primary tumor. These clusters survive better in the circulation than single tumor cells and have therefore a higher probability to from metastases. In human samples, more clusters were indicative of a shorter time to disease progression (Aceto et al., 2014). Hence, sequencing of these clusters in the circulation might be more helpful for choosing effective therapies to treat metastasis than the analysis of primary tumors.

2.2 The Estrogen Receptor α

The estrogen receptor α (ER) plays an important role in breast cancer, as a high percentage of human breast tumors are positive for ER expression (Zafrani et al., 2000). The ER, encoded by the *ESR1* gene (Menasce et al., 1993), is a ligand-dependent transcription factor that belongs to the nuclear receptor superfamily. The sequence of ER contains a DNA-binding domain (DBD) that binds to estrogen response elements (EREs) in the DNA, a ligand binding domain (LBD), as well as two transcriptional activation function (AF) domains. While the N-terminal AF1 domain can mediate ligand-independent activation of ER, the C-terminal AF2 domain harbors the ligand-dependent activation function. Both AF domains are responsible for the recruitment of several transcriptional coregulators (Figure 2.3) (Heldring et al., 2007).

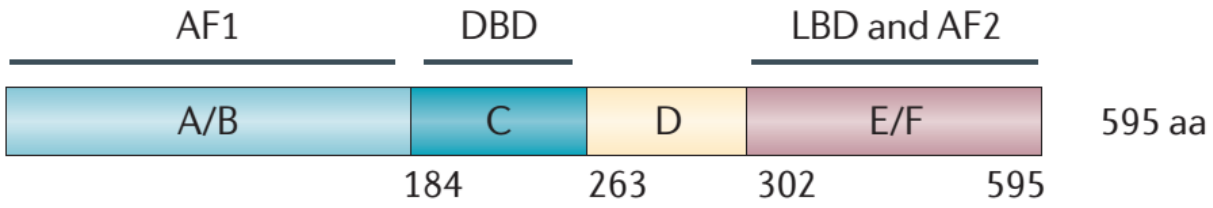

Figure 2.3 Schematic representation of ER and its functional domains. The ER consists of six nuclear receptor structural domains (A-F). Activation function 1 (AF1) and AF2, DNA binding domain (DBD), and ligand binding domain (LBD). Adjusted from (Thomas and Gustafsson, 2011)

The ER is expressed in various tissues including breast, brain, kidney, liver, ovaries and bone (Nilsson and Gustafsson, 2011). While ER KO mice are viable, reproductive functions are severely impaired (Lubahn et al., 1993). ER has been best studied in the breast, where it was demonstrated to be essential for ductal outgrowth and morphogenesis in normal mammary gland development (Mallepell et al., 2006). ER-signaling leads to changes in transcription of a large set of genes. In cancer cells, pro-proliferative genes are generally upregulated, while a significant fraction of genes that are downregulated upon ER-signaling, encode proteins with anti-proliferative and pro-apoptotic functions (Carroll et al., 2006; Dutertre et al., 2010; Frasor et al., 2003). The ER controls gene transcription through several mechanisms. The classical mechanism involves binding of the ER ligand estrogen (E2) that causes a conformational change and dissociation from the chaperone protein Hsp90. This allows ER dimerization and subsequently translocation to the nucleus where it binds DNA at EREs. Once ER is bound, coregulatory proteins are recruited that regulate gene expression (Figure 2.4 [1]) (Aumais et al., 1997; Kumar and Chambon, 1988). Another mechanism of ER gene transcription regulation, is via interaction with other transcription factors such as activating protein 1 (AP1) (Kushner et al., 2000), NFκB (Quaedackers et al., 2007) and specificity protein 1 (SP1) (Saville et al., 2000). The interaction of ER with DNA via transcription factors does not require a full ERE, instead the ER binds chromatin indirectly via transcription factors (Figure 2.4 [2]). Furthermore, ER-signaling can be mediated through a so called non-genomic mechanism. Ligand binding of ER, which is localized in the cytoplasm or at the membrane, induces the recruitment of SRC and PI3K, activating the MAPK and PI3K/AKT pathway, resulting in transcription factor activation (Figure 2.4 [3]). However, ER can also control transcription in the absence of its ligand. Growth factor induced activation of receptor tyrosine kinases (RTKs) including EGFR, ErbB2, and the insulin-like growth factor 1 receptor (IGF1R), leads to the activation of the kinases ERK and AKT, which in turn phosphorylate and activate ER in a ligand-independent manner (Figure 2.4 [4]) (Thomas and Gustafsson, 2011). The transcriptional responses of ER largely depend on the recruitment of coactivators including SRC3, CBP and p300, or corepressors such as NCoR and HDACs (Barnes et al., 2004).

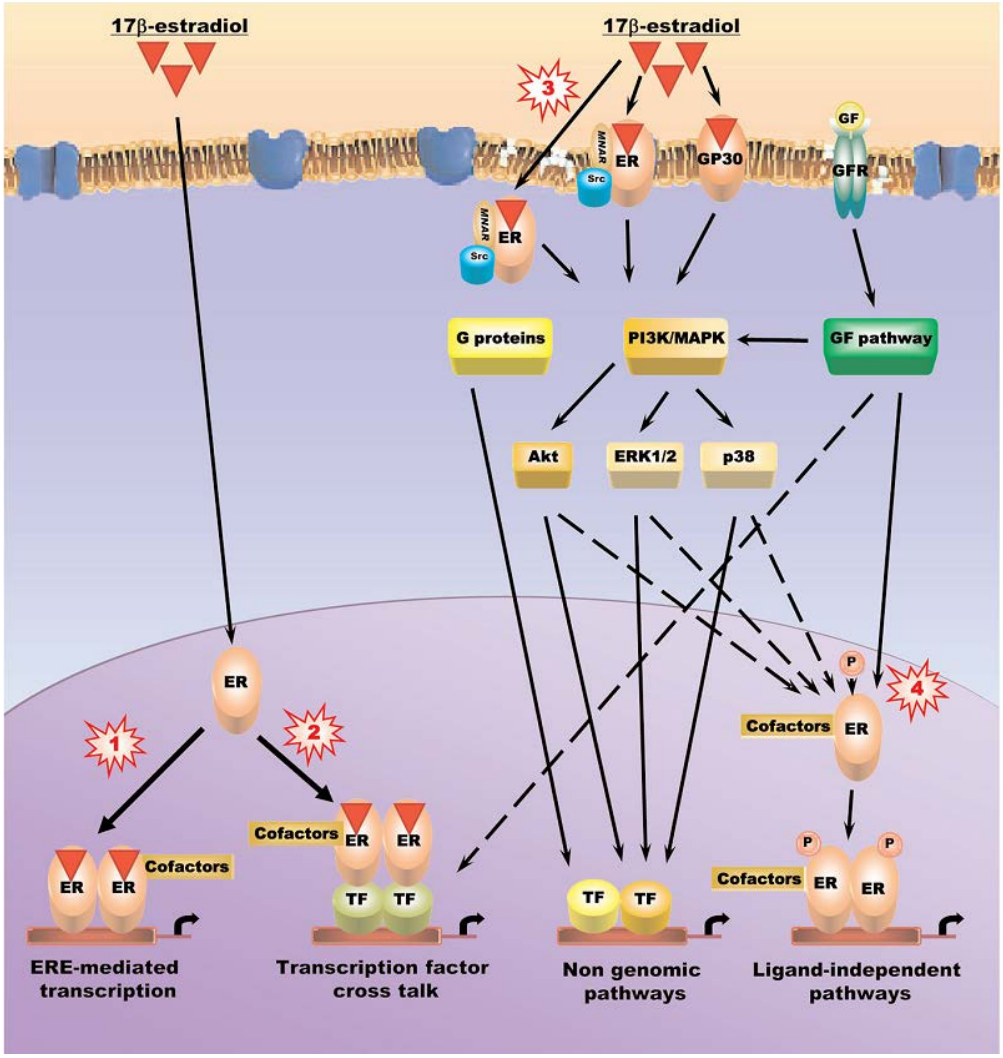

Figure 2.4 ER signaling pathways. Ligand dependent and ligand independent activation of ER are shown. (1) Activation of the classical genomic pathway involves the release of ligand-bound ER from chaperone Hsp90, dimerization, translocation to the nucleus and binding of DNA at estrogen response elements (EREs), and recruitment of coregulatory proteins. (2) Ligand bound ER can interact with other transcription factors (TFs) that bind to their own response elements. (3) The non-genomic pathway involves a small pool of ER located at the cell membrane that upon activation recruit protein kinases, leading to the activation of AKT and ERK and subsequent activation of transcription factors. (4) Activation of growth factor receptor (GFR) by growth factors (GF) lead to the phosphorylation and activation of ER in a ligand-independent manner (Roman-Blas et al., 2009).

2.2.1 ER-Signaling Is Controlled by Post-Translational Modifications

The ER is target for several post-translational modifications (PTMs) including phosphorylation, ubiquitination, acetylation and palmitoylation. These can influence ER functions, for example by affecting protein stability, DNA binding, ligand sensitivity, dimerization, subcellular localization and interaction with coregulators (Le Romancer et al., 2011).

Phosphorylation was the first PTM demonstrated to enhance ligand binding of the ER (Auricchio and Migliaccio, 1980). Since then, numerous phosphorylation sites have been described that affect various ER functions. For example, ER transcriptional activity is induced upon ligand-dependent phosphorylation of serine residue 118 (Ali et al., 1993), as well as upon ligand-independent phosphorylation of serine 118 or 167 (Bunone et al., 1996; Sun et al., 2001). Moreover, phosphorylation at serine 236 inhibits receptor dimerization, thereby preventing DNA binding (Chen et al., 1999a). Furthermore, ubiquitin-dependent degradation of ligand-bound ER is suggested to be critical for promoter clearance and additional rounds of transcription (Reid et al., 2003). The effect of ER acetylation will be discussed later (section 2.3.4). Thus, a plethora of PTMs tightly regulate ER-mediated functions.

2.2.2 ER in Breast Cancer

The ER is expressed in about 70% of breast cancer, promoting tumor proliferation and survival (Brünner et al., 1989; Zafrani et al., 2000). Endocrine therapies are commonly used to treat patients with ER-positive breast cancer, including tamoxifen, a selective estrogen modulator (SERM) that competes for ligand binding to the ER, the selective estrogen down regulator (SERD) fulvestrant, and aromatase inhibitors (letrozole, anastrozole and exemestane) that suppress estradiol production by blocking the aromatase enzyme . Despite the general success of endocrine agents, resistance towards these therapies often occurs leading to disease progression and death (Johnston, 2010). Several mechanisms have been suggested that alone or in combination might account for the development of resistance. Interestingly, loss of ER expression, an obvious resistance mechanism, is only observed in 15-20% of patients with tamoxifen resistant breast cancer (Encarnación et al., 1993; Gutierrez et al., 2005). Loss of ER

expression has been suggested to be caused by extensive methylation of the *ESR1* gene that was observed in primary ER-negative breast cancer but not in normal breast samples and ER-positive tumors (Lapidus et al., 1998). Indeed, demethylating agents have been shown to cause re-expression of ER in ER-negative breast cancer cells (Ferguson et al., 1995).

However, in the majority of endocrine resistant tumors, ER is still expressed and active, suggesting that these tumors acquired alternative mechanisms to become resistant. One possible mechanism of resistance is through activation of signaling pathways that activate ER by ligand-independent mechanisms. Indeed, upregulation of ErbB2 has been found in some tamoxifen resistant tumors (Gutierrez et al., 2005). Furthermore, activation of signaling pathways downstream of RTKs such as PI3K/AKT (Kirkegaard et al., 2005) that lead to altered phosphorylation of ER (Holm et al., 2009), and its coregulators (Carascossa et al., 2010), has been associated with tamoxifen resistance. Another recently reported resistance mechanism, is the occurrence of *ESR1* mutations that render ER less sensitive to endocrine therapy (Jeselsohn et al., 2015). While mutations in *ESR1* are rarely detected in primary breast cancer (Fuqua et al., 1993; The Cancer Genome Atlas Network, 2012), several point mutations have been found in metastatic breast cancer from patients that were treated with endocrine therapy (Jeselsohn et al., 2014; Merenbakh-Lamin et al., 2013; Robinson et al., 2013), suggesting a role for them in the development of metastatic disease and endocrine resistance. Indeed, the majority of these missense point mutations cluster within the LBD and several mutations have been shown to result in constitutive ER activity (Figure 2.5) (Jeselsohn et al., 2014; Merenbakh-Lamin et al., 2013; Robinson et al., 2013).

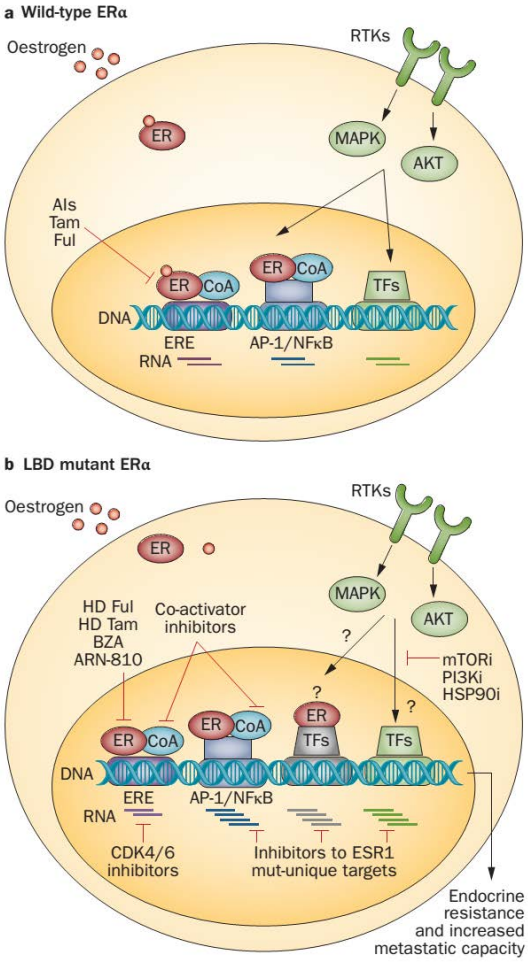

Figure 2.5 Treatment of ER-positive breast cancer. (a) ER wild-type expressing tumors are largely sensitive to endocrine therapies such as aromatase inhibitors (AIs), tamoxifen (TAM) and fulvestrant (Ful). (b) Tumors expressing ligand-binding domain (LBD) mutant ER, might also have enhanced ligand-independent activity, rendering them insensitive to standard endocrine therapy. Alternative therapeutic strategies might include higher doses (HD) of Ful or TAM, or more potent or mutant-specific inhibitors (BZD and ARN-810), inhibitors targeting ER gene-products (e.g. cyclinD1 blockade by CDK4/6 inhibitors), LBD mutant-unique gene products, inhibitors for coactivators (CoA) or other signaling molecules involved in ligand-independent activation of ER (mTORi, PI3Ki, Hsp90i) (Jeselsohn et al., 2015)

A better understanding of the underlying mechanisms driving resistance will help to better predict response to endocrine therapy and might lead to new treatment strategies in order to overcome resistance. For example, it has been shown that ER mutants are still sensitive to endocrine therapy, however at higher concentrations (Jeselsohn et al., 2014; Merenbakh-Lamin et al., 2013; Robinson et al., 2013). This opens new treatment strategies for patients with tumors harboring these mutations, for example using higher doses or more potent new endocrine therapies. Furthermore, combination therapies of endocrine therapies together with drugs targeting proteins involved in endocrine resistance, might lead to better responses of endocrine resistant tumors (Figure 2.5). Of note, a phase 2 clinical trial using an aromatase inhibitor in combination with a cyclin dependent kinase inhibitor for advanced breast cancer patients, showed promising results, and a phase 3 clinical trial is ongoing (Finn et al., 2014). Moreover, a phase 2 study combining an aromatase inhibitor with an ERBB2- and an mTOR-inhibitor is ongoing (https://clinicaltrials.gov/ct2/show/NCT01499160?term=GCC+0901&rank=1).

Despite these promising results, the treatment of endocrine resistant tumors remains a challenge and future studies are required to gain more insight in the underlying mechanisms of resistance. Furthermore, personalized therapies based on the present resistance mechanisms, as well as analysis of tumors throughout the course of disease to monitor the development of novel resistances, might lead to strategies that improve patient outcome.

2.3 Epigenetic Modifications in Cancer

The underlying mechanisms driving tumorigenesis are diverse. They include genomic alterations such as amplifications, translocations, deletions and point mutations, but also epigenetic modifications. These epigenetic modifications alter DNA-based processes, such as transcription, replication and DNA repair, without changing the nucleotide sequence of the DNA. As epigenetic modifications are reversible, they allow dynamic changes in gene

transcription, a process which needs to be tightly controlled in order for a cell to produce a given gene product at the appropriate time and level. Epigenetic modifications include methylation of the DNA, as well as PTMs of histone proteins, for example acetylation, methylation, ubiquitination and phosphorylation (Figure 2.6) (Dawson and Kouzarides, 2012).

Methylation of the DNA is mediated by methyltransferases (DNMTs) that transfer a methyl group to a cytosine (Bestor et al., 1988). DNA methylation occurs predominantly, but not exclusively, at CpG sites, regions in the DNA where a cytosine nucleotide is located next to a guanine and is linked by a phosphate (Lister et al., 2009; Ramsahoye et al., 2000). Methylation of the DNA is generally negatively associated with gene expression. Hence, DNA hypermethylation has been shown to inhibit the expression of genes (DeSmet et al., 1999), as well as transposons (Reik, 2007), and is involved in the inactivation of the X-chromosome (Plath et al., 2003).

The function of histone proteins is to organize the DNA into nucleosomes, in order to package DNA into chromatin. Nucleosomes consist of a histone octamer, with two of each of the histones H2A, H2B, H3 and H4, around which 146 bp of DNA are wrapped (Luger et al., 1997). PTMs on histone tails can influence the interaction between histones and DNA, thereby modulating the accessibility of the DNA to proteins involved in gene transcription (Dawson and Kouzarides, 2012). Many different histone modifications have been identified, one of the most common ones, the acetylation of lysine residues regulated by histone acetyltransferases (HATs) (Brownell et al., 1996) and histone deacetylases (HDACs) (Taunton et al., 1996), will be discussed below (section 2.3.1).

In cancer, deregulation of epigenetic modifications of DNA and histones are often observed. These include massively hypomethylated DNA (Ehrlich, 2002; Goelz et al., 1985), which is associated with increased chromosomal instability (Eden et al., 2003), as well as focal hypermethylation causing transcriptional repression of tumor suppressor genes like retinoblastoma (Rb) (Greger et al., 1989). Moreover, loss of acetylation on specific lysine residues from histone 4 (K16 and K20) has been shown to be a common event in human cancer (Fraga et al., 2005). It is therefore not surprising, that several epigenetic modifiers including

DNMTs, HATs and HDACs are often deregulated in cancer. For example, DNMT3B is overexpressed in leukemia, the HAT p300 was found to be overexpressed in colorectal carcinoma (Ishihama et al., 2007), and HDAC1, HDAC2 and HDAC6 are overexpressed in human breast cancer (Krusche et al., 2005; Müller et al., 2013; Zhang et al., 2004). Furthermore, aberrant recruitment of HDACs to specific gene promoters by oncogenic fusion proteins, such as PML-RARα, PLZF-RARα and AML1-ETO, is known to contribute to leukemogenesis (Dawson and Kouzarides, 2012).

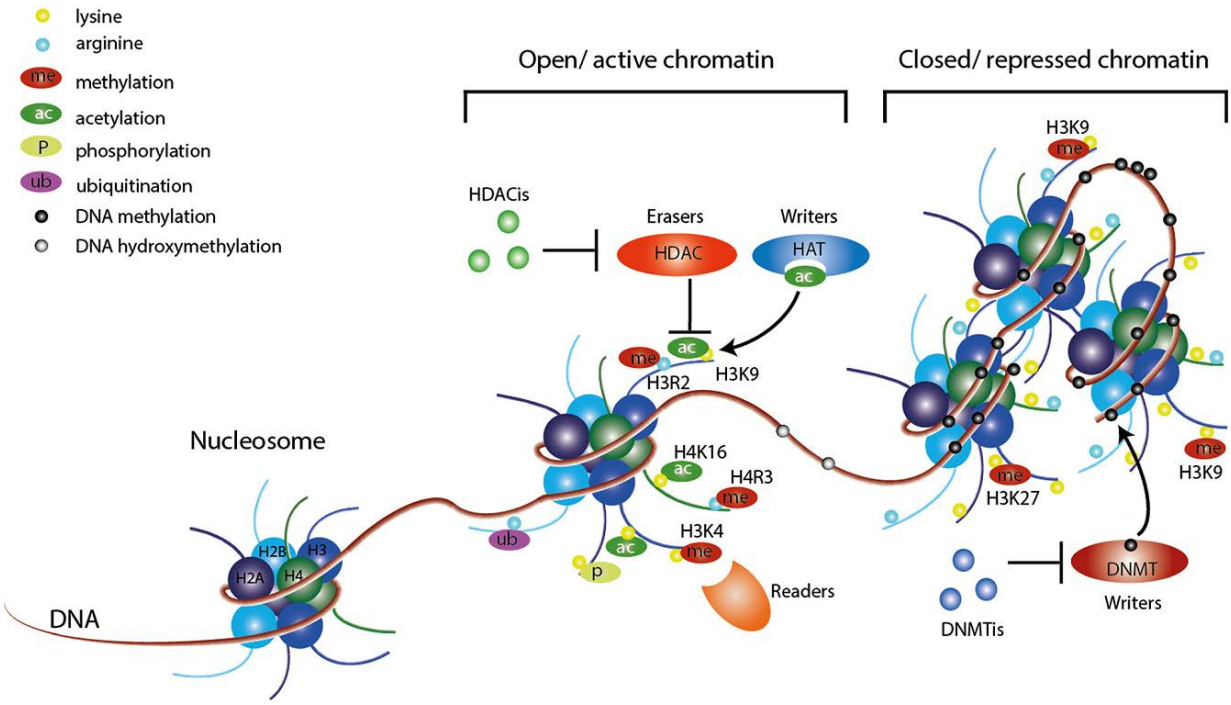

Figure 2.6 Epigenetic modifications of the DNA and histone proteins. Post-translational modifications on histone proteins, such as methylation, acetylation, ubiquitination and phosphorylation induce changes in the chromatin structure and thereby alter transcription. Histone acetyltransferases (HATs) transfer acetyl groups to lysine residues which can be removed by histone deacetylases (HDACs) that can be inhibited with HDAC inhibitors (HDACis). DNA methylation by DNA methyltransferases (DNMTs) is generally associated with transcriptional repression, which can be counteracted by DNMT inhibitors (DNMITs). Epigenetic modifications can recruit proteins that are able to read the modifications (readers) (Falahi et al., 2014).

2.3.1 Acetylation of Histones and Non-Histone Proteins

Acetylation is a dynamic process that is controlled by the opposing activities of HATs and HDACs. While HATs catalyze the transfer of an acetyl moiety from acetyl co-enzyme A to lysines, the removal of acetyl groups is mediated by HDACs (Parbin et al., 2013). Acetylation of histone tails plays an important role in the regulation of gene transcription, as acetylation neutralizes the positive charge on lysine residues and thereby weakens the interaction between histones and the negatively charged DNA (Figure 2.7) (Hong et al., 1993). This leads to a more open chromatin structure, rendering the DNA accessible for transcriptional regulators (Figure 2.6) (Lee et al., 1993). Furthermore, bromodomain-containing proteins including HATs and transcriptional coactivators, recognize and bind to acetylated histones and modulate gene transcription (Figure 2.7) (Dhalluin et al., 1999; LeRoy et al., 2008). Thus, acetylation is generally associated with increased transcriptional activity. As HDACs revert the action of HATs and cause a more condensed chromatin structure (Taunton et al., 1996), they are regarded as transcriptional repressors. Moreover, they are often found in complexes with transcriptional repressors such as NCoR and mSin3 (Heinzel et al., 1997)

In addition to its role in transcriptional regulation, acetylation of non-histone proteins has a big impact on protein functions. Acetylation is involved in protein stability, activity, cellular localization and protein-protein interactions (Singh et al., 2010). For example de-acetylation of the tumor suppressor p53 decreases its transcriptional activity, and thereby prevents p53-dependent apoptosis in response to DNA damage (Luo et al., 2001). More than 1750 proteins have been shown to be acetylated; these are involved in many cellular processes such as cell cycle, cell migration, splicing, chromatin remodeling and DNA replication (Choudhary et al., 2009). Thus, acetylation not only regulates gene transcription but also numerous cellular processes. Furthermore, acetylation of lysine residues competes with other post-translational modifications such as ubiquitination, methylation and sumoylation and therefore can also indirectly affect protein functions (Figure 2.7) (Yang and Seto, 2008).

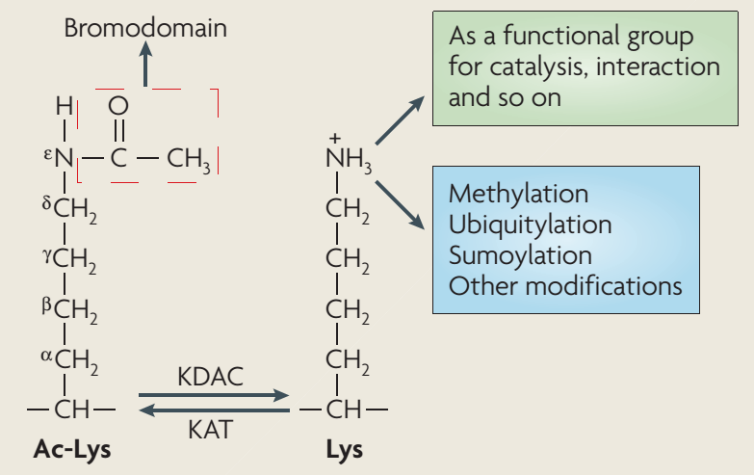

Figure 2.7 Acetylation and de-acetylation of lysine residues. Histone acetyltransferases (HATs), also called lysine (K) acetyltransferases (KATs), transfer acetyl groups to lysine residues, while histone deacetylases (HDACs), also called lysine deacetylases (KDACs), remove them and restore the positive charge on the lysine residue. Acetylated lysines are recognized by proteins containing bromodomains. De-acetylated lysines can serve for catalysis and interaction with the DNA. Furthermore, acetylation competes with other post-translational modifications such as methylation, ubiquitination and sumoylation (Yang and Seto, 2008).

2.3.2 The Histone Deacetylase Family

The family of HDACs contains 18 members and can be divided in two distinct groups. The so called "classic" HDACs consist of 11 members and require zinc for their catalytic activity (de Ruijter et al., 2003). In contrast, the second group of HDACs, called sirtuins (SIRT1, -2, -3, -4, -5, -6 and -7), are not dependent on zinc but require NAD^+ as a cofactor (Afshar and Murnane, 1999; Frye, 1999).

The classical HDACs are further divided into four different classes, based on their homology to yeast proteins and their subcellular localization (Figure 2.8). Class I (HDAC1, -2, -3 and -8) share homology with the yeast HDAC Rpd3 and are primarily localized in the nucleus (Dangond et al., 1998; de Ruijter et al., 2003; Taunton et al., 1996). This class of HDACs are ubiquitously expressed and have been implicated in several cellular processes such as cell cycle regulation, tissue development and cell differentiation. Class I HDACs are generally components of multi-protein complexes and interact with various transcription factors (Reichert et al., 2012). HDAC1

and HDAC2 originate from a common ancestor, have overlapping functions and can partially compensate for each other (Gregoretti et al., 2004; Montgomery et al., 2007).

The class II HDACs are most closely related to the yeast protein Hda1 and in contrast to class I HDACs, their expression seems to be tissue specific. They are further divided in class IIa (HDAC4,-5, -7 and -9) and class IIb (HDAC6 and 10) HDACs (Fischle et al., 1999, 2001; Grozinger et al., 1999; Guardiola and Yao, 2002; Kao et al., 2000; Yang and Seto, 2008). HDACs of both classes, IIa and IIb, can shuttle between the nucleus and cytoplasm, however class IIb HDACs are mainly localized in the cytoplasm (Hubbert et al., 2002; Parra et al., 2007; Tong et al., 2002). The shuttling of class IIa HDACs is mediated by phosphorylation. Phosphorylation of HDACs leads to binding of 14-3-3 proteins and subsequent export of HDACs from the nucleus, causing de-repression of target genes (Grozinger and Schreiber, 2000).

In contrast to class IIa, class IIb HDACs have two catalytic domains, although one of them is inactive in HDAC10 (Yang and Seto, 2008). While little is known about the functions of HDAC10, HDAC6 has been shown to affect cell migration through de-acetylation of α-tubulin as well as cortactin (Hubbert et al., 2002; Zhang et al., 2007a). Another target of HDAC6 is the chaperone protein Hsp90. It has been shown that knockdown of HDAC6 caused acetylation of Hsp90 which led to loss of chaperone activity (Kovacs et al., 2005). Furthermore, HDAC6 is the only HDAC with an ubiquitin binding site which allows binding of ubiqitinated proteins and the formation of aggresomes that organize misfolded proteins into a single location (Kawaguchi et al., 2003).

HDAC11, the most recently identified HDAC, is the sole member of class IV (Gao et al., 2002). As it shares sequence homology to both, class I and class II HDACs, it was assigned to a separate class. Because class III was already assigned to the sirtuins, HDAC11 was defined as a class IV HDAC (Gregoretti et al., 2004; de Ruijter et al., 2003). HDAC11 is mainly localized in the nucleus and its expression is restricted to specific tissues (Gao et al., 2002). This protein will be discussed in more detail later (see in section 2.4)

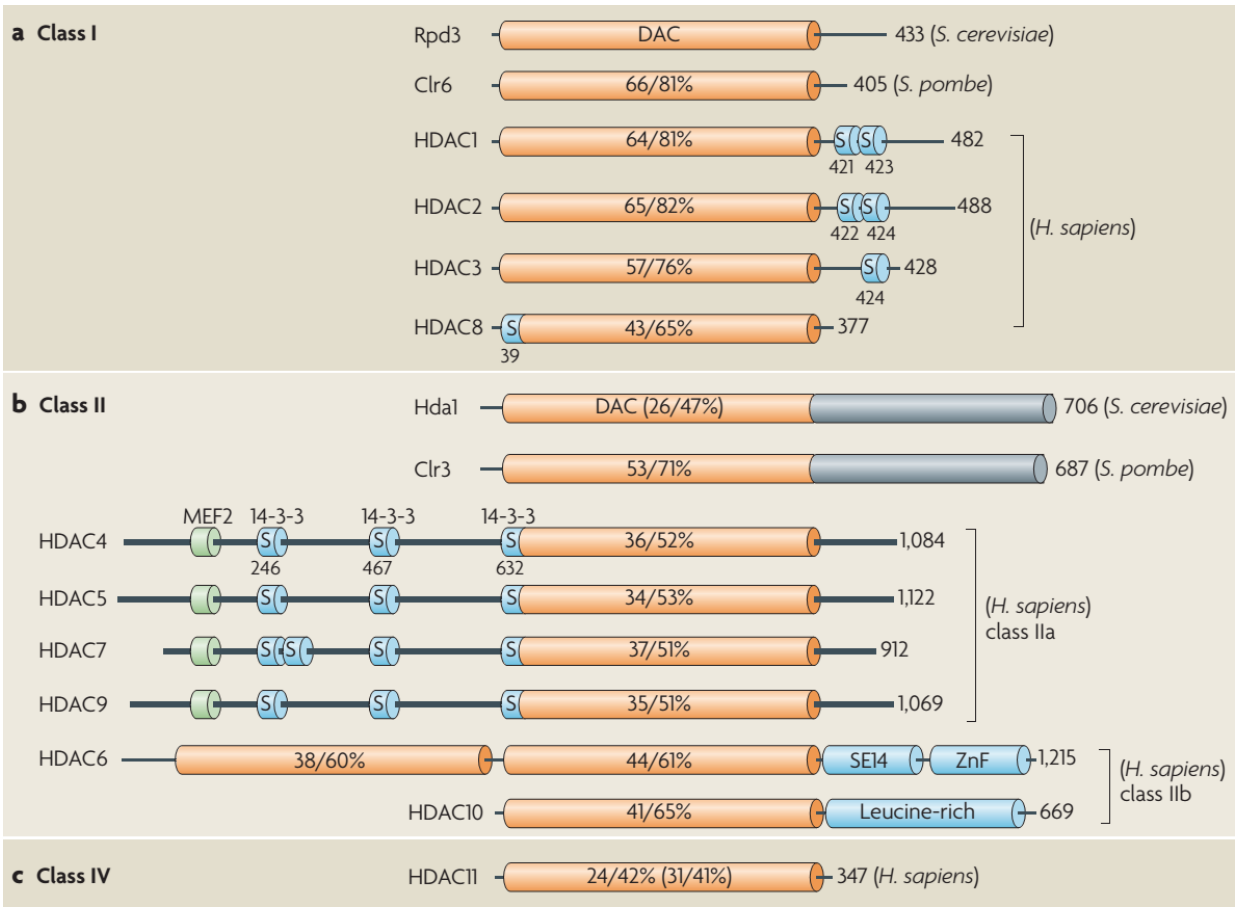

Figure 2.8 Classification of classical HDAC family members. HDACs are grouped into different classes based on their sequence homology to yeast proteins. Class I HDACs are homologous to the yeast protein Rpd3 and consist of HDAC1, -2, -3 and 8. Class II HDACs are structurally related to class II HDACs and further divided into class IIa (HDAC4, -5, -7 and 9) and class IIb (HDAC6 and -10). Class IV consists of HDAC11. The deacetylase (DAC) domain is depicted as an orange cylinder. The numbers in the cylinder reflect the percentage of amino acid sequence identity/similarity to Rpd3 (for class I) or to Hda1 (for class II and IV). The sequence identity/similarity of Hda1 and HDAC11 to Rpd3 is given in brackets. Myocyte enhancer factor-2 (MEF2)-binding motifs are shown as green cylinders and blue small cylinders represent 14-3-3 binding motifs. The larger blue cylinders show SE14: Ser-Glu-containing tetradecapeptide repeats; ZnF: ubiquitin-binding zinc finger and Leucine-rich motif. On the right, the total number of amino acid residues of each deacetylase is shown (Yang and Seto, 2008).

2.3.3 Targeting HDACs in Cancer

To date, a wide range of HDAC inhibitors (HDACi) that vary in structure, activity and specificity, have been identified. Most of the HDACi are pan-inhibitors targeting several HDACs, however, with different affinities (Ververis et al., 2013). The only specific HDACi identified to date, is the HDAC6 inhibitor tubacin, which induces hyperacetylation of α–tubulin but has no effect on histone acetylation (Haggarty et al., 2003). HDACi can be classified into several groups based on their chemical structure, including hydoxamic acid (tichostatin A and vorinostat, also known as SAHA), benzamides (entinostat, mocetinostat), cyclic peptides (romidepsin), short-chain fatty acids (valporic acid and butyrate) (Table 2-1) (Ververis et al., 2013).

HDACi Groups	HDACi	Specificity (Class)	Reference
Benzamides	Mocetinostat	I and IV	(Fournel et al., 2008)
	Entinostat	I	(Khan et al., 2008)
Short chain fatty acid based	Valporic acid	I	(Khan et al., 2008)
	Phenylbutyrate	I and IIa	(Mottamal et al., 2015)
Cyclic peptide	Romidepsin	I	(Furumai et al., 2002)
Hydroxamic acid	Pracinostat	I, II and IV	(Novotny-Diermayr et al., 2010)
	Trichostatin A	I, IIb and IV	(Lobera et al., 2013)
	Vorinostat (SAHA)	I and II	(Khan et al., 2008)
	Tubacin	HDAC6	(Haggarty et al., 2003)
	Belinostat	I and II	(Khan et al., 2008)
	Panobinostat	I and II	(Khan et al., 2008)

Table 2-1 Selection of HDAC inhibitors with different specificities.

Numerous preclinical studies using these inhibitors have been performed, which revealed that HDACi can have beneficial effects on tumor cells. Originally they were discovered through their ability to induce tumor cell differentiation (Leder and Leder, 1975; Riggs et al., 1977), but are now known to affect additional cellular functions such as cell-cycle arrest, apoptosis, angiogenesis and DNA repair (West and Johnstone, 2014). HDACi exert these multiple cellular effects through transcriptional control by modifying histones, but also through their action on non-histone proteins (Figure 2.9). For example, HDACi have been shown to disrupt the chaperone function of Hsp90 through deacetylation, exposing HIF1α to proteasomal degradation and preventing transcription of pro-angiogenic factors such as VEGF (Zhang et al., 2010a). Furthermore, most HDACi, induce cell cycle arrest at the G1/S transition (Bolden et al., 2006), which is mediated by upregulation of the cyclin-dependent kinase inhibitor 1 ($p21^{WAF1}$) (Gui et al., 2004), as well as by downregulation of cyclins (Sandor et al., 2000). Moreover, HDACi induce apoptosis in cancer cells through induction of extrinsic (death receptor) and intrinsic (mitochondrial) pathways, through upregulation of death receptors such as FAS and TRAIL (Insinga et al., 2005), and of pro-apoptotic proteins such as Bim, Bmf and Bax (Cohen et al., 2004; Zhang et al., 2006; Zhao et al., 2005). HDACi have also been demonstrated to sensitize cancer cells to DNA-damaging agents through downregulation of proteins involved in DNA-repair such as BRCA1 (Zhang et al., 2007b), and RAD51 (Figure 2.9) (Adimoolam et al., 2007).

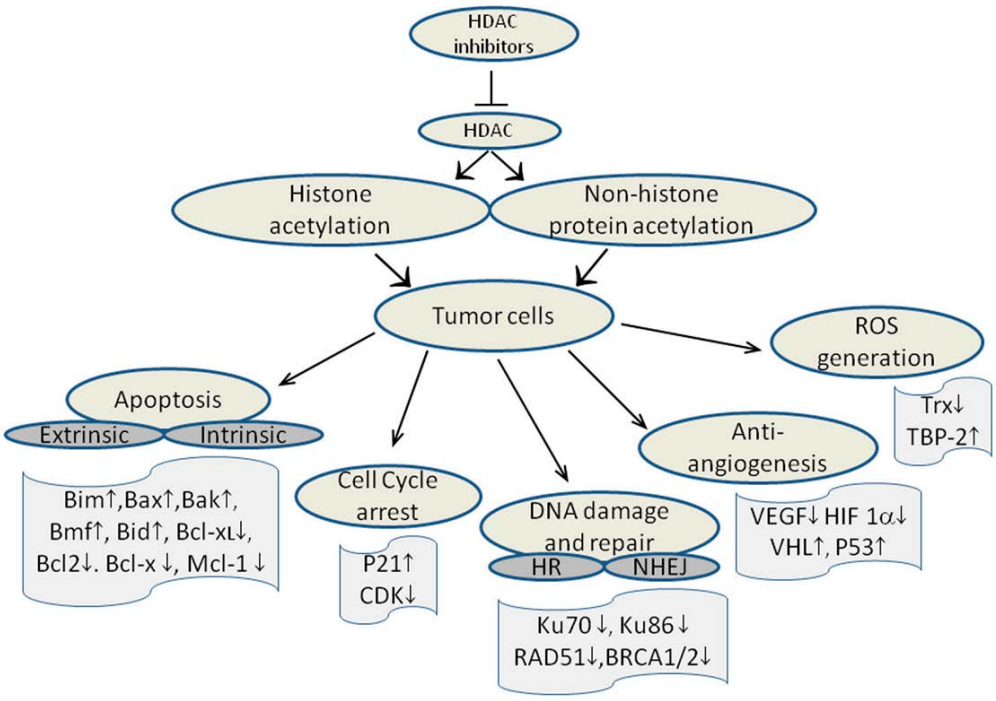

Figure 2.9 HDACi activate multiple anti-tumor pathways by affecting histone acetylation and non-histone protein acetylation. Abbreviation: homologous recombination (HR), non-homologous end joining (NHEJ) (Mottamal et al., 2015)

To date, the four HDACi vorinostat, romidepsin, belinostat and panobinostat have been approved by the US Food and Drug Administration (FDA) for the treatment of hematological malignancies (Mann et al., 2007; Mottamal et al., 2015; San-Miguel et al., 2014). However, despite the successful treatment of hematological malignancies, as well as numerous promising preclinical studies using HDACi to target different cancer cells, clinical studies with HDACi on solid tumors showed little success (West and Johnstone, 2014). This might be caused by the unspecific nature of HDACs targeting several HDACs at the same time, which could have different cellular functions. In breast cancer for example, high HDAC6 expression is correlated with better prognosis (Zhang et al., 2004), while high levels of HDAC2 and HDAC3 are associated with more aggressive disease (Müller et al., 2013). Furthermore, HDACi cause deregulation of large numbers of genes (Peart et al., 2005), which might cause re-expression of tumor suppressor genes, but could also contain genes that are tumor promoting. A better knowledge about the individual roles of specific HDACs in different cancer types, together with

development of more specific inhibitors might help to improve HDACi-based therapies. Furthermore, combining HDACi with other therapeutic agents might lead to improved anti-tumor responses. Indeed, promising results come from clinical trials using a multitargeted inhibitor of HDACs, EGFR and ErbB2 for patients with advanced solid tumors (Shimizu et al., 2014), as well as from a phase II clinical study combining a HDACi with an aromatase inhibitor for patients with ER-positive endocrine resistant tumors (Yardley et al., 2013). Several clinical studies using HDACi in combination with other cancer therapies for the treatment of solid tumors are ongoing (Mottamal et al., 2015), which might lead to new strategies for cancer therapy.

2.3.4 HDACs and the Estrogen Receptor

Several HDACs such as HDAC1, HDAC3 and HDAC6 (Krusche et al., 2005; Saji et al., 2005), have been reported to be expressed in ER-positive breast cancer and numerous studies have revealed a role for HDACs in the regulation of ER expression and signaling (Cavailles et al., 2011).

In most studies, treatments with different pan-HDACi (De los Santos et al., 2007; Reid et al., 2005; Yi et al., 2008) as well as KD of HDAC1, HDAC2 and HDAC6 (Biçaku et al., 2008) in ER-positive breast cancer cells, has been shown to decrease ER protein and mRNA levels, generally resulting in reduced ER transcriptional activity and inhibition of cell proliferation. The reduction in ER levels is mediated on the transcriptional as well as on the post-transcriptional level, as combination of HDACi with a proteasomal inhibitor, could partially rescue receptor downregulation (De los Santos et al., 2007). The mechanism by which inhibition of HDACs decreases *ESR1* transcription is largely unknown. However, as several transcription factors have been reported to be acetylated (Singh et al., 2010), HDACi might induce their hyperacetylation, altering transcriptional activity and/or recruitment of cofactors, thereby inducing *ESR1* transcriptional repression (Figure 2.10). Furthermore, as HDACs are generally known to act as transcriptional repressors by deacetylation of histone proteins (Taunton et al., 1996), they could control ER expression by repressing the transcription of miRs known to target *ESR1* mRNA (Figure 2.10) (Adams et al., 2007; Zhao et al., 2008).

On the protein level, HDACi have been shown to alter ER stability. This is mediated by hyperacetylation of the ER chaperone Hsp90 in response to HDACi treatment, which decreases its binding to ER, leading to polyubiquitylation and proteasomal degradation of ER (Figure 2.10) (Fiskus et al., 2007). In this study, pan-HDACi (targeting class I and II HDACs) have been used. However, as HDAC6 levels were decreased in response to these inhibitors, together with the previous finding that HDAC6 deacetylates Hsp90 (Kovacs et al., 2005), this effect was likely caused by the reduced HDAC6 levels. In contrast to this negative regulation of ER protein stability by HDACi, direct acetylation of ER by overexpression of the HAT p300, or treatment with the HDACi trichostatin A (targeting class I, IIb and IV HDACs), prevents its ubiquitylation and proteasomal degradation, thereby increasing ER protein stability (Figure 2.10) (Kim et al., 2010a). Furthermore, HDACi have been shown to induce re-expression of ER in ER-negative breast cancer cell lines rendering them sensitive to endocrine therapy (Sabnis et al., 2011; Yang et al., 2000). Taken together these data show that the effect of HDACi on ER expression is complex and likely to be dependent not only on the breast tumor sub-type but also the targeted HDAC.

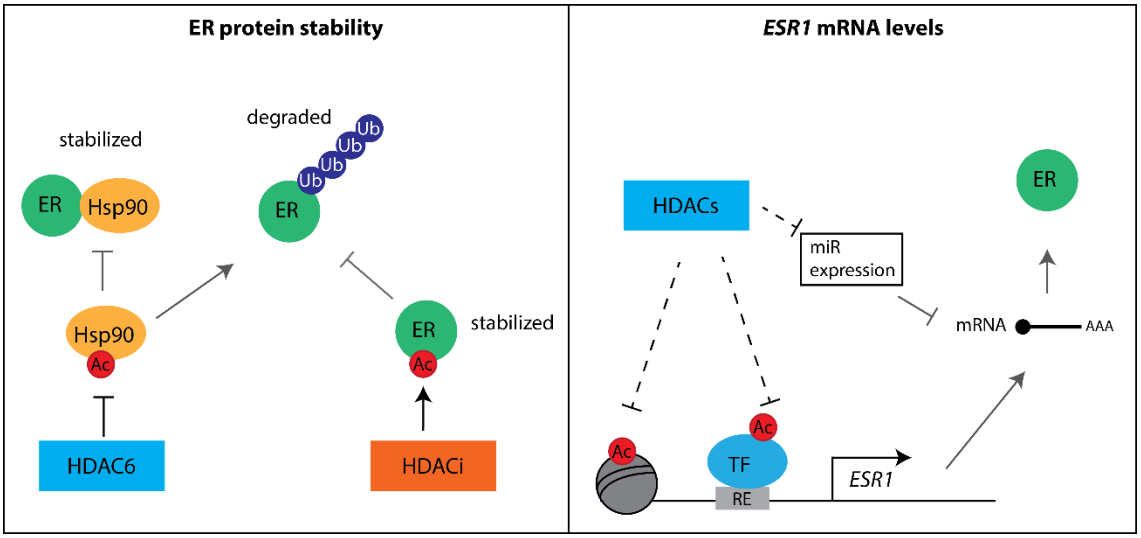

Figure 2.10 Crosstalk between HDACs and ER. HDAC6 deacetylates Hsp90, allowing interaction with ER, preventing its ubiquitylation and thereby increasing ER protein stability. HDACi promote ER acetylation, preventing its ubiquitylation, increasing ER protein stability. HDACi lead to alterations in *ESR1* mRNA levels, potentially resulting from various mechanisms, including enhanced acetylation of histone proteins at the *ESR1* promoter, altering the transcriptional activity of transcription factors and/or by repressing miRs that target *ESR1* mRNA for degradation.

In addition, HDACi alter ER-target gene transcription, which is also very likely to be mediated by various mechanisms, including downregulation of ER levels, histone acetylation as well as acetylation of ER and its coregulators (Figure 2.11) (Cavailles et al., 2011). Interestingly, ER has been shown to be acetylated by the HAT p300 at different lysine residues. While acetylation at lysine 266 and 268 enhances DNA-binding activity and transcriptional activity of ER (Kim et al., 2006), acetylation of lysine 302 and 303 results in suppressed ligand sensitivity (Wang et al., 2001). Thus, the function of ER acetylation is site specific. Moreover, several ER coregulators such as SRC3 (Chen et al., 1999b), RIP140/NRIP1 (Vo et al., 2001) and HDAC1 (Qiu et al., 2006) are also modified by acetylation, increasing the complexity of how HDACi could alter ER-target gene transcription. Unfortunately, little is known about the roles of individual HDACs with respect to ER. HDAC1 and HDAC4 have been shown to interact with ER and overexpression of these HDACs decreases ER transcriptional activity (Kawai et al., 2003; Leong et al., 2005). Furthermore, both HDAC1 and HDAC7 have been found on the promoter of *pS2*, a well-studied ER-target gene (Métivier et al., 2003). Interestingly, HDAC1 and HDAC3 have been found on the promoter of *c-myc* in the presence of tamoxifen, suggesting that the transcriptional repression by tamoxifen-bound ER of ER-target genes, involves the recruitment of HDACs (Liu and Bagchi, 2004). On the other hand, in breast cancer cells HDAC6 expression is induced by estrogen signaling, and this HDAC promotes cell migration by deacetylation of tubulin (Saji et al., 2005). Future studies might reveal additional functions of HDACs in breast cancer and help to better understand the action of HDACi in ER-positive breast cancer.

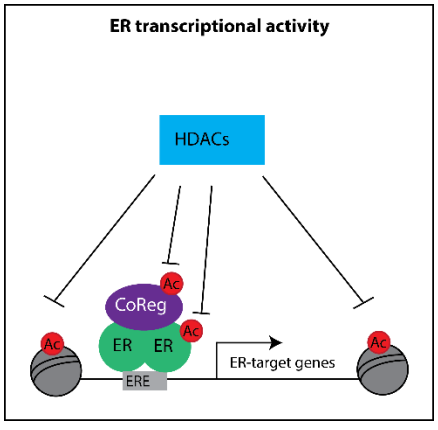

Figure 2.11 HDACs alter transcription of ER-target genes potentially by decreasing acetylation of ER, its coregulators and histone proteins.

2.4 The Histone Deacetylase 11

HDAC11 is the most recently discovered HDAC and was found through its sequence homology with the yeast protein HOS3 (Gao et al., 2002). The *HDAC11* gene is localized on chromosome 3 and two HDAC11 transcripts were found, resulting from alternative gene splicing. HDAC11 is the smallest member of the HDAC family and consists essentially of the catalytic domain (Figure 2.12). Its cellular localization was found to be mainly nuclear. In contrast to class I HDACs which are ubiquitously expressed, HDAC11 expression is, like class II HDACs, restricted to certain tissues. Expression of HDAC11 has been reported for testis, brain, heart, skeletal muscle and kidney, indicating a tissue-specific role for HDAC11. Furthermore, high levels of HDAC11 were detected in different human cancer cell lines, which suggests that HDAC11 not only plays a role in normal tissues but also in cancer (Gao et al., 2002).

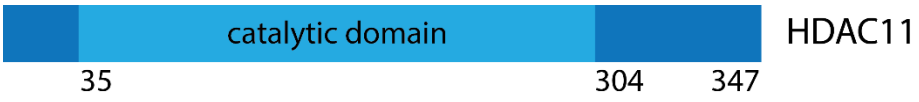

Figure 2.12. Schematic representation of HDAC11 with its catalytic domain.

2.4.1 Functions of HDAC11 in Normal Physiology

This section will summarize studies describing HDAC11 in normal physiology including the brain and immune system.

HDAC11 is expressed in human brain cells (Gao et al., 2002), and throughout the murine brain, it is one of the most highly expressed member of the HDAC family as demonstrated by *in situ* hybridization (Broide et al., 2007). Interestingly, expression levels of HDAC11 increase in specific areas of the mouse brain during the postnatal development of the central neural system (Liu et al., 2008). Furthermore, elevated HDAC11 levels have been found in a screen for nuclear receptors and their coregulators involved in the differentiation of neural stem cells (NSCs) (Androutsellis-Theotokis et al., 2013). NSCs differentiate into astrocytes, neurons and oligodendrocytes and expression of HDAC11 has been found in nuclei of oligodendrocytes and neurons, however only low levels have been detected in astrocytes (Broide et al., 2007; Liu et

al., 2008). Furthermore, during maturation of oligodendrocytes, HDAC11 mRNA levels accumulate and coincide with reduced acetylation levels of histones within the two oligodendrocyte-specific genes encoding proteolipid protein (PLP) and myelin basic protein (MBP). HDAC11 binds to the promoter regions of these two genes and interacts with histone H3 in mature oligodendrocytes, reducing its acetylation. Interestingly, although histone de-acetylation is commonly linked to transcriptional repression, de-acetylation of histones in the promoter region of *PLP* and *MBP* genes led to an increased recruitment of RNA Polymerase II and subsequently increased mRNA levels of PLP and MBP. Thus, HDAC11 positively regulates the transcription of PLP and MBP and thereby influences oligodendrocyte maturation (Liu et al., 2009).

HDAC11 has also been implicated in the regulation of immune activation versus immune tolerance. A tight regulation of these two processes is mandatory in order to allow an appropriate immune response against pathogens and at the same time prevent the system from over-reacting and causing self-tissue damage. Antigen presenting cells (APCs), such as macrophages, are important players in keeping this balance, as they modulate the antigen-specific activation of T-cells against pathogens, as well as their tolerance against self-antigens. In macrophages, HDAC11 represses the transcription of *il-10* (Cheng et al., 2014), encoding a cytokine with key function in tolerance induction (Moore et al., 2001), thereby promoting immune activation of T-cells and preventing T-cell tolerance (Figure 2.13) (Villagra et al., 2009). The levels of HDAC11 in macrophages are negatively controlled by miR-145. IFNβ downregulates miR-145 in a JAK1-STAT1 dependent manner, leading to increased HDAC11 levels and subsequently to *il-10* repression (Lin et al., 2013). Interestingly, while HDAC11 represses *il-10* gene transcription, HDAC6 interacts with HDAC11 and binds to the same DNA sequence within the *il-10* gene promoter, where it acts as a transcriptional activator. These divergent roles of HDAC11 and HDAC6 could allow the dynamic regulation of *il-10* transcription that is important for immune regulation by APC (Cheng et al., 2014).

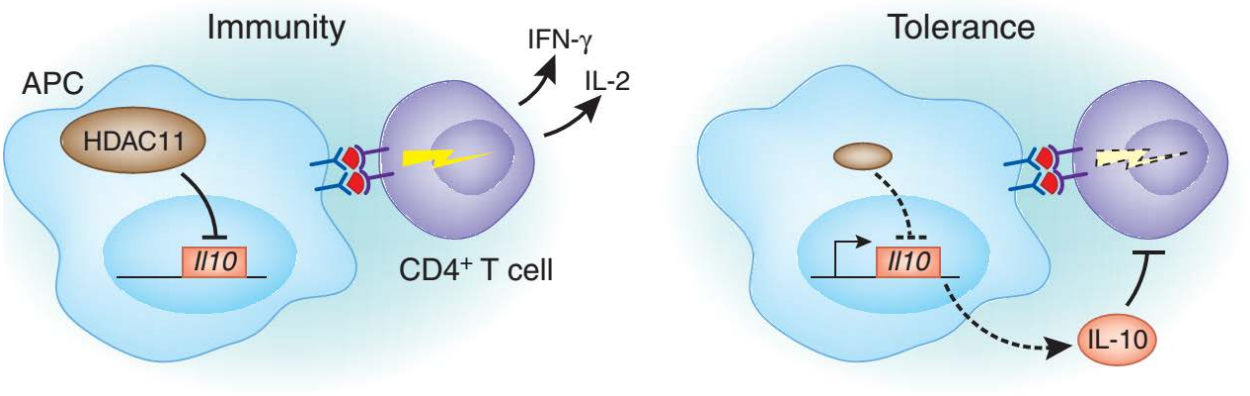

Figure 2.13 HDAC11 influences immune activation versus immune tolerance. HDAC11 represses transcription of *il-10* in antigen presenting cells (APCs), thereby promoting T-cell activation. Inactivation of HDAC11 in APCs increases IL-10 expression, which results in T-cell tolerance. Adjusted from (Georgopoulos, 2009).

2.4.2 HDAC11 Mediates DNA Replication and Proliferation

HDAC11 alters DNA replication by inducing chromatin condensation, as well as by decreasing the protein stability of Cdt1, a replication licensing factor (Glozak and Seto, 2009; Wong et al., 2014). Replication licensing is an important process to prevent re-replication and thus assuring that chromosomes are only replicated once per cell cycle to maintain genomic integrity. The initiation of DNA replication starts with the binding of the Origin Recognition Complex (ORC) to origins of replication and the recruitment of Cdc6 and Cdt1 that are required to load the hexameric Mini-Chromosome Maintenance (MCM) helicase complex (Machida et al., 2005). During G1, Cdt1 recruits HBO1, a histone acetyltransferase (HAT), to replication origins, causing chromatin de-condensation. Upon entering S phase, HDAC11 interacts with the replication licensing factor Cdt1 and binds to origins of replication. This causes chromatin condensation that alters the recruitment of MCMs and thereby prevents re-replication (Figure 2.14) (Wong et al., 2014). Furthermore, HDAC11 prevents re-replication by altering Cdt1 protein stability. During S phase Cdt1 is negatively regulated to ensure that the MCM2 helicase complex is not recruited to origins of replication which already fired. HDAC11 affects protein stability of Cdt1 through its de-acetylation. Acetylation can protect proteins from ubiquitination, as these post-translational modifications occur on the same lysine residues. Thus, de-acetylation of Cdt1 by

HDAC11 increases ubiquitylation that mediates its subsequent proteasomal degradation (Glozak and Seto, 2009). As replication licensing is important for proliferation (Stoeber et al., 2001), the authors suggest that HDAC11 might be negative regulator of cell proliferation (Glozak and Seto, 2009).

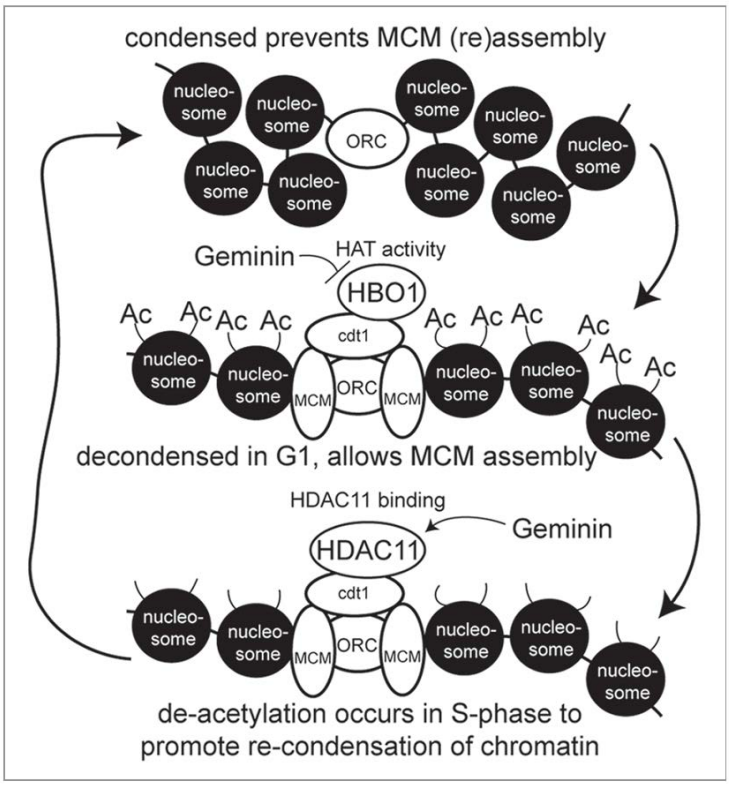

Figure 2.14 Model for replication licensing influenced by HDAC11. During G1 Cdt1 binds to origin recognition complex (ORC) and allows binding of the MCM helicase complex. Cdt1 recruits the histone acetyltransferase (HAT) HBO1, which induces chromatin de-condensation. Geminin inhibits HAT activity and recruits HDAC11, leading to chromatin condensation and preventing re-replication (Wong et al., 2014)

However, other studies have revealed that KD of HDAC11 decreases proliferation in oligodendrocytes (Liu et al., 2009), and different human cancer cell lines such as prostate, colon, ovarian and breast cancer (Deubzer et al., 2013). Thus, HDAC11's role in proliferation might be dependent on the cell type.

2.4.3 The Role of HDAC11 in Disease

HDAC11 has been described to be involved in several different diseases. Interestingly, in some cases HDAC11 expression contributes to the malignant phenotype, while in others it is involved in disease prevention.

For example, HDAC11 suppresses neurodegeneration in a drosophila model of the fragile X tremor ataxia syndrome (FXTAS), an inherited neurodegenerative disorder. This disease is caused by an expansion of a CGG trinucleotide repeat in the 5'UTR of the fragile X syndrome (FXS) gene, *FMR1*. FXTAS patients show an increase in mRNA levels of *FMR1*, while FMR protein levels are normal or decreased, as the expanded CGG repeat is insufficiently translated. It is thought that the CGG repeat-containing mRNA sequesters proteins and prevents them from performing their normal functions. Overexpression of HDAC11, HDAC6 or HDAC3 represses transcription of CGG-repeat containing *FMR1*, thereby suppressing neurodegeneration (Todd et al., 2010).

HDAC11 has been suggested to be oncogenic in cancer as KD of HDAC11 in colon, prostate, breast and ovarian cancer cell lines decreased metabolic activity while non-transformed cell lines were not affected (Deubzer et al., 2013). Furthermore, another study revealed that HDAC11 can induce repression of the tumor suppressor gene *ARHI*, which is expressed in normal cells but not in breast and ovarian cancer cells. Knockdown of HDAC11 increases acetylation of E2F1 (Feng et al., 2007), which has been shown to increase DNA-binding of E2F1 (Martínez-Balbás et al., 2000), suggesting that HDAC11 controls *ARHI* transcription through deacetylation of E2F1 (Feng et al., 2007).

These studies suggest, that HDAC11 might be a target for cancer therapy. However, targeting HDAC11 might also cause unwanted side effects, as it has been shown to play a role in immune responses. Two studies have looked at the role for HDAC11 in the immune defense against cancer cells. In the first study, HDAC11 has been shown to be a negative regulator of myeloid-derived suppressor cell (MDSC) expansion and function, a heterogeneous population of myeloid cells such as immature dendritic cells, macrophages and granulocytes (Sahakian et al., 2014). These cells interact with T-cells and negatively regulate their function to prevent

damage caused by excessive inflammation. Tumor infiltrating MDSCs can suppress anti-tumor T cell function in the tumor microenvironment and thereby modulate the immune response towards cancer cells (Serafini et al., 2006). HDAC11 is highly expressed in immature myeloid cells (IMCs), but decreased in MDSCs, which have increased IL-10 levels and promote T-cell tolerance against cancer cells. Consequently, mouse lymphoma cells injected into HDAC11 KO mice grew faster than in control mice, suggesting that the anti-tumor T cell response was suppressed in HDAC11 KO mice. These results suggest, that it might be unfavorable to treat cancer patients with HDAC11-inhibitors as this might decrease anti-tumor responses (Sahakian et al., 2014).

However, in a study investigating the role of HDAC11 in Hodgkin Lymphoma (HL), HDAC11 KD induced favorable anti-tumor immune responses. HL is a B-cell lymphoid cancer characterized by Hodgkin and Reed-Sternberg (HRS) cells which are surrounded by inflammatory cells such as T cells and regulatory T cells (T_{Reg}) that are involved in immune tolerance to self-antigens. Activated T cells, natural killer T cells and T_{Reg} cells express OX40 which is a receptor for the OX40 ligand (OX40L) that is produced by antigen-presenting cells like dendritic cells, macrophages, activated B cells, T cells and endothelial cells. The binding of OX40L by its receptor induces the generation of antigen-specific memory T cells that are important for antitumor responses. Furthermore, OX40L has been shown to suppress the generation of T_{Reg} cells. In HL cells, OX40L is not expressed but KD of HDAC11 induces its expression as well as the expression of TNF-α, interferon-γ, IL-17 and IL-6, but not IL-10, and causes apoptosis of HL cells. Additionally, expression of OX40L induced by HDACi in HL cells inhibited the generation of T_{Reg} cells. Thus, HDAC11 inhibition might be a promising approach to treat patients with HL (Buglio et al., 2011).

The contrasting observations of HDAC11's function in immune response against cancer cells suggest that OX40L and IL-10 signaling might vary in different cell types and in the presence of different cytokines. Whether HDAC11 inhibitors could cause favorable responses in the clinic might largely depend on the disease and the role HDAC11 is playing in the different contexts. Further studies are required to investigate the genomic- as well as non-genomic targets of

HDAC11 that might help to better understand the normal- as well as the malignant-function of HDAC11.

2.5 Memo (Mediator of ErbB2-Driven Cell Motility)

Memo, for Mediator of ErbB2-driven cell motility, was initially discovered through its interaction with the phosphotyrosine site Tyr-1227 of the ErbB2 receptor (Marone et al., 2004). Structural analysis revealed homology with the iron-dependent dioxygenase LigB (Qiu et al., 2008), a bacterial enzyme that catalyzes oxidative cleavage of carbon-carbon bonds of aromatic catechol ring systems (Noda et al., 1990). In LigB, three histidine amino acids (His-12, His-61, His-195) and one glutamic acid (Glu-242) are responsible for iron binding and its catalytic activity (Sugimoto et al., 1999). Interestingly, the three histidines (His-49, His81, and His-192) are conserved in Memo, while the glutamic acid is replaced by a cysteine (Cys-244). Indeed, we have shown that Memo binds copper via this site and functions as a redox protein (MacDonald et al., 2014). Memo is conserved in all branches of life, from bacteria to human, with a high sequence homology close to its active site (Qiu et al., 2008; Schlatter et al., 2012).

In cells, Memo is expressed in the cytoplasm and the nucleus (Schlatter et al., 2012) and upon heregulin (HRG)-stimulation Memo translocates to the cell membrane (Marone et al., 2004). While Memo contains a nuclear export sequence, and its nuclear export can be blocked by the nuclear export inhibitor Lebtomycin B, it remains unknown how Memo enters the nucleus. Given its small size of 34kDa, it might well be that it freely diffuses through the nuclear pores (Schlatter et al., 2012). In mammals, Memo is expressed in most adult organs, which suggests an important role for Memo in normal physiology. Indeed, Memo conditional full body knockout (KO) mice, where Memo deletion is induced after birth, have a reduced life span and show characteristics of premature aging that was accompanied by elevated serum levels of vitamin D and calcium (Haenzi et al., 2014). Furthermore, Memo deletion was demonstrated to be embryonic lethal, showing a bleeding phenotype that is likely caused by vascular defects (Kondo et al., 2014). However, the exact physiological role of Memo remains largely unknown.

2.5.1 Memo in Migration

Memo is required for cell migration downstream of several receptor tyrosine kinases (RTKs) as stimulation with HRG, fibroblast growth factor 2 (FGF2) and epidermal growth factor (EGF) in breast cancer cell lines (Marone et al., 2004), and platelet derived growth factor (PDGF) in mouse embryonic fibroblast (Kondo et al., 2014), induced cell migration in control cells, but was decreased in cells with reduced Memo levels. Thus, Memo harbors a widespread role in RTK-induced cell motility. Cell migration is a dynamic process that requires the remodeling of the actin and microtubule network, as well as the formation of adhesion sites (Ridley, 2011). Actin polymerization at the cell front pushes the plasma membrane forward leading to the formation of cell protrusions. Several different protrusions exist, including lamellipodia and filopodia that form at the leading edge of moving cells (Abercrombie et al., 1970; Gustafson and Wolpert, 1999; Wood and Martin, 2002). Furthermore, invadapodia and podosomes have been discovered that are matrix-degrading structures appearing on the ventral surface of cells (Chen, 1989; Tarone et al., 1985). The formation of adhesion sites, which link the actin cytoskeleton to the extracellular matrix, stabilizes the protrusions and generates traction forces. Contractile tension induces the disassembly of adhesions at the cell rear that allows tail retraction and cell movement (Ridley et al., 2003). Furthermore, microtubules extend within protrusions and regulate the turnover of focal adhesions and contribute to maintain cell polarity (Figure 2.15) (Watanabe et al., 2005).

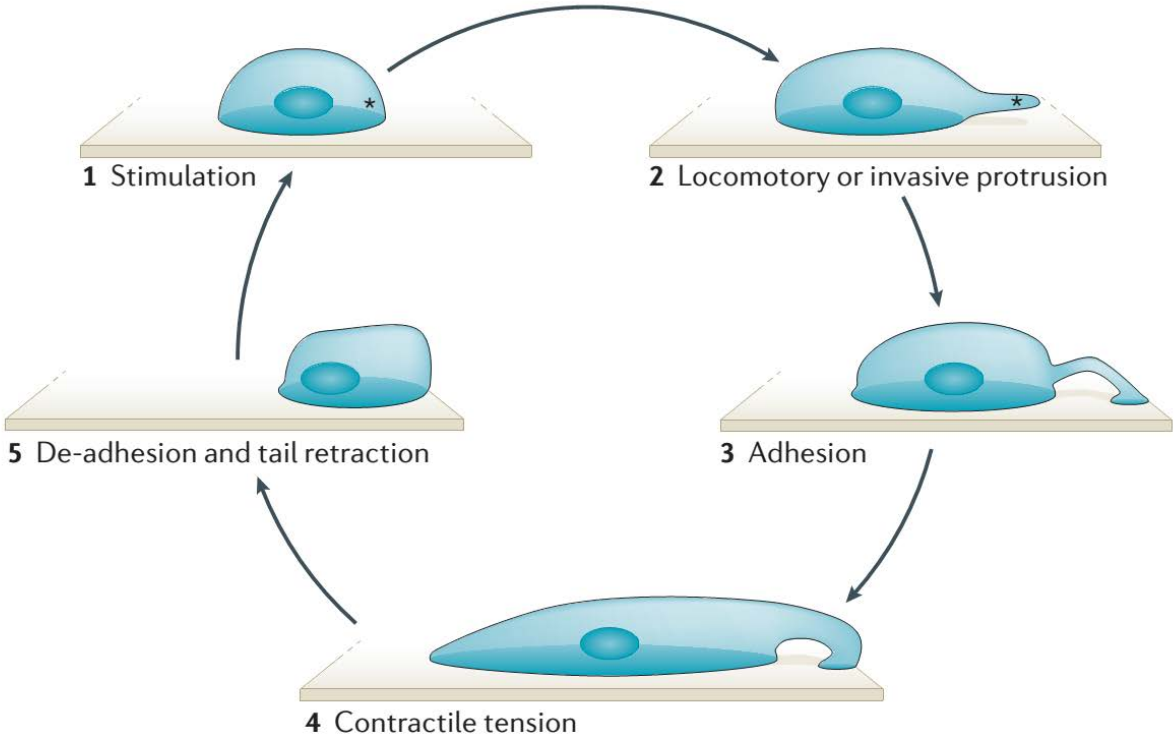

Figure 2.15 Steps involved in cell motility. 1) External stimuli induce actin polymerization and 2) the formation of cellular protrusions. 3) Protrusions adhere to the extracellular matrix via adhesion sites. 4) Contractile tension creates cell elongation. 5) Adhesion sites at the cell rear are disassembled, allowing the cell to move forward (Bravo-Cordero et al., 2013).

Memo mediates cell migration by controlling microtubule outgrowth into lamellipodia, adhesion site formation and organization of the actin network in lamellipodia in response to HRG-stimulation by localizing active RhoA, a small GTPase, and its effector mDia1 to the cell membrane (Zaoui et al., 2008). The growth of microtubules is mediated though dynamic changes between phases of growth and shrinkage at their plus ends until stabilized at the cell cortex. Microtubule capture and stabilization is required for cell polarization and directed cell migration (Watanabe et al., 2005). Memo mediates this process by controlling the localization of two microtubule binding and stabilizing proteins, adenomatous polyposis coli (APC) and cytoplasmic linker-associated protein 2 (CLASP2), to the plasma membrane in response to HRG-stimulation (Zaoui et al., 2010). The binding of APC and CLASP2 to microtubules is negatively regulated by glycogen synthase kinase-3β (GSK3β) (Wittmann and Waterman-Storer, 2005;

Zumbrunn et al., 2001). Memo inhibits GSK3β through HRG-induced phosphorylation of GSK3β most likely via AKT (Cross et al., 1995; Zaoui et al., 2010), which inhibits its activity and allows APC and CLASP2 to bind microtubules. Subsequently, membrane-bound APC recruits the protein ACF7 to the plasma membrane, which then mediates microtubule capture and stabilization at the cell cortex, allowing directed cell migration (Zaoui et al., 2010). Thus, the Memo-RhoA-mDia1 signaling pathway promotes cell migration through capturing microtubules to the cell cortex and causing their stabilization. Furthermore, Memo has been shown to interact with the actin-binding protein cofilin that controls actin dynamics and regulates actin filament turnover. Cofilin generates a pool of actin monomers that are required for lamellipodium extension at the cell leading edge. Memo is required for the localization of cofilin at the plasma membrane, and was shown to enhance the actin depolymerizing- and severing activity of cofilin and thereby controlling directed cell migration (Meira et al., 2009). Thus, Memo controls cell migration through the recruitment of several proteins involved in the organization of the microtubule- and actin network to the leading edge of migrating cells.

In addition, overexpression of Memo was reported to induce epithelial to mesenchymal transition (EMT), leading to increased cell migration and invasion. Stimulation of the insulin-like growth factor 1 receptor (IGF1R) was shown to induce the interaction between its effector insulin receptor substrate 1 (IRS1) and Memo, which leads to the upregulation of the transcriptional repressor Snail and subsequently repression of the epithelial cell-cell junction protein E-cadherin (Sorokin and Chen, 2013). Hence, Memo is involved in many cellular processes that promote cell migration.

2.5.2 Memo in Cancer

Several studies have suggested a role for Memo in cancer. For example, increased Memo mRNA levels were found in a human pancreatic cancer cell line compared to normal pancreas (Kalinina et al., 2010). In another study, the tumor suppressor miR-125b, which represses the expression of Memo, has been shown to be downregulated in pre-invasive breast cancer compared to normal breast epithelium, suggesting that Memo might play a role in early breast cancer

development (Hannafon et al., 2011). Furthermore, we have shown that Memo is expressed at low levels in normal breast, while it is overexpressed in 40% of human breast cancer. Moreover, we found that high cytoplasmic Memo is prognostic for early distant metastasis and death (MacDonald et al., 2014). Together these studies suggest that high Memo levels might promote malignancy.

2.6 Reactive Oxygen Species Acting as Signaling Molecules

Reactive oxygen species (ROS) are highly reactive molecules that are generated by the partial reduction of oxygen to form superoxide (O_2^-), hydrogen peroxide (H_2O_2), and hydroxyl radical ($HO^\cdot$). Depending on the species, these ROS have different reactivity. $HO^\cdot$ is highly oxidizing, H_2O_2 is a relatively weak oxidant and O_2^- can act as both a mild oxidant and a weak reductant (Lambeth and Neish, 2014). In the cell, reactive oxygen species are generated as natural by-products during mitochondrial electron transport (Boveris et al., 1972; Loschen et al., 1971) or by oxidases that are involved in diverse cellular processes including lipoxygenases (Los et al., 1995), xanthine oxidase (Fridovich, 1970) and cytochrome P450 (Gorsky et al., 1984). However, the first identified oxidases that produce ROS not as a byproduct, but as its primary function are the enzymes NADPH oxidases (NOX). The NOX family consists of seven membrane spanning catalytic isoforms NOX1-NOX5, DUOX-1 and DUOX-2, which differ in their subcellular localization, activation, cytoplasmic subunits, organ specificity and type of ROS release (Brandes et al., 2014). NOX complexes generate ROS by transferring an electron from NADPH across membranes to oxygen, thereby generating superoxide. This superoxide is then converted by superoxide dismutase (SOD) to hydrogen peroxide, which is then imported or can freely diffuse through the plasma membrane (Figure 2.16) (Gough and Cotter, 2011).

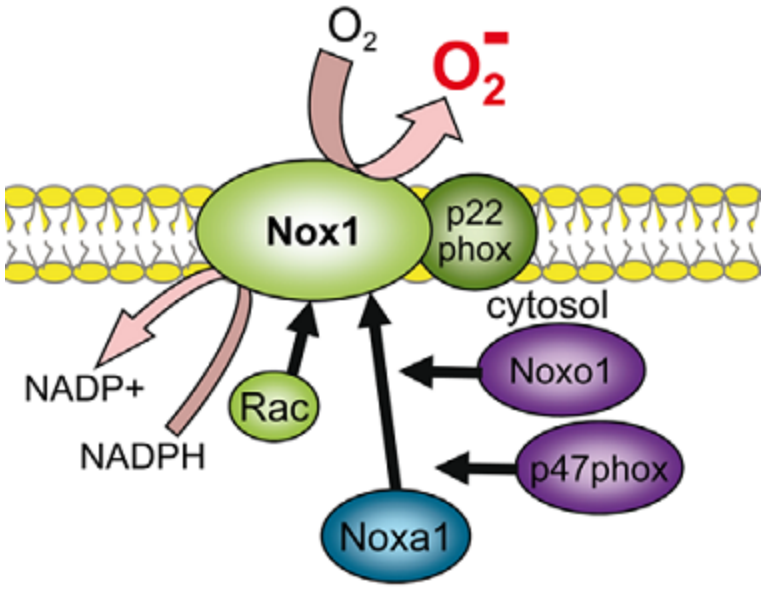

Figure 2.16 Superoxide production by the NADPH oxidase 1 (NOX1). Upon assembly of the NOX-complex through binding of its subunits, an electron from NADPH is transferred through the membrane to oxygen (O_2), generating superoxide (O_2^-). Adjusted from: (Brandes et al., 2014)

Traditionally, ROS has been viewed as a molecular damaging agent that can react with nucleic acids, proteins and lipids, disrupting biochemical functions and causing genome instability and apoptosis (Ray et al., 2012). Antioxidant enzymes including superoxide dismutase (SOD), catalase, glutathione peroxidase (GPX) and peroxiredoxin protect cells against ROS induced damage. Peroxiredoxin and GPX convert hydrogen peroxyde into water, or in the case of SOD catalyze the breakdown of O_2^- into H_2O_2 that can then be further oxidized into H_2O (Table 2-2) (Gough and Cotter, 2011). Furthermore, cysteine-rich proteins and peptides such as glutathione and thioredoxins function as redox sinks, as their cysteine residues rapidly get oxidized by ROS, quenching further biochemical reactivity (Lambeth and Neish, 2014).

Imbalance between ROS generation and detoxifying reactions leads to a disturbed cellular redox state and results in oxidative stress, which has been implicated in carcinogenesis (Szatrowski and Nathan, 1991; Toyokuni et al., 1995), neurodegeneration (Andersen, 2004), diabetes (Tanaka et al., 2002) and atherosclerosis (Kisucka et al., 2008). However, localized ROS in phagolysosomes of macrophages mediates microbial killing and thus serves as an important

protection against infections (Babior et al., 1973, 1975). Furthermore, low concentrations of ROS act as signaling molecules, causing reversible alterations in protein structure and/or activity. Redox-reactive cysteine residues are oxidized by ROS, which leads to the formation of sulfenic acid (-SOH) that can form disulfide bonds with cysteines in close proximity (-S-S-). These cysteine oxidations can be reversed by mechanisms involving glutathione or thioredoxins, which results in an off/on regulation similar to phosphorylation and dephosphorylation. However, high ROS concentrations lead to irreversible oxidation of cysteine residues to sulfinic ($-SO_2H$) or sulfonic ($-SO_3H$) acid, resulting in cell damage (Ray et al., 2012).

Several proteins have been shown to be redox-controlled. For example, the activity of protein tyrosine phosphatases (PTPs), including PTP-1B (Lee et al., 1998), SHP1 (Cunnick et al., 1998) and SHP2 (Meng et al., 2002), are negatively controlled by ROS. Oxidation of the cysteine residue that normally acts as a phosphate acceptor results in the inhibition of the phosphatase-activity thereby altering downstream signaling pathways (Lee et al., 1998). Furthermore, the protein tyrosine kinase SRC has been shown to be activated upon oxidation of two cysteines (Giannoni et al., 2005). ROS-mediated signaling has also been shown to be involved in gene transcription as several transcription factors including NF-κB, p53 and activator protein-1 (AP1) (Sun and Oberley, 1996) were shown to be redox-regulated. Thus, ROS can act as signaling molecules and regulate many cellular processes such as proliferation, apoptosis, migration and adhesion (Gough and Cotter, 2011).

Enzymatic antioxidant	Cellular location	Substrate	Reaction
Superoxide dismutase (Mn/Cu/ZnSOD)	Mitochondrial matrix (MnSOD) Cytosol (Cu/ZnSOD)	Superoxide ($O_2 \cdot^-$)	$O_2 \cdot^- \rightarrow H_2O_2$
Catalase	Peroxisomes Cytosol	Hydrogen peroxide (H_2O_2)	$2H_2O_2 \rightarrow O_2 + H_2O$
Glutathione peroxidase (GPX)	Cytosol	Hydrogen peroxide (H_2O_2)	$H_2O_2 + GSH \rightarrow GSSG + H_2O$
Peroxiredoxin I→VI (Prx)	Cytosol	Hydrogen peroxide (H_2O_2)	$H_2O_2 + TrxS_2 \rightarrow Trx(SH)_2 + H_2O$

Table 2-2 Enzymatic antioxidants: Superoxide dismutases (SODs) are located in the cytosol and mitochondria, and require a metal ion cofactor such as copper (Cu), zinc (Zn) or manganeses (Mn). These enzymes convert superoxide (O_2^-) into hydrogen peroxide (H_2O_2). Catalase converts hydrogen peroxide to water (H_2O) and is found in peroxisomes and in the cytoplasm. Glutathione peroxidases and peroxiredoxins reduce hydrogen peroxide to water and are localized in the cytoplasm. (Gough and Cotter, 2011)

2.6.1 ROS Involvement in Cell Migration

Numerous studies have demonstrated that ROS play a role in cell migration. For example, reduction of ROS by antioxidants or NOX-inhibitors has been shown to impair cell migration towards growth factors (Kim et al., 2010b). Furthermore, several growth factors, such as PDGF (Adachi et al., 2005), FGF (Schröder et al., 2007) and vascular endothelial growth factor (VEGF) (Evangelista et al., 2012), have been demonstrated to induce NOX-dependent ROS production during cell migration.

The activation of some of the NOX complexes, including NOX1, NOX2 and NOX3, require the assembly of regulatory subunits including p47phox and p21-activated kinase-1 (PAK1), as well as the recruitment of GTP-bound Rac (Brandes et al., 2014). Upon stimulation with growth factors, Rac is activated either through G-protein-mediated guanine exchange factor (GEF) activation or through PIP3-mediated GEF activation downstream of RTK signaling. The recruitment of p47phox is controlled by protein kinase C (PKC) activation that phosphorylates p47phox and allows its association with the NOX-complex and induction of superoxide production (Figure 2.17) (Brandes et al., 2014). Due to the unspecific nature of ROS, localized ROS production at specific cellular compartments is required in order to gain specificity. Indeed, NOX-complexes have been found to localize to the leading edge of migrating cells (Ikeda et al., 2005; Wu et al., 2005). This is thought to be mediated through the interaction of p47phox with myosin (Wientjes et al., 2001), cortactin (Touyz et al., 2005) and WASP-family verprolin-homologous protein 1 (WAVE1) (Figure 2.18 B-D) (Wu et al., 2003), three actin binding proteins that are enriched within lamellipodia.

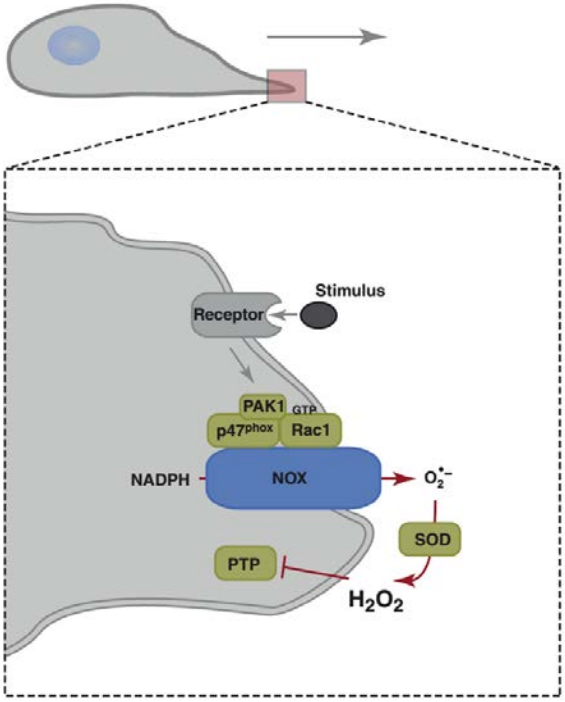

Figure 2.17 Growth factor induced superoxide production by NADPH oxidases (NOX) to promote cell migration. Ligand-activation of receptor tyrosine kinase (RTK) induces the recruitment of activated Rac1, p47phox, PAK1 and other NOX-subunits to the leading edge of the cell, where superoxide ($O_2^{\bullet-}$) is produced. Extracellular superoxide is converted to hydrogen peroxide (H_2O_2) by superoxide dismutase (SOD) and enters the cytoplasm of the cell. Intracellular hydrogen peroxide oxidizes proteins including protein tyrosine phosphatases (PTPs) and thereby promotes cell migration (Hurd et al., 2012).

While it is well established that NOX-generated ROS influences cell migration, the exact signaling involved in these processes is largely unknown. However, several proteins involved in the remodeling of the actin cytoskeleton during cell migration are known to be redox-regulated. Interestingly, actin itself has been shown to be controlled by redox-signaling, as ROS indirectly enhanced G-actin binding to glutathione, which has been demonstrated to decrease its ability to polymerize into F-actin (Dalle-Donne et al., 2003). Indeed, inhibition of ROS in neutrophils decreased actin glutathionylation, leading to increased F-actin formation that resulted in a higher number of pseudopodia and impaired directed cell migration (Figure 2.18 F) (Sakai et al., 2012).

Another protein involved in actin remodeling in lamellipiodia that has been shown to be directly- and indirectly controlled by ROS is cofilin, which harbors actin depolymerizing activity.

Cofilin is activated through de-phosphorylation by the phosphatase Slingshot-1L (SSH-1L). NOX-dependent ROS leads to oxidation of 14-3-3 and auto-dephosphorylation of SSH-1L, causing the disruption of the SSH-1L/14-3-3 complex, and therefore cofilin activation and cell migration (Figure 2.18 A) (Kim et al., 2009; Maheswaranathan et al., 2011). Moreover, direct oxidation of cofilin at two cysteine residues (Cys139 and Cys147) has been shown to decrease binding of cofilin to F-actin, thereby decreasing F-actin severing. Expression of an oxidation-resistant cofilin mutant has been shown to impair cell migration, suggesting that direct oxidation of cofilin at the cell front contributes to directed cell migration by enhancing F-actin stability at the cell leading edge (Cameron et al., 2015).

Furthermore, Rho GTPases have been shown to be sensitive to oxidation. This protein family is known to regulate many processes during cell migration. Ligand-induced activation of the Rac subfamily enhances actin polymerization and promotes lamellipodia formation, while members of the Rho subfamily stimulate cell contractility and adhesion by controlling the assembly of actin stress fibers and focal adhesions (Parri and Chiarugi, 2010). The regulation of these opposing processes needs to be balanced in order to allow directed cell migration. Interestingly, Rac mediated ROS production has been shown to indirectly inhibit RhoA activity. Oxidation of LMW-PTP (low-molecular-weight protein tyrosine phosphatase), resulted in its inhibition causing increased phosphorylation of p190Rho-GAP. This subsequently increased the GAP-mediated hydrolysis of RhoA-bound GTP to GDP, leading to its inactivation and allowing Rac-mediated lamellipodia formation (Nimnual et al., 2003). However, RhoA has also been shown to be regulated through direct oxidation of two cysteine-residues, leading to its activation and increased stress fiber formation (Aghajanian et al., 2009). Thus, redox-signaling is involved in many aspects of Rho GTPase mediated cell migration.

In addition to the role of Rac in the formation of lamellipodia, Rac is also required for the induction of a functional NOX-complex. Interestingly, it has been demonstrated that Rac can act both, upstream and downstream of NOX-dependent ROS production. ROS-induced oxidation of phosphatase and tensin homolog (PTEN) that counteracts the formation of PtdIns(3,4,5)P_3 by PI3Ks, leads to an accumulation of PtdIns(3,4,5)P_3 at the cell leading edge and

subsequently to activation of Rac and directed cell migration (Kuiper et al., 2011). Thus, Rac provides a positive feedback loop that promotes directed cell migration.

Localized and tightly regulated ROS in cellular protrusions has emerged as a signaling molecule, promoting cell migration by regulating proteins involved in cell migration. Future studies are likely to reveal additional redox-regulated proteins, which will lead to a better understanding how ROS controls cell migration.

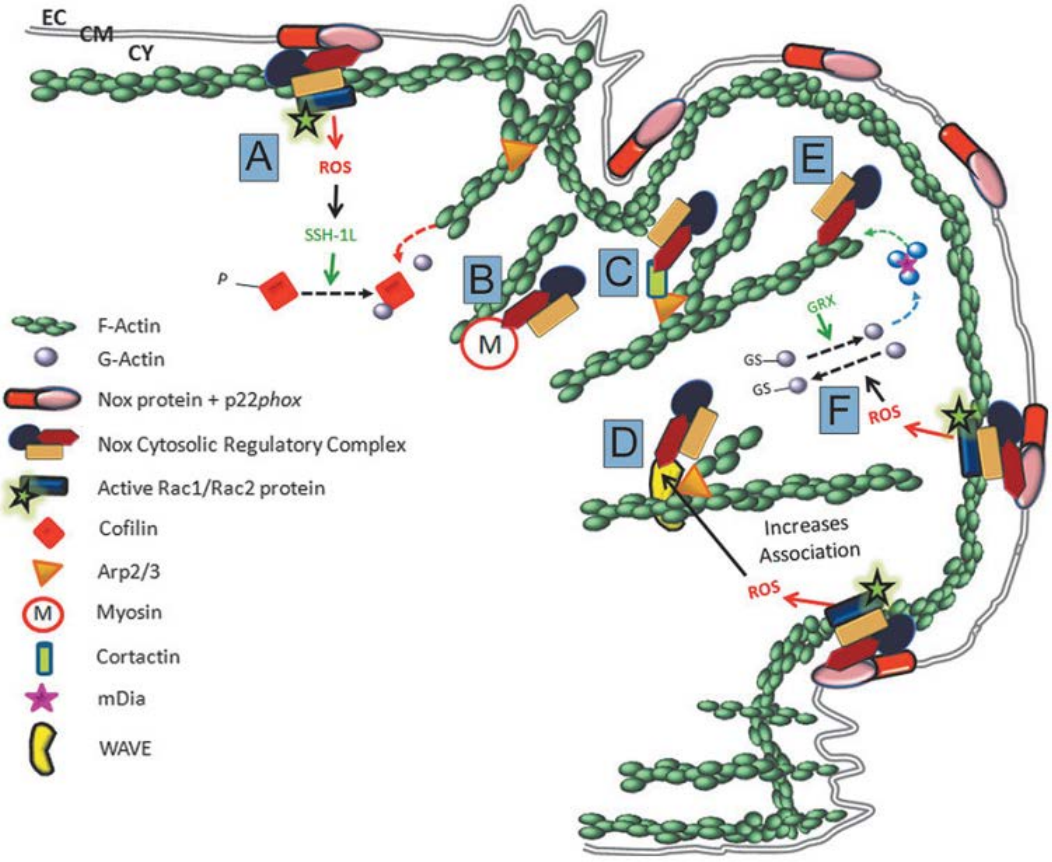

Figure 2.18 Schematic representation of ROS-mediated effects on the cellular actin network during cell migration. Red solid arrows represent NOX-mediated ROS production, black solid arrows show redox regulation, green solid arrows show protein regulation, black dashed arrows show post-translational modifications of proteins, red dashed arrows show actin depolymerization, the blue dashed arrow shows actin nucleation and the green dashed arrow shows actin polymerization. (**A**) NOX-mediated ROS production leads to oxidation of 14-3-3, release of the phosphatase Slingshot-1L (SSH-1L), and dephosphorylation of Cofilin, which leads to activation of its actin depolymerization activity. (**B-E**) p47phox is recruited to the cell membrane probably via its interaction with myosin (**B**), cortactin (**C**), the WASP-family verprolin-homologous protein (WAVE) (**D**) or actin (**E**). (**F**) NOX-dependent ROS increases actin binding to glutathione (GS), thereby decreasing actin polymerization, supporting an ordered migration process. Glutathionylated actin needs to undergo deglutathionylation by glutaredoxin (GRX) (Stanley et al., 2014).

3. Results

3.1 Manuscript: Histone Deacetylase 11 is an Estrogen-Induced Mediator of Breast Cancer Cell Proliferation

Anna Frei,[1,2] Francisca Maurer,[1] Patrice Zeis,[1,2] Nancy E. Hynes, [1,2] Marinus R. Heideman[1]

[1]Friedrich Miescher Institute for Biomedical Research, Maulbeerstrasse 66, CH-4058 Basel, Switzerland

[2]University of Basel, Petersplatz 1, CH-4003 Basel, Switzerland

ABSTRACT

Breast cancer is a heterogeneous disease that affects approximately 1 in 8 women worldwide. Despite improvements in cancer therapy and development of novel therapeutic agents, successful treatment of some breast cancer subtypes remains challenging and resistance often occurs. Therefore, it is important to find new strategies for the treatment of breast cancer patients. The inhibition of histone deacetylases (HDACs), a family of epigenetic regulators, is a promising therapeutic approach in cancer. However, knowledge about the role of individual HDACs in breast cancer is largely missing. We aimed to identify HDACs that are oncogenic in breast cancer and that might be potential targets for breast cancer therapy. Screening HDACs in publicly available databases revealed that HDAC11 is overexpressed in breast cancer. Moreover, we found a correlation between HDAC11 expression and estrogen receptor (ER) levels. By applying a knockdown (KD) approach, we demonstrated that HDAC11 promotes proliferation, in the ER-positive breast cancer cell lines T47D, MCF7 and J110. Furthermore, we identified HDAC11 as an estrogen-induced gene, which regulates a part of the estrogen responsive transcriptional program. In addition, Kaplan-Meier analysis revealed that high HDAC11 expression correlates with a decreased probability of recurrence-free survival (RFS) and distant metastasis-free survival (DMFS). In summary, we showed that HDAC11 has oncogenic potential in ER-positive breast cancer, and therefore might be a new target for therapy.

INTRODUCTION

Breast cancer is the most diagnosed cancer type in women and the first leading cause of cancer death among women worldwide (Torre et al., 2015). Several drugs are successfully used in the clinic to treat breast cancer patients, including chemotherapeutic agents as well as targeted therapies. One example of targeted therapies commonly used in the clinic, are endocrine agents that target the ER (EBCTCG, 2005). The ER is a transcription factor that is overexpressed in over 70% of breast cancer cases (Zafrani et al., 2000). Moreover, it plays a key role in breast cancer progression as it promotes proliferation and survival of breast cancer cells (Brünner et al., 1989). Upon binding to its ligand, 17-β-estradiol (E2), the ER dimerizes and translocates to the nucleus where it controls the expression of a large set of genes (Frasor et al., 2003; Kumar and Chambon, 1988). For example, it induces the expression of several pro-proliferative genes such as *MYC*, *CCND1* and *CDK1* (Frasor et al., 2003). Interestingly, besides acting as a transcriptional activator, studies have shown that the ER can also act as a transcriptional repressor (Carroll et al., 2006; Dutertre et al., 2010; Frasor et al., 2003). Targeting the ER by endocrine therapy has turned out to be a very efficient strategy to treat ER-positive breast cancer patients. For instance, inhibitors targeting aromatase, an enzyme responsible for the synthesis of estrogen, are successfully used for the treatment of postmenopausal women, while tamoxifen that directly binds to the ER and prevents binding of its natural ligand, is the standard therapy for premenopausal women. However, resistance towards these agents often occurs (Johnston, 2010). Therefore, it is important to gain better insight into the molecular mechanisms involved in cancer development, as well as in the occurrence of resistance, as this might lead to novel therapeutic approaches.

Numerous studies have described that epigenetic modifiers play important roles in breast cancer (Huang et al., 2011). Histone deacetylases (HDACs) are a family of epigenetic modifiers that de-acetylate lysine residues in histones, which results in a more compact chromatin structure, rendering the DNA less accessible for transcription factors. Thus, HDACs are generally associated with transcriptional repression (Grunstein, 1997). Furthermore, HDACs can also de-acetylate non-histone proteins, thereby affecting major cellular processes (Choudhary et al., 2009). HDACs are classified based on their homology to yeast proteins and their subcellular

localization. Class I HDACs (HDAC1, -2, -3 and -8) are highly homologous to the yeast HDAC Rpd3 and are primarily localized in the nucleus. Class II HDACs are homologous to yeast protein Hda1 and are further divided in class IIa HDACs (HDAC4, -5, -7 and -9) that can shuttle between the nucleus and cytoplasm, and class IIb HDACs (HDAC6 and -10) that are mainly localized in the nucleus. HDAC11, the most recently identified HDAC, is the sole member of the class IV HDACs, based on homology to both class I and class II, and is mainly found in the nucleus (Gregoretti et al., 2004; de Ruijter et al., 2003). It has been demonstrated, that HDAC11 harbors de-acetylation-activity and can target histone and non-histone proteins (Gao et al., 2002; Glozak and Seto, 2009). Moreover, a recent study revealed that HDAC11 mediates the balance between T-cell activation versus T-cell tolerance through repression of *il-10* (Villagra et al., 2009). Furthermore, several publications have linked HDAC11 to proliferation. HDAC11 KD-studies in oligodendrocytes and several human cancer cell lines demonstrated that HDAC11 promotes proliferation. (Deubzer et al., 2013; Liu et al., 2009). Interestingly, others have reported that HDAC11 is a negative regulator of proliferation in cancer- and non-transformed cells (Bagui et al., 2013; Wong et al., 2014).

Overexpression and aberrant recruitment of HDACs has been found in different types of cancer (Gelmetti et al., 1998; Weichert, 2009). As inhibition of HDACs can drive the re-expression of silenced genes, including tumor suppressors, HDAC-inhibitors (HDACi) are promising drugs for cancer therapy (Cooper et al., 2012; Feng et al., 2007). Therefore, many clinical trials using HDACi as single therapy or in combination with other drugs have been initiated (Mottamal et al., 2015). These trials revealed that HDACi are potent drugs for treating several hematopoietic malignancies. For example, the HDACi vorinostat and romidepsin are FDA-approved and have been successfully used for treating patients with cutaneous T-cell lymphoma (Mann et al., 2007; Mottamal et al., 2015). Unfortunately, targeting solid tumors with HDACi revealed in general no significant responses (West and Johnstone, 2014). However, combinations of HDACi with other therapies has occasionally been shown to yield responses in patients with solid tumors. For example, treating patients with metastatic endocrine-therapy resistant breast cancer, with a combination of the HDACi entinsostat and the aromatase inhibitor exemestane showed a significant clinical response (Yardley et al., 2013).

An important reason for the limited successes of HDACi-based therapies is their generally non-specific nature. Most of these inhibitors target many HDACs, which might lead to opposing activities and unwanted side effects (Mottamal et al., 2015). In order to improve HDACi-based cancer therapy, it is therefore crucial to gain more knowledge about specific HDACs in the context of specific cancers. It is especially important to learn which HDACs are oncogenic and should be targeted. This knowledge could be used as a rationale to develop more specific HDACi and to choose the best available HDACi for the treatment of a specific cancer type.

In our study, we aimed to identify HDACs that are oncogenic in breast cancer. Screening HDACs in publicly available databases revealed that HDAC11 is overexpressed in breast cancer. Moreover, we found a correlation between HDAC11 expression and ER levels. By applying a knockdown (KD) approach, we demonstrate that HDAC11 promotes proliferation, specifically in ER-positive breast cancer cells. In addition, we identified HDAC11 as an estrogen-induced gene, which regulates a part of the estrogen responsive transcriptional program.

RESULTS

Overexpression of HDAC11 in Breast Cancer

To identify HDACs that have oncogenic potential in breast cancer, we examined HDAC mRNA levels in cancer cell lines and breast tumors using publicly available databases. Interestingly, a comparison of HDAC11 transcript level, between collections of cancer cell lines from different origin (Barretina et al., 2012), revealed that HDAC11 mRNA shows significantly higher expression in breast cancer cell lines, compared to all other cancer types (Figure 3.1 A). A similar comparison for HDAC1-10 did not show any significant increase in breast cancer cell lines (data not shown). Moreover, when we analyzed HDAC1-11 expression specifically in breast cancer subtypes, we observed a clear accumulation of tumors that express high levels of HDAC11. In contrast, we did not observe such a specific accumulation in breast cancer subtypes for any of the other tested HDACs (Figure 3.1 B). Previous findings by others demonstrated that HDAC11 mRNA expression in normal breast is marginal (Gao et al., 2002), suggesting that overexpression of HDAC11 might play a role in breast tumorigenesis. In agreement, a comparison between HDAC11 transcript levels in normal human mammary gland and different groups of human breast tumor samples showed significant elevation of the HDAC11 transcript in breast tumor samples (Figure 3.1 C). In addition, analysis of mutations in HDAC11 shows that the majority of HDAC11 alterations involve amplification (Figure 3.1 D), providing a potential mechanism for the elevation of HDAC11 mRNA expression in breast cancer. As overexpression of several HDACs was demonstrated to be tumor promoting in many malignancies (Hayashi et al., 2010; Marquard et al., 2008; Tang et al., 2013; Weichert, 2009), we hypothesized that HDAC11 overexpression in breast cancer has oncogenic potential.

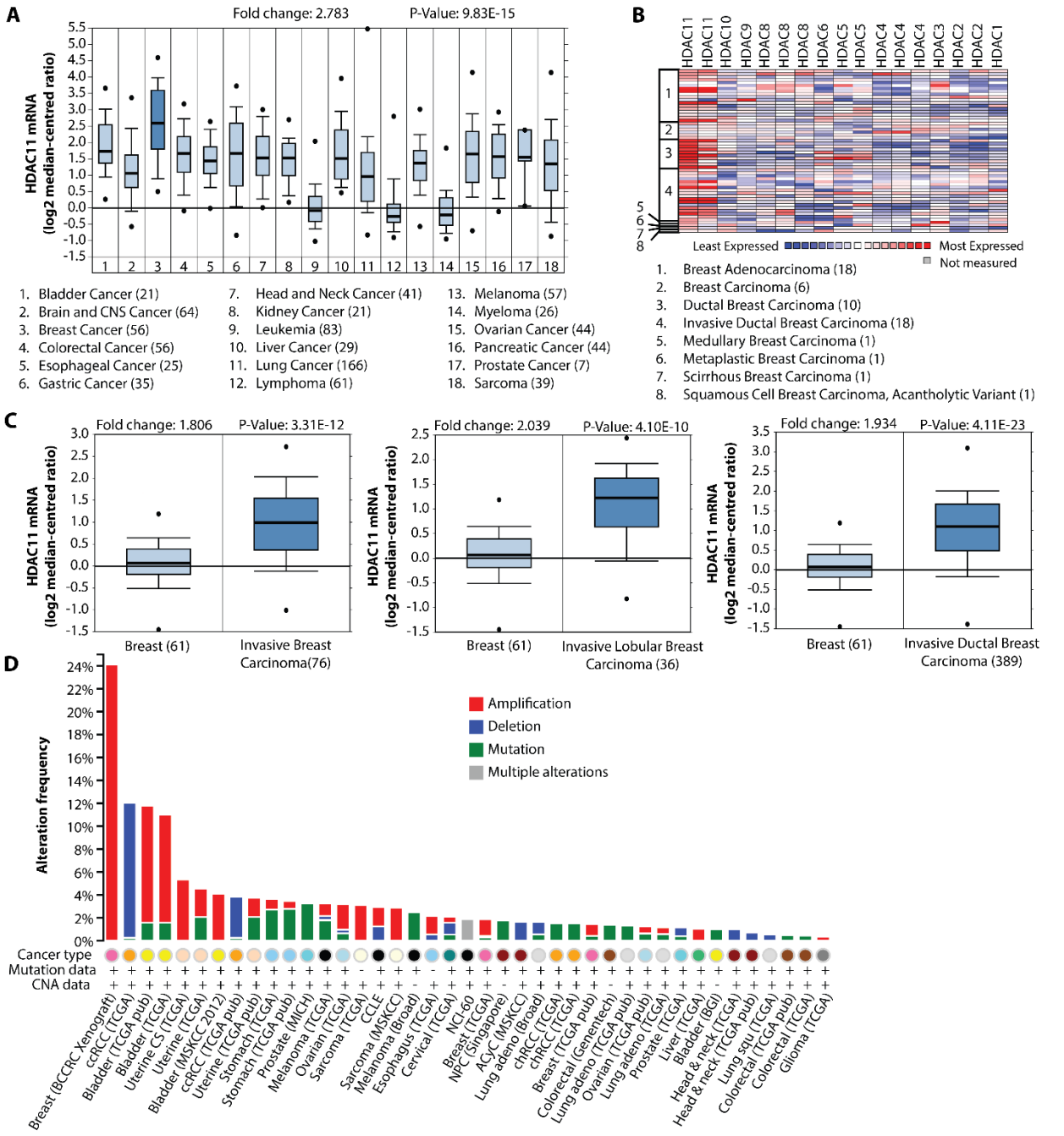

Figure 3.1 HDAC11 is overexpressed in Breast Cancer. (**A** and **B**) Expression levels of several HDACs were analyzed across different cancer cell lines in the Barretina CellLine dataset (Barretina et al., 2012) using the microarray database Oncomine. (**A**) Box plots showing HDAC11 mRNA expression (y-axis) in collections of different cancer cell lines (x-axis). (**B**) Section of the heat map from the Barretina Cell Line dataset, showing the expression profile of several HDACs (x-axis) in breast cancer cell lines (y-axis). Note: Colors are z-score normalized to depict relative values within columns. Levels between different HDACs cannot be compared. (**C**) Box plots generated in Oncomine using datasets of different breast cancer types and normal breast from the breast cancer dataset of The Cancer Genome Atlas (TCGA). Normal breast tissue samples and different types of breast cancer samples (x-axis) are plotted against the level of HDAC11 mRNA expression (y-axis). (**D**) Cross-cancer summary of genomic alterations in HDAC11 for "All Cancer Studies" in the cBioPortal for Cancer Genomics.

HDAC11 promotes Proliferation of ER-Positive Breast Cancer Cells

Several members of the HDAC family have been shown to positively regulate cell proliferation and survival in normal- and cancer cells (Reichert et al., 2012). For example, HDAC1 and HDAC2, have been shown to control cell cycle progression by regulating transition from the G1 to S phase in fibroblasts (Wilting et al., 2010).

To examine a possible role for HDAC11 in breast cancer cell proliferation and/or survival, we applied a knockdown approach. Therefore, we generated stable HDAC11 knockdown (KD) in ER-positive (T47D and MCF7) (Figure 3.2 A - D), and ER-negative (MDA-MB-231 and SUM159) (Figure 3.3 A and C) breast cancer cell lines. To exclude off target effects we used three different shRNAs targeting HDAC11. In addition, to control our experiments we used an empty vector (ev) and a non-targeted shRNA (shNT). KD efficiencies were tested by qPCR (Figure 3.2 A and C, Figure 3.3 A and C) and by western blot analysis (Figure 3.2 B and D), revealing KD of HDAC11 in all four breast cancer models ranging from 60-90%. To investigate the effect of HDAC11 KD on proliferation we generated growth curves, comparing cell growth between KD and control cells in time. While no consistent differences in proliferation were observed in the tested ER-negative breast cancer cell lines (Figure 3.3 B and D), we observed a consistent decrease in proliferation, in ER-positive HDAC11 KD lines (Figure 3.2 E and F). In agreement, when testing clonogenic potential, only in the ER-positive cell lines did we observe a significant reduction in both colony number and size (Figure 3.2 G and H, Figure 3.3 E and F). These findings can be the result of either a proliferation- and/or a survival defect in HDAC11 KD cells. To investigate survival we measured apoptosis performing YoPro assays, which revealed no increase in apoptosis in HDAC11 KD cells (Figure 3.2 I and J). This finding suggests that decreased cell growth in HDAC11 KD cells is caused by defective proliferation. In conclusion, our data reveal that HDAC11 promotes proliferation in ER-positive breast cancer cells.

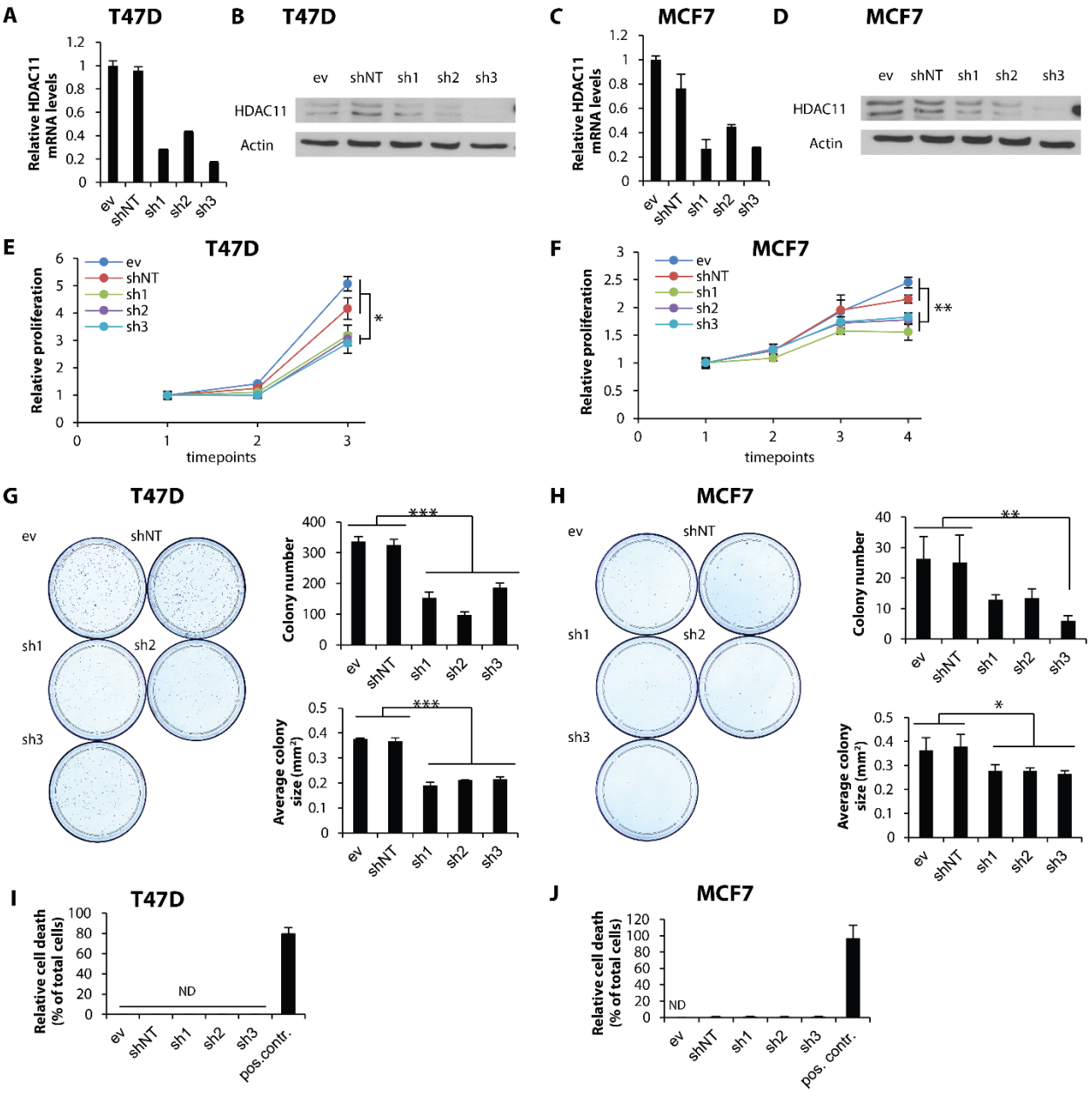

Figure 3.2 HDAC11 promotes Proliferation of ER-positive Breast Cancer Cells. (**A** and **C**) Relative HDAC11 mRNA expression levels in T47D and MCF7 cells, that stably express shRNAs against HDAC11, were measured by qPCR. (**B** and **D**) Western blot analysis of HDAC11 levels. (**E** and **F**) Proliferation assay showing relative proliferation of control and HDAC11 KD lines at different timepoints normalized to day 1 after seeding. Experiment was performed in triplicates. Error bars represent stdev. *p<0.05, **<0.01 by t-test. (**G** and **H**) Colony assay of T47D and MCF7 control and HDAC11 KD cells. Cells were seeded at low density and colonies stained with crystal violet after 1 week of culturing. Left panel: Representative pictures of colony assay. Right panel: Colony numbers were quantified and the average colony size was calculated. Experiment was performed in triplicates. Error bars represent stdev. *p< 0.05, **p< 0.01, ***p< 0.001 by t-test. (**I** and **J**) Apoptosis of control and HDAC11 KD cells was detected with the YoPro assay and plotted in percentage to total cells. As a positive control, cells were treated with 50µM Camptothecin in DMSO for 30min to induce apoptosis. Experiment was performed in quadruplicates.

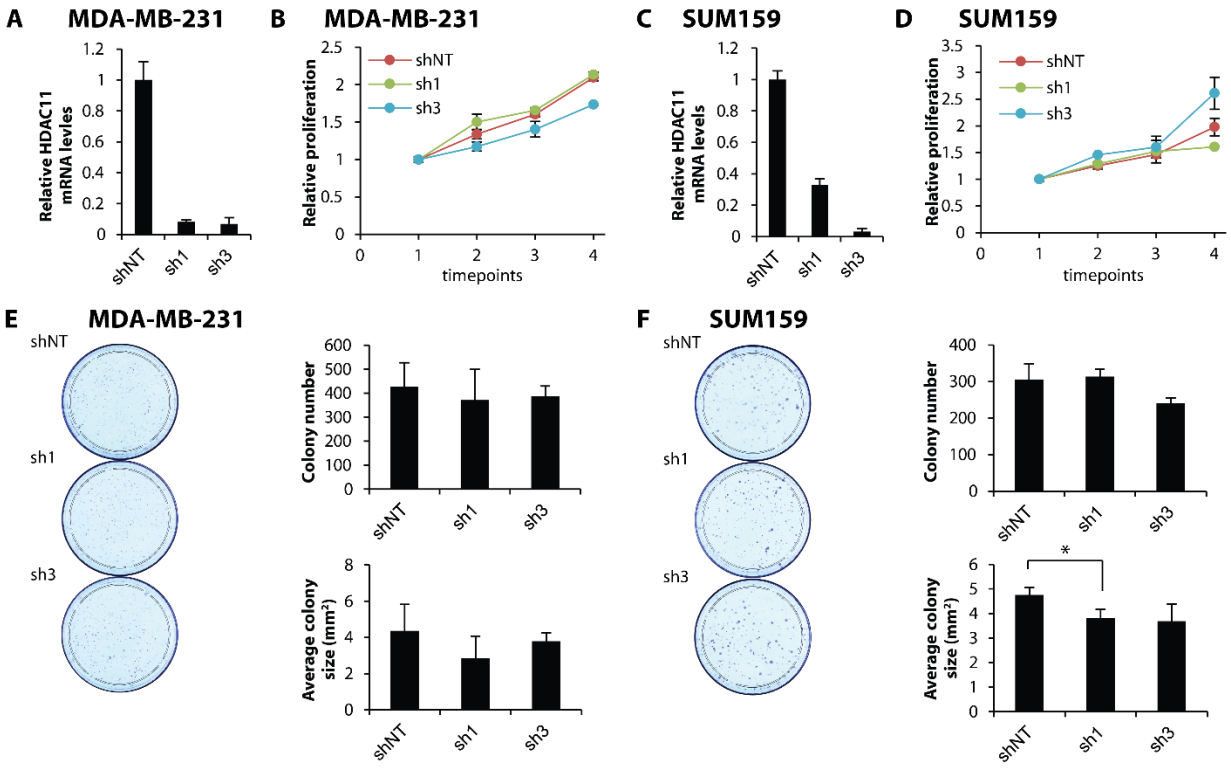

Figure 3.3 HDAC11 has no mayor effect on Proliferation of ER-negative Breast Cancer Cells. (**A** and **C**) Relative HDAC11 mRNA expression levels were measured by qPCR in MDA-MB-231 and SUM159 cells that stably express shRNAs against HDAC11. (**B** and **D**) Proliferation assay showing relative proliferation of control and HDAC11 KD lines at different timepoints, normalized to day 1 after seeding. Experiment was performed in triplicates. (**E** and **F**) Colony assay of MDA-MB-231 and SUM159 control and HDAC11 KD cells. Cells were seeded at low density and colonies stained with crystal violet after 1 week of culturing. Left panel: Representative pictures of colony assay. Right panel: Colony numbers were quantified and the average colony size was calculated. Experiment was performed in triplicates. Error bars represent stdev. *p< 0.05 by t-test.

Knockdown of HDAC11 reduces Tumor Growth *in vivo*

To investigate, whether HDAC11 affects tumor growth *in vivo*, we performed allografts using an ER-positive murine mammary cancer cell line (J110) (Torres-Arzayus et al., 2010). We generated HDAC11 KD cells using two hairpins targeting the mouse homologue of HDAC11 (Figure 3.4 A). As KD of HDAC11 in J110 recapitulated the results obtained with human ER-positive cancer cell lines (Figure 3.4 B and C), we used this cell line to assess the effect of HDAC11 KD on tumor growth *in vivo*.

HDAC11 knockdown cells, injected in the mammary fat pad of mice, showed a significant reduction in tumor growth compared to control tumors and a reduction in tumor weight at the end of the experiment (Figure 3.4 D and E). To examine if HDAC11 KD was stable throughout the experiment, we performed qPCR using RNA isolated from tumors. This analysis revealed lower HDAC11 expression in KD tumors, indicating that HDAC11 KD was stable (Figure 3.4 F). In summary, our data suggest that HDAC11 promotes proliferation both *in vivo* and *in vitro* in ER-positive breast cancer cell lines. As it has been shown that estrogen signaling controls proliferation in ER-positive breast cancer cells (Brünner et al., 1989) our findings suggest a possible link between HDAC11 and estrogen signaling.

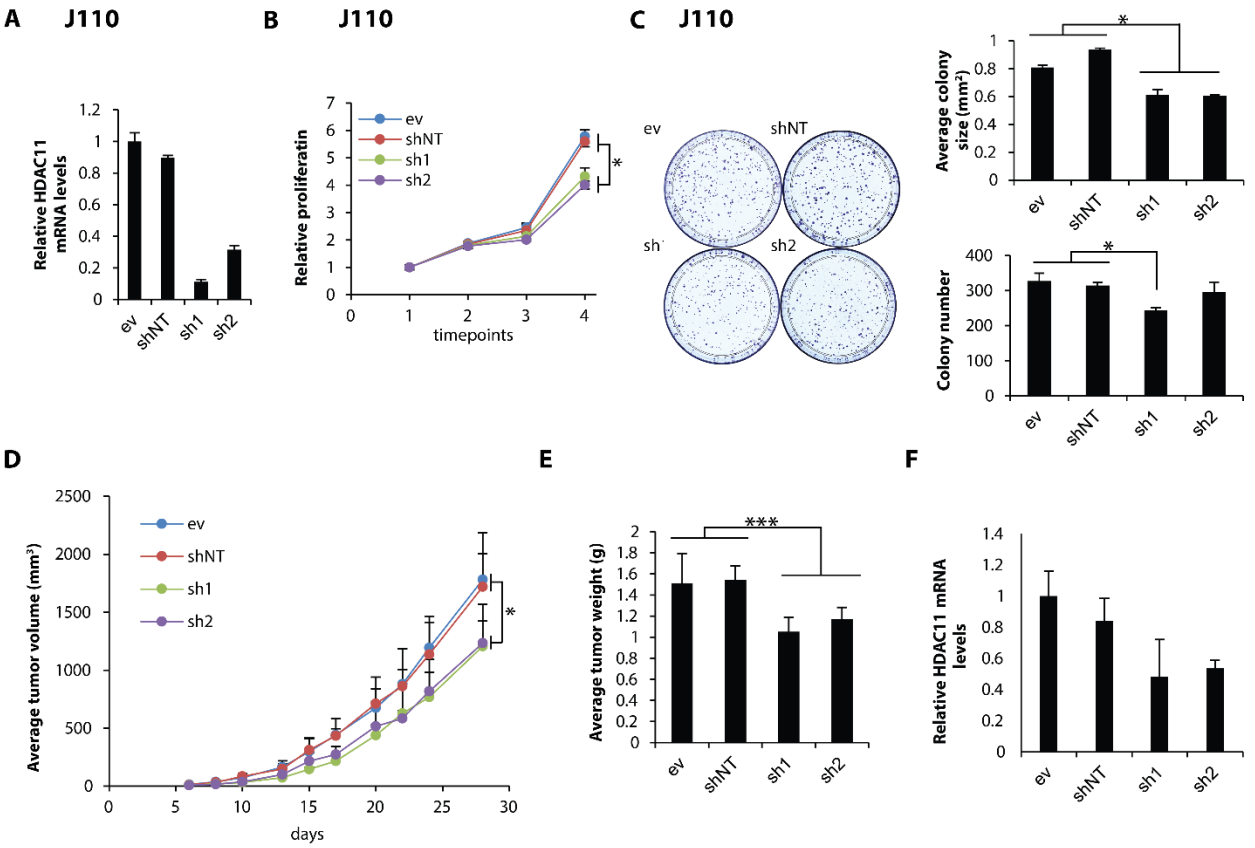

Figure 3.4 Knockdown of HDAC11 Reduces Tumor Growth *in vivo*. (**A**) qPCR analysis of HDAC11 mRNA levels in the ER-positive murine breast cancer cell line J110. (**B**) Proliferation assay showing relative proliferation of control and HDAC11 KD cells at different timepoints normalized to day 1 after seeding. Experiment was performed in triplicates. Error bars represent stdev. *p< 0.05, by t-test (**C**) Colony assay of J110 control and HDAC11 KD cells. Cells were seeded at low density and colonies stained with crystal violet after 1 week of culturing. Left panel: Representative pictures of colony assay. Right panel: Colony numbers were quantified and the average colony size was calculated. Experiment was performed in triplicates. Error bars represent stdev. *p< 0.05 by t-test. (**D**) Orthotopic tumor growth of J110 control and HDAC11 KD cells in mice. Curves show the mean tumor volumes (n= 5-6 mice per group). Error bars represent stdev. *p< 0.05, by t-test. (**E**) Tumor weight measured at the end of the experiment. Error bars represent stdev. ***p< 0.001 by t-test. (**F**) qPCR analysis of HDAC11 mRNA levels of tumor lysates (n= 2-3 tumor lysates).

HDAC11 Expression Correlates with ER Levels

To investigate a possible link between HDAC11 and ER signaling, we analyzed the correlation between HDAC11- and ER-expression using several publicly available datasets. Meta-analysis of 25 independent gene expression datasets comparing ER-negative versus ER-positive breast cancer revealed a significant association between *ESR1* (encoding ER) and *HDAC11* mRNA

expression (Figure 3.5 A). Furthermore, using the van't Veer breast dataset (van't Veer et al., 2002), which includes gene expression data and ER protein level of 117 breast carcinoma samples, we found a clear correlation between ER protein level and *HDAC11* mRNA expression (Figure 3.5 B). We could verify this result using the TCGA Breast Invasive Carcinoma dataset, which contains gene- and protein expression data of 1104 breast cancer samples (Figure 3.5 C). In summary, these findings suggest a link between estrogen signaling and HDAC11 expression in breast cancer.

To investigate a potential link between ER and HDAC11, we grew T47D and MCF7 cells in steroid-deprived conditions and subsequently stimulated these cells with the ER ligand 17-β-estradiol (E2). Comparing *HDAC11* mRNA levels of stimulated versus steroid-deprived cells, revealed a significant up-regulation of *HDAC11* mRNA upon E2 stimulation for both cell types (Figure 3.5 D). Conversely, inhibition of ER with the selective estrogen receptor modulator (SERM) 4-hydroxytamoxifen (TAM) or the selective estrogen receptor down-regulator (SERD) fulvestrant (Fulv) decreased *HDAC11* mRNA levels in a dose-dependent manner in MCF7 cells, as well as in T47D cells in response to Fulv (Figure 3.5 E).

Previous studies have shown that the ER can directly bind to estrogen induced genes (Kumar and Chambon, 1988), suggesting that *HDAC11* might be a direct target of the ER. Indeed, a genome-wide ER binding-profile performed by the Brown lab (Carroll et al., 2006), revealed that *HDAC11* has ER binding sites within the gene and in close proximity (Figure 3.5 F). In conclusion, we demonstrated that HDAC11 expression is induced by ER signaling and findings by others suggest *HDAC11* as a direct target of the ER.

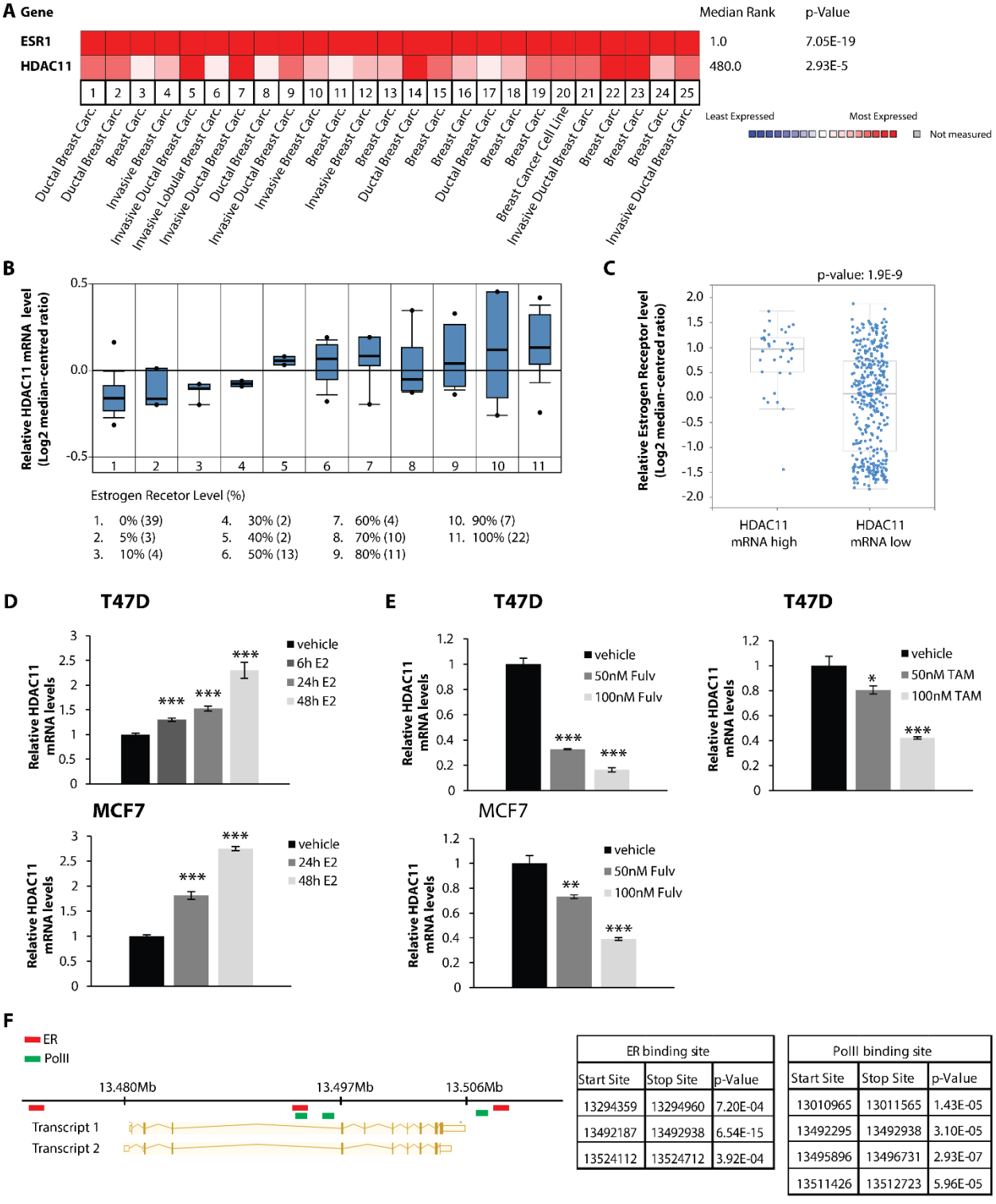

ER binding site		
Start Site	Stop Site	p-Value
13294359	13294960	7.20E-04
13492187	13492938	6.54E-15
13524112	13524712	3.92E-04

PolII binding site		
Start Site	Stop Site	p-Value
13010965	13011565	1.43E-05
13492295	13492938	3.10E-05
13495896	13496731	2.93E-07
13511426	13512723	5.96E-05

Figure 3.5 HDAC11 Expression Correlates with ER Levels. (**A**) Meta-analysis of 25 independent gene expression datasets comparing HDAC11 expression in ER-negative versus ER-positive breast carcinoma (carc.). Analysis was performed with Oncomine using studies from [1] Bittner, Not Published, 2005; [2] (Boersma et al., 2008); [3] (Chin et al., 2006); [4-6] (Curtis et al., 2012); [7] (Desmedt et al., 2007); [8] (Esserman et al., 2012); [9] (Ginestier et al., 2006); [10] (Glück et al., 2012), [11] (Gruvberger et al., 2001); [12] (Hatzis et al., 2011); [13] (Ivshina et al., 2006); [14] (Julka

et al., 2008); [15] (Kao et al., 2011); [16] (Korde et al., 2010); [17] (Lu et al., 2009); [18] (Minn et al., 2005); [19] (Miyake et al., 2012); [20] (Neve et al., 2006); [21] TCGA 2011 [http://cancergenome.nih.gov/.]; [22] (Marc J. Van De V Ijver, 2002); [23] (Waddell et al., 2010); [24] (Wang et al., 2005); [25] (Zhao et al., 2004). The rank for a gene is the median rank for that gene across each of the analyses. The p-value for a gene is its p-value for the median-ranked analysis. (**B**) Box plots generated in Oncomine using the Van't Veer breast cancer dataset showing ER expression levels (0-100%) (x-axis) against *HDAC11* mRNA expression levels (y-axis). (**C**) Analysis of the dataset Breast Invasive Carcinoma (TCGA, Provisional) using cBioportal. The dataset includes 1104 cases of breast cancer patients. Box plots showing breast cancer samples expressing high (expression >1.5) and low (expression <1.5) *HDAC11* mRNA expression (x-axis) against ER protein levels (y-axis) measured by Reverse Phase Protein Array (RPPA). (**D**) Q-PCR analysis of HDAC11 mRNA levels of T47D (upper panel) and MCF7 (lower panel) grown for 3 days in steroid-deprived medium and subsequently stimulated with 50nM E2 for different time points. HDAC11 levels were normalized to vehicle treated cells. Error bars represent stdev. ***p< 0.001 by t-test. (**E**) Relative *HDAC11* mRNA levels of T47D (upper panel) and MCF7 (lower panel) treated with vehicle or indicated doses of Fulv or TAM for 2 days. HDAC11 levels were normalized to vehicle treated cells. Error bars represent stdev. *p< 0.05, **p< 0.01, ***p< 0.001 by t-test. (**F**) Schematic representation of *HDAC11* transcript 1 and 2 modified from Ensembl [www.ensembl.org], with ER- and PolII-binding sites on chromosome 3 as described by the Brown lab (Carroll et al., 2006). Tables are showing start- and stop-site on chromosome 3 for ER- and PolII-binding with corresponding p-values. Data was generated by ChIP-on-chip experiments.

HDAC11 KD does not affect Protein Levels of other HDACs.

Several HDACs have been shown to be functionally redundant in promoting proliferation. For example, knocking-out either HDAC1 or HDAC2 leads to functional compensation by the other HDAC in heart-, skin- and B cells (LeBoeuf et al., 2010; Montgomery et al., 2007; Yamaguchi et al., 2010). Thus, we tested the possibility that HDAC11 affects proliferation in ER-positive breast cancer cells, by stimulating expression of other HDACs. For this, we carried out western blot analysis of several class I HDACs and the class II HDAC6, which has been shown to interact with HDAC11 (Cheng et al., 2014; Gao et al., 2002). This analysis revealed no changes in protein level for these HDACs in HDAC11 KD cells (Figure 3.6 A and B). Therefore, we exclude the possibility that HDAC11 mediates proliferation by interplay with these HDACs.

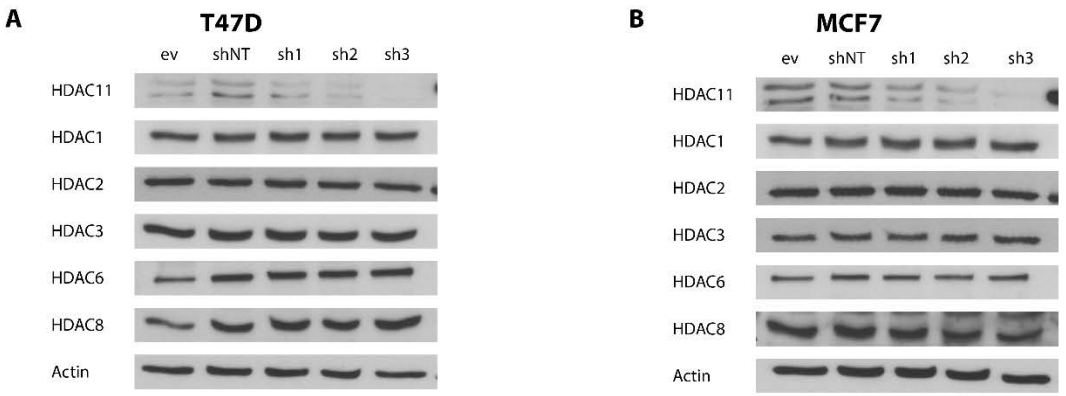

Figure 3.6 HDAC11 KD does not affect Protein Levels of other HDACs. (A and B) Western blot analysis of several HDACs in HDAC11 KD and control T47D and MCF7 lysates.

HDAC11 controls ER Levels

The ER is a transcription factor that induces genes that promote proliferation, like *MYC*, *CCND1*, *GREB1* and others (Dubik and Shiu, 1988; Rae et al., 2005; Shiozawa et al., 2004) Therefore, another mechanism by which HDAC11 might promote proliferation is by directly controlling ER activity and/or levels. Thus, we first analyzed ER protein levels in HDAC11 KD cells, revealing that they were reduced compared to control cells (Figure 3.7 A and B). Moreover, a qPCR analysis revealed decreased *ESR1* mRNA levels in HDAC11 KD cells (Figure 3.7 C and D). Suggesting, that HDAC11 controls ER expression at the transcriptional level. As HDAC11 is described as both a repressor and inducer of transcription (Liu et al., 2009; Villagra et al., 2009), the observed decrease in *ESR1* mRNA might be caused by a direct or indirect effect.

Phosphorylation of ER has been shown to modulate its transcriptional activity. For example it has been described that phosphorylation of residues Serine 118 and 167 affect transcriptional activity of ER either ligand-dependent and/or –independent (Ali et al., 1993; Bunone et al., 1996; Sun et al., 2001). We analyzed ER phosphorylation at these residues by western blot. This analysis showed no changes in phosphorylation levels upon HDAC11 KD (Figure 3.7 E).

Subsequently we took a direct approach to measure ER transcriptional activity. We performed reporter assays using an ER-inducible luciferase construct, which includes several ER-binding sites (EREs) preceding a luciferase gene. As a negative-control we used a non-inducible luciferase construct, lacking ERE-sites. This experiment did not show consistent differences in

luciferase-signal between HDAC11 KD and controls in both MCF7 and T47D cells (Figure 3.7 F and G). In summary, our findings demonstrate that HDAC11 positively regulates ER levels. However, it does not affect the phosphorylation status or the transcriptional activity of the ER. Hence, it is unlikely that HDAC11 promotes proliferation by directly controlling ER-activity.

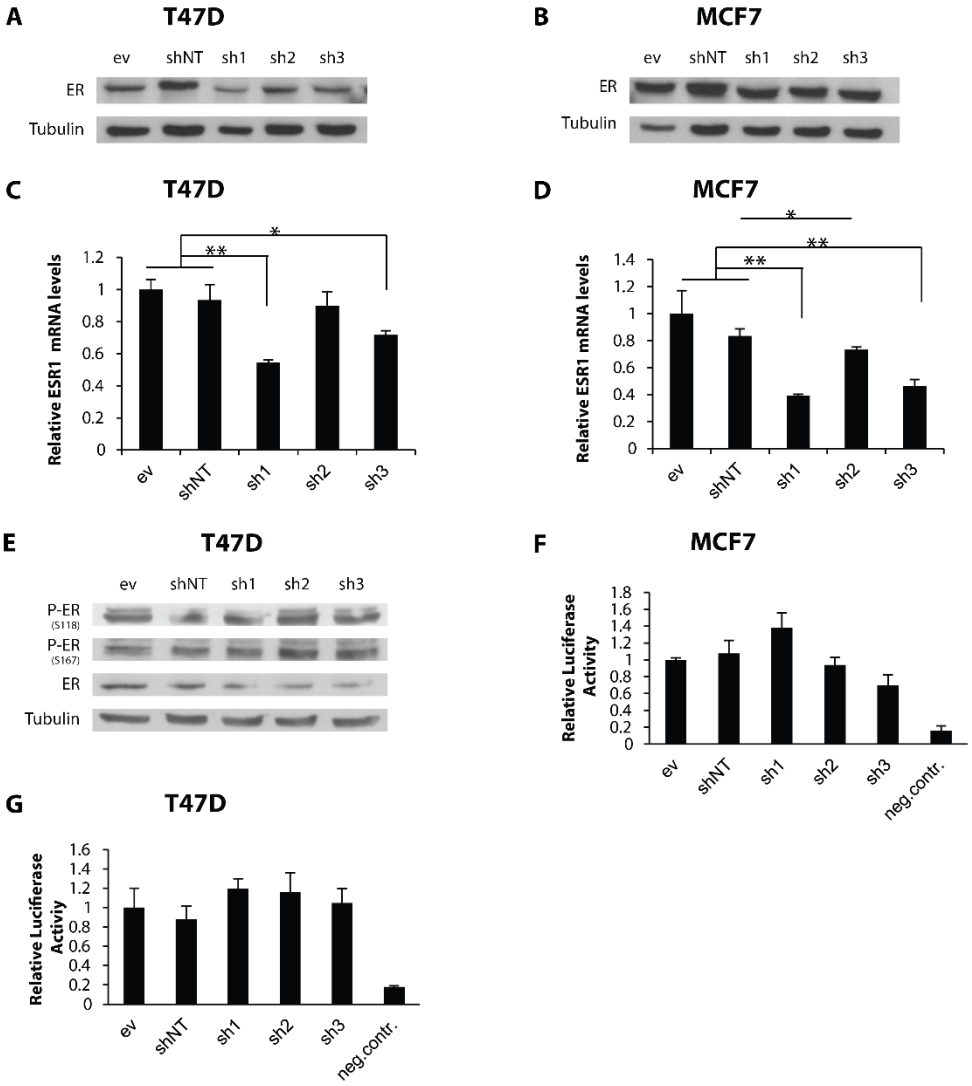

Figure 3.7 HDAC11 controls ER Protein Level. (A and B) Western blot analysis of ER levels in HDAC11 KD and control T47D and MCF7 lysates. (C and D) Relative *ESR1* mRNA expression levels in T47D and MCF7 cells, that stably express shRNAs against HDAC11, were measured by qPCR. Expression levels were normalized to ev control cells. Error bars represent stdev. *p< 0.05, **p<0.01 by t-test. (E) Western blot analysis of ER-phosphorylation in HDAC11 KD and control T47D lysates. (F and G) T47D and MCF7 cells were transfected with an ER-inducible luciferase reporter construct. ER transcriptional activity was measured by luciferase assay and normalized to Renilla-luciferase activity. As a negative control, cells were transfected with a non-inducible luciferase construct.

HDAC11 KD does not Affect Global Histone-Acetylation but Deregulates a Subgroup of Genes

Most HDACs act as transcriptional repressors by de-acetylation of histones (Thiagalingam et al., 2003), and HDAC11 has also been shown to harbor histone de-acetylation activity (Gao et al., 2002). For example, HDAC11 has been shown to directly repress expression of *il-10* in antigen presenting cells (Villagra et al., 2009). Knockout (KO) studies have shown that some HDACs, like HDAC1,-2 and -3, affect global histone acetylation (Bhaskara et al., 2010; Yamaguchi et al., 2010). To examine if HDAC11 KD affects global histone acetylation in ER-positive breast cancer cells, we compared histone acetylation between HDAC11 control and KD cells. This analysis revealed no difference in histone acetylation, indicating that HDAC11 is not a global histone-deacetylase (Figure 3.8 A and B).

Another possibility is that HDAC11 controls histone acetylation of a subset of genes in ER-positive breast cancer cells. To identify possible direct and indirect genomic targets of HDAC11, we generated genome wide expression profiles using RNA sequencing (RNAseq). We compared mRNA of three different T47D HDAC11 KD cell lines and control cells harboring either a non-targeted shRNA (shNT) or that were infected with an empty vector (ev). This revealed a modest number of differentially regulated genes, varying from 130-210 genes depending on the comparison. Interestingly, we could clearly observe that the number of up-regulated genes is much higher than the one of down-regulated genes (Figure 3.8 C). As HDAC11 can act as a repressor of transcription, this finding suggests that these genes might be direct targets. Among the highly significant de-regulated genes in all KD cells are genes that are related to estrogen signaling (Figure 3.8 D). For instance, interleukin 1 receptor type I (IL1R1) has been shown to be down-regulated in response to E2 in uterine epithelial cells (Schaefer et al., 2005).

Although HDAC11 does not affect global histone-acetylation, gene-expression profiling revealed that HDAC11 KD deregulates a subset of genes, which includes estrogen responsive genes. These findings suggest, that HDAC11 might affect proliferation downstream of the ER at the level of transcriptional regulation of estrogen responsive genes.

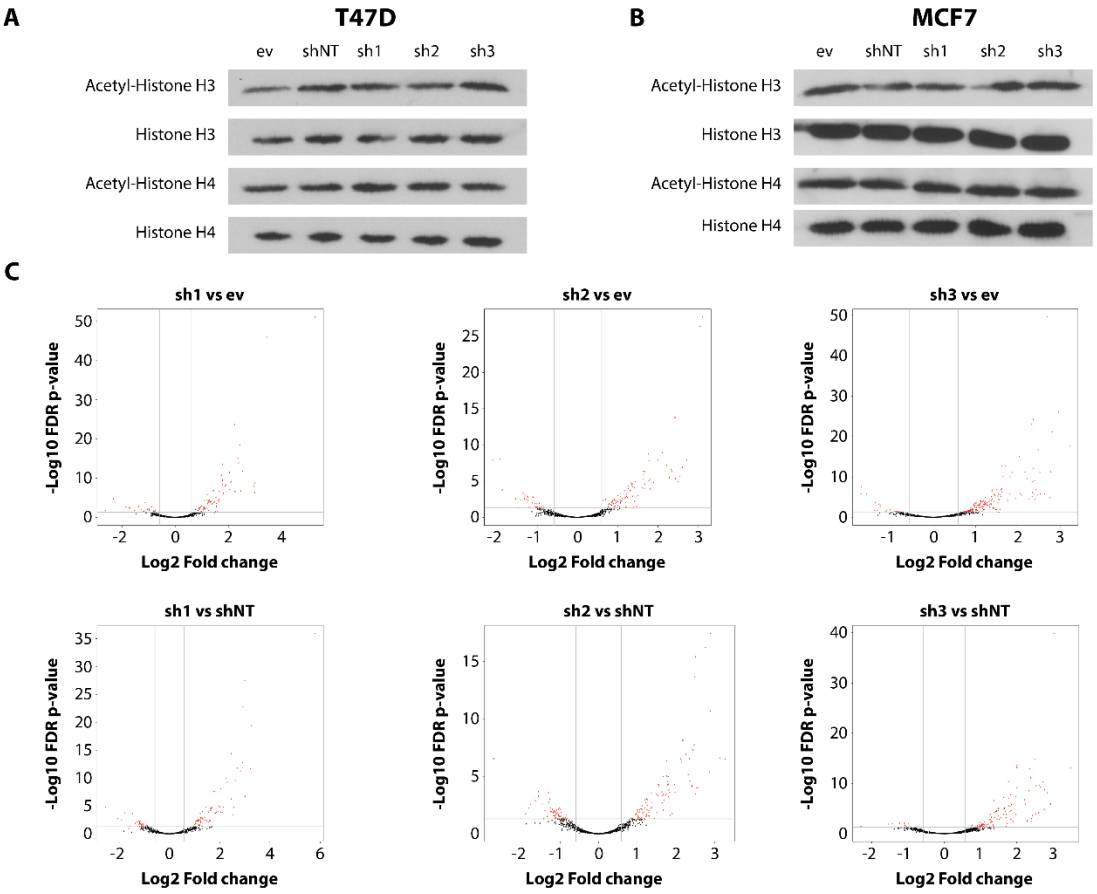

D

	Log2 Fold Change					
upregulated genes	sh1 vs. ev	sh2 vs. ev	sh3 vs. ev	sh1 vs. shNT	sh2 vs. shNT	sh3 vs. shNT
sulfatase 1	1.8	1.3	1.6	2.8	2.3	2.7
distal-less homeobox 1	1.1	0.7	0.7	1.0	0.6	0.6
cytochrome P450, family, subfamily A, polypeptide 1	1.0	2.1	0.9	1.0	2.1	1.0
cytoplasmic FMR1 interacting protein 2	0.8	1.3	1.1	1.4	1.9	1.7
interleukin 1 receptor, type I	0.8	0.7	0.6	1.1	1.1	0.9
2'5'-oligoadenylate synthetase 2, 69/71kDa	0.6	1.4	1.2	0.9	1.7	1.6
albumin	0.5	1.6	1.5	0.9	2.1	1.9
downregulated genes						
HDAC11	-2.1	-1.3	-2.5	-2.4	-1.6	-2.7
family with sequence similarity 178, member B	-0.9	-0.6	-1.1	-1.2	-0.8	-1.3
differentially expressed in FDCP 6 homolog (mouse)	-0.5	-0.6	-0.7	-0.6	-0.7	-0.7

Figure 3.8 HDAC11 KD does not affect global histone-acetylation but deregulates a subgroup of genes. (**A** and **B**) Western blot analysis of acetylation-levels of histone H3 and H4 upon knockdown of HDAC11 in T47D and MCF7 cells. (**C**) Volcano plots of log2 fold-change (x-axis) of gene expression between two genotypes (sh1 vs. ev; sh1 vs. shNT; sh2 vs. ev; sh2 vs. shNT; sh3 vs ev; sh3 vs. shNT) versus $-\log_{10}$FDR p-value (y-axis, representing the probability that the gene is differentially expressed). Expression profiles of T47D HDAC11 KD and control cells were obtained by RNAseq. (**D**) List of genes differentially regulated in all comparisons between HDAC11 KD and controls cells with a Fold change >1.4, p-value <0.05 and FDR<0.15 in the RNAseq experiment. Shown is the Log2 Fold change.

HDAC11 partially controls the Estrogen induced Transcriptional Program

To investigate with an unbiased approach if the estrogen responsive transcriptional program is affected by HDAC11 KD, we performed gene set enrichment analysis (GSEA) (Mootha et al., 2003; Subramanian et al., 2005). In this analysis we projected 3395 gene sets representing expression signatures of genetic and chemical perturbations (CGP: chemical and genetic perturbations) on our RNAseq datasets comparing HDAC11 KD versus control cells. Interestingly, the gene sets "Estradiol_Response_6HR_DN" and "Estradiol_Response_24HR_DN" (Dutertre et al., 2010), which include estrogen responsive genes down-regulated in MCF7 cells at time points 6 and 24 hours after E2 stimulation, were in general significantly enriched among genes that are upregulated in HDAC11 KD cells (Figure 3.9 A and B). Thus, genes which are normally down-regulated upon E2-stimulation, are upregulated in HDAC11 KD cells. In contrast, the gene-sets "Estradiol_Response_6HR_UP" and "Estradiol_Response_24HR_UP", which include genes up-regulated upon estrogen stimulation after 6 or 24 hours respectively, were in general not significantly enriched among genes that are down regulated in HDAC11KD cells (data not shown).

The gene sets, generated by Dutertre, were obtained from MCF7 cells, while our gene expression profile of HDAC11 KD cells was generated using T47D cells. To strengthen our findings, we created similar gene sets, from T47D cells. Therefore, we generated gene expression profiles of T47D cells stimulated with E2 for 8 and 24 hours and compared these expression profiles to vehicle-treated cells (Figure 3.10 A). From these datasets we extracted four gene sets which include 1) up-regulated after 8h E2 stimulation 2) down-regulated after 8h E2 stimulation 3) up-regulated after 24h E2 stimulation 4) down-regulated after 24h E2 stimulation. When projecting these gene sets on the HDAC11 KD versus control datasets, we observed that a significant number of genes that are normally down-regulated upon E2 stimulation, are up-regulated in HDAC11 KD cells (Figure 3.10 B and C). However, the gene set of normally up-regulated genes upon E2 stimulation, were generally not enriched in HDAC11 KD cells (Figure 3.10 D and E). In summary, these findings indicate that especially genes that normally are repressed by estrogen signaling are up-regulated in HDAC11 KD cells, strongly suggesting that HDAC11 might be a direct repressor of these estrogen responsive genes.

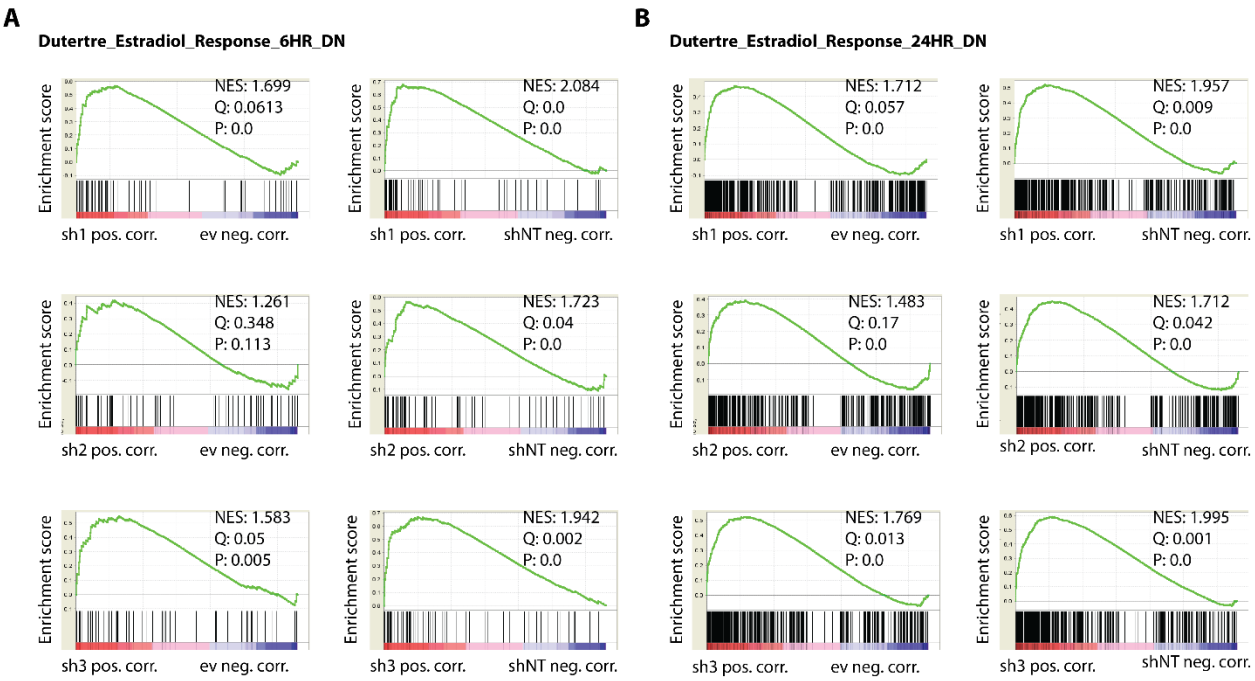

Figure 3.9 Enrichment of Estrogen-induced down-regulated gene sets in HDAC11 KD cells. (**A** and **B**) Enrichment plots generated by GSEA analysis of ranked gene expression data of HDAC11 KD versus control cells. The enrichment score is shown as a scattered green line, and the black bars indicate position of the genes from the gene set. The color-bar shows the gene list used in the GSEA ordered by differential gene expression. Red indicates higher (positively correlated) and blue indicates lower (negatively correlated) signal to noise in HDAC11 KD compared to control lines. Shown are Enrichment Score (ES), Normalized Enrichment Score (NES), Nominal p value (P) and Q-value of False discovery rate (Q). The enrichment for the gene set "Dutertre_Estradiol_Response_6HR_DN" in HDAC11 KD cells is shown in (**A**) and the enrichment for the gene set "Dutertre_Estradiol_Response_24HR_DN" in (**B**).

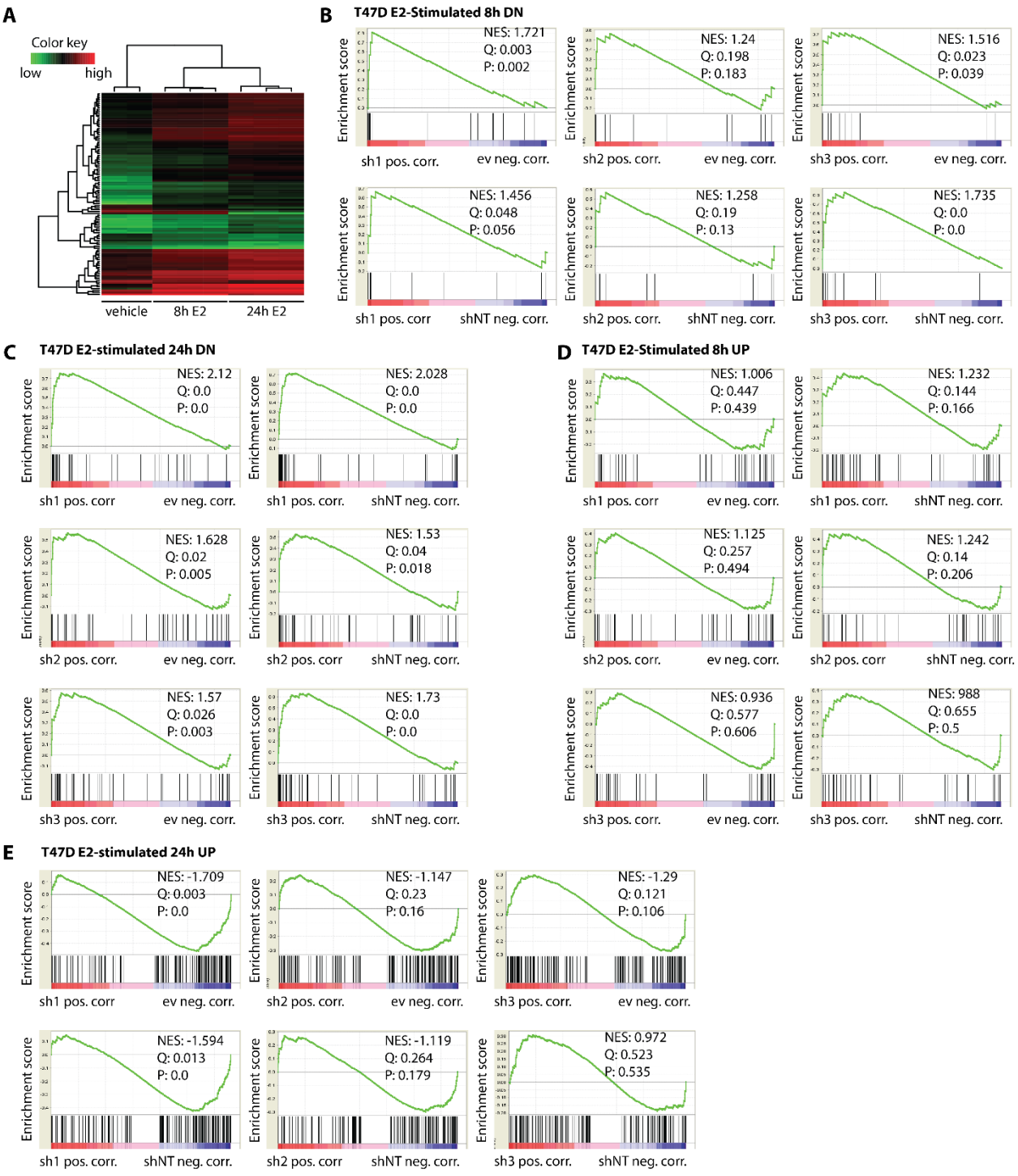

Figure 3.10 HDAC11 controls a subset of the Estrogen induced Transcriptional Program. (A) Heat map from microarray of T47D cells stimulated with vehicle or E2 for 8 or 24 hours, showing clustering of genes up- or down-regulated in response to E2 treatment. Fold change >2, p-value <0.01 (**B-E**) Enrichment plots of ranked gene expression data of HDAC11 KD versus control cells for the gene sets generated from the T47D microarray analysis. Enrichment plots of gene-sets for genes up-regulated after E2-stimulation for 8 (**B**) and 24 hours (**C**) and for genes down-regulated after E2-stimulation for 8 (**D**) and 24 hours (**E**) are shown with respective Normalized Enrichment Scores (NES), P-values (P) and FDR q-values (Q).

HDAC11 levels correlate with worse prognosis

As our findings reveal that HDAC11 is a regulator of proliferation in ER-positive breast cancer cells, we asked if HDAC11 expression level has prognostic value for breast cancer patients. Therefore, we performed several Kaplan-Meier analyses, using the KM-plotter which includes gene expression data of breast tumors and matched clinical data from breast cancer patients (Gyorffy et al., 2013). In this analysis breast cancer patients were split in two groups based on HDAC11 transcript level expression in their tumor samples. Subsequently, the probability of recurrence-free survival (RFS) and distant metastasis-free survival (DMFS) over time between these groups were compared. For our first analysis, we used the complete dataset, consisting of both ER-positive and –negative tumors. This analysis demonstrates that high levels of HDAC11 correlated with an increased probability of RFS and DMFS (Figure 3.11 A and B). These results were expected, as HDAC11 levels positively correlate with ER-expression and ER-positive tumors have in general a better prognosis (Figure 3.11 C). Intriguingly, when we performed a similar analysis, in a subgroup that includes patients with ER-positive, high grade breast tumors, that received endocrine therapy, the probability of RFS and DMFS was worse for the HDAC11-high group (Figure 3.11 D and E). As this group of patients likely includes many patients harboring therapy-resistant tumors, this finding suggest that high levels of HDAC11 might play a role in endocrine therapy resistance. Future and ongoing studies should reveal if HDAC11 has real potential as a drug-target for endocrine resistant breast cancer.

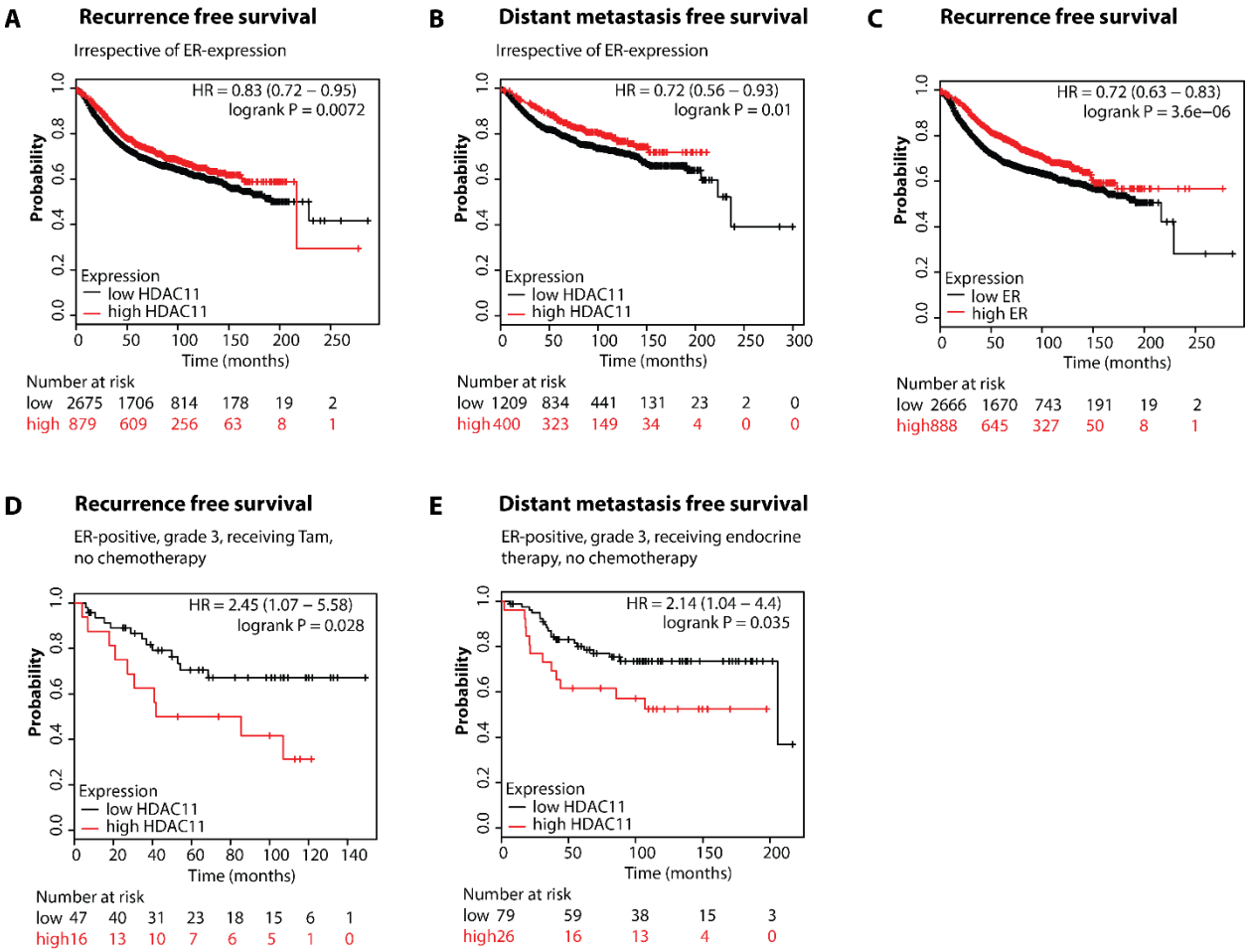

Figure 3.11 HDAC11-expression has prognostic-value for Breast Cancer Patients. Kaplan-Meier plots showing probability for recurrence-free survival (RFS) or distant metastasis-free survival (DMFS) for patients with tumors expressing high HDAC11 or ER (upper quartile) in red, and in black for patients with low HDAC11 or ER levels. Hazard ratio (HR) with 95% confidence intervals and log rank p-value are shown. (**A** and **B**) Kaplan-Meier plots showing probability of RFS and DMFS for patients with tumors expressing high or low levels of HDAC11, irrespective of ER-status. (**C**) Plot showing probability of RFS for patients with tumors expressing high or low levels of ER. (**D**) Plots showing probability of RFS for patients with ER-positive, grade 3 tumors who received tamoxifen but no chemotherapy, expressing high or low levels of HDAC11. (**E**) Plots showing probability of DMFS for patients with ER-positive, grade 3 tumors who received endocrine therapy but no chemotherapy, expressing high or low levels of HDAC11.

DISCUSSION

In this study, we aimed to identify HDACs with oncogenic potential in breast cancer. Screening HDACs in publicly available databases revealed that HDAC11 is overexpressed in breast cancer and that its expression correlates with ER expression levels. HDAC11 KD studies revealed a role for HDAC11 in proliferation, specifically in ER-positive breast cancer cells. In addition, we show that HDAC11 expression is induced by estrogen and that it might be a direct transcriptional target of the ER. Interestingly, genomic and bioinformatics approaches suggest that HDAC11 affects the estrogen responsive transcriptional program, as genes that are downregulated upon estrogen signaling are upregulated in HDAC11 KD cells. Finally, Kaplan-Meier analysis, using a group of patients that received endocrine therapy, revealed that HDAC11 expression has prognostic value, as the probability of RFS and DMFS decreased significantly for patients having tumors with high levels of HDAC11 expression.

Overexpression of HDACs has been shown in several cancer types and has been associated with tumor promotion. For example, overexpression of HDAC1 has been found in breast (Zhang et al., 2005), gastric (Choi et al., 2001) and colon (Ishihama et al., 2007) cancer. In addition, overexpression of HDAC6 has been observed in breast cancer (Zhang et al., 2004) and increased expression levels of HDAC1, HDAC2 and HDAC3 have been reported in prostate cancer (Weichert et al., 2008). Interestingly, our data base screening revealed that HDAC11 is overexpressed in ER-positive breast cancer, suggesting an oncogenic role for HDAC11 in that breast cancer subtype. Overexpression of HDAC11 in cancer cells has been reported in previous studies. In these studies the authors showed that HDAC11 is highly expressed in several cancer cell lines, but only marginal expression was observed in normal tissues, except for brain, testis, kidney, skeletal muscle and heart (Deubzer et al., 2013; Gao et al., 2002). For most cases it remains unknown why HDACs are overexpressed in cancer. One explanation for HDAC11 overexpression in breast cancer could be gene amplification. Indeed, a cross-cancer analysis of genomic alterations in *HDAC11* revealed that *HDAC11* is amplified in some breast cancer samples (Figure 3.1 D). As amplification of *HDAC11* cannot explain the general elevation of HDAC11 in ER-positive breast cancer, another explanation might be that active ER signaling in breast tumors induces HDAC11 expression. This is supported by our findings in several ER-

positive breast cancer cell lines, in which we observed that E2 stimulation induced activation of ER signaling which in turn increased *HDAC11* mRNA levels. In addition, we have shown that inhibition of the pathway by tamoxifen or fulvestrant decreased *HDAC11* transcription. Previous studies from the Brown lab, in which they constructed genome wide binding maps of the ER, revealed that the *HDAC11* locus harbors two binding sites, suggesting that *HDAC11* is a direct target of the ER (Carroll et al., 2006).However, it still remains to be tested if these binding sites control transcription of *HDAC11*. Finally, HDAC11 could also be affected indirectly by estrogen signaling, as *HDAC11* mRNA has been shown to be negatively regulated by the miR-145 (Lin et al., 2013), a micro RNA down-regulated upon E2 stimulation (Dai et al., 2008).

To test if HDAC11 has oncogenic potential in breast cancer cells that overexpress it, we applied a KD approach which revealed that HDAC11 promotes proliferation. This finding is in line with previous studies showing a role for HDAC11 in proliferation. For example, it has been demonstrated that KD of HDAC11 in oligodendrocytes decreased proliferation (Liu et al., 2009). In addition, similar findings were observed in ovarian-, breast-, prostate-, and colon cancer cell lines (Deubzer et al., 2013). Our findings revealed that HDAC11 specifically affects proliferation in ER-positive breast cancer cells, suggesting that HDAC11 might promote proliferation via ER signaling. ER signaling is known to promote proliferation by inducing a transcriptional program, in which activators of proliferation such as MYC, cyclin D1 and cyclin-dependent kinase 1 are upregulated upon ER activation (Frasor et al., 2003). Interestingly, previous studies revealed that acetylation affects ER function directly, as it was demonstrated that ER acetylation, depending on the acetylation site, can either positively (Kim et al., 2006) or negatively (Wang et al., 2001), affect its activity. Moreover, several studies demonstrated that treating breast cancer cells with HDACi resulted in a decrease of total ER protein levels (De los Santos et al., 2007; Yi et al., 2008). Excitingly, we found a direct link between HDAC11 and the ER, as ER protein- and mRNA levels were reduced in HDAC11 KD cells. As HDAC11 is a known transcriptional repressor, for example, it was shown to directly repress *il-10* (Villagra et al., 2009), it is unlikely that HDAC11 regulates ER levels in a direct manner. We consider it more likely that HDAC11 represses genes encoding proteins that repress *ESR1* transcription. In addition, HDAC11 might also affect ER protein level. This could involve the Hsp90 chaperone which binds

ER to maintain the receptor in a conformation capable of ligand binding (Fliss et al., 2000; Redeuilh et al., 1987), and whose inhibition results in the degradation of ER (Bagatell et al., 2001). Interestingly, the chaperone function of Hsp90 has been shown to be affected by acetylation (Kovacs et al., 2005). Inhibition of HDAC6, an interaction partner of HDAC11 (Cheng et al., 2014; Gao et al., 2002), causes Hsp90 hyperacetylation, decreases its association with ER and results in proteasomal degradation of ER (Figure 3.12) (Fiskus et al., 2007). Therefore, HDAC11 could indirectly control ER levels by contributing to the de-acetylation of Hsp90, a hypothesis which will be addressed in future studies. Surprisingly, the reduced ER levels in HDAC11 KD cells do not affect transcription from an ERE-containing reporter construct. However, the activity of ER on specific genes might be affected.

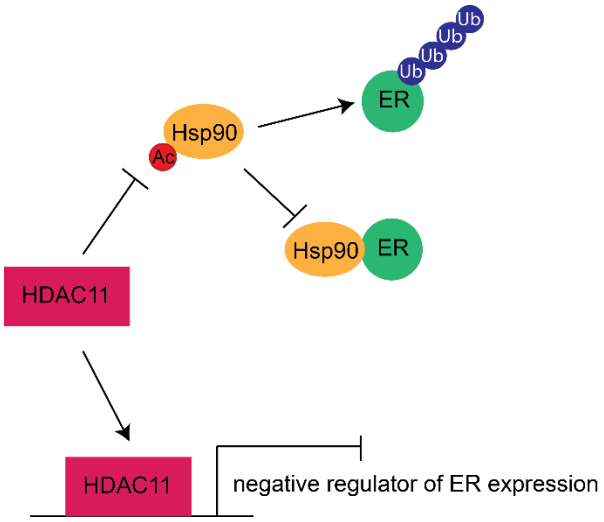

Figure 3.12 Potential mechanisms by which HDAC11 could control ER levels.

Using genomic and bioinformatics approaches we then examined if HDAC11 acts downstream of the ER by affecting transcription of estrogen responsive genes, in particular the ones that are normally silenced upon estrogen stimulation. These include genes known to decrease proliferation, such as *CDKN1A* encoding cyclin-dependent kinase inhibitor p21 (Cariou et al., 2000; Frasor et al., 2003), *CCNG2* encoding cyclin G2, a negative regulator of cell proliferation (Frasor et al., 2003; Liu et al., 2004) and *BTG2* encoding the BTG family member 2, another negative regulator of proliferation (Frasor et al., 2003; Zhang et al., 2010b). Our RNA-sequence analysis revealed that in HDAC11 KD cells, the number of upregulated genes is much higher compared to the down regulated genes, suggesting that HDAC11 can act as a direct repressor.

Interestingly, several of the significantly upregulated genes are associated with estrogen signaling, such as the cytokine receptor *IL1R1* shown to be down-regulated upon estrogen signaling (Schaefer et al., 2005), *CYP1A1*, a member of the cytochrome P450 (CYP) superfamily that contains proteins involved in hormone synthesis (Go et al., 2015) and albumin shown to regulate binding of estrogen to the ER (Baker, 1998). Moreover, our GSEA analysis using these RNA-sequence datasets demonstrated that genes, which are normally downregulated upon estrogen signaling, are enriched in HDAC11 KD cells. In summary, our findings suggest that HDAC11 might be a direct repressor of genes that are silenced by estrogen signaling, including anti-proliferative genes. Ongoing studies, in which we aim to generate a genome wide binding profile of HDAC11, should reveal if HDAC11 binds directly to these genes.

Finally, we tested if HDAC11 expression has prognostic value for breast cancer patients. Indeed, when we analyzed a group of endocrine therapy treated patients, we found that the probability of RFS and DMFS decreased significantly for patients with high levels of HDAC11. These findings in combination with HDAC11's role in proliferation in ER-positive breast cancer cells, imply that HDAC11 might be a new target for breast cancer therapy.

As ER-positive breast cancer patient are already effectively targeted by endocrine therapy (Criscitiello et al., 2011), our findings might have implications for patients that become resistant to endocrine agents. Therefore, it would be interesting to examine HDAC11 levels in these resistant tumors and select the cases that express high levels of HDAC11 for targeted therapy.

HDACs are currently targeted by non-specific inhibitors that target many HDACs at the same time, some of these inhibitors also target the activity of HDAC11 (Mottamal et al., 2015). However, using pan-inhibitors to target HDAC11 might cause opposing effects, like inhibition of HDACs that are tumor suppressive. Previous studies, for example, revealed that HDAC1 and HDAC2 have both oncogenic and tumor suppressive potential (Heideman et al., 2013; Winter et al., 2013). To avoid these problems, an increasing number of more selective HDACi are becoming available, which are either class specific or in the case of HDAC6 specific (tubacin) (West and Johnstone, 2014). Ideally, to test the full potential of HDAC11 targeting in breast cancer it would be crucial to develop a specific HDAC11 inhibitor, which might be feasible, as

the catalytic domain of HDAC11 is distinct from all other HDACs (Gao et al., 2002; Yang and Seto, 2008).

Numerous clinical trials have been performed using HDACi to target different cancer types, either as single therapy or in combination with another therapy (Mottamal et al., 2015). Promising results have been observed for hematological malignancies, like multiple myeloma (San-Miguel et al., 2014) and cutaneous T cell lymphoma (Mann et al., 2007). However, treatment of most other cancer types showed in general no or only marginal response. An exception is a clinical study in which patients with endocrine therapy resistant tumors were treated with a combination of the class I HDACi entinostat and the endocrine agent exemestane. This study revealed a clinical response and showed that the HDACi could re-sensitize the endocrine-resistant tumors to endocrine therapy (Yardley et al., 2013). In our opinion, the overall marginal outcomes of HDACi treatment of cancer patients in the clinical setting reflects our lack of knowledge about the function of specific HDACs in specific cancer types. Therefore future studies should reveal the oncogenic HDACs and drugs should be used and designed to target these specifically.

MATERIALS AND METHODS

Antibodies, reagents, plasmids

For western blot analysis the following antibodies were used: HDAC1, HDAC2, HDAC6 and HDAC11 (BioVision); HDAC3 and HDAC8 (Abcam); P-ERα Ser118 (Upstate); P-ERα Ser167 (Cell Signaling); ERα and Tubulin-α (NeoMarkers); Actin (Chemicon); Acetyl-Histone H3 (Millipore); Histone H3, Acetyl-Histone H4 and Histone H4 (Abcam).

17-β-estradiol (E2) (Sigma) was dissolved in ethanol at 1mM and 10mM concentration and stored at -20°C. The inhibitors 4-OH-tamoxifen (Sigma) and fulvestrant (Sigma) were dissolved in DMSO at 10mM and stored at 4°C.

Data Mining in Online Platforms

The online platform Oncomine [www.oncomine.com, March 2015, Thermo Fisher Scientific] was used for the following analyses and visualizations: **1.** The expression levels of several HDACs in different cancer cell lines were analyzed using the Barretina Cell Line dataset (Barretina et al., 2012). **2.** For comparison of *HDAC11* mRNA levels in normal breast versus different types of breast cancer samples (Invasive Breast Carcinoma, Invasive Lobular Breast Carcinoma, Invasive Ductal Breast Carcinoma) the breast dataset (No Associated Paper 2011/09/02) of The Cancer Genome Atlas (TCGA) [http://cancergenome.nih.gov/.] was used. **3.** The comparison of HDAC11 expression in ER-negative versus ER-positive breast cancer samples and cell lines was performed using the following 25 independent gene expression datasets: [1] Bittner, Not Published, 2005; [2] (Boersma et al., 2008); [3] (Chin et al., 2006); [4-6] (Curtis et al., 2012); [7] (Desmedt et al., 2007); [8] (Esserman et al., 2012); [9] (Ginestier et al., 2006); [10] (Glück et al., 2012), [11] (Gruvberger et al., 2001); [12] (Hatzis et al., 2011); [13] (Ivshina et al., 2006); [14] (Julka et al., 2008); [15] (Kao et al., 2011); [16] (Korde et al., 2010); [17] (Lu et al., 2009); [18] (Minn et al., 2005); [19] (Miyake et al., 2012); [20] (Neve et al., 2006); [21] TCGA 2011 [http://cancergenome.nih.gov/.]; [22] (Marc J. Van De V Ijver, 2002); [23] (Waddell et al., 2010); [24] (Wang et al., 2005); [25] (Zhao et al., 2004). **4.** For the correlation analysis of HDAC11 and ER expression, the van't Veer breast cancer dataset (van't Veer et al., 2002) was used.

The database of the cBioPortal for Cancer Genomics [www.cbioportal.org] (Cerami et al., 2012; Gao et al., 2013) was used to analyze the prevalence of genomic alterations of HDAC11 in "All Cancer Studies". The same platform was used for the correlation between ER protein and HDAC11 mRNA levels in the dataset Breast Invasive Carcinoma (TCGA, Provisional) including 1104 cases of breast cancer patient.

The prognostic value for HDAC11 was analyzed using the Kaplan-Meier plotter [http://kmplot.com/analysis], a database containing gene expression data and clinical data of breast cancer patients (Gyorffy et al., 2013). The two patient groups for high (upper quartile) and low HDAC11 expression were compared for RFS and DMFS in different cancer subtypes (ER-status and grade) and in selected cohorts (including or excluding patients receiving

chemotherapy and/or endocrine therapy). The hazard ratios with 95% confidence intervals and log rank p-values were calculated.

Cell culture, transfection, virus production and infection

HEK293T, T47D, MCF7, MDA-MB-231 and SUM159 cells were routinely grown in Dulbecco's modified Eagle's medium (DMEM) supplemented with 10% fetal bovine serum (FBS) at 37°C, 5% CO_2. The murine breast cancer cell line J110 was obtained from Dr.Myles Brown (Dana Farber Cancer Institute, Boston) and grown in RPMI 1640 supplemented with 10% FBS. For E2-stimulations, cells were steroid-deprived using phenol red-free DMEM supplemented with 10% charcoal-stripped FBS (Gibco) for 2-3 days before stimulation with 10 – 50nM E2. For HDAC11 mRNA analysis upon tamoxifen and fulvestrant treatment, cells were grown in normal growth condition and 100nM of either inhibitor was added for 48 hours.

Lentiviruses for generation of HDAC11 knockdown cells were produced by transient transfection of HEK293T cells with 0.8 µg pLKO.1-puro vectors containing different shRNA sequences from sigma (MISSION shRNA library: shNT (SHC016); ev (SHC001); sh1 (TRCN0000199149); sh2 (TRCN0000330937); sh3 (TRCN0000330863)), 0.4 µg HDM-tat16, 0.4 µg HDM-HgPM2, 0.4 µg pRC-CMV-Rall and 0.8 µg HDM-VSV-G using polyethylenimine (PEI) (Polysciences Inc.) or ProFection (Promega) and incubated o.n. at 37°C. Viruses were collected 72 h post-transfection, filter sterilized and used for infection of cells in the presence of 8 µg polybrene (Sigma) for 24 h. Successfully infected cells were selected using 2 µg puromycin (Sigma).

Proliferation and Colony assay

Proliferation was measured by growing cells in 12-well plates for 1 week. Cells were fixed with 2.5% Glutaraldehyde (Fluka) at different time points and stained with crystal violet (0.5% crystal violet, 25% Methanol). The dye was dissolved using 10% Acetic acid (Alfa Aesar) and absorption was measured using a spectrophotometer plate reader (Molecular Devices). Experiments were performed in triplicates.

Clonogenic potential was measured by seeding 1000 cells into 10cm dishes and colony formation was analyzed after 1 week. Cells were fixed and stained as described in the proliferation assay and colony numbers were counted. Total covered area was measured with the image processing program Fiji. The mean colony size was calculated by dividing the total covered area by the number of colonies. Experiments were performed in triplicates.

YoPro apoptosis assay

Effect of HDAC11 KD on apoptosis was measured by the YoPro assay (Idziorek et al., 1995). Cells were grown in 96-well plates in quadruplicates and cells for the positive apoptosis control were treated for 30min with medium containing 50µM camtothecin (Sigma) dissolved in DMSO. A final concentration of 2.5 µM YO-PRO-1 (Invitrogen) was diluted in 5x YO-PRO buffer (100mM Na-citrate pH4, 134mM NaCl) and added to the cells. After 10min incubation apoptosis was determined by measuring the fluorescence intensity (485nm excitation, 529nm emission) using a Cytofluor II Plate Reader. After the first reading, cells were lysed with lysis buffer (500mM EDTA, 500mM EGTA, 10% NP40, 1x YO-PRO buffer) and incubated for 30 min in the dark before fluorescence was measured to determine the total number of cells. The measured fluorescence intensity of the lysed cells was used to calculate the percentage of apoptotic cells. The experiment was performed in quadruplicates.

Lysates and Western blot analysis

Whole cell lysates were extracted in NP-40 buffer (50mM Hepes pH7.4, 150mM NaCl, 20mM β-glycerophosphate, 2.5mM NaF, 5mM EGTA, 1mM EDTA, 15mM PPI, 1% NP-40, 10µg/ml Leupeptin, 10µg/ml Aprotinin, 2mM Na Ortho Vanadate, 1mM DTT and 1mM PMSF). Lysates were cleared by centrifugation and protein concentration was measured by Bradford (Bio-Rad) using bovine serum albumin as a standard. Samples were boiled in SDS-sample buffer. The proteins were separated by SDS-PAGE, blotted onto nitrocellulose membranes (Whatmann) and probed with the specific antibodies after blocking with 10% horse serum (Gibco) in 1x TBS and 0.05% Tween 20 (Sigma-Aldrich), or for probing with HDAC11 antibodies, with 5% milk and

2.5% BSA (Sigma) in 1x TBS and 0.05% Tween 20. Tumor lysates were homogenized in NP-40 buffer using a polytron (Kinematica) and debris were removed by centrifugation.

Luciferase Reporter Assay

The Cignal Reporter Assay Kit (Qiagen) for ER-responsive firefly luciferase reporter activity was performed according to the manufacturer's protocol. Cells were seeded in 12-well plates and the following day transfected with 150ng of a mixture of the ER-responsive luciferase construct, encoding the firefly luciferase reporter gene under the control of a basal promoter element (TATA box) joined by tandem repeats of the estrogen transcriptional response element (ERE), and of a construct constitutively expressing the Renilla luciferase reporter gene under the control of a CMV promoter. The Renilla luciferase reporter was used as an internal control for normalizing transfection efficiencies. As a negative control, cells were transfected with 150ng of a mixture of a non-inducible firefly luciferase construct, encoding firefly luciferase under the control of a basal promoter (TATA box) without any additional transcriptional response elements, and the constitutively expressing Renilla luciferase construct. Transfections were performed using FuGENE HD (Promega). After 24 hours cells were washed and after 48h hours lysed with 1x Passive lysis buffer from the Dual-Luciferase Reporter Assay System (Promega). Luciferase activity was measured using the Dual-Luciferase reporter assay kit (Promega). Data were normalized for transfection efficiency by dividing firefly luciferase activity with that of Renilla luciferase. In all luciferase assays, values represent mean ± SDEV from 3 independent biological replicates.

Animal experiments

Animal experiment was performed according to the Swiss guidelines governing animal experimentation and approved by the Swiss veterinary authorities. $2x10^5$ J110 HDAC11 KD and control cells were injected into the fourth mammary fat pad of 6 week old female FVBN mice (Harlan). Tumors were measured and volume calculated (height x $(\text{diameter}/2)^2 \times \pi$). At the end of the experiment, mice were euthanized, tumors dissected and tumor weight measured.

Quantitative real-time PCR

RNA was isolated from cells using the QIAshredder and RNeasy Mini Kit (Qiagen). Synthesis and amplification of cDNA was carried out with the Ready-To-Go You-Prime First-Stand Beads (GE Healthcare) using oligo-dT(15) primers (Promega) according to the manufacturer's instruction. Quantitative real-time polymerase chain reaction (qPCR) was performed using SYBR Green ROX Mix (Thermo Scientific) and StepOnePlus Real-Time PCR System instrument and software (Applied Biosystems). The following primer sequences were used: HDAC11_fw: GAGCTCAAGTGGTCCTTTGC; HDAC11_rw: CTCCTGTCTGGGTCCGAAG; ESR1_fw: CCACCAACCAGTGCACCATT; ESR1_rw: GGTCTTTTCGTATCCCACCTTTC; Actin_fw: TGTCCACCTTCCAGCAGATGT; Actin_rw: CGCAACTAAGTCATAGTCCGCC. mRNA levels were measured in triplicates and normalized to respective actin levels.

Genomic and bioinformatics analysis

Microarray processing and analysis

T47D cells were grown in steroid-deprived condition for 3 days before stimulated with 10nM E2 for 8 and 24 hours. RNA from three biological replicates was isolated using the QIAshredder and RNeasy Mini Kit (Qiagen). 100ng of extracted total RNA was amplified using the Ambion WT Expression kit (Ambion, Life Technologies, Thermo Fisher Scientific, Waltham, MA, USA) and the resulting sense-strand cDNA was fragmented and labeled using the Affymetrix GeneChip WT Terminal Labeling kit (Affymetrix, Santa Clara, CA, USA). 2.75ug of labeled material for each sample was hybridized to an Affymetrix Human Gene 1.0 ST Array following the "GeneChip Whole Transcript (WT) Sense Target Labeling Assay Manual" (Affymetrix) with a hybridization time of 16h. The Affymetrix Fluidiscs protocol FS450_0007 was used for washing. Scanning was performed with Affymetrix GCC Scan Control v. 3.0.0.1214 on a GeneChip Scanner 3000 with autoloader. Arrays were normalized and probeset-level expression values were calculated with R/Bioconductor's (v2.14) 'affy' package using the rma() function.

Arrays were analyzed using R/Bioconductor version (version 3.2.1). The function featureFilter() of the genefilter package was used to filter out probesets without Entrez Gene ID. For Entrez

genes with several mapping probesets only the probeset with the most significant interquartile range (IQR) was kept. Of the remaining probesets, those with a linear fold-change >= 2, an log2 average expression of >= 4 across all arrays and an FDR <= 0.01 in the contrast "WT8hr – WT24hr" were plotted with the heatmap.2() function of the gplots package.

Gene set enrichment analysis (GSEA) was performed using the GSEA software (Mootha et al., 2003; Subramanian et al., 2005). Probesets differential in the contrast WT8hr-WT with adjusted p-value <= 0.05, linear fold-change >= 1.0 and average expression >= 4.0 and for the contrast WT24hr-WT with adjusted p-value <= 0.05, linear fold-change >= 1.3 and average expression >= 4.0 were identified and a .gmx file was created according to the specifications on http://www.broadinstitute.org/gsea/index.jsp and loaded into GSEA calculate geneset enrichments.

RNA-sequencing experiment

RNA from T47D HDAC11 KD (sh1, sh2 and sh3) and control lines (ev and shNT) were isolated using the QIAshredder and RNeasy Mini Kit (Qiagen). Libraries for RNA-seq were prepared with the TruSeq STrandend mRNA Sample Prep LS Protocol Rev.C (Illumina, CA, USA) starting from 2ug total RNA, pooled equimolarly. 50bp reads were sequenced on a one lane of a HiSeq2500 instrument (Illumina) using RTA 1.13.48 for basecalling. Demultiplexing and fastq generation was performed with bcl2fastq (bcl2fastq-1.8.4). Adapter sequences (GATCGGAAGAGCACACGTCTGAACTCCAGTCAC) were removed from the 3' end of the read.

Raw read counts for all hg19 refseq genes were extracted and analyzed with the edgeR packagel, in short, common and tagwise dispersions were calculated for all genes with at least 1 count per million in at least 2 samples. Statistics for contrasts were calculated fitting a negative binomial generalized log-linear model to the read counts for each gene and conduct genewise statistical tests for a given contrast. Genes were considered differential when having a fold-change of >= 1.4, p-value of <0.05 and an FDR of <=0.15.
Volcano plots were created by plotting log2 fold-changes against the –log10 of the FDR.

For GSEA-analysis, read counts normalized for library size were extracted and a gct file was created according to GSEA instructions, uploaded to GSEA and analyzed for enrichments of curated genesets of chemical and genetic pertubations (cgp) from GSEAs MSigDB.

3.2 "In the Spotlight" – Published in Cancer Discovery *

Targeting a novel ER/HOXB7 signaling loop in tamoxifen resistant breast cancer

Marinus R. Heideman[1], Anna Frei[1,2] and Nancy E. Hynes[1,2]

[1]Friedrich Miescher Institute for Biomedical Research, Maulbeerstrasse 66, 4058 Basel, Switzerland. [2] University of Basel, 4002 Basel, Switzerland.

Corresponding Author: Nancy E. Hynes Friedrich Miescher Institute for Biomedical Research, Maulbeerstrasse 66, 4058 Basel, Switzerland. Phone 41 61 6978107; FAX 41 61 6973576; E-mail: nancy.hynes@fmi.ch

Summary: The majority of breast cancer patients present with an estrogen receptor positive (ER+) tumor and the endocrine agent tamoxifen is a mainstay for their treatment; unfortunately, however, resistance remains a major problem since most patients who respond eventually have a recurrence. Thus, an enduring challenge in the breast cancer field is to identify mechanisms underlying tamoxifen resistance. In the current issue of *Cancer Discovery*, Jin and colleagues describe a novel ER/HOXB7 signaling loop in tamoxifen-resistant breast cancer models. Importantly, they reveal that targeting this signaling loop has great promise as an approach to treat tamoxifen-resistant breast cancer.

The approximately 70% of breast cancer patients whose tumors are ER+ are treated with endocrine agents, including tamoxifen, the first clinically successful ER modulator (SERM), and the more recently introduced agents fulvestrant, an ER degrader (SERD), and aromatase inhibitors that block estradiol production. Endocrine agents have increased the survival of hundreds of thousands of breast cancer patients since the introduction of tamoxifen into the clinic in the mid-1970s (Jordan, 2008). Unfortunately, tumor recurrence caused by acquired

* Repreinted by permission from the American Association for Cancer Research: Marinus R.Heideman, Anna Frei, and Nancy E. Hynes; Targeting a Novel ER/HOXB7 Signaling Loop in Tamoxifen-Resistant Breast Cancer; Cancer Discovery; September 2015; 5:909-911; doi:10.1158/2159-8290.CD-15-0871

resistance often occurs (reviewed in refs. Jeselson et al., 2015 and Musgrove et al., 2009). Therefore, it is crucial to gain an understanding of the mechanisms underlying endocrine therapy resistance.

ER biology is quite complex and it is likely that multiple, non-exclusive mechanisms contribute to endocrine resistance. For example, loss of ER, which is observed in 15-20% of recurrences, is an obvious resistance mechanism (Hoefnagel et al., 2012). RTK overexpression has also been proposed to contribute to endocrine resistance. Indeed, breast tumors with high expression and activity of EGFR and ERBB2 are less sensitive to tamoxifen (Newby et al., 1997). Moreover, the sub-group of breast cancer patients with ER+ tumors and the *ERBB2* amplicon generally do not respond to tamoxifen (Borg et al., 1994). These clinical data suggest that ERBB RTK signaling can circumvent the requirement for ER signaling. Recent findings demonstrate that mutations in the ER are also linked to acquired resistance. Genomic sequencing efforts revealed that metastatic tumors have a higher frequency of *ESR1* mutations than primary tumors (~20% vs 0.5%). The *ESR1* missense mutations identified in metastatic disease generally lead to ligand-independent constitutive activation of the receptor and are thought to be acquired during treatment (Jeselsohn et al., 2015). Biochemical analyses of some of the mutant ERs suggest that treatment of these patients with higher doses of current endocrine agents or with newer more potent agents might provide clinical benefit (Toy et al., 2013).

In this issue of *Cancer Discovery*, the Sukumar lab follows up on their 2012 *Proceedings of the National Academy of Sciences* paper (Jin et al., 2012), in which they showed that the HOXB7 transcription factor renders breast cancer cells resistant to tamoxifen through activation of the EGFR pathway. Their new manuscript (Jin et al., 2015) provides novel mechanistic insight into the regulation of HOXB7 in tamoxifen-resistant breast cancer models and proposes novel approaches to target tamoxifen-resistant breast cancer.

Interestingly, their data indicate that a direct interaction between HOXB7 and the ER is crucial for the upregulation of ER target genes in tamoxifen resistant cells. By performing co-immunoprecipitations they revealed a physical interaction between these two proteins. Moreover, ChIP experiments demonstrated increased binding of both HOXB7 and the ER at EREs in known ER target genes like *MYC*, *GREB1* and *CCND1*, suggesting that HOXB7 binds to

these sites in association with the ER. Of note, binding between HOXB7 and ER was shown to be enhanced upon E2 or tamoxifen treatment.

An important question that the authors answer then is "Why do these tamoxifen-resistant cells have increased HOXB7 levels?" To summarize the answer, the authors demonstrate that MYC is stabilized by phosphorylation mediated by ERBB2-EGFR signaling. Subsequently, stabilized MYC represses the expression of miRNA-196a, a known repressor of HOXB7 (Braig et al., 2010), resulting in increased HOXB7 levels (Figure 3.13).

One interesting aspect of this work is the direct relation between HOXB7 and ERBB2-EGFR expression and activation. The authors convincingly showed increased levels of phosphorylated ERBB2 and EGFR in cells that overexpress HOXB7. Furthermore, their data suggest that ERBB2 levels are directly regulated by ER/HOXB7 in tamoxifen resistant cells. This is based on chromatin immunoprecipitations revealing increased HOXB7 and transcriptional cofactor binding at an ERE site in the *ERBB2* locus of HOXB7 overexpressing, tamoxifen-resistant, MCF7 cells. In addition, quantitative PCR data show an increase in ERBB2 mRNA upon tamoxifen treatment. Data demonstrating increased HOXB7 and ER binding upon E2 or tamoxifen treatment is lacking, so it still remains a question whether or not ERBB2 is regulated in a similar manner as the other ER/HOXB7 targets described in the paper. Moreover, it cannot be ruled out that HOXB7 controls ERBB2 and EGFR level and phosphorylation by other direct or indirect mechanisms.

Another important finding in the HOXB7 overexpressing tamoxifen-resistant models is the stabilization of MYC by HER2/EGFR signaling leading to repression of miR-196a, which in turn represses HOXB7. Overexpression of miR196a was shown to reduce expression of ER targets and could reverse resistance to tamoxifen. In agreement, *in vivo* xenograft studies, using miR-196a overexpressing tamoxifen resistant BT474 cells, revealed a highly significant decrease in primary tumor growth.

Importantly, uncovering this new ER/HOXB7 signaling loop implies that targeting the ER associated HOXB7, either directly, or indirectly by ERBB2, MYC or miR-196a might have potential for treating tamoxifen-resistant breast cancer (Figure 3.13). To test targeting different nodes of this loop, the authors used several tamoxifen-resistant xenograft models. In BT474 xenografts, a model for ER+/*ERBB2* amplicon positive breast cancer, HOXB7 knock-down

almost totally blocked tumor outgrowth. This block was associated with a strong decrease in ERBB2 and EGFR levels and a subsequent decrease in AKT signaling. As there are currently no drugs directly targeting HOXB7, the authors targeted MYC, using the inhibitor 10058-F4 and targeted ERBB2 using trastuzumab. As anticipated, treatment of BT474 xenografts with trastuzumab caused a strong reduction in tumor growth. MYC inhibition reduced primary tumor growth only slightly but, interestingly, the combination of 10058-F4 and trastuzumab revealed synergy and tumor stasis. In another model, HOXB7-overexpressing MCF7 cells, treatment with fulvestrant resulted in complete remission. These data suggest that breast cancer patients with high HOXB7 levels might be the target population for fulvestrant treatment after tamoxifen-resistance emerges. It would be interesting to examine how the BT474 xenograft model responds to fulvestrant combined with the other inhibitors. Overall, these pre-clinical findings reveal that tamoxifen resistant tumors expressing high levels of HOXB7 can be targeted at several nodes of the ER/HOXB7 signaling loop.

Finally, the authors show analyses utilizing several independent databases harboring information of endocrine therapy treated ER+ breast cancer patients. These analyses revealed that patients expressing high HOXB7 have a worse probability of overall survival. Interestingly, elevated HOXB7 in combination with high ERBB2 and MYC showed an even stronger decrease in the probability of overall-survival. In summary, their findings imply that it could be beneficial to select tamoxifen-resistant patients based on these three markers, for rationalized targeting of the ER/HOXB7 signaling loop.

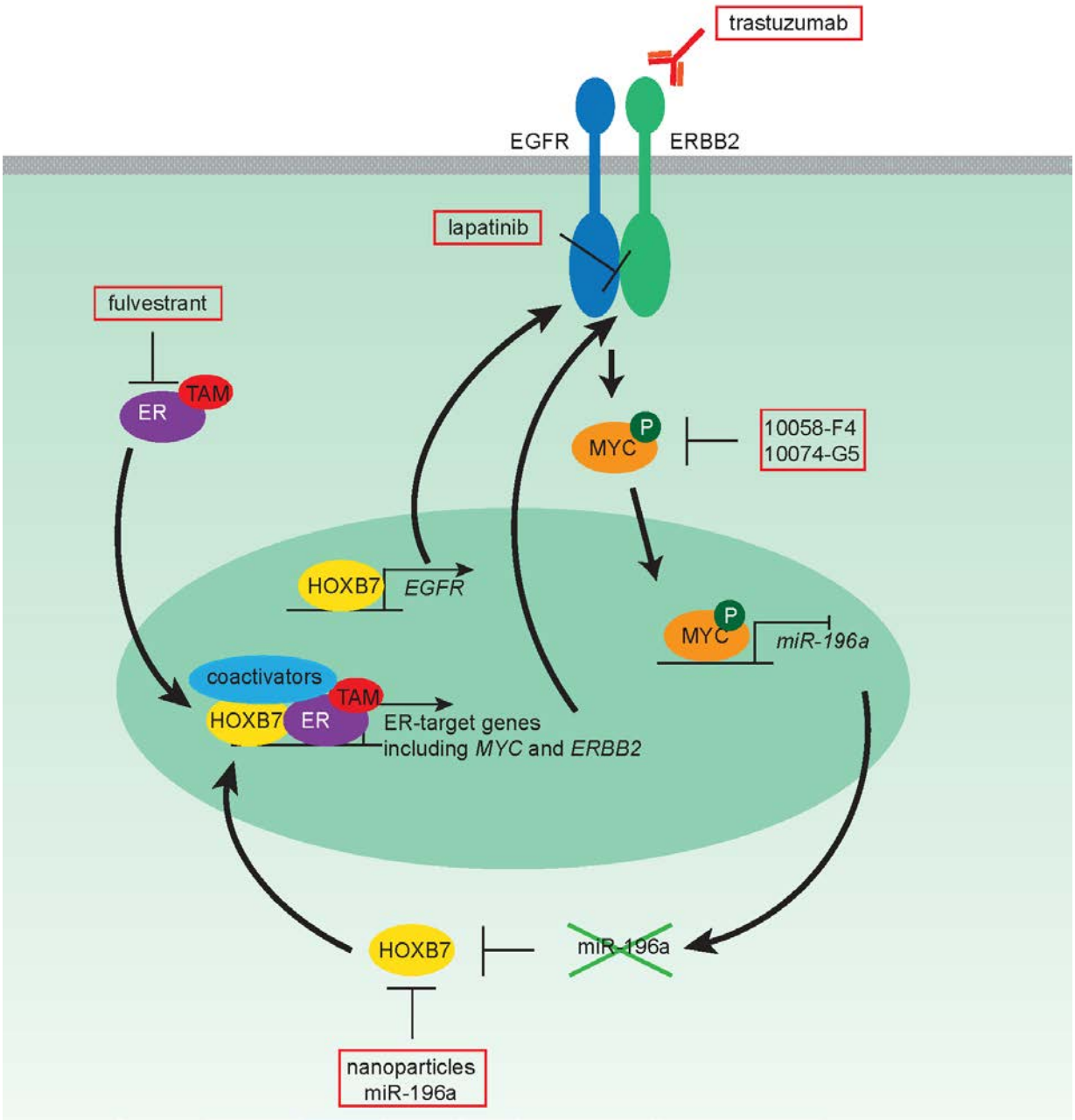

Figure 3.13 Targeting the ER/HOXB7 signaling loop in tamoxifen-resistant breast cancer. HOXB7 interacts with the tamoxifen (TAM) bound estrogen receptor (ER) and coactivators, inducing ER-target gene expression including MYC and ERBB2. HOXB7 binds the EGFR promoter directly increasing EGFR transcription. Increased signaling through ERBB2 and EGFR leads to MYC phosphorylation and stability. MYC represses miR-196a transcription, a repressor of HOXB7. Red boxes represent potential treatment strategies to target the ER/HOXB7 signaling loop: ERBB2 by trastuzumab, EGFR/ERBB2 by lapatinib, MYC by 10058-F4 or 10074-G5, miR-196a by nanoparticles containing miR-196 and ER by fulvestrant.

REFERENCES

Borg, A., Baldetorp, B., Ferno, M., Killander, D., Olsson, H., Ryden, S., and Sigurdsson, H. (1994). ERBB2 amplification is associated with tamoxifen resistance in steroid-receptor positive breast cancer. Cancer letters *81*, 137-144.

Braig, S., Mueller, D.W., Rothhammer, T., and Bosserhoff, A.K. (2010). MicroRNA miR-196a is a central regulator of HOX-B7 and BMP4 expression in malignant melanoma. Cellular and molecular life sciences : CMLS *67*, 3535-3548.

Hoefnagel, L.D., Moelans, C.B., Meijer, S.L., van Slooten, H.J., Wesseling, P., Wesseling, J., Westenend, P.J., Bart, J., Seldenrijk, C.A., Nagtegaal, I.D*., et al.* (2012). Prognostic value of estrogen receptor alpha and progesterone receptor conversion in distant breast cancer metastases. Cancer *118*, 4929-4935.

Jeselsohn, R., Buchwalter, G., Angelis, C., Brown, M., and Schiff, R. (2015). ESR1 mutations-a mechanism for acquired endocrine resistance in breast cancer. Nature reviews Clinical oncology.

Jin, K., Kong, X., Shah, T., Penet, M.F., Wildes, F., Sgroi, D.C., Ma, X.J., Huang, Y., Kallioniemi, A., Landberg, G*., et al.* (2012). The HOXB7 protein renders breast cancer cells resistant to tamoxifen through activation of the EGFR pathway. Proceedings of the National Academy of Sciences of the United States of America *109*, 2736-2741.

Jin K , Park S , Teo WW , Korangath P , Cho SS , Yoshida T , et al. (2015). HOXB7 is an ERα cofactor in the activation of HER2 and multiple ER target genes leading to endocrine resistance . Cancer Discov 2015 ;5: 944 – 59 .

Jordan, V.C. (2008). Tamoxifen: catalyst for the change to targeted therapy. European journal of cancer *44*, 30-38.

Musgrove EA , Sutherland RL (2009). Biological determinants of endocrine resistance in breast cancer . Nat Rev Cancer ; 9 : 631 – 43 .

Newby, J.C., Johnston, S.R., Smith, I.E., and Dowsett, M. (1997). Expression of epidermal growth factor receptor and c-erbB2 during the development of tamoxifen resistance in human breast cancer. Clinical cancer research : an official journal of the American Association for Cancer Research *3*, 1643-1651.

Toy, W., Shen, Y., Won, H., Green, B., Sakr, R.A., Will, M., Li, Z., Gala, K., Fanning, S., King, T.A*., et al.* (2013). ESR1 ligand-binding domain mutations in hormone-resistant breast cancer. Nature genetics *45*, 1439-1445.

3.3 Research Article – Published in Science Signaling*

Memo Is a Copper-Dependent Redox Protein with an Essential Role in Migration and Metastasis

Gwen MacDonald[1]*, Ivan Nalvarte[1*¶], Tatiana Smirnova[1], Manuela Vecchi[3,4], Nicola Aceto[1,2π], Arno Dolemeyer[5], Anna Frei[1], Susanne Lienhard[1], Jeffrey Wyckoff[1θ], Daniel Hess[1], Jan Seebacher[1], Jeremy J. Keusch[1], Heinz Gut[1], Daniele Salaun[6], Giovanni Mazzarol[7], Davide Disalvatore[8], Mohamed Bentires-Alj[1], Pier Paolo Di Fiore[3,4,9], Ali Badache[6], & Nancy E. Hynes[1,2,$]

[1] Friedrich Miescher Institute for Biomedical Research; Basel, 4058; Switzerland

[2] University of Basel; Basel, 4002; Switzerland

[3] IFOM, Fondazione Istituto FIRC di Oncologia Molecolare; Milan, 20139; Italy

[4] Molecular Medicine Program, Department of Experimental Oncology; European Institute of Oncology; Milan, 20141; Italy

[5] Novartis Institutes for Biomedical Research; Basel, 4057; Switzerland

[6] Centre de Recherche en Cancérologie de Marseille (CRCM), Inserm U1068, Institut Paoli-Calmettes; Aix-Marseille Université; CNRS, UMR7258 ; Marseille, 13009 ; France

[7] Division of Pathology and Laboratory Medicine; European Institute of Oncology; Milan, 20141; Italy

[8] Division of Epidemiology and Biostatistics, European Institute of Oncology; Milan, 20141; Italy

[9] Dipartimento di Scienze della Salute; Università degli Studi di Milano; Milan, 20122; Italy

[$] Corresponding author: Tel- 41 61 6978107, Fax-41 61 6973976, email nancy.hynes@fmi.ch

*Contributed equally

[¶] Current address: Department of Biosciences and Nutrition, Karolinska Institute, 14183 Huddinge, Sweden

[π] Current address: Massachusetts General Hospital Cancer Center, Harvard Medical School, Boston, MA 02129, USA

[θ] Current address: Koch Institute for Integrated Cancer Research, MIT, 500 Main St. Cambridge, MA 02138, USA

* From: Gwen MacDonald, Ivan Nalvarte et al.; Memo Is a Copper-Dependent Redox Protein with an Essential Role in Migration and Metastasis; Science Signaling; June 2014; Vol. 7;Issue 329, pp. ra56; DOI:10.1126/scisignal.2004870. Reprinted with permission from AAAS.

ABSTRACT

Memo is a conserved protein that has a critical role in cell motility. We show here that Memo was required for migration and invasion of breast cancer cells, and for *in vivo* spontaneous lung metastasis from MDA-MB-231 xenografts. Biochemical assays revealed that Memo is a novel copper-dependent redox enzyme that affected the intracellular redox milieu and levels of reactive oxygen species (ROS) in specific cellular locations. Memo also modulated the activity of NADPH oxidase (NOX), and was required for sustained O_2^- production in response to NOX activation. Memo abundance was increased in >40% of the primary breast tumors, was correlated with clinical parameters of aggressive disease and was an independent prognostic factor of early distant metastasis.

Summary Sentence

Memo is a redox enzyme that affects localized ROS levels, modulates NOX-mediated O_2^- production, and is required for metastasis.

INTRODUCTION

The majority of breast cancer patients die from metastases, making it crucial to identify proteins and signaling pathways involved in tumor cell dissemination. Our group previously identified Memo as being essential for breast cancer cell motility in response to several receptor tyrosine kinases. Tumor cells with Memo knockdown fail to migrate in response to epidermal growth factor, heregulin, fibroblast growth factor or serum (*1-4*). Memo has also recently been reported to interact with insulin receptor substrate 1 and insulin-like growth factor receptor 1 (*5, 6*). Thus, Memo links extracellular signals to intracellular responses through multiple receptors.

Memo is evolutionarily conserved, with homologs found in all branches of life (*7, 8*). The 2.1 Å crystal structure of Memo revealed its structural homology with iron- and zinc-binding enzymes, however, no evidence for metal binding was found in these studies (*7*). In this manuscript, we present evidence that Memo is a metal-binding enzyme that required Cu(II) for

its oxidase activity. Reactive oxygen species (ROS) function as intracellular second messengers regulating physiological processes by controlling the activity of redox-regulated proteins including transcription factors, kinases and phosphatases (*9-12*). We showed here that Memo affected localized ROS production, cell migration and *in vivo* metastasis. NADPH oxidases (NOX) are major cellular ROS generating complexes. We present results showing that Memo was required for sustained O_2^- production in response to NOX activation. Moreover, we showed that elevated Memo levels were present in >40% of primary human breast tumors and correlated with poor prognostic factors and distant recurrence-free survival.

RESULTS

Memo is required for cell motility and invasion

Memo knockdown has been shown to decrease directed motility of breast cancer cell lines in transwell and Dunn chamber assays (*1, 2, 13*). In the following experiments, we examined the effect of Memo knockdown using wound-closure and invasion assays. In the MDA-MB-231 breast cancer model, a control shRNA line (shLZ) and two lines expressing independent Memo shRNAs (sh2, sh5), were established; both shRNAs were efficient in decreasing Memo levels (Figure 1A, lower panel). Loss of Memo significantly impaired the cellular migration of both of the knockdown cells lines in wound-closure assays and (Figure 1A) and was also seen with SKBR3 and T47D sh5 lines (Figure S1A). The invasiveness of MDA-MB-231 tumor cells in Matrigel-coated assays was also lower in the Memo knockdown cells (Figure 1B), although significance was only achieved with the sh5 pool, which had the lowest amount of Memo (Figure 1B, lower panel). Rescue of Memo levels, achieved by expressing a non-targetable (NT) Myc-tagged Memo in the sh5 cells restored invasiveness to control levels, confirming the specificity of the shRNA knockdown for Memo (Figure 1B). We further analyzed the invasion phenotype using MCF10A-ErbB2/ErbB3 cells, which form hyperproliferative, invasive structures and display loss of polarity when grown in 3D (*14*). Doxycycline-induced Memo knockdown in these cells had no effect on proliferation (Ki67 staining, Figure 1C), but led to a significant reduction in the number of invasive structures and a concomitant increase in the number of polarized structures, defined by the basal marker Laminin V and the apical golgi marker GM130

staining, respectively (Figure 1C; Figure S1B). Together these data confirmed that Memo is important for breast tumor cell migration and invasion. Additionally, increased Memo levels alone did not appear to be transforming, as Memo overexpression did not change the invasion, proliferation, nor luminal filling of MCF10A or MCF10A-ErbB2 cells cultured in 3D (Figure S1C). Memo overexpression in MCF10A and HEK293 cells, however, increased migration in wound-closure assays (Figure S1D).

Memo is required for breast cancer metastasis

In the following experiments we used the MDA-MB-231 model, which represents the poor-outcome triple negative subtype and is one of few xenograft models known to spontaneously metastasize in mice (*15*), to test the *in vivo* role of Memo in tumor progression. The parental line, a control shRNA (shLZ) line and the two lines expressing independent Memo shRNAs (sh2, sh5) were injected into mice and tumor growth and metastasis were monitored. Control and Memo knockdown tumors grew with similar kinetics to similar volumes (Figure 2A), Memo knockdown was retained in the tumors (Figure S2A) and there were no significant differences in proliferation or angiogenesis by immunohistochemistry comparing the control and sh5 groups (Figure S2B). Our *in vitro* analyses with other Memo knockdown and reconstituted tumor cell lines also revealed no changes in cellular proliferation (Figure S2C).

To quantify metastases, lungs of the tumor-bearing animals were sectioned and stained for human vimentin. No difference in lesion number was seen between parental and shLZ tumors, however, Memo knockdown reduced these numbers, which was significant for the sh5 group (Figure 2B). To examine if Memo knockdown impacts on proliferation of lung metastases, we measured the area of each individual lung lesion. Compared to the control groups, there was no difference in the median lung lesion size in the sh2 knockdown mice, however, the mean lesion size in the sh5 knockdown mice was significantly lower (Figure S2D). Sh5 knockdown cells have lower Memo levels compared to the sh2 cells (Figures S2A). This suggests that Memo levels can influence the proliferative ability of the tumor cells in the lung environment.

To monitor the ability of the cells to extravasate we performed tail vein injection of the control shLZ and two Memo knockdown cell lines. The number of experimental lung metastases was

significantly decreased for both Memo knockdown cell lines (Figure 2C). To analyze the role of Memo in the early stages of metastasis, we used intravital imaging to look at the periphery of GFP-expressing shLZ and Memo knockdown sh5 primary tumors. In comparison to controls, Memo knockdown tumors had a greater number of cells extending protrusions, however, the number of motile cells was significantly lower (Figure 2D; Movies S1-2). Taken together, these data suggest that the decreased number of spontaneous lung metastases observed in mice with Memo knockdown tumors is due at least in part to a defect in intravasation from the primary site as well as a decreased potential to extravasate into the lungs. The results show that Memo has an essential role in metastatic dissemination.

Reconstitution of Memo knockdown cells with non-targetable Memo rescues the *in vivo* phenotype

In the next experiments, we tested the *in vivo* effect of reconstituting MDA-MB-231 Memo knockdown sh5 cells with Myc-tagged NT Memo rescue vector (sh5-NT). GFP-expressing- shLZ control, -sh5 and -sh5-NT cell lines (Figure 3A) were injected into mice and tumor growth and metastasis were monitored. All tumors grew with similar kinetics to similar volumes (Figure S3A) and Memo knockdown and NT-Memo levels were retained in the tumors (Figure S3B). We used intravital imaging to quantify the number of cells extending protrusions and the number of motile cells in the periphery of the primary tumor. Sh5 tumors had a significant increase in the number of cells extending protrusions and a significant decrease in motile cells (Figures 3B), as observed in Figure 2D. The reconstituted sh5-NT tumors were similar to the control shLZ tumors in the numbers of protruding and motile cells (Figure 3B). Likewise, reconstitution of Memo in sh5 tumors caused a significant increase in lung metastases (Figure 3C). We also monitored the tumor blood burden (Figure S3C). Although there were no significant differences between the three groups, due to large intra-group variation in the number of circulating tumor cells, there was a trend for lower circulating tumor cells in the sh5-tumor-bearing mice and this trend was reversed in the sh5-NT tumor-bearing mice (Figure S3C). These results confirm that the defects in metastatic dissemination to the lungs were specific to Memo loss, as reexpression of Memo recapitulated the phenotypes seen with the control tumors.

Memo is a copper-dependent redox enzyme

Although Memo's role in migration is well documented (*1, 2, 4, 13*), nothing is known about its biochemical function. Memo is structurally homologous to a class of bacterial non-heme, iron-dependent dioxygenases (*7*), but these enzymes (for example, protocatechuate dioxygenase, PD) hydrolyze catechols and Memo lacks this activity (Figure S4A). Memo does, however, have a putative metal-binding pocket (3 His, 1 Asp, 1 Cys) that resembles those of metal-dependent redox enzymes (Figure 4A). To test if Memo has redox activity, we measured its ability to generate O_2^-, an intermediate product of many metal-catalyzed redox reactions. Out of 8 common metal ions tested, only Cu(II) specifically generated O_2^- in Memo's presence (Figure S4B). Indeed, Memo has oxygen-dependent, copper-reducing activity (Figure 4B) which the dioxygenase PD lacks (Figure S4C).

The amino acid residues in Memo's putative active site (Figure 4A) were mutated and the proteins analyzed for Cu(II) reducing activity. The three histidine mutants had the lowest activities both as recombinant proteins (Figure 4C) and when expressed in HEK293T cells as Myc-tagged proteins (Figure S4D-E). The H192A mutant produced significantly less O_2^- in the presence of Cu(II) compared to WT Memo; the production of O_2^- by both proteins was abolished upon addition of superoxide dismutase (Figure 4D).

We next asked if Cu(II) is stably or transiently present in the active site by incubating Memo with Cu(II), followed by extensive dialysis to remove free Cu(II) and measurement of O_2^- production. Cu(II)-preloading of Memo resulted in approximately 20-fold higher activity, as compared to no preloading or to preloading with Fe(II) (Figure 4E), suggesting that Memo retained Cu(II) once it was bound; Cu(II)-preloaded H192A-Memo produced significantly less O_2^- than WT (Figure 4E).

Next we determined the enzymatic properties of WT and H192A Memo using Cu(II) as a substrate. For this, O_2^- production, in the presence of increasing amounts of Cu(II) or Memo, was measured (Figure S4F-G). This revealed that WT Memo had a lower affinity (K_m) for Cu(II) than H192A Memo (Figure 4F). However, the catalytic turnover (K_{cat}) of Cu(II) by WT Memo was 4-fold higher than that of the mutant (Figure 4F). This suggests that Cu(II) binds the mutant more readily than the WT, but is either not efficiently reduced, or rapidly dissociates; the end result

being that WT Memo reduces Cu(II) more efficiently than the mutant (K_{cat}/K_m). During this process, the active-site histidines could act as bases to donate an electron to Cu(II), generating a Cu(I) intermediate that is able to reduce and activate molecular oxygen to produce O_2^- (Figure S4H). In order for Memo to remain active *in vivo* it would need to be regenerated, namely reduced, either actively (for example, by reductases) or passively (for example, by reduced glutathione), something that will be analyzed in the future.

Finally, we examined the influence of Memo on RhoA, a protein that interacts with Memo (*16*) and has been reported to be redox sensitive (*17, 18*). For this we used recombinant proteins and a quantitative mass spectrometric (MS) approach (Figure 4G). We quantified the effects of WT and H192A Memo, with or without Cu(II) preloading, on the net oxidation state of RhoA cysteines. These results showed that without Cu(II) pre-loading Memo has no effect on RhoA oxidation (Figure S4I). With CuI(II) preloaded Memo, we observed a significant increase in the net oxidation status (Figure S4I), as well as the oxidation of individual cysteines in RhoA (Figure 4G). The increase in RhoA oxidation status was also significant, albeit slightly lower, with H192A Memo (Figure 4G and S4I), which is in line with its lower catalytic activity.

Memo influences the cellular redox status

We established that Memo is a copper-binding redox enzyme. In the following experiments we explored Memo's cellular activity. First, we tested invasion in the presence of the copper chelator tetrathiomolybdate (TM). Treatment of MDA-MB-231 shLZ cells with TM resulted in a 40% decrease in invasion (Figure 5A), showing that inhibition of copper impacts on signaling pathways required for this process. Memo knockdown sh5 cells, which exhibited impaired invasion capacity, were not affected by TM treatment (Figure 5A), suggesting that Memo might be the major copper binding target involved in invasions in the MDA-MB-231 model.

Next, we asked if the presence or absence of Memo has an influence on the cellular redox status, first by examining specific proteins, including RhoA, Shc, and actin, which have been shown to interact with Memo (*1, 2, 16*), as well as Rac1, another important protein involved in migration. For this experiment, lysates from MDA-MB-231 control shLZ, sh5, and sh5 reconstituted (sh5-NT) cells were treated with the heavy thiol-binding probe AMS, and then

run on non-reducing SDS-PAGE. This revealed a shifted band of reduced RhoA (Red.), which is only present in the sh5 lysates (Figure 5B, quantification below). These results support the MS results obtained with the recombinant proteins. In the same lysates, the redox status of Rac1 and actin were not altered (Figure 5B). Lysates from SKBR3 control and Memo knockdown cells were also examined and we detected elevated levels of reduced RhoA, as well as p52 Shc, in the Memo knockdown cells (Figure S5A).

Finally we examined expression levels of key redox homeostasis enzymes; namely catalase, glutamate-cysteine ligase (GCLC) and glutathione peroxidase (GPx1) in the MDA-MB-231 and SKBR3 shLZ control and Memo knockdown cell lines. RNA levels of catalase, which converts H_2O_2 to H_2O, was decreased in sh5 MDA-MB-231 (Figure 5C) and SKBR3 cells (Figure S5B). In addition, GCLC, a rate-limiting enzyme for glutathione synthesis, was also lower in MDA-MB-231 sh5 cells (Figure S5B). Conversely, GPx1, which oxidizes GSH to GSSG, was elevated in both SKBR3 and MDA-MB-231 knockdown cells (Figure 5D, Figure S5B). These changes were reversed in the sh5-NT reconstituted MDA-MB-231 cells (Figure 5C). Taken together these results suggest that the cellular environment is more reduced when cells have low Memo levels, both at the level of individual proteins, and more generally, using key redox enzymes as a read-out.

Memo regulates ROS in protrusions and O_2^- production

Memo is a redox enzyme, which prompted us to study ROS levels in Memo knockdown cells. There are several major ROS sources within cells including the mitochondrial transport chain, peroxisomes and redoxisomes (*19*). We investigated levels of intracellular ROS, using Carboxy-H_2DCF-DA (DCF-DA) followed by fluorescence activated cell sorting (FACS) and found no significant differences between MDA-MB-231 control shLZ and sh5 Memo knockdown cells (Figure 6A). However, by visualization and quantification of ROS using the CellROX Deep Red reagent, we determined that ROS levels in cellular protrusions, specifically the lamellipodium and lamella (example seen in Figure 6B), were significantly lower in sh5 cells (Figure 6C). In control cells, 3.5% of total cellular ROS was found in these protrusions and in Memo knockdown cells the amount was significantly decreased to 1% (Figure 6C, quantification right graph).

Reconstitution of Memo in MDA-MB-231 sh5 cells restored ROS to the values measured in the control cells (Figure 6C, quantification right graph). Similar results were obtained with SKBR3 and T47D cells (Figure S6A-B). Expression of GFP-tagged Memo in SKBR3 cells confirmed that Memo co-localized with ROS in these protrusions (Figure S6C). Thus, Memo is required for production of a small percentage of cellular ROS, which can be visualized due to its localized nature, but is not measurable by FACS.

The plasma membrane is a site of localized ROS signaling (*20, 21*). The ROS-producing NOXes, which have well established roles in migration (*11, 12, 22*), localize to cellular membranes and have been shown to be concentrated in the lamellae of motile cells (*23*). We examined if Memo might influence the activity of a specific pool of NOX. MDA-MB-231 cells express NOX1 and NOX2 (Figure S6D), both of which are protein kinase C (PKC) activated (*19, 22*). We thus measured extracellular O_2^- levels in the medium of live MDA-MB-231 cells following stimulation with the PKC activator phorbol 12-myristate 13-acetate (PMA). Following PMA addition to control shLZ cells, there is a rapid peak of O_2^- production at 60 sec (Figures S6E), then a second broader wave between 0 and 200 min, peaking at 60 min (Figure 6D). There was no significant between shLZ, sh5 or sh5-NT cells in the 60 sec peak of O_2^- produced in response to PMA (Figure S6E). However, Memo knockdown cells were missing the second wave of O_2^- produced during the 200 min time course and this was restored in the sh5-NT cells (Figure 6D); these data were quantified by measuring the area under the curve (Figure 6D, right panel). The higher amounts of O_2^- produced in the sh5-NT cells compared to control cells, likely reflect the higher Memo levels in the reconstituted cells (Figure 3A). The general NOX inhibitor diphenyleneiodonium chloride (DPI) blocked both basal and PMA-induced O_2^-production (Figure S6F), providing evidence that the O_2^- generated in response to PMA was NOX-mediated. It is tempting to speculate that the ROS visualized in the protrusions is due to NOX activity; however, as these protrusions are not formed following DPI treatment, we were not able to confirm this. In summary, the results suggest that Memo promotes a more oxidized environment in cellular protrusions formed upon stimulation with growth factors and that Memo is required for sustained O_2^- production in response to NOX activation.

Elevated Memo levels in breast cancer correlates with aggressive disease parameters and early events

We know very little about the role of Memo in human tumors, however, Memo has been reported to be overexpressed in a human pancreatic adenocarcinoma cell line (*24*). Moreover, Memo is a target of miR-125, a microRNA that is downregulated early in breast cancer development, at the pre-invasive stage (*25, 26*). To investigate if Memo plays a role in human breast disease, immunohistochemistry (IHC) was carried out on a breast cancer cohort arrayed on tissue microarrays (TMA) (*27, 28*), (Table S1). We determined that Memo levels are low in normal breast tissue and significantly higher > 40% of the tumors (Figure 7A-B).

Memo is present in the cytoplasm and nucleus in normal cells and in breast tumor cells lines (*8*). To examine if the sub-cellular localization of Memo correlates with any clinical or histopathological parameters, we categorized the breast tumor samples according to Memo levels and localization. In this analysis Memo was found at low levels in both the cytoplasm and nucleus of > 90% of normal breast samples and displayed high nuclear Memo in the remaining cases (Figure 7A, normal breast, high). In the tumor samples Memo was found to be low in both the nuclear and cytoplasmic compartments in 56.3%; high in both of these compartments in 23.3%; high exclusively in the cytoplasm (C-Memo) in 6.6%; and high exclusively in the nucleus (N-Memo) in 13.8% (Figure 7C-D; Figure S7A). We next performed a correlation analysis of Memo status with the different molecular subtypes and various clinical and histopathological parameters (Figure 7E; Table S2). As the function of Memo could vary between cellular compartments, a correction for the possible confounding effect of the contribution of C-Memo to the N-Memo analysis, and *vice versa*, was made. A significant correlation was observed between predominantly high C-Memo and many parameters indicative of aggressive disease (high grade, ER/PgR$^-$, Ki67$^+$, ErbB2$^+$ and p53$^+$) (Figure 7E, C-Memo, p value red; Table S2), as well as with the poor-prognosis triple negative (TN) and Luminal B (Lum B) molecular subtypes (*29, 30*). Predominantly high N- Memo inversely associated with poor prognostic factors (high tumor grade, ER/PgR$^-$, and TN tumors) (Figure 7E, N-Memo; Table S2). These dichotomous results explain why none of the examined parameters, except p53$^+$ status, significantly correlate with total Memo staining (Figure 7E; Table S2, Total Memo) and suggest that Memo's

cellular localization can impact on tumor biology. Additionally, in a multivariate logistic regression model, elevated C-Memo retained its correlation with ER/PgR$^-$ and p53$^+$ (odds ratio (OR): 2.87, confidence interval (CI) 95% 1.03-7.98, p-value 0.043; OR: 2.73, CI 95% 1.34-5.57, p-value 0.006; respectively).

Finally, in a time-dependent survival analysis, C-Memo was strongly prognostic of distant metastasis (HR: 3.89, CI 95% 1.16-13.07, p-value 0.028) and overall survival (OS) (HR: 8.36, CI 95% 1.31-53.42, p-value 0.025) within 5 years (Figure 7F, Tables S3-S4), outperforming lymph node status, the single most important indicator of disease-free survival and overall survival in breast cancer (*31*) (Table S4). Given the limited size of the breast subtype groups, we could not evaluate the independent prognostic value of C-Memo with regard to the different molecular subtypes. Nonetheless, these results provide evidence that C-Memo is an independent prognostic factor for more aggressive tumors, with higher risk of early distant recurrence and death.

DISCUSSION

Metastasis is the major cause of breast cancer-related death. Accordingly, studies aimed at understanding the molecular underpinnings of tumor cell spread, as well as their survival and proliferation in metastatic sites, are of utmost importance in order to identify new anti-cancer approaches. Herein we demonstrated that Memo is crucial for breast tumor cell migration, *in vivo* metastasis and is prognostic of poor patient outcome. In addition, we showed that Memo is an oxidase, required for sustained NOX-mediated O_2^- production, and influencing localized ROS levels. Furthermore, loss of Memo altered the redox status of several proteins involved in important biological processes, including migration.

In our study of 407 human breast tumors we found that Memo abundance was prognostic of poor patient outcome. This is noteworthy as the breast cancer patients in the studied cohort generally had a good prognosis. Indeed, 65% had no involved lymph nodes; > 90% are ER/PgR+ and had low grade tumors, and/or had no distant recurrence at 12.1 years. Increased levels of C-Memo, which were observed in ~7% of the tumors, significantly predicted early metastasis

and death, and outperformed nodal status for both outcomes. We propose that Memo's cytoplasmic role is to promote tumor cell motility. In our *in vitro* analyses we have consistently observed that Memo is required for cell motility, be it chemotactic transwell migration (*1, 2, 4*), invasion in 3D matrices or wound closure (this paper). Moreover, we showed herein that tumors with Memo knockdown had significantly fewer motile cells and lung metastatic lesions. How does Memo influence motility and metastasis? As discussed below, we know that Memo has a role in many pathways that influence migration. Related to the new results in this paper, Memo's role in promoting localized ROS production in the lamellae may be important. The NOXs, which have well-established roles in migration (*11, 12, 22*), have been shown to be concentrated in the lamellae of motile cells (*21, 23*). NOX activation contributes to spatially-controlled increases in ROS levels, thereby modulating the function of proteins important for cell motility (*10, 32*). NOXs produce ROS and, in turn, are activated by ROS, suggesting that a positive feed-forward mechanism might amplify O_2^- production. We propose a model (Figure 8) whereby Memo, which is also present at the cell cortex (*8*), influences activity of redox sensitive proteins that are required for sustained activation of specific NOX complexes.

Considering ErbB2-induced migration, the model in which we discovered Memo (*1*), a pathway linking Memo to RhoA-mDia1 and microtubule capture and chemotaxis has been elucidated (*33*). ErbB2-induced phospholipase C gamma has also been shown to converge on Memo and participate in microtubule capture (*13*). Whether RhoA redox status influences its activation in this pathway is not known. Moreover, we have shown that cofilin, an actin regulator is subjected to Memo control (*2*). Taken together, these results suggest, that Memo regulates various pathways that have roles in migration (Figure 8).

Our results also showed that in Memo knockdown cells there are general changes in the redox environment that are reflected in alterations in the RNA levels of enzymes controlling redox homeostasis. These changes were consistent with a more reduced cellular environment in the absence of Memo. This was further reflected in the redox status of RhoA and p52 Shc, both of which showed an increase in their reduced forms in Memo knockdown cells. On the other hand, actin and Rac1, both known to be subject to redox control (*34, 35*) were not altered in Memo knockdown cells. The redox status of a protein is controlled by multiple inputs including ROS concentration, cellular localization, and upstream signaling pathways (*9, 19, 21*). The different

outcome of Memo loss on the examined proteins likely reflects the complex nature of ROS control. Since RhoA activation has been shown to be ROS dependent (*17*) and to lie downstream of NOX (*36*), it is possible that the observed redox changes in RhoA in the absence of Memo reflect alterations in NOX activity. Alternatively, RhoA might be a direct Memo substrate since using recombinant proteins we showed that Memo oxidizes RhoA. Further analyses will be necessary to sort out the pathway by which Memo controls the redox status of cellular proteins.

In the TMA analysis a significant correlation was observed between high cytoplasmic Memo and the proliferative marker Ki67. We have examined normal (*4*) and cancer cell lines (this work) and have not observed an effect of Memo loss on proliferation. It is possible that cultured cell lines cannot respond to Memo levels. However, while Memo knockdown MDA-MB-231 xenografts grew the same as controls, lung metastatic lesions from Memo knockdown tumors were significantly smaller. These results suggest that in the lung environment Memo levels might impact on survival or proliferation.

The data from the TMA also suggested that Memo has distinct roles in different cellular compartments and that elevated nuclear Memo, which was present in approximately 14% of the tumors, correlated with good prognostic parameters. We have not explored Memo's nuclear role, however, Memo has recently been shown to interact with ER and to influence its transcriptional activity (*6*). Moreover, it has been reported that Memo regulates some transcriptional pathways. Indeed, overexpressing Memo in MCF10A cells triggers epithelial-to-mesenchymal transition by upregulating levels of Snail and Zeb1/2 transcription factors (*5*). We did not specifically examine epithelial-to-mesenchymal transition in our analyses, but considering its importance in migration, the results are in line with our studies. It is also interesting to discuss our recent paper showing that Memo conditional knock-out mice have a reduced life-span which is accompanied by other characteristics of premature aging (*3*). It is possible that the reduced lifespan of the mice is related to the redox activity of Memo, but this question remains open.

The crystallization of Memo revealed its structural homology with metal binding enzymes (*7*). Herein we showed that the active site pocket of Memo most likely coordinates a copper ion. The importance of other copper-dependent proteins such as SOD1 (*37*), or indirectly HIF-

1alpha (*38, 39*), in tumor growth and angiogenesis has been documented (*40-42*). We showed that treatment of control MDA-MB-231 cells with the copper chelator TM reduced their ability to invade, however, Memo knockdown cells were not affected, suggesting that Memo might be the major copper-bound enzyme promotin invasion in this model. Early clinical trials with copper chelators are ongoing (http://clinicaltrials.gov/show/NCT00195091) (*43*) and it is tempting to speculate that Memo inhibition might contribute to the anti-tumor effects of these compounds. To conclude, our data suggest that further analyses of Memo's mechanisms of activation, downstream targets and localized functions are warranted, based on its integral role in human metastatic disease and its novel function as a modulator of cellular ROS signaling.

MATERIALS AND METHODS

Ethics Statement

A TMA from 407 female breast cancer patients was analyzed retrospectively under protocols approved by the Institutional Ethical Committee of the European Institute of Oncology. All animal experiments were carried out according Swiss guidelines governing animal experimentation, approved by the Swiss veterinary authorities (Licenses 2286 and 1412).

Reagents and antibodies

Beta1-Heregulin (HRG) was from R&D systems (Minneapolis, MN, USA), 12-myristate 13-acetate (PMA), $CuCl_2$, $CuSO_4$, $(NH_4)_2Fe(SO_4)_2$, $ZnCl_2$, $FeCl_3$, $CoCl_2$, Na_2MoO_4, $MnCl_2$, $CaCl_2$, superoxide dismutase (SOD), doxycycline and ammonium tetrathiomolybdate (TM) were from Sigma (St. Louis, MO, USA). Diphenyleneiodonium Chloride (DPI) was from Millipore (Billerica, MA, USA). Carboxy-H_2DCF-DA, CellROX Deep Red reagent and 4-acetamido-4′-maleimidylstilbene-2,2′-disulfonic acid (AMS) were from Invitrogen (Pailsley, UK). TO-PRO-3 was from Molecular Probes Inc., (Eugene, OR, USA). Growth factor–reduced Matrigel was from BD Biosciences (San Jose, CA, USA). Doxycycline (Dox) chow was from BioServ (Frenchtown, NJ, USA). The monoclonal

mouse anti-human Memo antibody was purified in-house (*2*). Other antibodies: Beta-Actin MAB1501, Rac1 23A8 and Laminin V MAB19562 (Merck Millipore Corporation, Billerica, MA, USA); Vimentin NCL-VIM-V9 (Novocastra Leica Biosystems, Newcastle Upon Tyne, UK); CD31 550274 and GM130 610822 (BD Biosciences, San Jose, California, USA); pHistoneH3 9701 (Cell Signaling Technology, Inc. Danvers, MA, USA), Alpha-Tubulin MS-581-P1 (Thermo Fischer Scientific, Kalamazoo, MI, USA); Ki67 18-0191 and GFP A-11122 (Invitrogen Corporation, Camarillo, CA, USA); ErbB2 21N (*1*); and c-Myc 9E10 sc-40 and RhoA sc-179 (Santa Cruz Biotechnology, Dallas, TX, USA).

Cell culturing and proliferation assays

MDA-MB-231, T47D, SKBR3, HEK293 and HEK293T cells were cultured in DMEM supplemented with 10% fetal calf serum (FCS) (GIBCO Invitrogen, Basel, Switzerland) at 37°C, 5% CO_2. MCF10A-derived lines were cultured in 2D and 3D as described (*14*). For all experiments performed with dox-inducible lines, cells were pre-treated with dox for a minimum of 3 days and treatment was maintained for the duration of the experiment. To measure proliferation, cells were seeded in full growth medium and three wells were counted each day up to 4 days post-plating, using Trypan-blue exclusion, in a Beckman Coulter Vi-Cell counter (Beckman Coulter, Brea, CA, USA).

Vectors and Cloning

For a list of constructs and primers see Table S5. Lentiviral constructs were purchased from Sigma or cloned in house. Synonymous mutations were introduced into the sh5 recognition site of the N-terminally Myc-tagged Memo–construct in pcDNA3.1 (*7*). This construct was further subcloned to produce Myc-Memo-sh5-non targetable (NT)-pLHCX (referred to as sh5-NT). **Lenti- and retroviral infections**

Cells were infected over-night at 37°C with lenti- or retroviral particles at a multiplicity of infection of 2, in the presence of 5 µg/ml polybrene (Sigma). The media was then changed and the cells incubated 24 h at 37°C. Successfully infected cells were selected using puromycin, hygromycin (both from Sigma), or FACS sorted for GFP levels.

Wound-healing and Invasion Assays

Cells were grown to confluency and either maintained in full medium or starved over-night in DMEM containing 0.1% FCS. Monolayers were scratched and wound healing was monitored using a Widefield TILL5x, Axiovert 200M (5% CO_2 and 37°C chamber). Time-lapse images were digitally captured every 20 min with a CCD camera over 8 h. The area recovered by the migrating cells was calculated using ImageJ. Matrigel invasion assays were performed using BD BioCoat Growth Factor Reduced Matrigel Invasion Chambers as per the manufacturer's instructions (Becton Dickinson. Allschwil, Switzerland). Briefly, 2.5 x10^4 MDA-MB-231cells were seeded in the upper chamber in DMEM containing 0.1% BSA. The lower chamber was filled with DMEM containing 10% FCS. TM (1 nM top and bottom chambers) and DPI (5 µM top chamber) were added at the time of seeding. Cells were left to invade for 24 h at which point the upper chambers were cleaned using a cotton swab. Cells on the lower surface of the membrane were fixed with 4% PFA, stained with crystal violet, imaged, and quantified using ImageJ. MCF10A-ErbB2/ErbB3-derived lines were cultured in 3D in the presence of dox and 1.2 nM HRG. After 7 days the cells were fixed, stained for immunofluorescence and imaged as previously described (*14*).

Animal Experiments

All experiments were performed with 6 week old female NOD/SCID mice (Charles River Laboratories, Wilmington, MA, USA); 5×10^5 cells were injected into the second mammary fat pad, or into the tail vein. Mice were sacrificed 28 days post-injection. Lungs and tumors were processed as previously described (*44*). All IHC stainings were done using the Ventana DiscoveryXT biomarker platform. The right lobe of the lung was paraffin embedded and sections were taken every 50 µm, through the entire block and sections were stained using antibodies against human Vimentin or GFP. Tumor sections were stained using antibodies against phospho-HistoneH3 and CD31. Digital slide image data was generated using a slide scanner (Zeiss Mirax, v. 1.12, Zeiss, Germany) at a final magnification comparable to 400x. Whole slide automated quantitative assessment of stained tissue areas were performed using Definiens XD software (version XD 2.0, Definiens AG, Germany) and an in-house developed

image analysis algorithm. Blood burdens were assessed as described (*45*). Single tumor cells from blood were grown in DMEM 20% FBS media and counted 10 days after plating.

Intravital Imaging by Multiphoton Microscopy (IVI-MP)

For IVI-MP experiments, stable or dox-inducible shRNA GFP-expressing cells were injected into the second or fourth mammary fatpad of mice. Inducible lines were cultured in dox-containing medium for 3 days prior to injection. Recipient mice were fed dox-containing chow 2 days prior to injection and for the remainder of the experiment. Orthotopic primary tumors were imaged 5 weeks post injection. The animals were imaged as described previously in (*45*) on a custom-built microscope (*46*).

Cell and tumor lysates

Cells were lysed in Triton X-100 buffer as described (*2*). Tumors were homogenized in NP-40 lysis buffer (*44*) using the Precellys-24 tissue homogenizer in 2mL tubes with ceramic beads (20s at 5500 rpm at 4 °C). The extracts were clarified using a tabletop centrifuge at maximum speed for 20 min at 4°C and protein concentrations determined.

Expression and purification of recombinant proteins

Human Memo cDNA was cloned into pOPINF (*47*) and expressed in BL21(DE3) *E. coli* as described (*48*). Cell pellets were freeze-thawed, resuspended in lysis buffer (50 mM Tris pH 7.5, 500 mM NaCl, 20 mM imidazole 0.2% Tween, Complete EDTA-free protease inhibitor cocktail (Roche), and 3 U/ml Benzoase (Sigma)) and homogenized with the EmulsiFlex-C3 high-pressure homogenizer (Avestin GmbH, Mannheim, Germany). Cleared lysates were batch purified on Ni-NTA beads and bound protein was cleaved by incubating with His-tagged 3C enzyme for 2 h at +4°C in 50 mM Tris pH 7.5, 500 mM NaCl, and 20 mM imidazole. The eluted protein was monitored on ÄKTA Purifier (GE life sciences), concentrated and purified to >96% using sephadex-75 gel filtration in 20 mM Tris pH 7.5, 200 mM NaCl, 0.02% NaN_3. The ultrapure, eluted Memo was concentrated with an Amicon Ultra filtration unit. GST-RhoA in the pxRB096 vector

(provided by Dr. X. Bustelo, University of Salamanca, Spain) was induced in BL21(DE3) *E. coli* using 0.3 mM isopropyl thiogalactopyranoseide (IPTG) for 4 h at 30°C. Cell pellets were freeze-thawed and incubated with BugBuster lysis buffer (Millipore) supplemented with 2 mg lysozyme, 60U benzonase and Complete EDTA-free protease inhibitor cocktail for 20 min at RT. Cleared lysates were batch purified on Glutathione Sepharose 4B resin (GE Healthcare) and the bound GST-RhoA was incubated in thrombin buffer (20 mM Tris-HCl, pH 8.4, 150 mM NaCl, 2.5 mM $CaCl_2$, 15 U biotinylated thrombin (Novagen)). To remove free thrombin, beads were sedimented and the supernatant was incubated with 50 µl Neutravidin beads (Thermo Fischer Scientific) that were then sedimented and the concentration of cleaved RhoA in the supernatant was measured.

qPCR analyses of selected targets

Total RNA was collected from cells using the QIAShredder and RNeasy Mini Kit (Qiagen, Hombrechtikon, Switzerland). cDNA synthesis and amplification was performed using GE Healthcare Ready-to-go You-Prime First-Strand Beads according to the manufacturer's instructions. Quantitative real-time PCR (qPCR) was performed with the Absolute qPCR Master Mix (Thermo Fischer Scientific), SetpOnePlus real-time PCR (Applied Biosystems, Pailsley, UK). Data were normalized to h18S levels. See Table S5 for primer sequences.

Dioxygenase activity measurements

Intra- or extradiol dioxygenase activity was measured as described (*49*). In brief, 400 µM protocatechuic acid was added to each well of a 96- well plate containing either 0.1 nmol Memo or 0.1 nmol Protocatechuate dioxygenase (PD) in 10 mM Tris-HCl pH 8.5. The cleavage of protocatechuic acid was monitored spectrophotometrically by the decrease in absorbance at 290 nm. The absorbance of the blank sample was subtracted from each reading.

Cu(II) reduction assays.

The Cu(II) reduction capacity of 0.1 nmol recombinant Memo was assayed as described (Cell Biolabs, San Diego, CA, USA). The spectrophotometric absorbance at 490 nm was read in a SpectraMax 190 absorbance plate reader (Molecular Devices, Sunnyvale, CA, USA) and correlated to a uric acid standard curve, yielding copper reducing equivalent values (µM CRE). The activity of protein-free samples was subtracted. To measure Memo activity in cells, pcDNA Myc-Memo and Myc-Memo mutants were transiently expressed in HEK293 cells for 72 hrs. Cells were lysed in RIPA buffer, and 500 µg of lysate was loaded onto 50 µl 50% EZ-view Anti-Myc sepharose slurry. Beads with bound Myc-Memo were resuspended in 35 µl 10 mM Tris-HCl, pH 8.5; 5 µl was used for western blot quantification and 30 µl for copper reduction activity measurements. Assays under hypoxic conditions were performed as described above except all buffers were flushed with N_2 for 2 h prior to the assay.

Superoxide detection assays

O_2^- production was determined by using a luminol oxidation assay (Sigma) with slight modifications. In brief, recombinant protein, or $1x10^6$ cells were used per reaction; in some assays 4U of SOD were added. To stimulate NOX activity 1µg/mL PMA was added to cultures; 10 µM DPI was added to block NOX. Values from blank samples, without Memo or PMA, were subtracted from each reading. For short-term (200s) and long-term (220 min) assays, luminol oxidation was measured as relative light units for 10s every 10 s or 30 min, respectively, using a Berthold Centro XS3 LB 960 plate reader (Berthold Technologies GmbH, Bad Wildbad, Germany). For assays done with metal-preloaded recombinant Memo, 50 pmol Memo (5µM final) was incubated with 50µM $CuCl_2$ or $(NH_4)_2Fe(SO_4)_2$ in 50 mM Tris-HCl, pH 6.8 for 30 min at 4°C. Excess metal ions were removed by dialysis against the same buffer for a minimum of 3 h at 4°C. For the assays in Figure S4F-G, the indicated amounts of Memo or Cu(II) were used.

Redox status of recombinant RhoA and other proteins

The oxidation status of cysteine residues in RhoA was determined by quantitative MS. Recombinant RhoA was incubated in the presence or absence of recombinant, Cu(II)-pre-loaded or non-preloaded WT-Memo or H192A-Memo, in 50 mM Tris-HCl, pH 6.8, for 30 min at RT. Then the samples were incubated 30 min at RT in the dark with 35 mM heavy iodoacetamide-$^{13}C_2$, 2-d_2 (heavy IAA) (Sigma). IAA was removed by trichloroacetic acid/acetone precipitation. The remaining oxidized cysteines were reduced with 20 mM Tris(2-carboxyethyl)phosphine hydrochloride (TCEP) for 30 min at RT, then alkylated by 35 mM IAA-$^{12}C_2$ (light IAA). Samples were then digested 6h at 37°C with endoproteinase Lys-C, followed by over-night digestion in trypsin at 37°C. Diluted samples were applied on an EASY n-LC 1000 liquid chromatography system, coupled to a LTQ Orbitrap Velos MS (both from Thermo Scientific). Quantitative analysis of the ratio light/heavy IAA incorporation was done with ProgenesisLC (Nonlinear Dynamics, Durham, NC, USA).

For intracellular redox status of different proteins, cells were harvested in PBS with inhibitors, then sonicated and supernatants collected. Equal amounts of protein extracts were treated 30 min at RT with 15 mM AMS. Samples were separated by 15% non-reducing and reducing SDS-PAGE.

Detection of intracellular ROS levels

For quantification of ROS levels by FACS, cells were washed 2 times with PBS and incubated with 20 µM carboxy-H_2DCF-DA in PBS for 10 min at 37°C. Cells were then washed 2 times, trypsinized, resuspended in PBS with 10% FCS, spun down for 3.5 min and resuspended in PBS with 0.1% BSA. Samples were then analyzed using a BD LSRII SORP (BD Biosciences). For quantification of ROS levels by imaging, growing or serum-starved cells, stimulated as indicated, were cultured in 5 µM CellROX Deep Red reagent. Then cells were incubated at 37°C for 30 min, washed with growth medium and imaged at excitation/emission maxima 640/665nm in a temperature and CO_2 controlled chamber using an OlympusIX81 spinning-disk microscope driven by Metamorph 7.7.10.0 software (Molecular Devices, Sunnyvale, CA, USA).

CellROX intensities in cell protrusions were measured and quantified relative to the total ROS levels in the cell, using ImageJ.

Analyses of breast cancer TMAs

Clinical and pathological characteristics of 407 female breast cancers (*27, 28, 50*) are shown in Table S1 and Table S2. Stainings for Memo were performed on 2 µm sections, using the EnVision Plus/HRP system (DAKO). The specificity of the Memo antibody was verified by staining breast tumor cells lines with Memo overexpression or Memo knockdown (Figure S7B). For scoring, a semi-quantitative approach with scores ranging from 0 to 3 was used. For the correlation analyses of Memo abundance with clinical parameters, 3 categories were defined: Total Memo, considering Memo levels in the nucleus and/or the cytoplasm; C-Memo, considering only cytoplasmic Memo; and N-Memo, considering only nuclear Memo. Memo scores in normal tissue (n=32) ranged between 0 and 1.0; tumor samples with IHC scores > 1.0 were considered high; those ≤ 1.0 were considered low.

Association between clinical parameters at surgery and probability of high Total Memo was evaluated by univariate analysis. To control for possible confounding effects of the contribution of C-Memo to N-Memo, and vice versa, the association of clinical variables with the probability of high C-Memo and high N-Memo was evaluated by bivariate logistic regression models, adjusted for N-Memo or C-Memo, respectively. The impact of patients' characteristics on the probability of high C-Memo or N-Memo (adjusted for N-Memo or C-Memo, respectively) was also assessed by multivariable logistic regression models adjusted for ER/PgR, Ki-67, ErbB2, p53, grade, and histology, and is expressed as odds ratios (ORs) with 95% confidence interval (CI). A time-dependent multivariable Cox model was used to estimate the hazard ratios (HRs) comparing C-Memo high vs low within 5 years and after 5 years from surgery, controlled for age at diagnosis, tumor size, lymph node status, grade, and status of ER/PgR, ErbB2, p53 and Ki-67, as well as N-Memo, when evaluating C-Memo and C-Memo, when evaluating N-Memo. SAS statistical software was used for all analyses (SAS Institute, Inc., Cary NC).

Statistical Methods

Unless stated otherwise, statistical significance of data following a normal distribution, as determined by the Shapiro-Wilk normality test, was determined using an unpaired, two-tailed Student's t–test, assuming unequal variances or a one-way ANOVA followed by Tukey's post-hoc test for multiple comparisons. Data that failed the normality test was analyzed using the Wilcoxon-Rank Sum Test (one and two-condition comparisons), or the Kruskal-Wallis test followed by Dunn's post-hoc test for multiple comparisons. Differences were considered significant if the p-value was ≤0.05; * $p \leq 0.05$, ** $p < 0.01$, *** $p < 0.001$, for all tests.

SUPPLEMENTARY MATERIALS

Figure S1. Memo is required for cellular migration and invasion; Memo overexpression is not transforming.

Figure S2. Memo does not affect *in vitro* cellular proliferation or primary tumor outgrowth, but may affect the survival or proliferation of disseminated tumor cells in the lungs.

Figure S3. Reconstitution of Memo restores invasion and tumor cell migration *in vivo*.

Figure S4. Analyses of Memo activity.

Figure S5. Memo influences the intracellular redox status.

Figure S6. Analysis of ROS and selected RNAs in Memo KD cell lines.

Figure S7. Memo immunohistochemistry.

Table S1, Clinico-pathological characteristics of the breast cancer cohort analyzed for Memo abundance.

Table S2, Correlations between Memo status and clinical and pathological parameters in the breast cancer cohort.

Table S3, Observed events in the breast cancer cohort.

Table S4, A Time-dependent multivariable Cox model to measure Hazard Ratios.

Table S5, Sequences of all primers and oligos used for cloning and qPCR.

Movie 1, shLZ tumor cell motility.

Movie 2, sh5 tumor cell protrusions.

Movie 3, sh5-NT tumor cell motility

REFERENCES

1. R. Marone, D. Hess, D. Dankort, W. J. Muller, N. E. Hynes, A. Badache, Memo mediates ErbB2-driven cell motility. *Nature cell biology* 6, 515-522 (2004).
2. M. Meira, R. Masson, I. Stagljar, S. Lienhard, F. Maurer, A. Boulay, N. E. Hynes, Memo is a cofilin-interacting protein that influences PLCgamma1 and cofilin activities, and is essential for maintaining directionality during ErbB2-induced tumor-cell migration. *Journal of cell science* 122, 787-797 (2009).
3. B. Haenzi, O. Bonny, R. Masson, S. Lienhard, J. H. Dey, O. M. Kuro, N. E. Hynes, Loss of Memo, a novel FGFR regulator, results in reduced lifespan. *FASEB journal : official publication of the Federation of American Societies for Experimental Biology*, (2013).
4. S. Kondo, A. Bottos, J. C. Allegood, R. Masson, F. G. Maurer, C. Genoud, P. Kaeser, A. Huwiler, M. Murakami, S. Spiegel, N. E. Hynes, Memo Has a Novel Role in S1P Signaling and Crucial for Vascular Development. *PloS one* 9, e94114 (2014).
5. A. V. Sorokin, J. Chen, MEMO1, a new IRS1-interacting protein, induces epithelial-mesenchymal transition in mammary epithelial cells. *Oncogene* 32, 3130-3138 (2013).
6. K. Jiang, Z. Yang, L. Cheng, S. Wang, K. Ning, L. Zhou, J. Lin, H. Zhong, L. Wang, Y. Li, J. Huang, H. Zhang, Q. Ye, Memo Promotes Extranuclear Estrogen Receptor Signaling Involving the Growth Factor Receptors IGF1R and ErbB2. *The Journal of biological chemistry*, (2013).
7. C. Qiu, S. Lienhard, N. E. Hynes, A. Badache, D. J. Leahy, Memo is homologous to nonheme iron dioxygenases and binds an ErbB2-derived phosphopeptide in its vestigial active site. *The Journal of biological chemistry* 283, 2734-2740 (2008).
8. I. D. Schlatter, M. Meira, V. Ueberschlag, D. Hoepfner, R. Movva, N. E. Hynes, MHO1, an evolutionarily conserved gene, is synthetic lethal with PLC1; Mho1p has a role in invasive growth. *PloS one* 7, e32501 (2012).
9. E. A. Veal, A. M. Day, B. A. Morgan, Hydrogen peroxide sensing and signaling. *Molecular cell* 26, 1-14 (2007).
10. K. Block, Y. Gorin, Aiding and abetting roles of NOX oxidases in cellular transformation. *Nature reviews. Cancer* 12, 627-637 (2012).
11. T. R. Hurd, M. DeGennaro, R. Lehmann, Redox regulation of cell migration and adhesion. *Trends in cell biology* 22, 107-115 (2012).
12. B. Diaz, S. A. Courtneidge, Redox signaling at invasive microdomains in cancer cells. *Free radical biology & medicine* 52, 247-256 (2012).
13. K. Benseddik, N. Sen Nkwe, P. Daou, P. Verdier-Pinard, A. Badache, ErbB2-dependent chemotaxis requires microtubule capture and stabilization coordinated by distinct signaling pathways. *PloS one* 8, e55211 (2013).

14. N. Aceto, N. Sausgruber, H. Brinkhaus, D. Gaidatzis, G. Martiny-Baron, G. Mazzarol, S. Confalonieri, M. Quarto, G. Hu, P. J. Balwierz, M. Pachkov, S. J. Elledge, E. van Nimwegen, M. B. Stadler, M. Bentires-Alj, Tyrosine phosphatase SHP2 promotes breast cancer progression and maintains tumor-initiating cells via activation of key transcription factors and a positive feedback signaling loop. *Nature medicine* 18, 529-537 (2012).
15. Y. Matsuda, T. Schlange, E. J. Oakeley, A. Boulay, N. E. Hynes, WNT signaling enhances breast cancer cell motility and blockade of the WNT pathway by sFRP1 suppresses MDA-MB-231 xenograft growth. *Breast cancer research : BCR* 11, R32 (2009).
16. K. Zaoui, S. Honore, D. Isnardon, D. Braguer, A. Badache, Memo-RhoA-mDia1 signaling controls microtubules, the actin network, and adhesion site formation in migrating cells. *The Journal of cell biology* 183, 401-408 (2008).
17. A. Aghajanian, E. S. Wittchen, S. L. Campbell, K. Burridge, Direct activation of RhoA by reactive oxygen species requires a redox-sensitive motif. *PloS one* 4, e8045 (2009).
18. J. Heo, S. L. Campbell, Mechanism of redox-mediated guanine nucleotide exchange on redox-active Rho GTPases. *The Journal of biological chemistry* 280, 31003-31010 (2005).
19. N. Y. Spencer, J. F. Engelhardt, The basic biology of redoxosomes in cytokine-mediated signal transduction and implications for disease-specific therapies. *Biochemistry* 53, 1551-1564 (2014).
20. M. Ushio-Fukai, Compartmentalization of redox signaling through NADPH oxidase-derived ROS. *Antioxidants & redox signaling* 11, 1289-1299 (2009).
21. M. Ushio-Fukai, Localizing NADPH oxidase-derived ROS. *Sci STKE* 2006, re8 (2006).
22. K. Bedard, K. H. Krause, The NOX family of ROS-generating NADPH oxidases: physiology and pathophysiology. *Physiological reviews* 87, 245-313 (2007).
23. R. F. Wu, Y. C. Xu, Z. Ma, F. E. Nwariaku, G. A. Sarosi, Jr., L. S. Terada, Subcellular targeting of oxidants during endothelial cell migration. *The Journal of cell biology* 171, 893-904 (2005).
24. T. Kalinina, C. Gungor, S. Thieltges, M. Moller-Krull, E. M. Penas, D. Wicklein, T. Streichert, U. Schumacher, V. Kalinin, R. Simon, B. Otto, J. Dierlamm, H. Schwarzenbach, K. E. Effenberger, M. Bockhorn, J. R. Izbicki, E. F. Yekebas, Establishment and characterization of a new human pancreatic adenocarcinoma cell line with high metastatic potential to the lung. *BMC cancer* 10, 295 (2010).
25. B. N. Hannafon, P. Sebastiani, A. de las Morenas, J. Lu, C. L. Rosenberg, Expression of microRNA and their gene targets are dysregulated in preinvasive breast cancer. *Breast cancer research : BCR* 13, R24 (2011).
26. M. V. Iorio, M. Ferracin, C. G. Liu, A. Veronese, R. Spizzo, S. Sabbioni, E. Magri, M. Pedriali, M. Fabbri, M. Campiglio, S. Menard, J. P. Palazzo, A. Rosenberg, P. Musiani, S. Volinia, I. Nenci, G. A. Calin, P. Querzoli, M. Negrini, C. M. Croce, MicroRNA gene expression deregulation in human breast cancer. *Cancer research* 65, 7065-7070 (2005).

27. U. Veronesi, G. Paganelli, G. Viale, A. Luini, S. Zurrida, V. Galimberti, M. Intra, P. Veronesi, C. Robertson, P. Maisonneuve, G. Renne, C. De Cicco, F. De Lucia, R. Gennari, A randomized comparison of sentinel-node biopsy with routine axillary dissection in breast cancer. *The New England journal of medicine* 349, 546-553 (2003).
28. S. Confalonieri, M. Quarto, G. Goisis, P. Nuciforo, M. Donzelli, G. Jodice, G. Pelosi, G. Viale, S. Pece, P. P. Di Fiore, Alterations of ubiquitin ligases in human cancer and their association with the natural history of the tumor. *Oncogene* 28, 2959-2968 (2009).
29. C. M. Perou, T. Sorlie, M. B. Eisen, M. van de Rijn, S. S. Jeffrey, C. A. Rees, J. R. Pollack, D. T. Ross, H. Johnsen, L. A. Akslen, O. Fluge, A. Pergamenschikov, C. Williams, S. X. Zhu, P. E. Lonning, A. L. Borresen-Dale, P. O. Brown, D. Botstein, Molecular portraits of human breast tumours. *Nature* 406, 747-752 (2000).
30. T. Sorlie, C. M. Perou, R. Tibshirani, T. Aas, S. Geisler, H. Johnsen, T. Hastie, M. B. Eisen, M. van de Rijn, S. S. Jeffrey, T. Thorsen, H. Quist, J. C. Matese, P. O. Brown, D. Botstein, P. E. Lonning, A. L. Borresen-Dale, Gene expression patterns of breast carcinomas distinguish tumor subclasses with clinical implications. *Proceedings of the National Academy of Sciences of the United States of America* 98, 10869-10874 (2001).
31. P. L. Fitzgibbons, D. L. Page, D. Weaver, A. D. Thor, D. C. Allred, G. M. Clark, S. G. Ruby, F. O'Malley, J. F. Simpson, J. L. Connolly, D. F. Hayes, S. B. Edge, A. Lichter, S. J. Schnitt, Prognostic factors in breast cancer. College of American Pathologists Consensus Statement 1999. *Archives of pathology & laboratory medicine* 124, 966-978 (2000).
32. A. Corcoran, T. G. Cotter, Redox regulation of protein kinases. *The FEBS journal* 280, 1944-1965 (2013).
33. K. Zaoui, K. Benseddik, P. Daou, D. Salaun, A. Badache, ErbB2 receptor controls microtubule capture by recruiting ACF7 to the plasma membrane of migrating cells. *Proceedings of the National Academy of Sciences of the United States of America* 107, 18517-18522 (2010).
34. R. J. Hung, C. W. Pak, J. R. Terman, Direct redox regulation of F-actin assembly and disassembly by Mical. *Science* 334, 1710-1713 (2011).
35. M. M. Harraz, J. J. Marden, W. Zhou, Y. Zhang, A. Williams, V. S. Sharov, K. Nelson, M. Luo, H. Paulson, C. Schoneich, J. F. Engelhardt, SOD1 mutations disrupt redox-sensitive Rac regulation of NADPH oxidase in a familial ALS model. *The Journal of clinical investigation* 118, 659-670 (2008).
36. Y. Zhang, F. Peng, B. Gao, A. J. Ingram, J. C. Krepinsky, High glucose-induced RhoA activation requires caveolae and PKCbeta1-mediated ROS generation. *Am J Physiol Renal Physiol* 302, F159-172 (2012).
37. J. C. Juarez, O. Betancourt, Jr., S. R. Pirie-Shepherd, X. Guan, M. L. Price, D. E. Shaw, A. P. Mazar, F. Donate, Copper binding by tetrathiomolybdate attenuates angiogenesis and tumor cell proliferation through the inhibition of superoxide dismutase 1. *Clinical cancer*

research : an official journal of the American Association for Cancer Research 12, 4974-4982 (2006).

38. F. Martin, T. Linden, D. M. Katschinski, F. Oehme, I. Flamme, C. K. Mukhopadhyay, K. Eckhardt, J. Troger, S. Barth, G. Camenisch, R. H. Wenger, Copper-dependent activation of hypoxia-inducible factor (HIF)-1: implications for ceruloplasmin regulation. *Blood* 105, 4613-4619 (2005).
39. W. Feng, F. Ye, W. Xue, Z. Zhou, Y. J. Kang, Copper regulation of hypoxia-inducible factor-1 activity. *Molecular pharmacology* 75, 174-182 (2009).
40. Q. Pan, D. T. Rosenthal, L. Bao, C. G. Kleer, S. D. Merajver, Antiangiogenic tetrathiomolybdate protects against Her2/neu-induced breast carcinoma by hypoplastic remodeling of the mammary gland. *Clinical cancer research : an official journal of the American Association for Cancer Research* 15, 7441-7446 (2009).
41. L. Finney, S. Vogt, T. Fukai, D. Glesne, Copper and angiogenesis: unravelling a relationship key to cancer progression. *Clinical and experimental pharmacology & physiology* 36, 88-94 (2009).
42. S. A. Lowndes, A. L. Harris, The role of copper in tumour angiogenesis. *Journal of mammary gland biology and neoplasia* 10, 299-310 (2005).
43. S. Jain, J. Cohen, M. M. Ward, N. Kornhauser, E. Chuang, T. Cigler, A. Moore, D. Donovan, C. Lam, M. V. Cobham, S. Schneider, S. M. Hurtado Rua, S. Benkert, C. Mathijsen Greenwood, R. Zelkowitz, J. D. Warren, M. E. Lane, V. Mittal, S. Rafii, L. T. Vahdat, Tetrathiomolybdate-associated copper depletion decreases circulating endothelial progenitor cells in women with breast cancer at high risk of relapse. *Annals of oncology : official journal of the European Society for Medical Oncology / ESMO* 24, 1491-1498 (2013).
44. J. H. Dey, F. Bianchi, J. Voshol, D. Bonenfant, E. J. Oakeley, N. E. Hynes, Targeting fibroblast growth factor receptors blocks PI3K/AKT signaling, induces apoptosis, and impairs mammary tumor outgrowth and metastasis. *Cancer research* 70, 4151-4162 (2010).
45. T. Smirnova, Z. N. Zhou, R. J. Flinn, J. Wyckoff, P. J. Boimel, M. Pozzuto, S. J. Coniglio, J. M. Backer, A. R. Bresnick, J. S. Condeelis, N. E. Hynes, J. E. Segall, Phosphoinositide 3-kinase signaling is critical for ErbB3-driven breast cancer cell motility and metastasis. *Oncogene* 31, 706-715 (2012).
46. L. Bonapace, J. Wyckoff, T. Oertner, J. Van Rheenen, T. Junt, M. Bentires-Alj, If you don't look, you won't see: intravital multiphoton imaging of primary and metastatic breast cancer. *Journal of mammary gland biology and neoplasia* 17, 125-129 (2012).
47. N. S. Berrow, D. Alderton, S. Sainsbury, J. Nettleship, R. Assenberg, N. Rahman, D. I. Stuart, R. J. Owens, A versatile ligation-independent cloning method suitable for high-throughput expression screening applications. *Nucleic acids research* 35, e45 (2007).
48. F. W. Studier, Protein production by auto-induction in high density shaking cultures. *Protein expression and purification* 41, 207-234 (2005).

49. M. Wojtas-Wasilewska, J. Trojanowski, Purification and properties of protocatechuate 3,4-dioxygenase from Chaetomium piluliferum induced with p-hydroxybenzoic acid. *Acta biochimica Polonica* 27, 21-34 (1980).
50. I. N. Colaluca, D. Tosoni, P. Nuciforo, F. Senic-Matuglia, V. Galimberti, G. Viale, S. Pece, P. P. Di Fiore, NUMB controls p53 tumour suppressor activity. *Nature* 451, 76-80 (2008).

Acknowledgements: We thank Dr. O. Pertz, Dr. S. Kondo and all members of the Hynes lab for fruitful discussions. We thank C. Luise for excellent technical assistance, Drs. P. Maisonneuve, S. Confalonieri, E. Dama and G. d'Ario for advice on the statistical analysis and Dr. G. Viale for human tissue samples. **Funding:** NEH was supported by grants from Susan G. Komen for the Cure SAC110041; SNF 310030A-121574 and 310030B-138674 and KFS 02528-02-2010 and the Novartis Research Foundation. PPDF was supported by grants from the Associazione Italiana per la Ricerca sul Cancro, from the Italian Ministries of Education-University-Research (MIUR) and of Health, the Monzino Foundation, and the European Research Council. AB was supported by Fondation ARC and INCa-DGOS-Inserm 6038. **Author contributions**: G.M.D, I.N., M. V. and N.E.H planned and wrote the paper; G.M,D, I.N. T.S., N.A., A.D, S.L., J.W., D.H., J.S., J.J.K., H.G., A.F., and D.S. planned and performed experiments; D.D. performed the statistical analysis of the breast tumor TMA; M.V., G.M. and P.P.D.F.created and performed the IHC analysis of the breast tumor TMA; M.B-A. and A.B. provided material, expertise and discussions over the course of the experiments and the preparation of the paper; **Competing interests**: the authors declare that they have no competing interests.

FIGURES

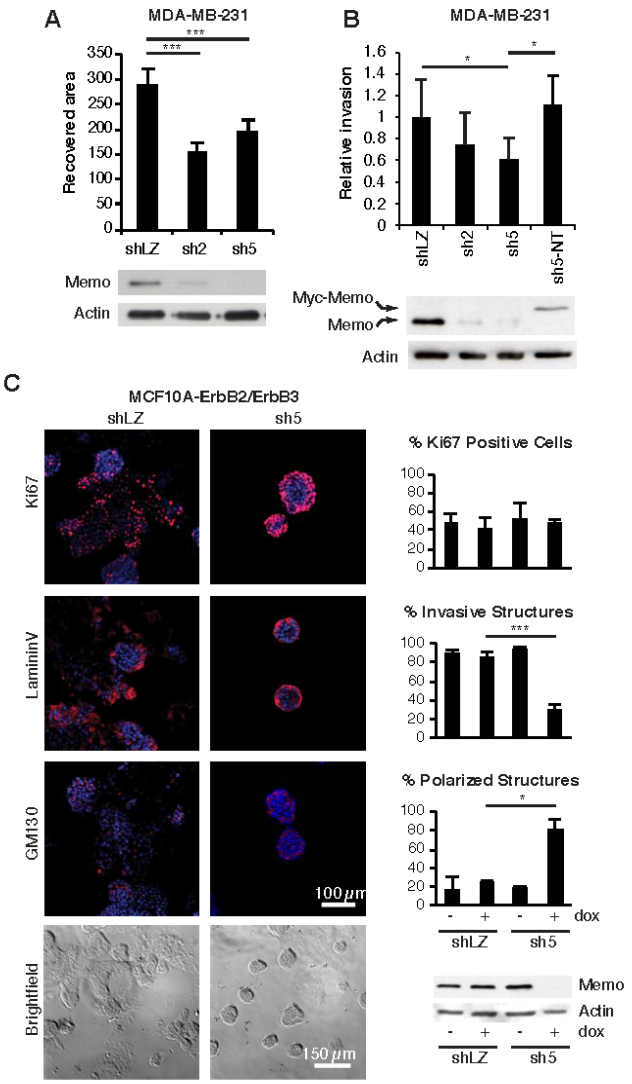

Figure 1. Memo is needed for migration and invasion in vitro. (A) Relative wound closure of MDA-MB-231 control shLZ and Memo knockdown (KD) sh2 and sh5 cells, grown in full medium. Data represent means ± SD of 6 fields. Western blot analysis of Memo levels is shown below. (B) Invasion of MDA-MB-231 shLZ control, Memo KD sh2 and sh5 cells, and sh5 non-targeting Memo-reconstituted cells (sh5-NT), through matrigel-coated Boyden chambers. Data represent means ± SD (n=4-8 chambers per condition). Western blot analysis of Memo levels is shown below. (C) Confocal images of MCF10A-ErbB2/ErbB3 inducible shLZ and sh5 cells grown in 3D culture in the presence of doxycycline (dox). Images are representative of 3 independent experiments. The percentages of Ki67-positive cells, invasive structures, and polarized structures were quantified. Data represent average percentages ± SEM (n=5 wells per condition). Western blot analysis of Memo levels is shown below.

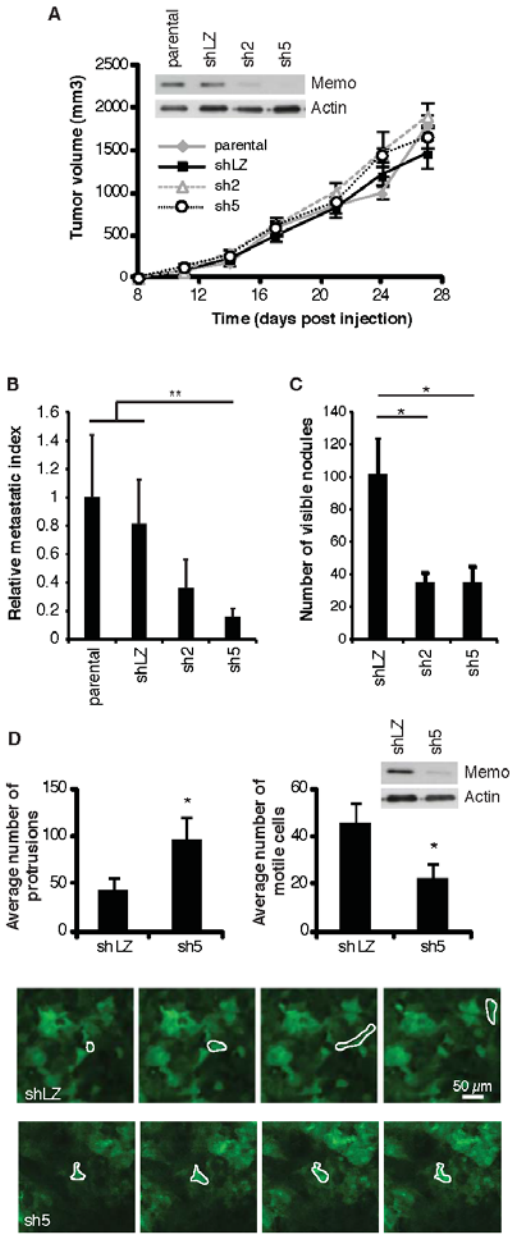

Figure 2. Memo is required for invasion and tumor cell migration *in vivo*. (A) Orthotopic tumor growth of MDA-MB-231 control (parental and shLZ) and Memo KD (sh2 and sh5) cells in mice. Curves are the mean tumor volumes ± SEM (n=8 mice per group). Inset: Western blot analysis of Memo levels in injected cells. (B) Relative number of spontaneous lung metastases per unit lung area, normalized to final tumor mass (Metastatic index), in the animals described in (A). Data are the means ± SEM (n=8 mice per group). For statistical analyses, each shMemo group was compared to the combined parental and shLZ control groups. (C) Average number of tail-vein derived lung surface metastases ± SEM 4 weeks post-injection (n=6-10 mice per group). (D) Intravital time-lapse imaging of orthotopic tumors from GFP-labeled MDA-MB-231 shLZ and sh5 cells. The average numbers of cells extending protrusions and motile cells were determined per z-stack. Data are the means ± SEM of 7-8 separate z-stacks (n=3 mice per group). Inset: Western blot analysis of Memo levels in injected cells. Lower panels: one motile shLZ tumor cell is outlined, frames are 4 min apart; one protruding sh5 tumor cell is outlined, frames are at 0, 8, 22 and 28 min.

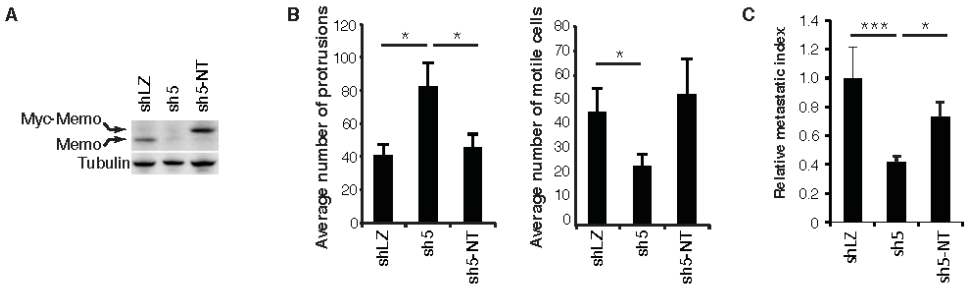

Figure 3. Reconstitution of Memo expression rescues tumor cell migration and invasion *in vivo*. (A) Western blot analysis of Memo levels in control shLZ, Memo sh5 KD and sh5 non-targeting Memo reconstituted cells (sh5-NT). (B) Intravital time-lapse imaging of orthotopic tumors from GFP-labeled MDA-MB-231 shLZ, sh5 and sh5-NT cells. The average numbers of cells extending protrusions (left graph) and motile cells (right graph) were determined per z-stack. Data are the means ± SEM of 7-8 separate z-stacks (n=3-5 mice per group). (C) Relative number of spontaneous lung metastases per unit lung area, normalized to final tumor mass (Metastatic index), from mice with orthotopic MDA-MB-231 shLZ, sh5 and sh5-NT MDA-MB-231-derived tumors. Data are the means ± SEM (n= mice per group).

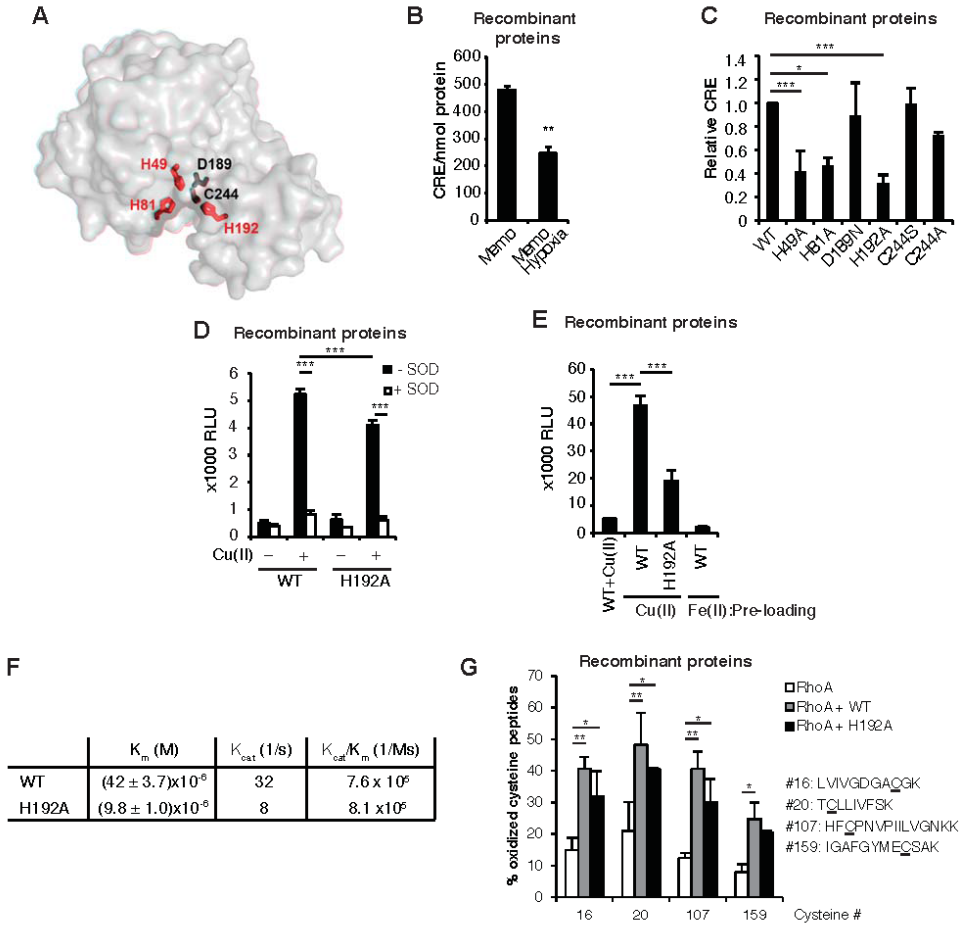

Figure 4. Memo has copper-dependent redox activity. (A) Structural model of Memo showing the putative active site pocket and residues (*7*). Histidine residues required for copper binding are shown in red. (B) Cu(II) reduction assay, measured as μM Cu(II) reducing equivalents (CRE) per nmol purified protein, in normoxic and hypoxic conditions. (C) Cu(II) reduction assay with Memo mutants, measured as CRE normalized to wild-type (WT) (normoxic conditions). (D) O_2^- production by WT or H192A Memo in the presence or absence of 50 μM $CuCl_2$ and 4U SOD, measured as relative light units (RLU). (E) O_2^- production by WT or H192A Memo, pre-loaded with the indicated metal or assayed in the presence of Cu(II). (F) Enzymatic properties of WT and H192A Memo during the generation of O_2^- using $CuCl_2$ as a substrate (K_m, substrate affinity; K_{cat}. substrate turnover; K_{cat}/K_m, enzymatic efficiency). K_{cat} was determined from figure S4G and is the maximum number of Cu(II) molecules converted per 50 nmol protein per 10 s. (G) Quantitative mass spectrometric analysis of the oxidation state of 4 cysteines in the indicated RhoA peptides. All data represent means ± SD of 4 independent experiments.

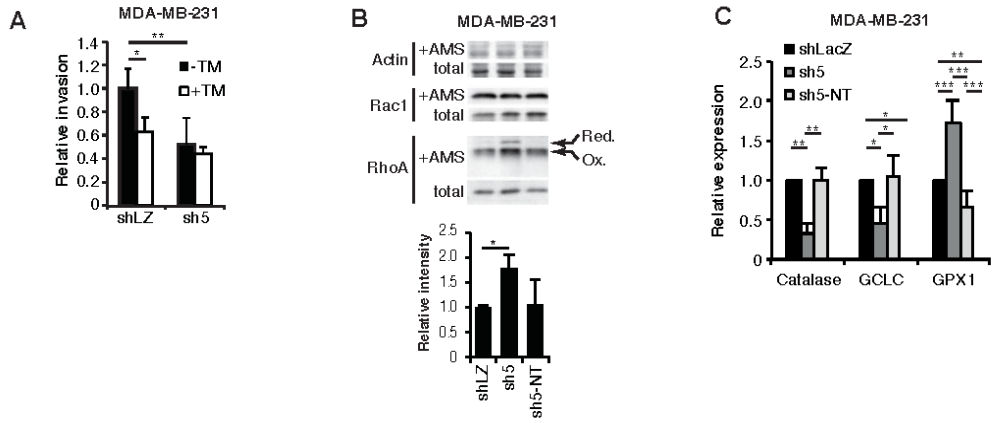

Figure 5. Memo influences the intracellular redox status. (A) Invasion of MDA-MB-231 control shLZ and Memo KD sh5 cells treated with 1 nM tetrathiomolybdate (TM), through matrigel-coated Boyden chambers. Data represent means ± SD (n=4 chambers per condition). (B) Western blot analysis of levels of reduced and total actin, Rac1 and RhoA in lysates incubated with AMS. Quantification of reduced RhoA, relative to total and normalized to shLZ, is shown below. Data represent means ± SD of 4 independent experiments. (D) Relative abundance of mRNAs encoding catalase, GCLC, and GPx1 in the indicated MDA-MB-231 cell lines. Data represent means ± SD of 6 independent experiments.

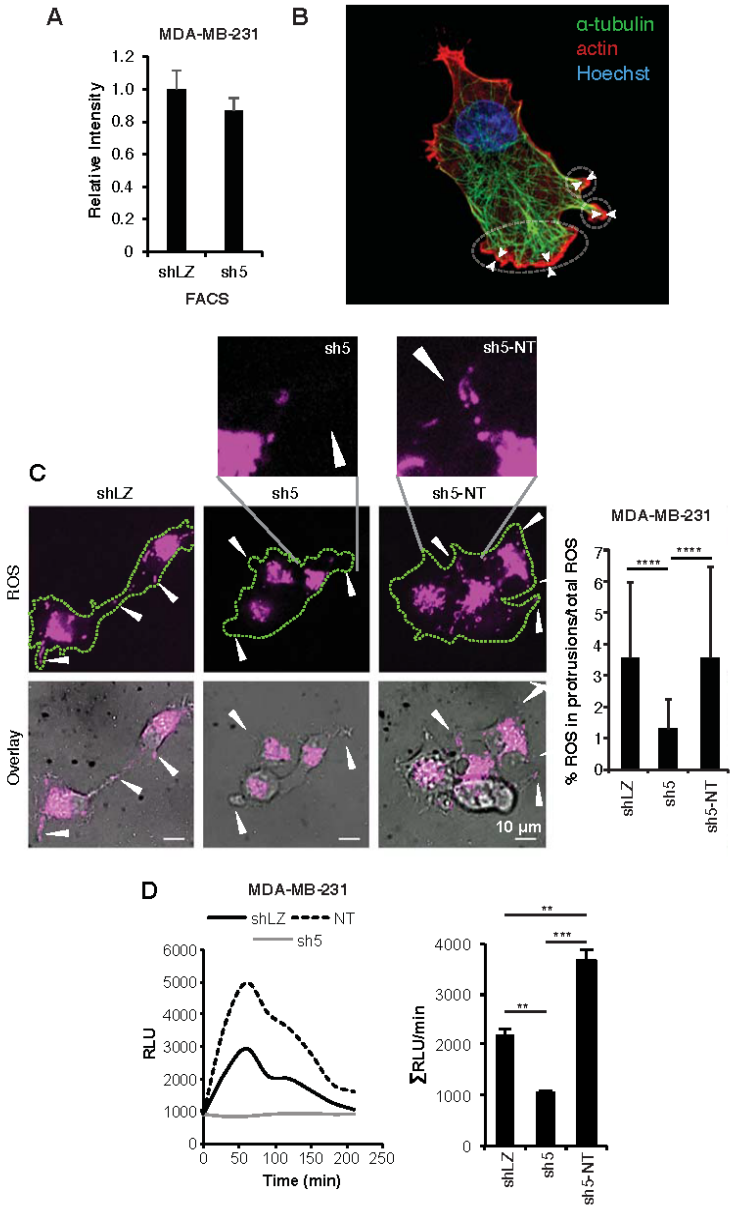

Figure 6. Memo regulates ROS levels in cellular protrusions and NOX-mediated O_2^- production. (A) Intracelllular ROS levels in MDA-MB-231 shLZ and sh5 Memo KD cells under normal growth conditions as determined by carboxy-H_2DCF-DA treatment followed by FACS. Data represent means ± SD of 3 biological replicates from 2 independent experiments. (B) MDA-MB-231 cell stained to visualize the nucleus (blue), microtubules (green) and actin (red). Protrusions (lamellae) are circled. The lamellipodia, actin-rich structures at the leading edge of the protrusion, are indicated by the white arrows. (C) CellROX staining of MDA-MB-231 shLZ control, sh5 Memo KD, and sh5-NT Memo reconstituted cells, after starvation and serum stimulation. Outlines indicate cell boundaries, arrows indicate protrusions (for magnifications see upper images). Images are representative of 3 independent experiments. The percentage of ROS present in protrusions relative to total intracellular ROS levels were quantified (graph, right). Data represent means ± SD (n=16 images/group). (C) Representative graph of long-term NOX activity, as measured by O_2^- production (relative light units, RLU), upon PMA stimulation of MDA-MB-231 shLZ, sh5, and sh5-NT cells (left). The area under the curve was quantified (right). Data represent means ± SD of 3 independent experiments.

A

Total Memo Expression

Tissue Type	Low (≤ 1.0)	High (> 1.0)	Total	p-value
Normal breast	29 (90.6%)	3 (9.4%)	32	0.0001
Breast cancer	229 (56.3%)	178 (43.7%)	407	

B

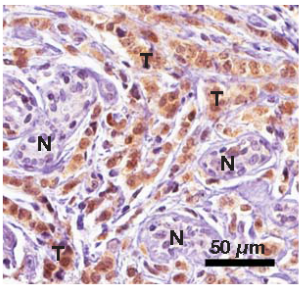

C

C-Memo \ N-Memo	Low (%)	High (%)	Total (%)
Low (%)	229 (56.3)	56 (13.8)	285 (70.0)
High (%)	27 (6.6)	95 (23.3)	122 (30.0)
Total (%)	256 (62.9)	151 (37.1)	407 (100.0)

p-value chi-square test: <0.0001

D

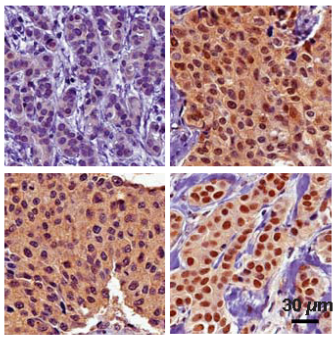

E

Variable	Total Memo (£) High vs Low OR	p	C-Memo (*) High vs Low OR	p	N-Memo ($) High vs Low OR	p
Grade						
2 vs 1	1.1	0.693	1.8	0.07	0.74	0.302
3 vs 1	0.92	0.765	2.93	0.007	0.34	0.005
ER/PgR - vs +	1.14	0.737	3.91	0.004	0.27	0.011
ErbB2 + vs -	0.97	0.943	3.36	0.028	0.33	0.067
Ki-67 ≥14% vs <14%	1.36	0.129	2.17	0.005	0.76	0.278
p53 ≥16% vs <16%	1.73	0.045	3.03	0.001	0.71	0.330
Subtype						
Lum B Ki67 High vs Lum A	1.29	0.238	1.69	0.07	0.9	0.706
Lum B ErbB2+ vs Lum A	1.32	0.609	5.51	0.012	0.34	0.123
ErbB2+ vs Lum A	0.75	0.748	4.55	0.139	0.15	0.138
TN vs Lum A	1.51	0.367	6.32	0.001	0.23	0.018

F

	Distant metastasis C-Memo High vs Low HR (95% CI)	p	Distant metastasis N-Memo High vs Low HR (95% CI)	p	Overall survival C-Memo High vs Low HR (95% CI)	p	Overall survival N-Memo High vs Low HR (95% CI)	p
≤ 5 years	3.89 (1.16;13.07)	0.028	0.44 (0.13;1.53)	0.2	8.36 (1.31;53.42)	0.025	0.38 (0.07;2.1)	0.27
> 5 years	0.44 (0.11;1.8)	0.25	0.57 (0.16;2.01)	0.38	1.05 (0.45;2.43)	0.92	0.54 (0.23;1.28)	0.16

Figure 7. Memo expression is upregulated in breast cancer and is correlated with aggressive disease. (A) IHC quantification of Memo in human normal and breast cancer samples. The number and percentage of samples with low and high Memo levels are shown. Statistical analysis was performed by Contingency Table analysis with Fisher's Exact Test (JMP 10). (B) An example of Memo expression in non-neoplastic (N) and invasive tumor (T) structures within the same core. (C) Distribution of the number of cases displaying low and high C- and N-Memo. C- and N-Memo levels are significantly correlated (p<0.0001). (D) Examples of C- and N-Memo staining. (E) Correlation between high total Memo (cytoplasm and/or nucleus), C-Memo and N-Memo with patients' clinical and histopathological parameters at surgery. £: the OR and p-value of the univariate logistic regression model, high total Memo. *: the OR and p-value of the bivariate logistic regression model, high C-Memo adjusted for N-Memo. $: the OR and p-value of the bivariate logistic regression model, high N-Memo adjusted for C-Memo. (F) Multivariate analysis of high C- or N-Memo with distant metastasis and OS. The HRs comparing C- or N-Memo high vs low were estimated with a multivariable Cox proportional hazards model, controlled for clinical and histopathological parameters at surgery within 5 years (≤ 5 years) and after 5 years (> 5 years) from surgery. Significant p-values are indicated in red.

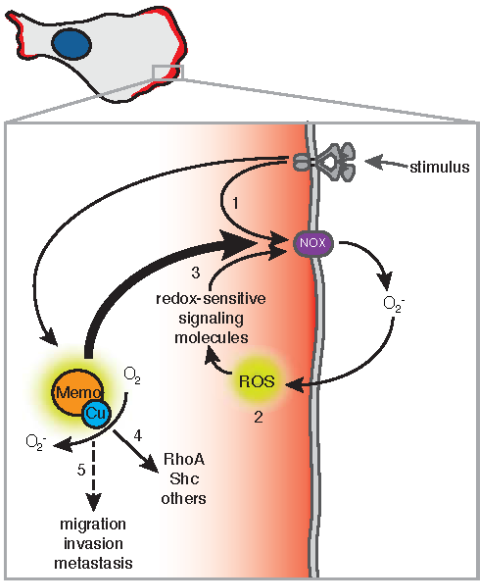

Figure 8. Model for Memo's function in intracellular ROS production and migration. Extracellular stimuli can induce signaling pathways, for example PKC, leading to NOX1 and NOX2 activation (1). NOX-dependent redox signaling, occurring at cellular membranes, leads to spatially-restricted increases in ROS levels, thereby modulating the function of proteins important for cell motility (2). In addition, NOX complexes themselves have been shown to be activated by ROS, suggesting that a positive feed-forward mechanism might amplify O_2^- production (3). Memo, which is also recruited to the cell cortex upon growth factor stimulation, is necessary for sustained activation of NOX signaling, perhaps by influencing the activity of redox sensitive proteins (3). Memo also controls the cellular redox status of RhoA, Shc and potentially other proteins (4). Memo is also known to influence pathways promoting cell motility and, as we show herein, invasion and metastasis (5).

SUPPLEMENTARY MATERIAL

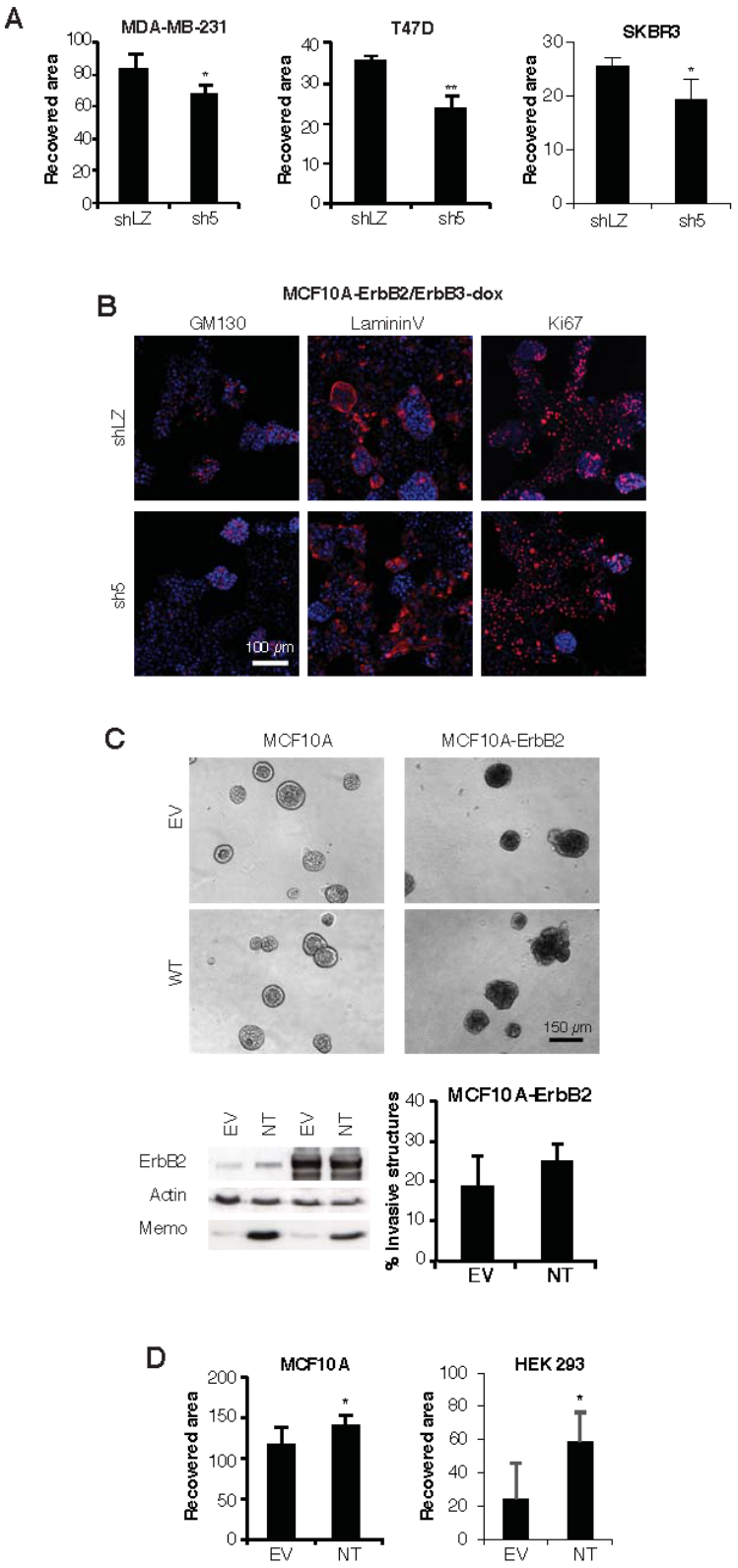

Figure S1. Memo is required for cellular migration and invasion; Memo overexpression is not transforming. (A) Wound closure assays with MDA-MB-231, T47D and SKBR3 control shLZ and Memo knockdown (KD) sh5 cells performed in medium containing 0.1% FCS. Data represent means ± SD of 5-6 fields. (B) Confocal images of MCF10A-ErbB2/ErbB3-derived inducible control shLZ and Memo KD sh5 cells grown in 3D culture in the absence of doxycycline (dox). Images are representative of 3 independent experiments. (C) Control empty vector (EV) and Memo over-expressing (NT) MCF10A and MCF10A-ErbB2 cells grown in 3D Matrigel in the presence of 1.2 nM HRG. Images are representative of 2 independent experiments. Western blot analysis of Memo and ErbB2 abundance is shown. Graph represents the number of invasive structures in each MCF10A-ErbB2 condition. Data represent average percentages ± SEM (n=5 wells per condition). (D) Relative wound closure of MCF10A and HEK293 control (EV) and Memo overexpressing (NT) cells in full growth medium. Data represent means ± SD of 5-6 fields.

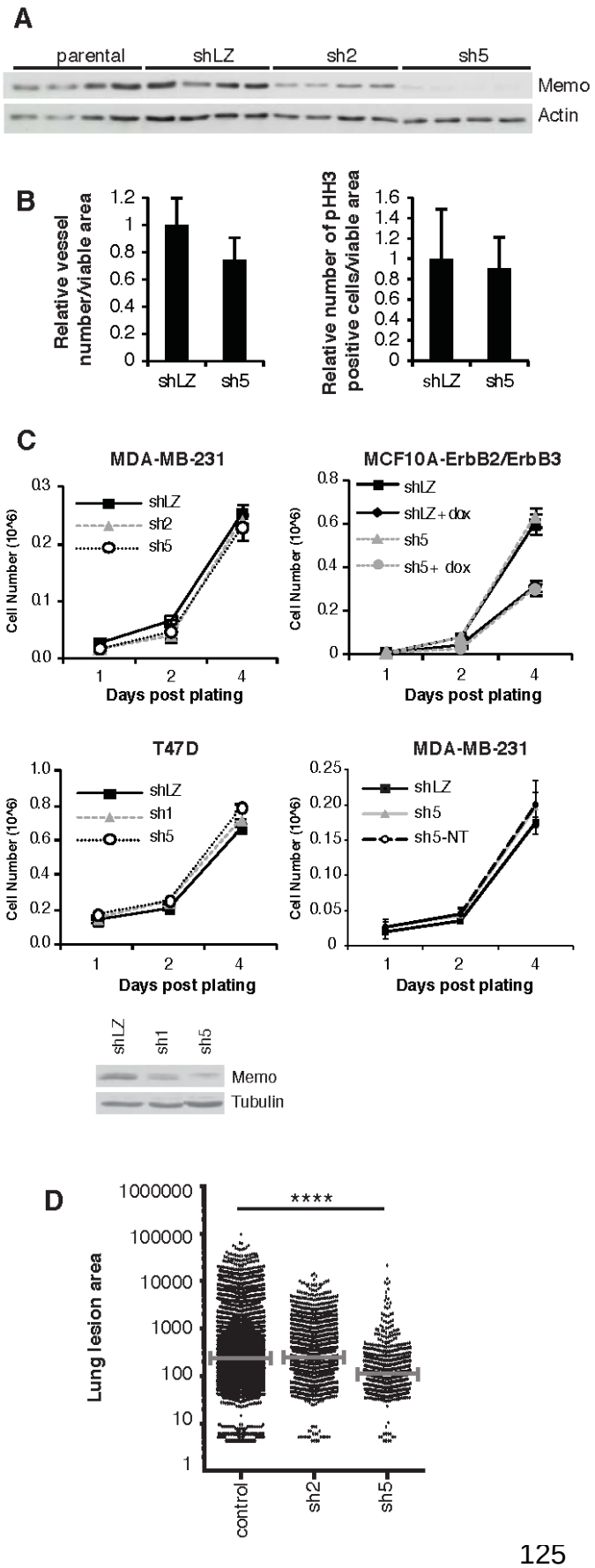

Figure S2. Memo downregulation does not decrease in vitro cellular proliferation or primary tumor outgrowth, but may decrease the survival or proliferation of disseminated tumor cells in the lungs. (A) Western blot analysis of Memo abundance in MDA-MB-231 control (parental and shLZ) and Memo KD (sh2 and sh5) tumor lysates. Each lane represents an individual tumor. (B) Quantification of CD31 and phospho-HistoneH3 staining of MDA-MB-231 control shLZ and Memo sh5 KD tumors to assess angiogenesis and cell proliferation, respectively. Data represent means ± SD (n=3 mice per group). (C) Proliferation of stable MDA-MB-231 and T47D and dox-inducible MCF10A-ErbB2/ErbB3 control (shLZ), Memo knockdown (sh1, sh2, sh5) and sh5 Memo NT-reconstituted cells. Data represent means ± SD of 3 wells; each experiment was performed at least 3 times. Western blot analysis of Memo in the indicated cell lines; each experiment was performed at least 3 times. (D) Area of individual lung lesions arising from MDA-MB-231 control (parental and shLZ groups) and Memo KD sh2 and sh5 tumors. Grey bars indicate the median lesion areas (n=8 mice per group).

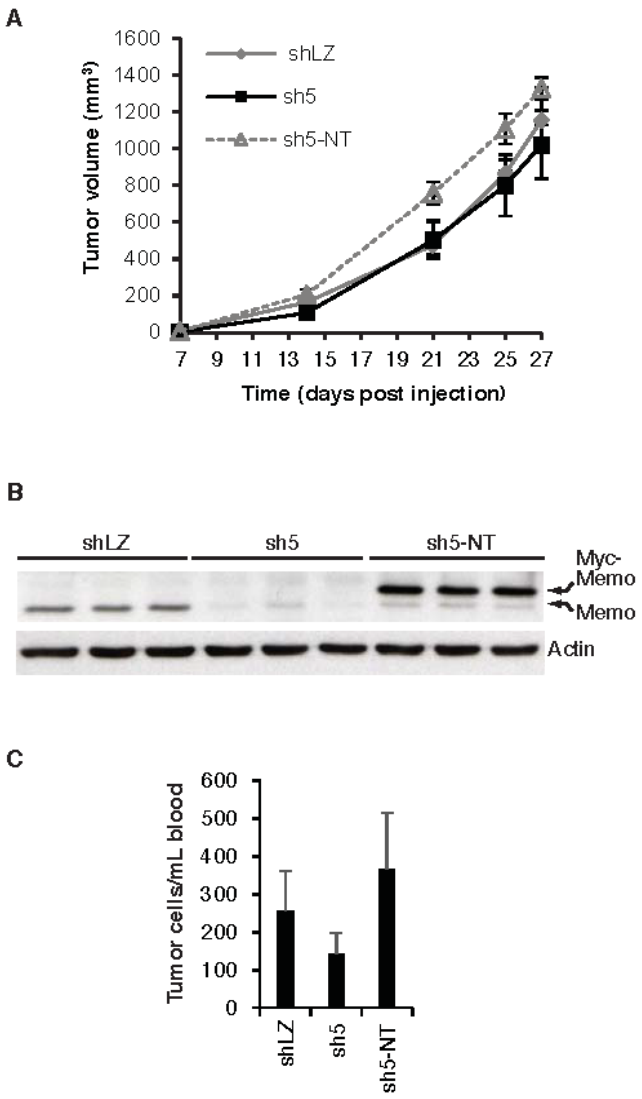

Figure S3. **Reconstitution of Memo restores invasion and tumor cell migration in vivo.** (A) Orthotopic tumor growth in mice of GFP-labeled MDA-MB-231 control shLZ, Memo sh5 KD and sh5 Memo NT-reconstituted cells. Curves are the mean tumor volumes ± SEM (n=9-15 mice per group). (B) Western blot analysis of Memo abundance in tumor lysates produced from mice described in (A). Each lane represents an individual tumor. (C) Number of tumor cells per mL blood taken from the mice described in (A). Data represent the means ± SEM (n=8-15 mice per group).

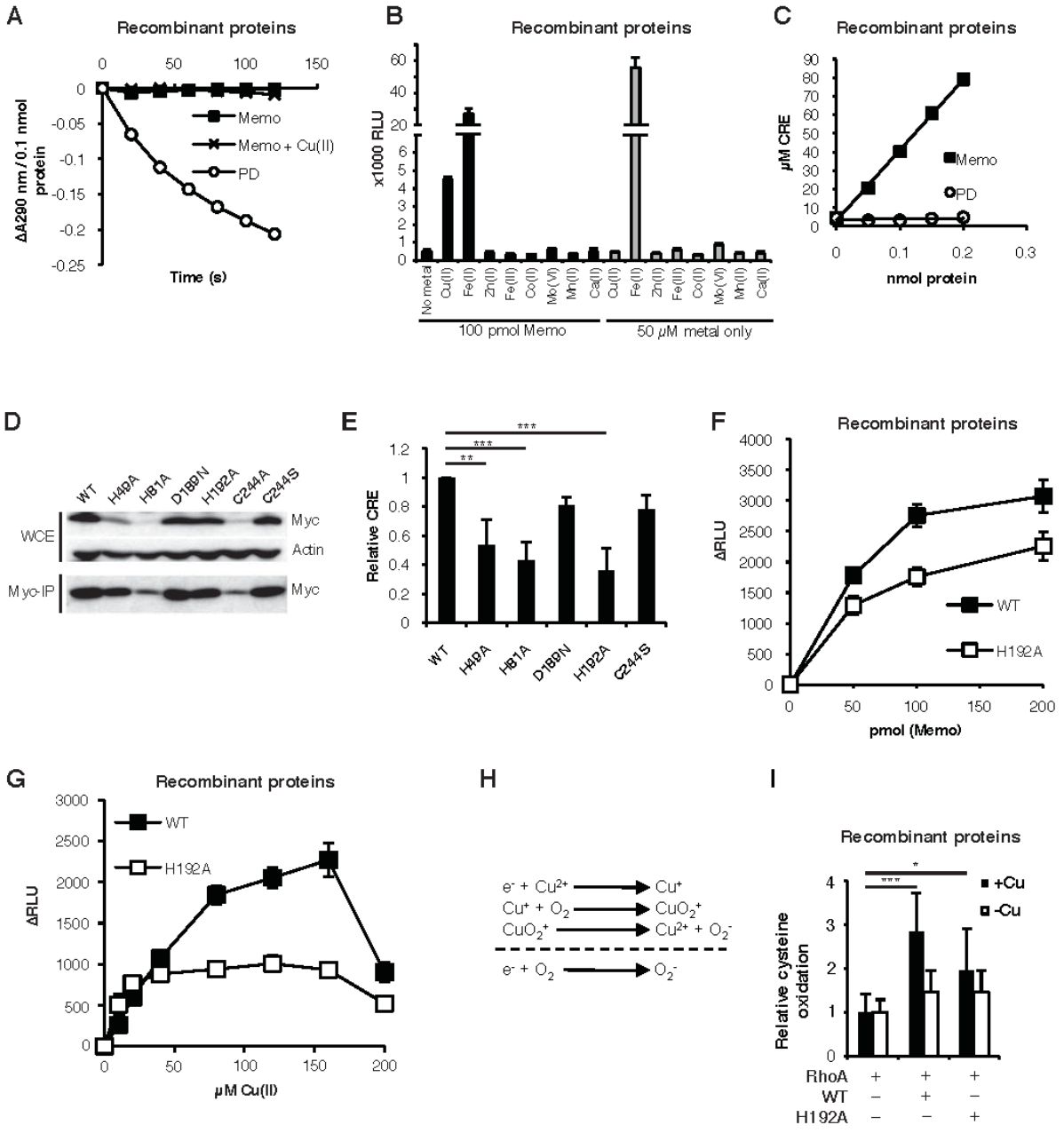

Figure S4. **Analyses of Memo activity.** (A) Measurement of the dioxygenase activity of 0.1 nmol protocatechuate dioxygenase (PD), Memo and Memo supplemented with 50 μM $CuCl_2$ (Cu(II)). The activity of PD is significantly greater than that of Memo alone (p=0.004) or Memo with $CuCl_2$ (p=0.004), as determined by regression analysis. (B) O_2^- production by 100 pmol Memo, assayed in the presence of 50 μM of the indicated metal. Fe(II)-generated O_2^- is a result of Fenton chemistry. (C) Cu(II) reducing equivalents (CRE) of increasing amounts of Memo or PD. The activity of PD is less than that of Memo ($p=7x10^{-5}$) as determined by regression analysis. (D) Western blot analysis of the abundance of WT and mutant Myc-tagged Memo proteins in whole cell extracts (WCE) and immunoprecipitates from transfected HEK293T cells. (E) Relative CRE of the immunoprecipitated Memo proteins shown in panel D. Values are relative to Memo protein levels and normalized to WT. (F) Measurement of O_2^- production in the presence of 50 μM $CuCl_2$ and increasing amounts of WT or H192A Memo. Values are significantly

different for measurements ≥ 50 pmol Memo ($p \leq 0.008$) (G) Measurement of O_2^- production in the presence of 50 pmol WT or H192A Memo and increasing amounts of $CuCl_2$. Values are significantly different for measurements > 50 µM Cu(II) ($p \leq 0.004$) (H) Putative Cu(II)-dependent mechanism of O_2^- production by Memo. (I) MS analysis of the relative average oxidation status of 4 cysteine residues within RhoA, in the presence or absence of Cu(II)-preloaded (+Cu) or non-preloaded (-Cu) WT or H192A Memo. Data for (A), (F-G) and (I) represent means ± SD of 4 independent experiments; data for (B) and (E) represent means ± SD of 3 independent experiments. Data for (C) are representative of 3 independent experiments.

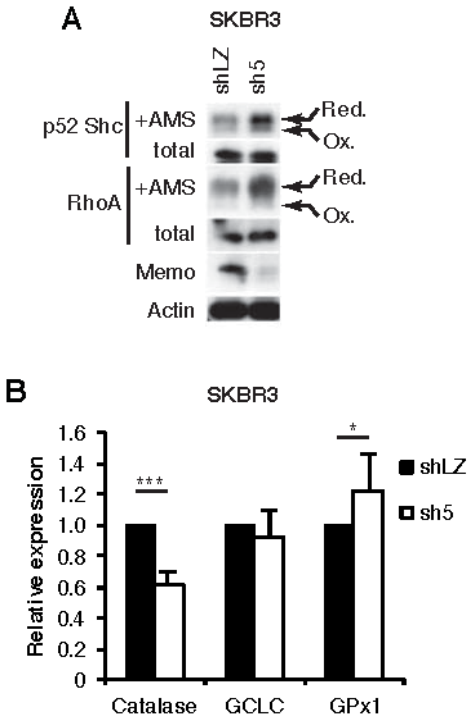

Figure S5. Memo influences the intracellular redox status. (A) Western blot analysis of the abundance of reduced (non-reducing SDS-PAGE) and total (reducing SDS-PAGE) p52 Shc and RhoA in SKBR3 lysates incubated with AMS. Data are representative of 3 independent experiments. (B) Relative abundance of mRNAs encoding catalase, GCLC, and GPx1 in the indicated SKBR3 cell lines. Data represent means ± SD of 6 independent experiments.

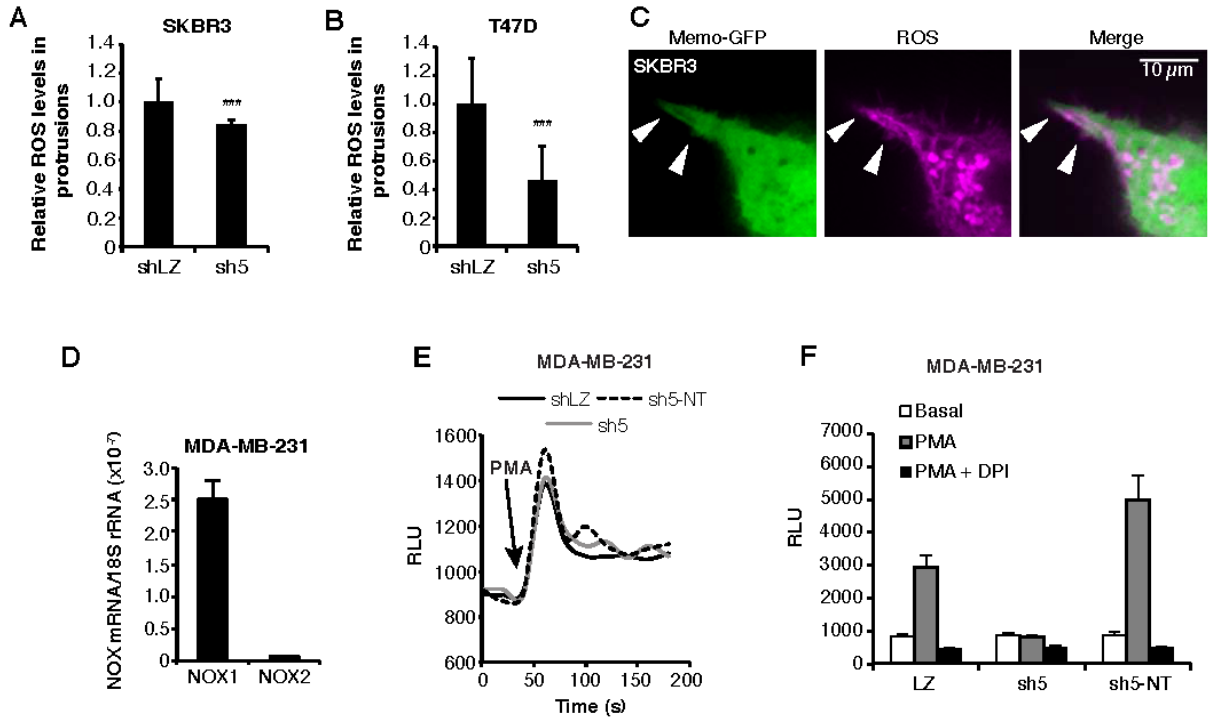

Figure S6. Analysis of ROS and selected mRNAs in Memo knockdown cell lines. Relative ROS concentrations in protrusions of (A) SKBR3 and (B) T47D shLZ and sh5 cells stimulated with 12 nM HRG, normalized to total ROS concentrations. Data represent means ± SD of 3 independent experiments. (C) Detection of GFP-Memo and CellROX Deep Red ROS reagent staining in HRG-stimulated SKBR3 cells. 100x magnification. Arrows indicate regions where Memo and ROS overlap. Images are representative of 2 independent experiments, with a total of 4 biological replicates. (D) Quantification of Nox1 and Nox2 mRNA abundance in MDA-MB-231 cells by qPCR, normalized to 18S RNA abundance. Data represent means ± SD of 3 independent experiments. (E) Representative graph of short-term NOX activity, as measured by O_2^- production (relative light units, RLU), upon PMA stimulation of MDA-MB-231 shLZ, sh5, and sh5-NT cells. Arrow indicates PMA addition. Graphs are representative of 3 independent experiments. (F) Quantification of O_2^- production (relative light units, RLU) in shLZ, sh5, and sh5-NT cells untreated (basal) or treated for 60 min with PMA or PMA + DPI. Data represent means ± SD of 3 independent experiments.

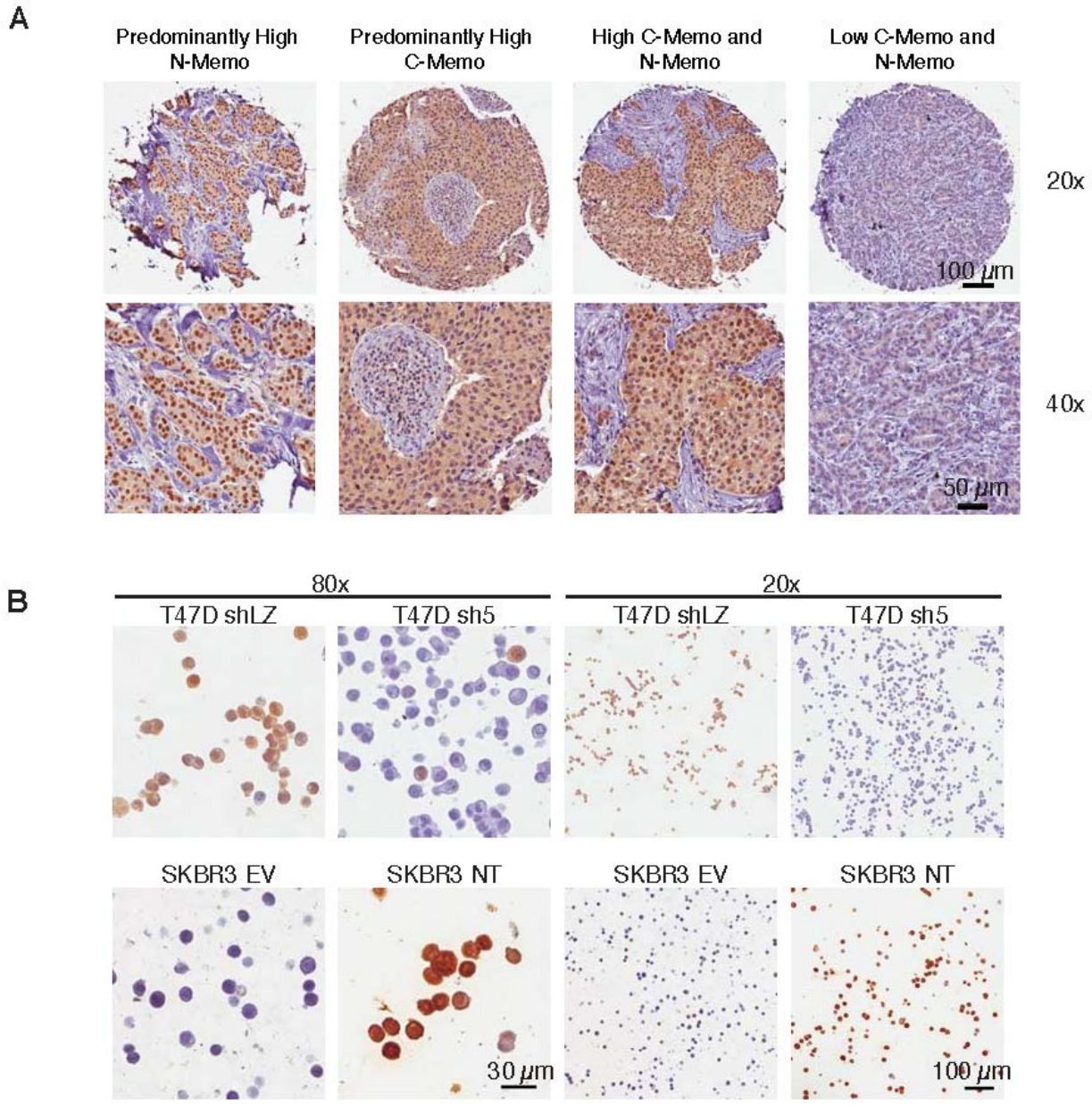

Figure S7. Memo immunohistochemistry. (A) Immunohistochemical quantification of Memo in human neoplastic breast samples. 20x and 40x magnifications of the tumor sections shown in Figure 7D are shown. (B) Memo immunohistochemistry on sections of paraffin-embedded: T47D shLZ and sh5 cells, and SKBR3 control (EV) and Memo overexpressing (NT) cells done to control for Memo antibody specificity (80X and 20x magnification).

Variable	Definition	N(% col)
All		407 (100.0)
Age at surgery	35-50	125 (30.7)
	51-65	217 (53.3)
	>65	65 (16)
Histology	Ductal	319 (78.4)
	No Ductal	88 (21.6)
pT	pT1a	4 (1)
	pT1b	91 (22.4)
	pT1c	277 (68.1)
	pT2	35 (8.6)
Positive lymph nodes	None	264 (64.9)
	1+	143 (35.1)
Grade	NA	12 (2.9)
	1	111 (27.3)
	2	197 (48.4)
	3	87 (21.4)
PVI	Absent	340 (83.5)
	Present	67 (16.5)
ER	ER=0	32 (7.9)
	ER>0	375 (92.1)
PgR	PGR=0	81 (19.9)
	PGR>0	326 (80.1)
ER/PgR	- (Both 0)	30 (7.4)
	+ (ER>0 or PgR>0)	377 (92.6)
ErbB2	NA	8 (2)
	-	378 (92.9)
	+	21 (5.2)
Ki67	<14%	175 (43)
	≥14%	232 (57)
p53	NA	92 (22.6)
	<16	244 (60)
	≥16	71 (17.4)
Subtype	NA	5 (1.2)
	LUM A	168 (41.3)
	LUM B Ki67 HIGH	191 (46.9)
	LUM B ErbB2+	15 (3.7)
	ErbB2+	6 (1.5)
	TN	22 (5.4)
Distant metastasis	No event	369 (90.7)
	Event	38 (9.3)
Overall Survival	Alive	360 (88.5)
	Dead	47 (11.5)

Table S1. Clinico-pathological characteristics of the breast cancer cohort analyzed for Memo abundance. pT, primary tumor stage; tumor grade; proliferation index (Ki-67); p53 IHC status; subtype (Luminal (LUM) A; LUM B with high Ki67; LUM B with positive ErbB2, ErbB2 positive and triple negative (TN) breast tumors (*46*). Distant metastasis is defined as the time from surgery to distant recurrence or death from breast cancer; overall survival (OS) as alive or dead, defined as the time from surgery until the date of death from any cause. NA, not available.

		Total Memo (£)				C-Memo (*)				N-Memo ($)			
Variable	Definition	LOW	HIGH	OR (95% CI)	p	LOW	HIGH	OR (95% CI)	p	LOW	HIGH	OR (95% CI)	p
Age at surgery	35-50	69 (55.2)	56 (44.8)	Ref.		82 (65.6)	43 (34.4)	Ref.		82 (65.6)	43 (34.4)	Ref.	
	51-65	127 (58.5)	90 (41.5)	0.87 (0.56;1.36)	0.549	160 (73.7)	57 (26.3)	0.5 (0.28;0.9)	0.021	135 (62.2)	82 (37.8)	1.68 (0.95;2.98)	0.073
	>65	33 (50.8)	32 (49.2)	1.19 (0.66;2.18)	0.561	43 (66.2)	22 (33.8)	0.78 (0.36;1.69)	0.53	39 (60)	26 (40)	1.48 (0.69;3.13)	0.325
Histology	Ductal	180 (56.4)	139 (43.6)	Ref.		222 (69.6)	97 (30.4)	Ref.		203 (63.6)	116 (36.4)	Ref.	
	No Ductal	49 (55.7)	39 (44.3)	1.03 (0.64;1.66)	0.901	63 (71.6)	25 (28.4)	0.77 (0.41;1.44)	0.415	53 (60.2)	35 (39.8)	1.32 (0.74;2.35)	0.346
pT	pT1a/b	47 (49.5)	48 (50.5)	Ref.		65 (68.4)	30 (31.6)	Ref.		55 (57.9)	40 (42.1)	Ref.	
	pT1c	163 (58.8)	114 (41.2)	0.68 (0.43;1.09)	0.113	198 (71.5)	79 (28.5)	1.02 (0.55;1.86)	0.957	178 (64.3)	99 (35.7)	0.78 (0.43;1.34)	0.341
	pT2	19 (54.3)	16 (45.7)	0.82 (0.38;1.79)	0.627	22 (62.9)	13 (37.1)	1.91 (0.71;5.16)	0.2	23 (65.7)	12 (34.3)	0.5 (0.19;1.34)	0.17
Positive lymph nodes	None	143 (54.2)	121 (45.8)	Ref.		182 (68.9)	82 (31.1)	Ref.		165 (62.5)	99 (37.5)	Ref.	
	1+	86 (60.1)	57 (39.9)	0.78 (0.52;1.18)	0.247	103 (72)	40 (28)	0.84 (0.49;1.44)	0.529	91 (63.6)	52 (36.4)	1.04 (0.63;1.73)	0.874
Grade	1	64 (57.7)	47 (42.3)	Ref.		85 (76.6)	26 (23.4)	Ref.		68 (61.3)	43 (38.7)	Ref.	
	2	109 (55.3)	88 (44.7)	1.1 (0.69;1.76)	0.693	135 (68.5)	62 (31.5)	1.8 (0.95;3.39)	0.07	121 (61.4)	76 (38.6)	0.74 (0.42;1.31)	0.302
	3	52 (59.8)	35 (40.2)	0.92 (0.52;1.62)	0.765	59 (67.8)	28 (32.2)	2.93 (1.34;6.38)	0.007	63 (72.4)	24 (27.6)	0.34 (0.18;0.72)	0.005
PVI	Absent	188 (55.3)	152 (44.7)	Ref.		237 (69.7)	103 (30.3)	Ref.		209 (61.5)	131 (38.5)	Ref.	
	Present	41 (61.2)	26 (38.8)	0.78 (0.46;1.34)	0.374	48 (71.6)	19 (28.4)	1.21 (0.6;2.43)	0.598	47 (70.1)	20 (29.9)	0.61 (0.31;1.22)	0.162
ER	ER=0	18 (56.2)	14 (43.7)	1 (0.48;2.07)	0.999	19 (59.4)	13 (40.6)	3.53 (1.43;8.74)	0.006	24 (75)	8 (25)	0.28 (0.09;0.71)	0.008
	ER>0	211 (56.3)	164 (43.7)	Ref.		286 (70.9)	109 (29.1)	Ref.		232 (61.9)	143 (38.1)	Ref.	
PgR	PGR=0	47 (58)	34 (42)	0.91 (0.56;1.5)	0.722	59 (72.8)	22 (27.2)	0.98 (0.51;1.88)	0.958	55 (67.9)	26 (32.1)	0.77 (0.41;1.42)	0.401
	PGR>0	182 (55.8)	144 (44.2)	Ref.		226 (69.3)	100 (30.7)	Ref.		201 (61.7)	125 (38.3)	Ref.	
ER/PgR	- (both0)	16 (53.3)	14 (46.7)	1.14 (0.54;2.4)	0.737	17 (56.7)	13 (43.3)	3.91 (1.55;9.85)	0.004	22 (73.3)	8 (26.7)	0.27 (0.1;0.74)	0.011
	+ (ER>0 or PgR>0)	213 (56.5)	164 (43.5)	Ref.		268 (71.1)	109 (28.9)	Ref.		234 (62.1)	143 (37.9)	Ref.	
ErbB2	-	213 (56.3)	165 (43.7)	Ref.		268 (70.9)	110 (29.1)	Ref.		237 (62.7)	141 (37.3)	Ref.	
	+	12 (57.1)	9 (42.9)	0.97 (0.4;2.35)	0.943	12 (57.1)	9 (42.9)	3.36 (1.14;9.86)	0.028	15 (71.4)	6 (28.6)	0.33 (0.1;1.08)	0.067
Ki67	<14%	106 (60.6)	69 (39.4)	Ref.		135 (77.1)	40 (22.9)	Ref.		113 (64.6)	62 (35.4)	Ref.	
	≥14%	123 (53)	109 (47)	1.36 (0.91;2.03)	0.129	150 (64.7)	82 (35.3)	2.17 (1.27;3.71)	0.005	143 (61.6)	89 (38.4)	0.76 (0.46;1.25)	0.278
p53	<16	143 (58.6)	101 (41.4)	Ref.		178 (73)	66 (27)	Ref.		158 (64.8)	86 (35.2)	Ref.	
	≥16	32 (45.1)	39 (54.9)	1.73 (1.01;2.94)	0.045	37 (52.1)	34 (47.9)	3.03 (1.53;5.99)	0.001	41 (57.7)	30 (42.3)	0.71 (0.36;1.41)	0.33
Subtype	LUM A	101 (60.1)	67 (39.9)	Ref.		129 (76.8)	39 (23.2)	Ref.		108 (64.3)	60 (35.7)	Ref.	
	LUM B Ki67 High	103 (53.9)	88 (46.1)	1.29 (0.85;1.96)	0.238	129 (67.5)	62 (32.5)	1.69 (0.96;2.99)	0.07	115 (60.2)	76 (39.8)	0.9 (0.54;1.52)	0.706
	LUM B ErbB2 POS	8 (53.3)	7 (46.7)	1.32 (0.46;3.81)	0.609	8 (53.3)	7 (46.7)	5.51 (1.46;20.8)	0.012	10 (66.7)	5 (33.3)	0.34 (0.08;1.34)	0.123
	ErbB2 POS	4 (66.7)	2 (33.3)	0.75 (0.13;4.23)	0.748	4 (66.7)	2 (33.3)	4.55 (0.61;33.98)	0.139	5 (83.3)	1 (16.7)	0.15 (0.01;1.84)	0.138
	TN	11 (50)	11 (50)	1.51 (0.62;3.67)	0.367	12 (54.5)	10 (45.5)	6.32 (2.07;19.28)	0.001	16 (72.7)	6 (27.3)	0.23 (0.07;0.78)	0.018

Table S2. Correlations between Memo status and clinical and pathological parameters in the breast cancer cohort. £: Odd Ratio (OR) and p-value of the univariate logistic regression model, association between patients' characteristics at surgery and probability of high Total Memo. OR and p-value of the bivariate logistic regression model, association between patients' characteristics at surgery and probability of high: * cytosolic Memo (C-Memo), adjusted for nuclear Memo (N-Memo); and $ N-Memo, adjusted for C-Memo, respectively. Significant p-values are indicated in red.

			Total Memo (N%)		C-Memo (N%)		N-Memo (N%)	
	Definition	All cases analyzed	Low	High	Low	High	Low	High
All cases analyzed	All	407 (100)	229 (100)	178 (100)	285 (100)	122 (100)	256 (100)	151 (100)
Distant Metastasis	No Event	369 (90.7)	204 (89.1)	165 (92.7)	259 (90.9)	110 (90.2)	228 (89.1)	141 (93.4)
	Event	38 (9.3)	25 (10.9)	13 (7.3)	26 (9.1)	12 (9.8)	28 (10.9)	10 (6.6)
Overall Survival	Alive	360 (88.5)	199 (86.9)	161 (90.4)	254 (89.1)	106 (86.9)	222 (86.7)	138 (91.4)
	Dead	47 (11.5)	30 (13.1)	17 (9.6)	31 (10.9)	16 (13.1)	34 (13.3)	13 (8.6)

Table S3. Observed events in the breast cancer cohort. Median follow-up time estimated in non-events: 12.1 years; Interquartile range: 11.3-12.9 years, according to Total memo, cytosolic Memo (C-Memo) or nuclear Memo (N-Memo) high compared low abundance; (% in parenthesis).

	Distant metastasis		Overall survival	
Variable	HR (95% CI)	p	HR (95% CI)	p
C-Memo <5 years: High vs Low	3.89 (1.16;13.07)	**0.028**	8.36 (1.31;53.42)	**0.025**
C-Memo ≥5 years: High vs Low	0.44 (0.11;1.8)	0.25	1.05 (0.45;2.43)	0.92
N-Memo <5 years: High vs Low	0.44 (0.13;1.53)	0.2	0.38 (0.07;2.1)	0.27
N-Memo ≥5 years: High vs Low	0.57 (0.16;2.01)	0.38	0.54 (0.23;1.28)	0.16
Age: 35-50 vs 65+	0.44 (0.17;1.18)	0.1	0.34 (0.15;0.76)	**0.008**
Age: 51-65 vs 65+	0.61 (0.26;1.43)	0.25	0.36 (0.18;0.74)	**0.005**
pT2 vs pT1	2.9 (1.26;6.71)	**0.013**	1.92 (0.85;4.35)	0.12
Positive lymph nodes: 1+ vs none	2.75 (1.42;5.32)	**0.003**	1.94 (1.06;3.53)	**0.031**
Grade 3 vs 1-2	1.42 (0.64;3.15)	0.39	1.64 (0.77;3.48)	0.2
ER/PgR: - vs +	1.98 (0.82;4.78)	0.13	1.42 (0.59;3.41)	0.43
ErbB2:+ vs -	1.52 (0.49;4.76)	0.47	1.26 (0.41;3.91)	0.69
Ki67 ≥14% vs <14%	1.63 (0.7;3.78)	0.25	1.13 (0.56;2.27)	0.74
p53 ≥16 vs <16	2.26 (1.06;4.81)	**0.034**	2.7 (1.31;5.56)	**0.007**

Table S4. A time-dependent multivariable Cox model was used to estimate the hazard ratios. The comparison is between cytosolic Memo (C-Memo) high compared to low, within 5 years and after 5 years from surgery; controlled for age, tumor size, lymph node status, grade, hormone-receptor status, ErbB2 status, p53 and Ki-67, and nuclear Memo (N-Memo) when evaluating C-Memo and C-Memo when evaluating N-Memo.

Lentiviral constucts:

pLKO.1-puro shMemo vectors purchased from Sigma:

Given construct name	Sigma order number
sh1	MISSION shRNA library TRCN0000122894
sh2	MISSION shRNA library TRCN0000122895
sh5	MISSION shRNA library TRCN0000122898

pLKO-tet-on-puro shRNA vectors cloned in house:

Given construct name	Forward/reverse oligo sequences
control shLZ: pLKO.1-puro and pLKO-tet-on-puro	5'-CCGGGCGGCTGCCGGAATTTACCTTCTCGAGGGTAAATTCCGGCAGCCGCTTTTT-3'
	5'-AATTAAAAAGCGGCTGCCGGAATTTACCCTCGAGAAGGTAAATTCCGGCAGCCGC-3
Memo sh5: pLKO-tet-on-puro	5'-CCGGGCAAGACAGTTCAGTGAGTTACTCGAGTAACTCACTGAACTGTCTTGCTTTTTG-3'
	5'-GAATTCAAAAAGCAAGACAGTTCAGTGAGTTACTCGAGTAACTCACTGAACTGTCTTGC-3'
GFP lenti	GFP-pWPXL

Retroviral expression constructs:

Oligos used to introduce synonymous mutations into the Memo sh5 recognition sequence:

5'- GCAGGATTCGAGTGTATCGTATGCAGCTGGAGCAC-3'

5'-CGATACACTCGAATCCTGCCAGTTTCTACACTGGC-3'

Given construct name	Description
NT	Myc-Memo with mutated sh5 recognition sequence in pLHCX
EV	pLHCX empty vector

Other vectors:

GFP-Memo	eGFP-Memo-pcDNA3.1

qPCR Primers:

gene	forward/reverse primers
hGPX1	5'-TTCCCGTGCAACCAGTTTG-3'
	5'-TTCACCTCGCACTTCTCGAA-3'
hGCLC	5'-GGCACAAGGACGTTCTCAAGT-3'
	5'-CAGACAGGACCAACCGGAC-3'
hCAT	5'-TGGGATCTCGTTGGAAATAACAC-3'
	5'-TCAGGACGTAGGCTCCAGAAG-3'
h18S	5'-GGACATCTAAGGGCATCACAGACC-3'
	5'-TGACTCAACACGGGAAACCTCAC-3'

Table S5. Primers, oligos, and vectors used.

Movie S1. Motility of MDA-MB-231 tumor cells expressing shLZ. Representative 30 min time lapse movie from multiphoton imaging of a shLZ tumor is shown. Movie shows several moving tumor cells. Tumor cells show GFP fluorescence (green). Scale is 0.994 μm/pixel.

Movie S2. Cell protrusions in MDA-MB-231 tumor cells with sh5-mediated Memo knockdown. Representative 30 min time lapse movie from multiphoton imaging of a sh5 tumor is shown. Movie shows an example of cell protrusions. Tumor cells show GFP fluorescence (green). Scale is 0.994 μm/pixel.

Movie S3. **Motility of sh5-expressing MDA-MB-231 tumor cells reconstituted with Memo**. Representative 30 min time lapse movie from multiphoton imaging of a sh5-NT tumor is shown. Movie shows several moving tumor cells. Tumor cells show GFP fluorescence (green). Scale is 0.994 μm/pixel.

3.3.1 Contributions

My contributions to the publication "Memo is a Copper-Dependent Redox Protein with an Essential Role in Migration and Metastasis" include: 1) preparation of lung sections for the staining of lung metastases; 2) generation of the T47D Memo rescue cell line and 3) Co-Immunoprecipitation experiments of Memo with ErbB2 and RhoA.

I also collaborated with Gwen MacDonald on a sub-project, in which we aimed to investigate the role of Memo in tumorigenesis in a transgenic mouse model (see following chapter).

3.4 Unpublished Results: Memo in Tumorigenesis

We have demonstrated that Memo is a redox protein involved in breast cancer metastasis. Furthermore, we have shown that Memo is expressed at low levels in normal mammary gland, while 40% of human breast cancer samples have elevated Memo expression, suggesting an oncogenic role for Memo. Moreover, high cytoplasmic localization of Memo is predictive for early metastasis and death, which is therefore a prognostic factor for aggressive disease (section 3.3). Interestingly, in a study comparing miRNA expression between normal epithelium of human breast samples with ductal carcinoma in situ (DCIS), miR-125b that targets Memo, was demonstrated to be downregulated early in breast cancer development (Hannafon et al., 2011). Thus, Memo might be involved in the progression from normal to cancer cells.

Memo is expressed in a subset of luminal cells in pubertal mice and changes its expression pattern during pregnancy, lactation and involution.

Before testing the role of Memo in tumorigenesis, we first aimed to analyze the expression of Memo in a normal physiological setting in the murine mammary gland. The mammary gland is a unique organ as it undergoes most of its developmental changes after birth in order to prepare for its function to produce and secrete milk for offspring. These changes include the development of secretory alveoli during pregnancy that are capable of producing milk, the induction of milk production and secretion during lactation and the re-establishment of the pre-pregnant gland, a process that is called involution (Inman et al., 2015). As each of these developmental programs requires diverse molecular mechanisms, we investigated Memo expression in the different developmental stages to see if Memo might be involved in these processes. Western blot analysis of lysates from mammary glands that were obtained from pubertal and older virgin mice as well as from mice during pregnancy, lactation and involution, revealed that Memo was expressed in all developmental stages (Figure 3.14 A). To investigate if Memo is localized to a specific compartment of the mammary gland, we first isolated mammary glands from pubertal mice and performed immunohistochemistry (IHC) for Memo. Interestingly, luminal cells that line the inner epithelial layer facing the lumen of the ducts, were

positive for Memo expression. However, not all luminal cells were positive for Memo (Figure 3.14 B). In myoepithelial cells, which comprise the outer layer of the ducts, no Memo expression could be detected (Figure 3.14 B).

Next, we analyzed Memo expression in mammary glands from pregnant (Figure 3.14 C), and lactating (Figure 3.14 D) mice, and from mice undergoing involution (Figure 3.14 E). In contrast to pubertal glands, where Memo was expressed in a subset of luminal cells (Figure 3.14 B), the majority of luminal cells express Memo during pregnancy, lactation and involution (Figure 3.14 C-E). This staining was not caused by non-specific binding of the secondary anti-mouse antibody as IHC staining without the primary anti-Memo antibody showed no signal (Figure 3.14 F-H). In summary, these observations suggest, that Memo could be involved in the development and/or remodeling of the mammary gland during different stages of development – a hypothesis that requires further investigation. However, we have clear evidence, that Memo is expressed in luminal cells of the murine mammary gland, therefore, we next studied the role of Memo in tumorigenesis in a mouse model.

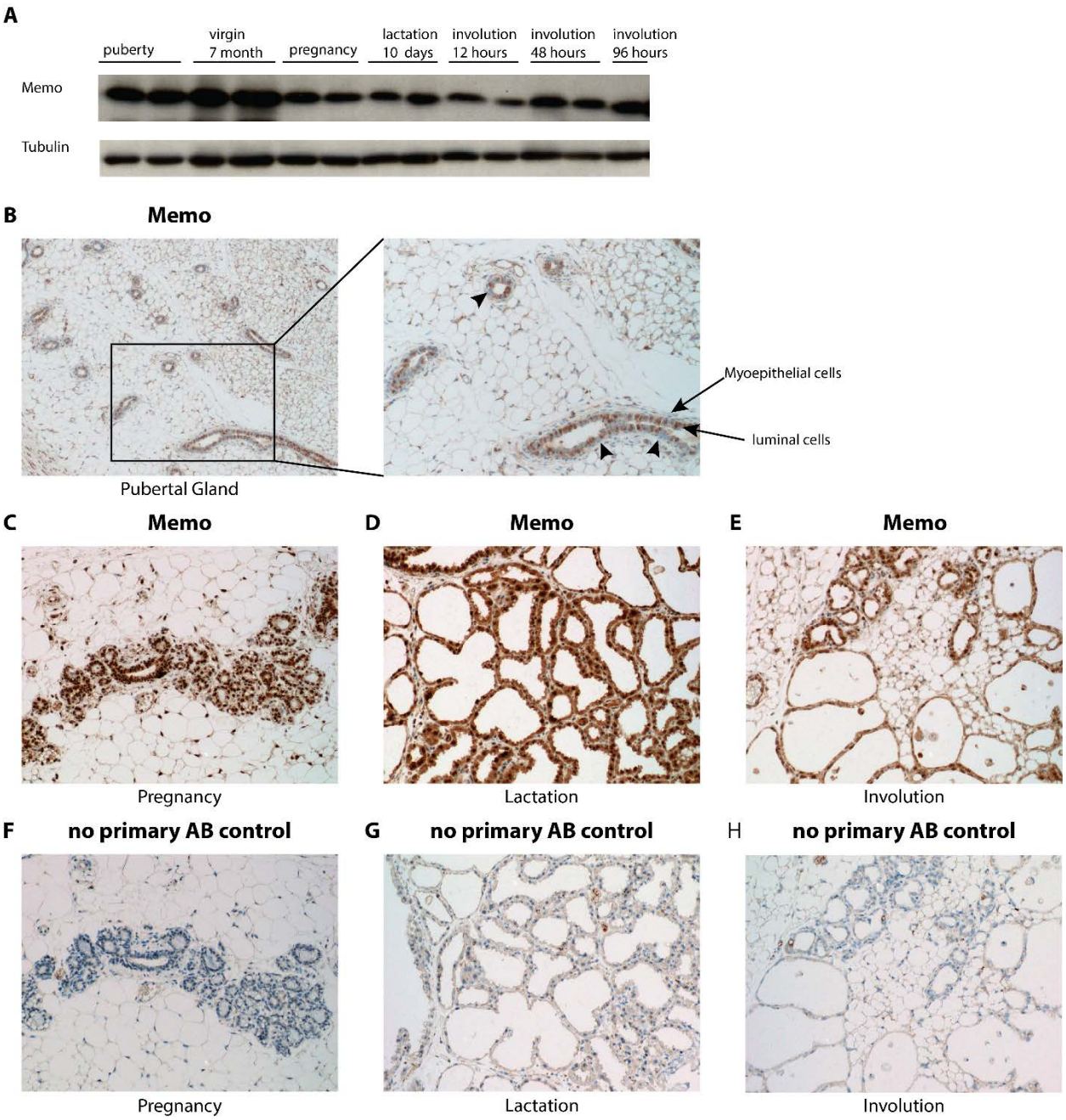

Figure 3.14 Expression pattern of Memo during mammary gland development. (**A**) Western blot analysis of Memo expression in mammary gland lysates from different stages of mammary gland development. (**B-E**) IHC staining of Memo on mammary glands from mice in different developmental stages. (**B**) Mammary gland from a 36 days old pubertal mouse. Memo is expressed in a subset of luminal cells but not in myoepithelial cells. Arrowheads indicate some Memo-negative cells. (**C**) Mammary gland from a pregnant mouse at day 16.5, (**D**) from day 10 of lactation and (**E**) from involution 48 hours after weaning. (**F-H**) IHC staining without primary anti-Memo antibody on same mammary gland sections as in B, C and D to rule out that staining is not caused by secondary anti-mouse antibody.

Memo might be required for tumorigenesis in a spontaneous murine tumor model

Memo is expressed at low levels in the human breast and overexpressed in 40% of breast cancer. Therefore, we hypothesized that Memo is involved in the transition from normal to cancerous cells. In order to investigate this hypothesis we made use of a spontaneous murine breast cancer model in which tumorigenesis is driven by an oncogene. In contrast to the experiments performed with the human breast cancer cell line MDA-MB-231 (section 3.3 Figure 2A), in which we studied the effect of Memo depletion in a tumor cell line that already underwent tumorigenesis, this spontaneous model allows us to investigate if Memo plays a role in the malignant transformation process. In this mouse tumor model, tumorigenesis is driven by the expression of a constitutively activated form of the ErbB2/HER2/Neu receptor, NeuNT, under the transcriptional control of the mouse mammary tumor virus (MMTV) long terminal repeat (LTR). The expression of NeuNT in the mammary epithelium is well known to result in the development of multifocal mammary tumors that metastasize to the lungs (Guy et al., 1996). We chose this model based on the initial discovery of Memo through its interaction with the receptor tyrosine kinase ErbB2 (Marone et al., 2004), and based on the observed correlation between high cytoplasmic Memo expression and ErbB2-positivity in human breast cancer samples (section 3.3 Figure 7E). To investigate if Memo affects MMTV-*NeuNT*-driven tumorigenesis, we generated a triple transgenic mouse line. In this mouse line the excision of LoxP-flanked (floxed) *Memo* alleles is mediated by a Cre-recombinase. As the *Cre*-transgene is under the control of the MMTV-LTR, *Memo* excision is expected to occur primarily in the mammary gland. However, MMTV-transgene expression was reported to occur at low levels in other tissues like salivary gland, thymus, lung and spleen (Guy et al., 1992). Furthermore, as both, *NeuNT*- and *Cre*- expression are under the control of the MMTV-LTR, oncogene expression and Memo excision are expected to occur at the same time. By crossing *Memo*$^{fl/+}$MMTV-*Cre*$^{tg/tg}$ mice with *Memo*$^{fl/+}$MMTV-*NeuNT*$^{tg/tg}$ mice, we generated Memo mammary gland wild-type (WT) mice (*Memo*$^{+/+}$MMTV-*Cre*$^{tg/+}$MMTV-NeuNT$^{tg/+}$), Memo mammary gland heterozygous (Het) mice (Memo$^{fl/+}$ MMTV-Cre$^{tg/+}$MMTV-NeuNT$^{tg/+}$) and Memo mammary gland knockout (KO) mice (Memo$^{fl/fl}$ MMTV-Cre$^{tg/+}$MMTV-NeuNT$^{tg/+}$) (Figure 3.15 A). IHC analysis with an antibody against ErbB2, which detects the mutated form of ErbB2 (NeuNT), of mammary glands isolated from

MMTV-NeuNT transgenic mice, revealed higher ErbB2 expression (Figure 3.15 B) compared to control mice without the transgene (Figure 3.15 C), indicating that the transgene is transcriptionally active. Indeed, multifocal adenocarcinomas developed in the mammary glands about five months after birth and were positive for ErbB2 expression as detected by IHC (Figure 3.15 D). Furthermore, IHC staining of ErbB2 on lung sections revealed that tumors were capable to metastasize to the lungs (Figure 3.15 E). We therefore monitored the different mouse lines for tumor onset, which revealed that mice from all lines developed tumors with the same latency (Figure 3.15 F), and also the average number of tumors within one mouse did not show significant differences (Figure 3.15 G). IHC and western blot analysis of the tumor samples revealed Memo expression in all tumors, independent of the mouse lines (Figure 3.15 H and I). Given the known mosaic expression pattern of MMTV-Cre (Lu et al., 2008; Wagner et al., 2001), this result suggests that either Memo-depleted mammary epithelial cells have a growth defect and are replaced by Memo expressing cells, or that only Memo expressing cells can give rise to tumors. Thus, to fully elucidate the role of Memo in tumorigenesis, further studies are required.

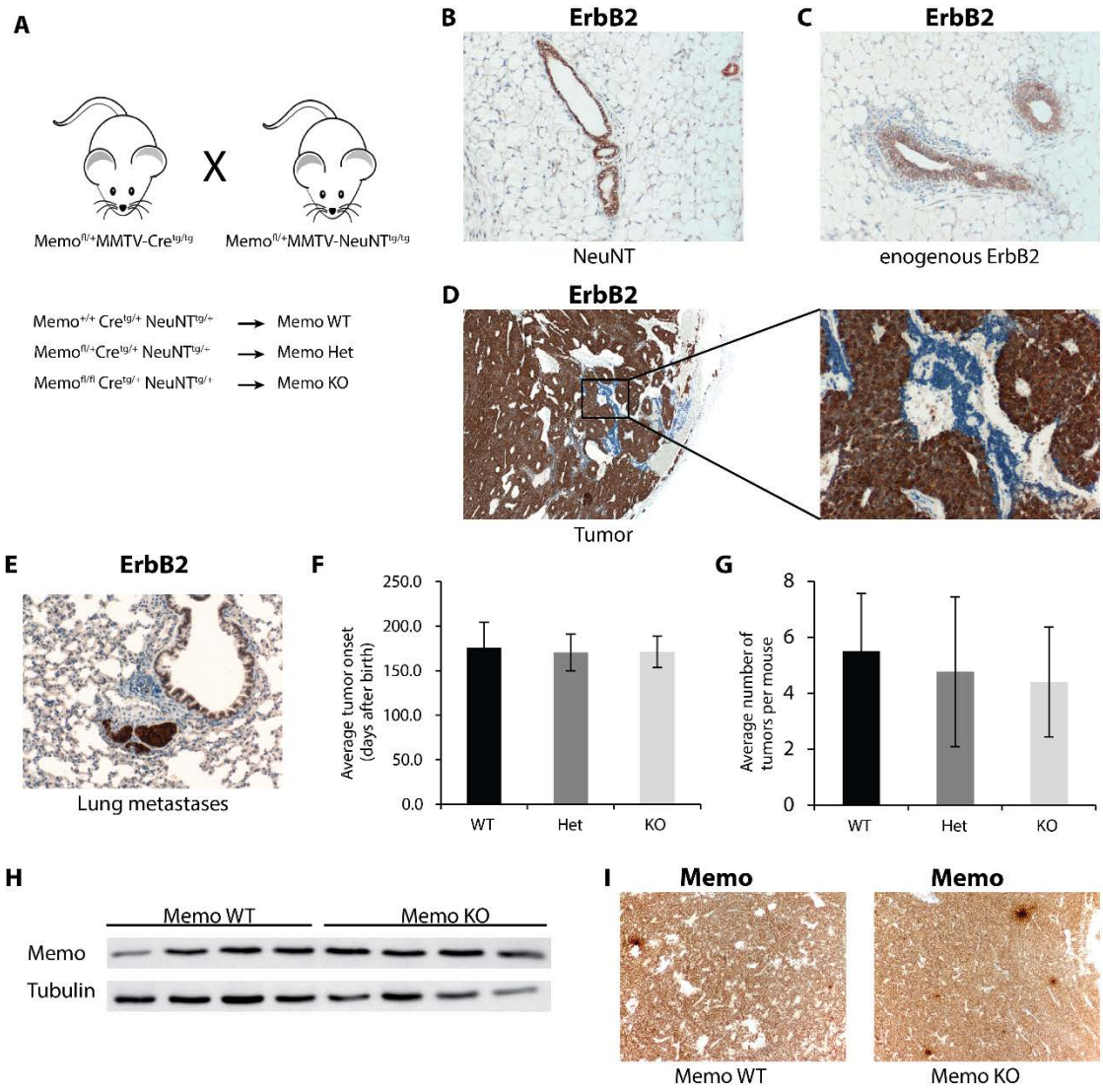

Figure 3.15 Effect of Memo expression on tumorigenesis in a spontaneous murine tumor model. (**A**) Scheme of the generation of a triple transgenic NeuNT-driven spontaneous murine tumor model in which Memo excision and NeuNT expression are expected to be accomplished primarily in the mammary gland and at the same time. *Memo*$^{fl/+}$MMTV-*Cre*$^{tg/tg}$ mice were crossed with *Memo*$^{fl/+}$MMTV-*NeuNT*$^{tg/tg}$ mice to obtain mice with mammary glands depleted for Memo (*Memo*$^{fl/fl}$MMTV-*Cre*$^{tg/+}$MMTV-*NeuNT*$^{tg/+}$), heterozygous (Het) for Memo (*Memo*$^{fl/+}$MMTV-*Cre*$^{tg/+}$MMTV-*NeuNT*$^{tg/+}$) and expressing Memo (*Memo*$^{+/+}$MMTV-*Cre*$^{tg/+}$MMTV-*NeuNT*$^{tg/+}$). (**B - E**) IHC analysis using an anti-ErbB2 antibody that detects NeuNT expression in (**B**) mammary glands from mice with the MMTV-*NeuNT*$^{tg/+}$ transgene and (**C**) without transgene, (**D**) in tumors derived from MMTV-NeuNT$^{tg/+}$ mice and (**E**) in lungs to detect metastases derived from NeuNT-driven tumors. (**F**) Mice were monitored for tumor onset. Average number of days until tumor onset was plotted. (**G**) Numbers of tumors per mouse were counted and the average number of tumors per mouse was calculated. (**H**) Western blot analysis of Memo expression in tumor lysates isolated from mice harboring *Memo*$^{fl/fl}$ (KO) or *Memo*$^{+/+}$ alleles (WT) as well as the MMTV-*Cre*$^{tg/+}$ and MMTV-*NeuNT*$^{tg/+}$ transgenes. (**I**) IHC staining of Memo on tumor sections from mice harboring *Memo*$^{fl/fl}$ (KO) or *Memo*$^{+/+}$ alleles (WT) as well as the MMTV-*Cre*$^{tg/+}$ and MMTV-*NeuNT*$^{tg/+}$ transgenes.

Memo does not affect tumor growth of established tumor cells

We have demonstrated that Memo KD does not affect tumor growth of the triple-negative human breast cancer cell line MDA-MB-231 (Section 3.3 Figure 2A). Nevertheless, the function of Memo might be different depending on the breast cancer subtype. We previously found that cytoplasmic localization of Memo correlates with ErbB2 expression (Section 3.3 Figure 7E). Therefore, we investigated if Memo affects proliferation in NeuNT-positive tumors derived from the spontaneous tumor model described above. As all tumors derived from this tumor model were positive for Memo expression (Figure 3.15 H and I), we applied a new strategy to deplete Memo in these tumor cells. In order to achieve the excision of the floxed Memo alleles, isolated tumor cells were infected with an adenovirus containing a sequence for the Cre-recombinase. It is important to note, that this strategy does not answer the question if Memo plays a role in tumorigenesis, as these cells already underwent malignant transformation. However, this system enables us to investigate if Memo affects tumor growth of NeuNT positive tumors.

To obtain Memo WT as well as Memo KO tumor cells, tumors from *Memo*$^{+/+}$MMTV-*NeuNT*$^{tg/+}$ and *Memo*$^{fl/fl}$MMTV-*NeuNT*$^{tg/+}$ animals were isolated, dispersed into single cell suspension and infected with an adenovirus containing a sequence for Cre-GFP. As a negative control, cells were infected with an adenovirus containing a sequence for GFP alone (Figure 3.16 A). An infection efficiency of about 80% was achieved, determined by the presence of GFP using a fluorescence microscope and FACS analysis (data not shown).

Infection of *Memo*$^{fl/fl}$MMTV-*NeuNT*$^{tg/+}$ tumor cells with Ad-Cre-GFP depleted Memo, while infection of *Memo*$^{+/+}$MMTV-*NeuNT*$^{tg/+}$ cells with Ad-Cre-GFP or cells infected with Ad-GFP did not lose Memo expression as determined by western blot analysis (Figure 3.16 B). Memo WT, KO and control cells were injected into mammary fat pads of immunodeficient mice and tumor growth measured. No significant differences were observed between the tumors formed by the different lines. This might be caused by the large variance between the tumors sizes across all cell genotypes and due to the small number of mice (Figure 3.16 C). However, closer analysis of the tumor growth of Memo WT and Memo KO tumors that originated from the same *Memo*$^{fl/fl}$MMTV-*NeuNT*$^{tg/+}$ tumor cells, which were infected once with Ad-Cre-GFP (Memo KO) and once with Ad-GFP (Memo WT), showed no difference (Figure 3.16 D), suggesting that Memo is not involved in tumor growth. Western blot analysis as well as IHC on tumor sections

revealed reduced Memo levels in Memo KO tumors (Figure 3.16 E and F) and that ErbB2 levels were not altered upon loss of Memo (Figure 3.16 E and G). As we have demonstrated that Memo plays a role in tumor metastasis (Section 3.3 Figure 2B and C), we analyzed the lungs of tumor bearing mice for the presence of metastases. Except for one mouse that was harboring a Memo WT tumor, no metastases were detected (data not shown). Thus, we could not analyze the effect of Memo deletion on metastasis in this tumor model. In summary, these results suggest that Memo does not affect proliferation of NeuNT-driven breast tumors.

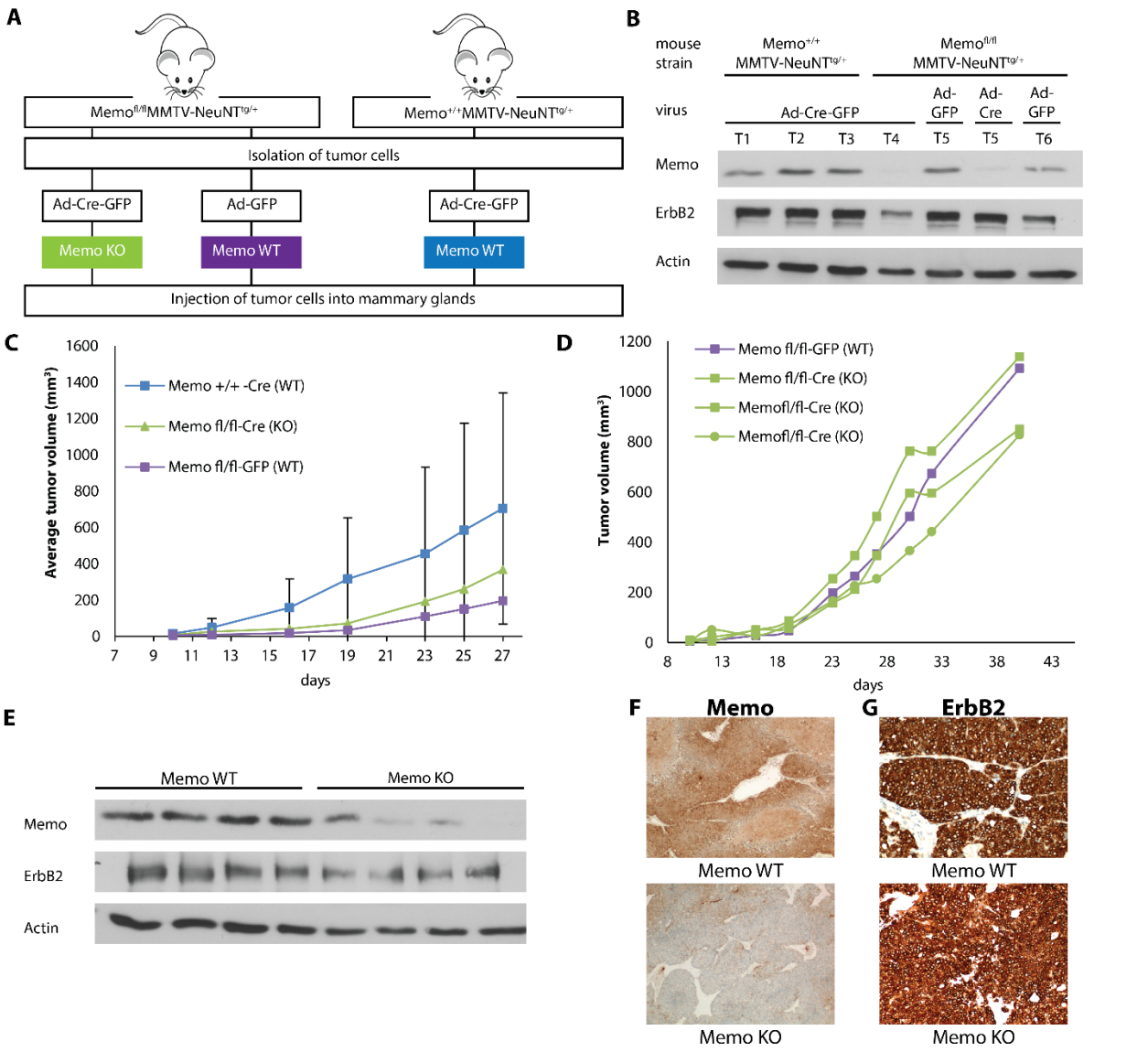

Figure 3.16 Memo deletion in MMTV-*NeuNT* tumor cells does not affect in vivo tumor growth. (**A**) Scheme shows the strategy of how to excise Memo in primary tumor cells derived from the MMTV-*NeuNT*$^{tg/+}$ mouse line. Tumors from *Memo*$^{fl/fl}$MMTV-*NeuNT*$^{tg/+}$ and *Memo*$^{+/+}$MMTV-*NeuNT*$^{tg/+}$ mice were isolated and dispersed into single cells. *Memo*$^{fl/fl}$ cells were infected with an adenovirus containing a sequence for Cre-GFP (Ad-Cre-GFP) to generate Memo KO cells or GFP alone (Ad-GFP) as a negative control. *Memo*$^{+/+}$ cells were infected with Ad-Cre-GFP to control for Cre-mediated effects. The obtained Memo KO and WT cells were injected into mammary glands of immunodeficient mice to test for tumor formation. (**B**) Western blot analysis of Memo and ErbB2 expression in cell lysates obtained from Ad-Cre-GFP or Ad-GFP infected tumor cells. Tumors were isolated from *Memo*$^{+/+}$MMTV-*NeuNT*$^{tg/+}$ mice (T1-3) and from *Memo*$^{fl/fl}$MMTV-*NeuNT*$^{tg/+}$ (T4-6). Ad-Cre-GFP induced the excision of the floxed Memo allele. (**C**) Tumor growth of *Memo*$^{+/+}$-Cre (WT) (n=6), *Memo*$^{fl/fl}$-Cre (KO) (n=3), *Memo*$^{fl/fl}$-GFP (WT) (n=2) cells (as shown in B) in Balb/c nude mice. (**D**) Tumor growth of individual mice from (C) that derived from same same *Memo*$^{fl/fl}$MMTV-*NeuNT*$^{tg/+}$ tumor and infected either with Ad-Cre-GFP (KO) or Ad-GFP (WT). (**E**) Western blot analysis of Memo and ErbB2 in tumor lysates from Memo WT and Memo KO tumors. (**F**) IHC staining of Memo on tumor sections from Memo WT and KO tumors. (**G**) IHC staining of NeuNT on tumor sections from Memo WT and KO tumors.

Materials and Methods – for unpublished results

Antibodies, reagents, plasmids

For western blot analysis and immunohistochemistry the following antibodies were used: Tubulin-α (NeoMarkers); Actin (Chemicon), ErbB2 (Graus-Porta et al., 1995), and the anti-Memo monoclonal antibody (aa 279-294 human Memo RNWQDSSVSYAAGALTVH) was produced in house as described previously (Haenzi et al., 2014).

Lysates and Western blot analysis

Whole cell lysates were extracted in NP-40 buffer (50mM Hepes pH7.4, 150mM NaCl, 20mM β-glycerophosphate, 2.5mM NaF, 5mM EGTA, 1mM EDTA, 15mM PPI, 1% NP-40, 10µg/ml Leupeptin, 10µg/ml Aprotinin, 2mM Na Ortho Vanadate, 1mM DTT and 1mM PMSF). Tumor lysates were homogenized in NP-40 buffer using a polytron (Kinematica). Lysates were cleared by centrifugation and protein concentration was measured by Bradford (Bio-Rad) using bovine serum albumin as a standard. Samples were boiled in SDS-sample buffer. The proteins were separated by SDS-PAGE, blotted onto polyvinylidene difluoride membranes (Millipore) and probed with the specific antibodies after blocking with 10% horse serum (Gibco) in 1x TBS and 0.05% Tween 20 (Sigma-Aldrich).

Immunohistochemistry

Tumors and mammary glands were fixed in 4% paraformaldehyde for 24 hours and transferred to 70% ethanol. Fixed tissues were embedded in paraffin and cut into 4 µm thick sections. Immunohistochemistry was performed using the anti-Memo (1:200) or anti-ErbB2 (1:1000) antibodies. Stainings were carried out using the Ventana Discovery XT biomarker platform (Roche Diagnostics).

Animal Experiments

Animal experiments were performed according to the Swiss guidelines governing animal experimentation and approved by the Swiss veterinary authorities. To generate the triple transgenic mouse lines MMTV-*NeuNT*/MMTV-*Cre*/*Memo*$^{fl/fl;fl/+;+/+}$ and the double transgenic mouse lines MMTV-Neu*NT*/*Memo*$^{fl/fl;fl/+;+/+}$ following lines were crossed: The conditional Memo KO (*Memo*$^{fl/fl}$) mice that were generated as described previously (Haenzi et al., 2014) and backcrossed into FVB/N background, were crossed with MMTV-*Cre* and/or with MMTV-*NeuNT* lines that were both a kind gift from Mohamed Bentires-Alj. For the allograft experiment with tumor cells isolated from MMTV-NeuNT/Memo$^{fl/fl;+/+}$ tumors that were infected with adenovirus containing a sequence for Cre-GFP or GFP alone, 1.5 x 10^6 tumor cells were injected with 25% Matrigel (BD Biosciences) into the mammary gland of Balb/c nude mice (Charles River). Mice were monitored twice weekly for tumor onset. Tumor growth was measured and tumor volume calculated (height x $(\text{diameter}/2)^2 \times \pi$). At the end of the experiment, mice were euthanized and tumors dissected.

Isolation of tumor cells and infection with adenovirus

Isolated tumors were cut into small pieces and digested for 1h in a 37°C water bath using 1mg/ml collagenase (Roche), 1mg/ml dispase (Roche) and 50KU/ml DNAse (Sigma). Single cells were plated and incubated o.n. at 37°, 5% CO_2. The next day, the cells were infected with adenovirus Ad-Cre-GFP or Ad-GFP (Vector Biolabs) at a MOI 100 and cultured for another four days before they were harvested and injected into mammary glands of immunodeficient mice.

4. Discussion and Outlook

4.1 HDAC11 in ER-positive breast cancer

Our study revealed that HDAC11 is overexpressed in human breast cancer compared to normal breast and it correlates with ER expression levels. Furthermore, HDAC11 expression is controlled by ER signaling, as E2 stimulation increases *HDAC11* mRNA levels, while inhibition of the pathway by tamoxifen or fulvestrant decreases *HDAC11* transcription. KD of HDAC11 in the ER-positive breast cancer cell lines T47D, MCF7 and J110, decreases cell proliferation, but does not significantly alter proliferation of the ER-negative breast cancer cell lines MDA-MB-231 and SUM159. Moreover, RNA-sequencing experiments revealed a higher number of upregulated than downregulated genes upon HDAC11 KD, underscoring its role as a transcriptional repressor. Interestingly, GSEA analysis suggests that HDAC11 affects the estrogen responsive transcriptional program, as genes normally downregulated upon estrogen signaling are upregulated in HDAC11 KD cells compared to control cells. Furthermore, Kaplan-Meier analysis revealed that HDAC11 has prognostic value for patients who received endocrine therapy, as the probability of RFS and DMFS was decreased for the HDAC11-high group.

HDAC11 affects ER expression levels

We observed a reduction in ER protein and mRNA levels upon HDAC11 KD in T47D as well as in MCF7 cells. As HDAC11 is a transcriptional repressor (Villagra et al., 2009), it is unlikely that HDAC11 induces *ESR1* transcription in a direct manner. However, HDAC11 might directly repress genes encoding proteins or miRNAs, which repress *ESR1* transcription or target *ESR1* mRNA, respectively (Figure 3.12). Indeed, several miRNAs, including miR-206 (Adams et al., 2007), miR-221 and miR-222 (Zhao et al., 2008) negatively regulate ER expression. Future experiments such as ChIP-sequencing, might identify genes directly repressed by HDAC11, and could reveal how HDAC11 affects ER levels.

Additionally, HDAC11 might also control ER protein levels through deacetylation of the ER chaperone Hsp90. Hyperacetylation of Hsp90 in response to HDAC6 inhibition decreases its

binding to ER, leading to polyubiquitylation and proteasomal degradation of ER (Fiskus et al., 2007). Thus, it would be interesting to investigate the acetylation status of Hsp90 in HDAC11 KD cells and to test if ER ubiquitylation is affected by HDAC11 (Figure 3.12).

HDAC11 controls part of the estrogen-induced transcriptional program

Genes normally downregulated in response to estrogen signaling are upregulated in HDAC11 KD cells compared to control cells. Thus HDAC11 might contribute to the estrogen induced transcriptional program by acting as a transcriptional repressor. However, it remains unknown how HDAC11 mediates gene repression in response to estrogen signaling. Several mechanisms are possible, which might include deacetylation of the ER directly and/or ER-interacting proteins such as transcription factors and coregulatory proteins.

The ER represses genes by recruiting corepressors such as NCoR1 and HDAC1 (Jackson et al., 1997; Kawai et al., 2003) to gene promoters. Thus, HDAC11 might be recruited to specific genes through interaction with ER and induce chromatin condensation and/or alter ER transcriptional activity. We did not observe differences in transcriptional activity of ER measured by an ER-responsive reporter construct, however this does not rule out that ER transcriptional activity is affected by HDAC11 on specific genes. As ER has been shown to be acetylated by the HAT p300, which, depending on the acetylation site, increases (Kim et al., 2006) or decreases (Wang et al., 2001) ER transcriptional activity, HDAC11 might control ER activity through its deacetylase function (Figure 4.1). Therefore, it would be interesting to analyze if HDAC11 and ER interact and if HDAC11 can deacetylate ER at specific sites.

Alternatively, HDAC11 might be recruited to ER target genes by interacting with transcription factors such as AP1, a known ER interacting protein (Kushner et al., 2000). Interestingly, genome wide analysis of ER binding sites revealed that late downregulated ER target genes (at 6 and 12h of E2 stimulation) are more likely to contain AP1 binding sites close to their promoter region, suggesting that AP1 promotes transcriptional repression of these genes (Carroll et al., 2006). AP1 interacts with the corepressor protein NRIP1/RIP140 (Teyssier et al., 2003), whose transcription is induced upon estrogen signaling, and KD of NRIP1 prevents repression of

several genes normally repressed by estrogen signaling (Carroll et al., 2006). Thus, it would be interesting to test if HDAC11 is recruited to ER target genes by AP1. Co-IP experiments should reveal if these two proteins can interact, and Re-ChIP experiments would be required to test whether HDAC11 and AP1 are found at the same gene promoters. Additionally, HDAC11 might also affect AP1 transcriptional activity, as the class II HDAC SIRT1 has been shown to deacetylate AP1, thereby repressing AP1 transcriptional activity (Figure 4.1) (Zhang et al., 2010c).

Moreover, several ER coregulatory proteins are regulated by acetylation. For example, acetylation of the two ER corepressor proteins NRIP1/RIP140 and HDAC1 (Carroll et al., 2006; Kawai et al., 2003; Lopez-Garcia et al., 2006), leads to loss of gene repression. In the case of NRIP1, acetylation prevents its association with the transcriptional regulator CtBP (Vo et al., 2001), while acetylation of HDAC1 inhibits its deacetylase function (Figure 4.1) (Qiu et al., 2006).

Thus, HDAC11 could repress gene transcription by various mechanisms. Future studies will be aimed to identify the genes directly regulated by HDAC11 as well as its interaction partners by ChIP-sequencing and mass spectrometric experiments, respectively.

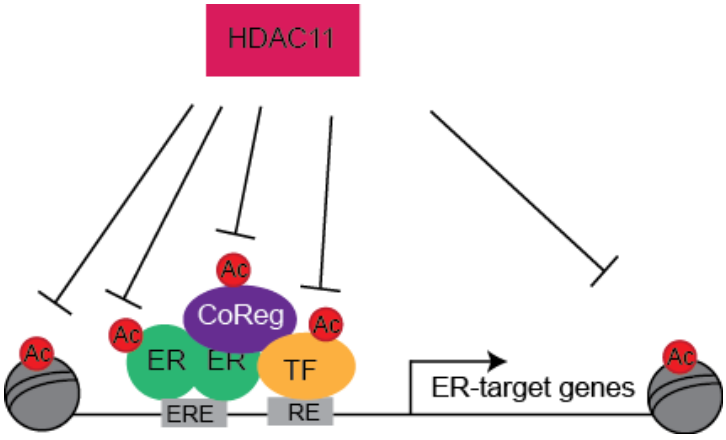

Figure 4.1 Potential mechanisms through which HDAC11 could mediate gene repression in response to estrogen signaling. HDAC11 could be recruited to ER-target genes by ER, coregulatory proteins (CoReg) or transcription factors (TF), where it could deacetylate histone proteins leading to chromatin condensation, decreased transcriptional activity of ER and/or other TF, or prevent binding of other coregulatory proteins. Abbreviations: response element (RE), estrogen response element (ERE)

HDAC11 as a therapeutic target for breast cancer

Searching online available databases revealed that HDAC11 is overexpressed in human breast cancer compared to normal breast, suggesting an oncogenic role for HDAC11. This is supported by our finding that HDAC11 controls proliferation of ER-positive breast cancer cell lines. Furthermore, allograft experiments using the ER-positive murine breast cancer cell line J110 revealed reduced tumor growth of HDAC11 KD cells. However, further experiments are required to test if HDAC11 might be a target for breast cancer therapy. Xenograft experiments using T47D and/or MCF7 control and HDAC11 KD cells could shed light on HDAC11's potential to affect tumor growth of human cell lines *in vivo*. Treatment of tumor bearing mice with an HDAC11-inhibitor, might give additional insight if targeting HDAC11 is beneficial, particularly since targeting HDAC11 in immune cells has been shown to decrease anti-tumor immune responses and to cause increased tumor growth (Sahakian et al., 2014). However, this experiment would require the development of HDAC11 specific inhibitors, as inhibitors that target HDAC11, generally also target class I and/or class II HDACs (Mottamal et al., 2015).

Kaplan-Meier analysis revealed a decrease in the probability for RFS and DMFS for patients treated with endocrine therapy, expressing high HDAC11 levels. As this group of patients is likely to contain endocrine resistant tumors, HDAC11 might play a role in resistance. In order to investigate if tumors expressing high HDAC11 levels are more likely to develop resistance, IHC for HDAC11 on primary tumors and matched relapsed tumors that developed resistance against endocrine therapies are needed. Furthermore, *in vitro* studies using tamoxifen resistant cell lines such as T47D-TMR and MCF7-TMR, might give additional insights into HDAC11's potential role in endocrine resistance.

To conclude, our study suggests that HDAC11 is an estrogen induced transcriptional repressor, promoting ER-positive breast cancer cell proliferation. Furthermore, HDAC11 is overexpressed in human breast cancer and high HDAC11 levels in endocrine treated patients correlates with an increased risk of early disease recurrence. Important areas for future research would be to learn more about HDAC11's potential role in the development of endocrine resistance and development of more specific HDAC11 inhibitors to test their effects in the clinic.

4.2 Memo in Metastasis and Tumorigenesis

We have shown that Memo is a copper-binding redox protein essential for cell migration and metastasis. Our data suggest that Memo promotes migration by sustaining NOX-mediated ROS production in cellular protrusions, which are the locations of proteins that are redox controlled and known to be important for cell migration. Furthermore, we found that Memo alters the redox state of RhoA and Shc. While Memo is required for breast cancer cell migration and metastasis, KD of Memo in several breast cancer cell lines did not affect cell proliferation *in vitro*, and tumor growth of the triple-negative as well as NeuNT-driven tumor models were not affected by Memo KD or KO, respectively. However, the average size of lung metastases that disseminated from Memo KD tumors, were smaller in size, suggesting that these cells have a growth disadvantage in the lung environment. Moreover, our observation that all developing tumors in the NeuNT-driven breast cancer model were Memo-positive, might have been caused by an early growth defect of Memo-negative cells in the mammary gland. In addition, high cytoplasmic localization of Memo in human breast cancer correlated with the proliferation marker Ki67. Together, this data suggest a role for Memo in proliferation during early tumor development and metastasis. Importantly, we provide evidence that Memo has prognostic value for breast cancer patients, as distant metastasis-free survival and overall survival decreased for patients with high cytoplasmic Memo. Furthermore, preliminary experiments suggest that Memo might have a role in normal mammary gland development.

Memo controls the redox-milieu in cellular protrusions and promotes migration

We and others have demonstrated that Memo is required for breast cancer cell migration (Marone et al., 2004; Meira et al., 2009; Zaoui et al., 2008, 2010). Our novel finding, that Memo is a copper-binding redox protein, sheds new light on how Memo might control cell migration.

KD of Memo causes a decrease in ROS levels in cellular protrusions upon serum stimulation, and ROS is known to be involved in affecting proteins located in these protrusions and important for the migration process (Moldovan et al., 2000; Wagner and Gorin, 2014). Localized, and tightly regulated ROS can act as signaling molecules, inducing reversible oxidation of

proteins, thereby altering protein structure, interaction and activity (Ray et al., 2012). Despite the increasing number of proteins found to be redox-regulated and known to be involved in cell migration, the exact targets of Memo and how these are involved in cell migration is still largely unknown.

The main source of ROS in cellular protrusions is generated by NOX-enzymes, which are membrane spanning proteins that require the assembly and activation of numerous NOX-specific cytoplasmic subunits for their enzymatic activity. Growth factors have been shown to induce the recruitment of these subunits to cellular protrusions where they form functional ROS-producing NOX complexes (Hurd et al., 2012). Many of the NOX-subunits are subject to functionally relevant phosphorylation, including p22phox, p47phox and p67phox (Brandes et al., 2014), which is controlled through the opposing actions of protein kinases and PTPs. The protein kinase MEK1/2 for example, phosphorylates and activates p67phox, while dephosphorylation by the PTP type 1 and type 2A (PP1/2A) causes its inhibition and suppresses ROS production (Dang et al., 2011). We have demonstrated that Memo is involved in sustained ROS production by NOX complexes. The initial NOX-dependent ROS production was not affected by Memo, which suggests that Memo does not control the assembly and activation of the NOX-complex. This is in concordance with the previous finding that Memo is not required for localization of Rac1 to the cell membrane (Zaoui et al., 2008), a protein whose recruitment is essential for NOX-activation (Diekmann et al., 1994).

As Memo mediates sustained ROS production, we hypothesize that Memo maintains the NOX-subunits in an active state. This might be achieved through regulation of PTPs, which are known to be redox-sensitive. PTPs have a cysteine residue in their active site that normally acts as a phosphate acceptor. Oxidation of this cysteine residue leads to inhibition of the PTP's phosphatase-activity (Cunnick et al., 1998; Lee et al., 1998). Thus, Memo might oxidize and inhibit specific PTPs, preventing the removal of phosphate groups from NOX-subunits, thereby sustaining NOX-activity. Furthermore, Memo might also regulate the activity of tyrosine kinases that phosphorylate and activate NOX-subunits. One such kinase is SRC, which can be activated via oxidation of two cysteine residues (Giannoni et al., 2005), and has been demonstrated to induce NOX-dependent ROS production (Gianni et al., 2008). Future studies will be aimed at

uncovering whether Memo can control the redox-state of PTPs and/or tyrosine kinases, and thereby alter NOX-mediated ROS production. Alternatively, Memo could maintain NOX-activity by shuttling proteins that regulate NOX-activity to the cell cortex. Indeed, Memo has been shown to control the localization of several proteins involved in cell migration, such as RhoA and mDia1, to the cell cortex (Zaoui et al., 2008). Future studies will reveal if Memo mediates sustained ROS production by NOX-complexes through controlling the activation and/or localization of NOX-subunits.

Interestingly, using *in vitro* biochemical assays we found that Memo can directly oxidize RhoA. Previous studies have revealed that RhoA is subject to different types of redox control in cells in a direct and indirect manner. For example, Rac1-dependent ROS production leads to inhibition of the low-molecular weight protein tyrosine phosphatase (LMW-PTP), resulting in an increase in the phosphorylation and activation of its target, p190Rho-GAP. Activation of p190Rho-GAP, a Rho-specific GTPase-activating protein, facilitates the hydrolysis of RhoA-bound GTP to GDP, leading to RhoA inactivation. Thus, ROS indirectly causes a decrease in RhoA activity (Nimnual et al., 2003). Moreover, it has been demonstrated that direct oxidation of two RhoA cysteine residues (Cys16 and Cys20) enhances RhoA activity, leading to increased actin stress fiber formation. This was lost in cells expressing an oxidation-insensitive mutant $RhoA^{C16/20A}$ (Aghajanian et al., 2009). However, it was not tested whether the increase in stress fiber formation, a well characterized readout of Rho activity (Ridley and Hall, 1992), subsequently increased cell migration. Thus, it remains unknown whether oxidation of RhoA is required for cell migration. Interestingly, we have shown that these two cysteine residues are oxidized by Memo *in vitro* and that Memo KD cells have increased levels of reduced RhoA (section 3.3 Figure 4G and 5B). Hence, Memo might control RhoA activity through oxidation, and thereby modulate cell migration. To test whether Memo's activity is required for RhoA-activation and thus cell migration, and if so, if RhoA is the main target of Memo, cell lines KD for both Memo and RhoA could be reconstituted with combinations of WT Memo or RhoA and mutant Memo (enzymatically impaired) or mutant RhoA (oxidation-insensitive) constructs. If these two proteins converge on the same pathway, the loss of activity of either should produce a similar migration phenotype.

Other proteins involved in cell migration could potentially be controlled through their redox status by Memo. Cofilin for example, a known interactor of Memo that mediates cell migration (Meira et al., 2009), is regulated by redox-signaling directly and indirectly. Specifically, oxidation of the protein 14-3-3 through Nox-generated ROS causes dissociation of the PTP Slingshot-1L (SSH-1L) from the 14-3-3/SSH-1L complex. This leads to SSH-1L-mediated dephosphorylation of cofilin and induces its actin-severing and dephosphorylating activities (Kim et al., 2009). Moreover, direct oxidation of two cofilin cysteine residues (Cys139 and Cys147) in cells, decreases its binding to F-actin, resulting in reduced F-actin severing (Cameron et al., 2015). It would therefore be interesting, to investigate if Memo directly, or indirectly alters cofilin activity through its redox-activity.

Future studies are required to investigate whether Memo's enzymatic activity is required for cell migration, or whether its main function in this process is to control the localization of important proteins to the cell membrane. Experiments in Memo KD cells, reconstituted with an enzymatic dead Memo mutant, should reveal if the redox-activity of Memo is required for cell migration.

Memo's role in the nucleus

Our analysis of human breast tumor samples revealed that high nuclear Memo expression inversely correlated with poor prognostic factors, including high tumor grade, ER/Progesterone-Receptor-negative, and triple-negative tumors, while high cytoplasmic localization positively correlated with these factors. This suggests that Memo might have different functions, depending on its cellular localization. Cytoplasmic Memo is involved in cell migration, while nothing is known about its nuclear function. Memo contains a nuclear export sequence, and its nuclear export can be blocked by leptomycin B, suggesting that Memo is actively exported from the nucleus via exportins. Memo does not contain a nuclear localization sequence, but due to its small size of 33kDa, it could enter the nucleus by passive diffusion through the nuclear pores. However, as Memo accumulates in the nucleus upon growth factor

stimulation of leptomycin B treated cells, this could be indicative of a potential active import mechanism for Memo (Schlatter et al., 2012).

Interestingly, Memo interacts with the ER (Jiang et al., 2013), a transcription factor that translocates to the nucleus upon activation to regulate gene transcription (Heldring et al., 2007). Intriguingly, transcriptional activity of ER has been reported to be modulated by Memo, which was suggested to be mediated by an extra nuclear function, as the interaction was thought to be only cytoplasmic (Jiang et al., 2013). However, as we have shown that Memo is also expressed in the nucleus (Schlatter et al., 2012), it would be interesting to test whether the interaction with ER also occurs in this cellular compartment or whether Memo enters the nucleus in a complex with ER. Furthermore, the question of what Memo's function is in the nucleus remains to be determined. An obvious first step would be to investigate if Memo can bind DNA, either directly or in a complex with ER. Interestingly, one study suggested that ER-transcriptional activity might be regulated by oxidation. Low levels of ROS decreased the DNA-binding capacity of ER, which was reverted through addition of thioredoxin (Hayashi et al., 1997), an antioxidant that facilitates the reduction of proteins by cysteine thiol-disulfide exchange (Holmgren, 1985). Indeed, several transcription factors have been shown to be redox-controlled, including p53, NF-κB and AP1 (Sun and Oberley, 1996). Thus, it would be interesting to explore if Memo controls the redox state of ER and thereby influences its transcriptional activity.

Furthermore, to study the role of the cytoplasmic- versus nuclear localization of Memo in cancer, *in vivo* experiments could be performed using cells expressing constructs targeting Memo specifically to the nucleus or to the cytoplasm. Immunoprecipitations using cytoplasmic- and nuclear cellular fractions, in combination with mass-spectrometry analysis, should identify new interaction partners of Memo, which might provide more insight in its cytoplasmic- and nuclear functions.

Memo in normal mammary gland development

In the normal mammary gland, Memo is expressed through all stages of development including puberty, virgin, pregnancy, lactation and involution. The mammary gland consists mainly of two cell types, the luminal epithelial cells that face the lumen of the ducts and are responsible for milk production, and the outer layer of myoepithelial cells that are contractile and participate in the delivery of milk (Inman et al., 2015). Interestingly, we discovered that Memo is specifically expressed in luminal cells, while myoepithelial cells are negative for Memo. Furthermore, in mammary glands from pubertal mice, Memo is expressed only in a subset of luminal cells, while all luminal cells express Memo during pregnancy, lactation and involution. This suggests that Memo-negative cells are either outcompeted, or that the expression of Memo increases after puberty, or during pregnancy. In order to know when exactly the expression of Memo in luminal cells changes, samples of adult virgin mice will have to be investigated in the future.

Memo is expressed during all stages of development and changes its expression pattern between puberty and later stages of mammary gland development, suggesting it may play a role during mammary gland development. The mammary gland is a unique organ, as the final stages of development occur postnatal. At birth, the mammary fat pad contains a rudimentary ductal tree, which at the onset of puberty, and in response to ovarian hormones, starts to invade into the mammary fat pad. The terminal end buds (TEBs), located on the tips of the ducts, are highly proliferative and penetrate into the fat pad until it is entirely filled with a network of branching ducts. During pregnancy, secretory alveoli are formed and are responsible for milk production and secretion during lactation. In order to re-establish the mammary gland after weaning, the mammary gland undergoes a process called involution (Inman et al., 2015). A large number of different hormones, cytokines and growth factors control these different stages of development (Hynes and Watson, 2010).

Interestingly, many receptors known to interact with Memo are implicated in these processes. For example the ER, which is expressed in about 15% of luminal cells (Clarke et al., 1997), plays an important role during ductal outgrowth (Mallepell et al., 2006). Moreover, ErbB2, which in contrast to ER is expressed in the majority of the luminal cells (Schroeder and Lee, 1998), is

required for morphogenesis during puberty, as evidenced by the fact that ErbB2 KO mammary glands have structural defects in TEBs (Jackson-Fisher et al., 2004). Similar findings were observed with a mutated IGF1R (Bonnette and Hadsell, 2001). As Memo has been found downstream of these receptors in breast cancer cells (Jiang et al., 2013; Marone et al., 2004; Sorokin and Chen, 2013), Memo could play a role during mammary gland development. To study this hypothesis, mammary gland specific Memo KO and/or Memo overexpression mice should be generated. Not only would this be a useful tool to elucidate the normal function of Memo in the mammary gland, it could also be used to examine the role of Memo in breast cancer tumorigenesis and metastasis.

The role of Memo in NeuNT-driven tumorigenesis

Our analysis of human breast tissue microarrays revealed Memo to be expressed at low levels in normal breast and at significantly higher levels in 40% of breast cancers, suggesting that it might be involved in tumorigenesis. However, in a spontaneous MMTV-*NeuNT*-driven mammary tumor model, in which Cre-mediated excision of floxed *Memo* alleles is achieved specifically in the mammary gland, no differences in tumor onset or in the average number of tumors per mouse were observed between mice harboring floxed *Memo* alleles and mice with non-floxed *Memo* alleles. Interestingly, tumors from all mice were positive for Memo expression, which could be explained by one of the following three hypotheses: 1) Memo is required for NeuNT-driven tumorigenesis; 2) Memo-depleted mammary epithelial cells have a growth defect and are selected out by Memo expressing cells; or 3) the Cre-recombinase was not active.

MMTV-*Cre* is well known to be expressed in a mosaic pattern in the mammary gland (Lu et al., 2008; Wagner et al., 2001). Thus, it is likely that the mammary glands from mice harboring the floxed Memo alleles still contain some Memo-expressing cells. Assuming that Memo deletion was achieved in a significant number of cells, and given our observation that all mice developed tumors, independent of the Memo phenotype, might suggest that Memo is required for NeuNT-driven tumorigenesis. However, one would expect that tumors would

develop less frequently, as statistically a lower number of Memo-expressing cells should lead to a reduced number of tumors, or a delayed tumor formation. Since all mouse lines developed tumors with the same latency, with no difference in the average tumor number per mouse, the lack of Memo-negative tumors cannot be explained by our first hypothesis.

Accordingly, our second hypothesis is based on the mosaic expression pattern of MMTV-*Cre*. In contrast to the first hypothesis, we assume that Memo KO cells have a growth and/or survival disadvantage that leads to mammary glands mainly consisting of Memo-expressing cells, independent of the presence or absence of floxed Memo alleles. Indeed, it has been previously reported that in the mammary glands of MMTV-*Cre* transgenic mice that harbored floxed *Fgfr2* alleles, FGFR2-negative cells in the TEBs were outcompeted by FGFR2-expressing cells. BrdU incorporation assays revealed that the remaining FGFR2-negative cells were less proliferative than FGFR2 positive cells (Lu et al., 2008). Similarly, Memo KO cells could potentially be outcompeted by Memo-expressing tumor cells.

In contrast to mammary glands from pubertal mice, mammary glands of mice during the stages of pregnancy, lactation and involution had no Memo-negative cells. One could speculate that also during normal development, and in the absence of the *Cre*-transgene, Memo-negative cells are outcompeted by Memo expressing-cells. However, we cannot rule out that the Cre-recombinase was not functional in our transgenic mouse lines. We did confirm the presence of the *Cre*-transgene in these mice, however we did not test for Cre-activity. To do this, one would have to cross these mice with reporter lines such as the R26R-line. This mouse line harbors a LacZ-transgene that is preceded by a floxed stop-cassette. Thus, active Cre leads to LacZ expression, which can then be assayed for β–galactosidase activity (Soriano, 1999). As we did not test for Cre-activity, we cannot rule out that our Cre was not functional. It should be mentioned, however, that the same Cre-transgenic line has been successfully used by another lab in the FMI (Balavenkatraman et al., 2011; Meyer et al., 2011).

To further investigate the function of Memo in tumorigenesis *in vivo*, the MMTV/NIC mouse line could be used in which an oncogenic mutant Neu and Cre-recombinase are linked by an internal ribosome entry site (IRES) and therefore expressed from the same transcript (MMTV-neu-IRES-cre) (Ursini-Siegel et al., 2008). This could verify, that Memo excision and *Neu*-

expression can occur in the same cells, at the same time. If Memo is required for Neu-driven tumorigenesis, one would expect no tumor formation in mice with floxed Memo alleles.

Memo does not affect primary tumor growth, but promotes metastasis.

Tumor xenograft experiments using the triple-negative human tumor cell line MDA-MB-231 revealed no differences in tumor onset or growth between Memo WT and KD cells. Similarly, tumor allograft experiments using tumor cells derived from MMTV-NeuNT transgenic mice, in which Memo deletion was achieved *in vitro*, revealed no significant differences between Memo WT and KO cells. The number of mice in this experiment was relatively small and we observed large variance within the different groups, potentially reflecting the different genetic profiles of these cells, as they were derived from different tumors. However, analysis of the tumor growth of Memo WT and KO tumors that originated from the same tumor, infected once with Cre-recombinase (Memo KO) or once with GFP-alone (Memo WT), showed no differences. Thus, Memo does not affect tumor growth of this MMTV-*NeuNT*-driven tumor cell line, which is in line with the results from the human triple-negative cell line MDA-MB-231.

Using breast cancer xenograft models, we demonstrated that Memo is required for spontaneous breast cancer metastasis. Memo KD tumors had less migrating cells than control tumors, leading to a decreased number of lung metastases. Furthermore, the average size of the metastases derived from Memo KD tumors was smaller, suggesting that these cells had a growth and/or survival disadvantage in the lung environment. Thus, Memo might be a promising target in breast cancer therapy to prevent or treat metastases.

Further studies are required to test if Memo's enzymatic function, which requires copper, is essential to promote metastasis. In our experiments, a copper chelator decreased the invasive potential of Memo WT MDA-MB-231 cells, but had no additive effect on Memo KD cells, suggesting the hypothesis that Memo's enzymatic activity contributes to its function in cell invasion and potentially metastasis. Interestingly, preclinical- and early clinical results have suggested that the use of copper chelators produces beneficial results with respect to tumor growth (Brady et al., 2014), angiogenesis (Juarez et al., 2006) as well as for re-sensitization to

platinum-based cancer therapies (Fu et al., 2014). Thus, as Memo's copper-dependent enzymatic activity might be involved in metastasis, copper chelators could be beneficial for the treatment of metastatic breast cancers over-expressing cytoplasmic Memo. Several clinical trials using copper chelators for different types of cancer are ongoing (https://clinicaltrials.gov/ct2/results?term=copper+chelator+cancer&Search=Search). If these trials are successful, it would be interesting to analyze the expression of Memo in tumors that responded to copper chelators and those that did not.

With this study, we identified a new redox protein playing an important role during cell migration. Here, we provide evidence that Memo expression is of relevance for human breast cancer, as it is expressed at high levels in 40% of breast cancer and its cytoplasmic localization is prognostic for aggressive disease. Moreover, Memo is required for breast cancer metastasis. The treatment of metastases remains a big challenge and new therapeutic targets are required. Future studies will reveal, if Memo could be a new target to treat or prevent metastases.

5. References

Abe, F., Dafferner, A.J., Donkor, M., Westphal, S.N., Scholar, E.M., Solheim, J.C., Singh, R.K., Hoke, T. a., and Talmadge, J.E. (2010). Myeloid-derived suppressor cells in mammary tumor progression in FVB Neu transgenic mice. Cancer Immunol. Immunother. *59*, 47–62.

Abercrombie, M., Joan, E., Heaysman, M., and Pegrum, S.M. (1970). The locomotion of fibroblasts in culture. Exp. Cell Res. *60*, 437–444.

Aceto, N., Bardia, A., Miyamoto, D.T., Donaldson, M.C., Wittner, B.S., Spencer, J.A., Yu, M., Pely, A., Engstrom, A., Zhu, H., et al. (2014). Circulating Tumor Cell Clusters Are Oligoclonal Precursors of Breast Cancer Metastasis. Cell *158*, 1110–1122.

Adachi, T., Togashi, H., Suzuki, A., Kasai, S., Ito, J., Sugahara, K., and Kawata, S. (2005). NAD(P)H oxidase plays a crucial role in PDGF-induced proliferation of hepatic stellate cells. Hepatology *41*, 1272–1281.

Adams, B.D., Furneaux, H., and White, B. a (2007). The micro-ribonucleic acid (miRNA) miR-206 targets the human estrogen receptor-alpha (ERalpha) and represses ERalpha messenger RNA and protein expression in breast cancer cell lines. Mol. Endocrinol. *21*, 1132–1147.

Adimoolam, S., Sirisawad, M., Chen, J., Thiemann, P., Ford, J.M., and Buggy, J.J. (2007). HDAC inhibitor PCI-24781 decreases RAD51 expression and inhibits homologous recombination. Proc. Natl. Acad. Sci. U. S. A. *104*, 19482–19487.

Afshar, G., and Murnane, J.P. (1999). Characterization of a human gene with sequence homology to Saccharomyces cerevisiae SIR2. Gene *234*, 161–168.

Aghajanian, A., Wittchen, E.S., Campbell, S.L., and Burridge, K. (2009). Direct Activation of RhoA by Reactive Oxygen Species Requires a Redox-Sensitive Motif. PLoS One *4*, e8045.

Ali, S., Metzger, D., Bornert, J.M., and Chambon, P. (1993). Modulation of transcriptional activation by ligand-dependent phosphorylation of the human oestrogen receptor A/B region. EMBO J. *12*, 1153–1160.

Andersen, J.K. (2004). Oxidative stress in neurodegeneration: cause or consequence? Nat. Med. *10*, S18–S25.

Androutsellis-Theotokis, A., Chrousos, G.P., McKay, R.D., DeCherney, A.H., and Kino, T. (2013). Expression profiles of the nuclear receptors and their transcriptional coregulators during differentiation of neural stem cells. Horm.Metab Res. *45*, 159–168.

Aumais, J.P., Lee, H.S., Lin, R., and White, J.H. (1997). Selective interaction of hsp90 with an estrogen receptor ligand-binding domain containing a point mutation. J. Biol. Chem. *272*, 12229–12235.

Auricchio, F., and Migliaccio, A. (1980). In vitro inactivation of oestrogen receptor by nuclei. Prevention by phosphatase inhibitors. FEBS Lett. *117*, 224–226.

Babior, B.M., Kipnes, R.S., and Curnutte, J.T. (1973). Biological defense mechanisms. The production by leukocytes of superoxide, a potential bactericidal agent. J. Clin. Invest. *52*, 741–744.

Babior, B.M., Curnutte, J.T., and Kipnes, R.S. (1975). Biological defense mechanisms. Evidence for the participation of superoxide in bacterial killing by xanthine oxidase. J. Lab. Clin. Med. *85*, 235–244.

Bagatell, R., Khan, O., Paine-Murrieta, G., Taylor, C.W., Akinaga, S., and Whitesell, L. (2001). Destabilization of steroid receptors by heat shock protein 90-binding drugs: A ligand-independent approach to hormonal therapy of breast cancer. Clin. Cancer Res. *7*, 2076–2084.

Bagui, T.K., Sharma, S.S., Ma, L., and Pledger, W.J. (2013). Proliferative status regulates HDAC11 mRNA abundance in nontransformed fibroblasts. Cell Cycle *12*, 3433–3441.

Baker, M.E. (1998). Albumin's role in steroid hormone action and the origins of vertebrates: Is albumin an essential protein? FEBS Lett. *439*, 9–12.

Balavenkatraman, K.K., Aceto, N., Britschgi, A., Mueller, U., Bence, K.K., Neel, B.G., and Bentires-Alj, M. (2011). Epithelial protein-tyrosine phosphatase 1B contributes to the induction of mammary tumors by HER2/Neu but is not essential for tumor maintenance. Mol. Cancer Res. *9*, 1377–1384.

Balko, J.M., Giltnane, J.M., Wang, K., Schwarz, L.J., Young, C.D., Cook, R.S., Owens, P., Sanders, M.E., Kuba, M.G., Sánchez, V., et al. (2014). Molecular profiling of the residual disease of triple-negative breast cancers after neoadjuvant chemotherapy identifies actionable therapeutic targets. Cancer Discov. *4*, 232–245.

Barnes, C.J., Vadlamudi, R.K., and Kumar, R. (2004). Novel estrogen receptor coregulators and signaling molecules in human diseases. Cell. Mol. Life Sci. *61*, 281–291.

Barretina, J., Caponigro, G., Stransky, N., Venkatesan, K., Margolin, A. a., Kim, S., Wilson, C.J., Lehár, J., Kryukov, G. V., Sonkin, D., et al. (2012). The Cancer Cell Line Encyclopedia enables predictive modelling of anticancer drug sensitivity. Nature *483*, 603–307.

Bestor, T., Laudano, A., Mattaliano, R., and Ingram, V. (1988). Cloning and sequencing of a cDNA encoding DNA methyltransferase of mouse cells. J. Mol. Biol. *203*, 971–983.

Bhaskara, S., Knutson, S.K., Jiang, G., Chandrasekharan, M.B., Wilson, A.J., Zheng, S., Yenamandra, A., Locke, K., Yuan, J.L., Bonine-Summers, A.R., et al. (2010). Hdac3 is essential for the maintenance of chromatin structure and genome stability. Cancer Cell *18*, 436–447.

Biçaku, E., Marchion, D.C., Schmitt, M.L., and Münster, P.N. (2008). Selective inhibition of histone deacetylase 2 silences progesterone receptor-mediated signaling. Cancer Res. *68*, 1513–1519.

Bidwell, B.N., Slaney, C.Y., Withana, N.P., Forster, S., Cao, Y., Loi, S., Andrews, D., Mikeska, T., Mangan, N.E., Samarajiwa, S. a, et al. (2012). Silencing of Irf7 pathways in breast cancer cells promotes bone metastasis through immune escape. Nat. Med. *18*, 1224–1231.

Bill, R., and Christofori, G. (2015). The relevance of EMT in breast cancer metastasis: Correlation or causality? FEBS Lett. *589*, 1577–1587.

Boersma, B.J., Reimers, M., Yi, M., Ludwig, J. a, Luke, B.T., Stephens, R.M., Yfantis, H.G., Lee, D.H., Weinstein, J.N., and Ambs, S. (2008). A stromal gene signature associated with inflammatory breast cancer. Int. J. Cancer *122*, 1324–1332.

Bolden, J.E., Peart, M.J., and Johnstone, R.W. (2006). Anticancer activities of histone deacetylase inhibitors. Nat. Rev. Drug Discov. *5*, 769–784.

Bonnette, S.G., and Hadsell, D.L. (2001). Targeted disruption of the IGF-I receptor gene decreases cellular proliferation in mammary terminal end buds. Endocrinology *142*, 4937–4945.

Boveris, a, Oshino, N., and Chance, B. (1972). The cellular production of hydrogen peroxide. Biochem. J. *128*, 617–630.

Brabletz, T. (2012). To differentiate or not — routes towards metastasis. Nat. Rev. Cancer *12*, 425–436.

Brady, D.C., Crowe, M.S., Turski, M.L., Hobbs, G.A., Yao, X., Chaikuad, A., Knapp, S., Xiao, K., Campbell, S.L., Thiele, D.J., et al. (2014). Copper is required for oncogenic BRAF signalling and tumorigenesis. Nature *509*, 492–496.

Brandes, R.P., Weissmann, N., and Schröder, K. (2014). Nox family NADPH oxidases: Molecular mechanisms of activation. Free Radic. Biol. Med. *76*, 208–226.

Bravo-Cordero, J.J., Magalhaes, M. a O., Eddy, R.J., Hodgson, L., and Condeelis, J. (2013). Functions of cofilin in cell locomotion and invasion. Nat. Rev. Mol. Cell Biol. *14*, 405–415.

Broide, R.S., Redwine, J.M., Aftahi, N., Young, W., Bloom, F.E., and Winrow, C.J. (2007). Distribution of histone deacetylases 1-11 in the rat brain. J. Mol. Neurosci. *31*, 47–58.

Brownell, J.E., Zhou, J., Ranalli, T., Kobayashi, R., Edmondson, D.G., Roth, S.Y., and Allis, C.D. (1996). Tetrahymena Histone Acetyltransferase A : A Homolog Acetylation to Gene Activation. Cell *84*, 843–851.

Brünner, N., Bronzert, D., Vindeløv, L.L., Rygaard, K., Spang-Thomsen, M., and Lippman, M.E. (1989). Effect on growth and cell cycle kinetics of estradiol and tamoxifen on MCF-7 human breast cancer cells grown in vitro and in nude mice. Cancer Res. *49*, 1515–1520.

Buglio, D., Khaskhely, N.M., Voo, K.S., Martinez-Valdez, H., Liu, Y.J., and Younes, A. (2011). HDAC11 plays an essential role in regulating OX40 ligand expression in Hodgkin lymphoma. Blood *117*, 2910–2917.

Bunone, G., Briand, P. a, Miksicek, R.J., and Picard, D. (1996). Activation of the unliganded estrogen receptor by EGF involves the MAP kinase pathway and direct phosphorylation. EMBO J. *15*, 2174–2183.

Camerer, E., Qazi, A. a., Duong, D.N., Cornelissen, I., Advincula, R., and Coughlin, S.R. (2004). Platelets, protease-activated receptors, and fibrinogen in hematogenous metastasis. Blood *104*, 397–401.

Cameron, J.M., Gabrielsen, M., Chim, Y.H., Munro, J., McGhee, E.J., Sumpton, D., Eaton, P., Anderson, K.I., Yin, H., and Olson, M.F. (2015). Polarized Cell Motility Induces Hydrogen Peroxide to Inhibit Cofilin via Cysteine Oxidation. Curr. Biol. *25*, 1520–1525.

Carascossa, S., Dudek, P., Cenni, B., Briand, P.A., and Picard, D. (2010). CARM1 mediates the ligand-independent and tamoxifen-resistant activation of the estrogen receptor α by cAMP. Genes Dev. *24*, 708–719.

Cariou, S., Donovan, J.C., Flanagan, W.M., Milic, a, Bhattacharya, N., and Slingerland, J.M. (2000). Down-regulation of p21WAF1/CIP1 or p27Kip1 abrogates antiestrogen-mediated cell cycle arrest in human breast cancer cells. Proc. Natl. Acad. Sci. U. S. A. *97*, 9042–9046.

Carroll, J.S., Meyer, C. a, Song, J., Li, W., Geistlinger, T.R., Eeckhoute, J., Brodsky, A.S., Keeton, E.K., Fertuck, K.C., Hall, G.F., et al. (2006). Genome-wide analysis of estrogen receptor binding sites. Nat. Genet. *38*, 1289–1297.

Cavailles, V., Linares, A., Dalenc, F., Balaguer, P., and Boulle, N. (2011). Manipulating protein acetylation in breast cancer: A promising approach in combination with hormonal therapies? J. Biomed. Biotechnol. *2011*.

Cerami, E., Gao, J., Dogrusoz, U., Gross, B.E., Sumer, S.O., Aksoy, B.A., Jacobsen, A., Byrne, C.J., Heuer, M.L., Larsson, E., et al. (2012). The cBio Cancer Genomics Portal: An open platform for exploring multidimensional cancer genomics data. Cancer Discov. *2*, 401–404.

Chen, W.-T. (1989). Proteolytic activity of specialized surface protrusions formed at rosette contact sites of transformed cells. J. Exp. Zool. *251*, 167–185.

Chen, D., Pace, P.E., Coombes, R.C., and Ali, S. (1999a). Phosphorylation of human estrogen receptor alpha by protein kinase A regulates dimerization. Mol. Cell. Biol. *19*, 1002–1015.

Chen, H., Lin, R.J., Xie, W., Wilpitz, D., and Evans, R.M. (1999b). Regulation of hormone-induced histone hyperacetylation and gene activation via acetylation of an acetylase. Cell *98*, 675–686.

Cheng, F., Lienlaf, M., Perez-Villarroel, P., Wang, H.-W., Lee, C., Woan, K., Woods, D., Knox, T., Bergman, J., Pinilla-Ibarz, J., et al. (2014). Divergent roles of histone deacetylase 6 (HDAC6) and histone deacetylase 11 (HDAC11) on the transcriptional regulation of IL10 in antigen presenting cells. Mol. Immunol. *60*, 44–53.

Chin, K., DeVries, S., Fridlyand, J., Spellman, P.T., Roydasgupta, R., Kuo, W.L., Lapuk, A., Neve, R.M., Qian, Z., Ryder, T., et al. (2006). Genomic and transcriptional aberrations linked to breast cancer pathophysiologies. Cancer Cell *10*, 529–541.

Choi, J.H., Kwon, H.J., Yoon, B.I., Kim, J.H., Han, S.U., Joo, H.J., and Kim, D.Y. (2001). Expression profile of histone deacetylase 1 in gastric cancer tissues. Jpn. J. Cancer Res. *92*, 1300–1304.

Choudhary, C., Kumar, C., Gnad, F., Nielsen, M.L., Rehman, M., Walther, T.C., Olsen, J. V, and Mann, M. (2009). Lysine acetylation targets protein complexes and co-regulates major cellular functions. Science *325*, 834–840.

Clarke, R.B., Howell, A., Potten, C.S., and Anderson, E. (1997). Dissociation between steroid receptor expression and cell proliferation in the human breast. Cancer Res. *57*, 4987–4991.

Clavel-Chapelon, F., Orsi, L., Paoletti, X., Rosé, M., Avenel, V., Hoang, L.A., Chaït, R., Follain, Y., Niravong, M., Thiébaut, A., et al. (2002). Cumulative number of menstrual cycles and breast cancer risk: Results from the E3n cohort study of French women. Cancer Causes Control *13*, 831–838.

Cohen, H.Y., Lavu, S., Bitterman, K.J., Hekking, B., Imahiyerobo, T. a., Miller, C., Frye, R., Ploegh, H., Kessler, B.M., and Sinclair, D. a. (2004). Acetylation of the C terminus of Ku70 by CBP and PCAF controls Bax-mediated apoptosis. Mol. Cell *13*, 627–638.

Cooper, S.J., von Roemeling, C. a., Kang, K.H., Marlow, L. a., Grebe, S.K., Menefee, M.E., Tun, H.W., Colon-Otero, G., Perez, E. a., and Copland, J. a. (2012). Reexpression of Tumor Suppressor, sFRP1, Leads to Antitumor Synergy of Combined HDAC and Methyltransferase Inhibitors in Chemoresistant Cancers. Mol. Cancer Ther. *11*, 2105–2115.

Di Cosimo, S., and Baselga, J. (2010). Management of breast cancer with targeted agents: importance of heterogeneity. Nat. Rev. Clin. Oncol. *7*, 139–147.

Creighton, C.J. (2012). The molecular profile of luminal B breast cancer. Biol. Targets Ther. *6*, 289–297.

Criscitiello, C., Fumagalli, D., Saini, K.S., and Loi, S. (2011). Tamoxifen in early-stage estrogen receptor-positive breast cancer: Overview of clinical use and molecular biomarkers for patient selection. Onco. Targets. Ther. *4*, 1–11.

Cross, D. a, Alessi, D.R., Cohen, P., Andjelkovich, M., and Hemmings, B. a (1995). Inhibition of glycogen synthase kinase-3 by insulin mediated by protein kinase B. Nature *378*, 785–789.

Cunnick, J.M., Dorsey, J.F., Mei, L., and Wu, J. (1998). Reversible regulation of SHP-1 tyrosine phosphatase activity by oxidation. Biochem. Mol. Biol. Int. *45*, 887–894.

Curtis, C., Shah, S., Chin, S., Turashvili, G., Rueda, O., Dunning, M., Speed, D., Lynch, A., Samarajiwa, S., Yuan, Y., et al. (2012). The genomic and transcriptomic architecture of 2,000 breast tumours reveals novel subgroups. Nature *486*, 346–352.

Dai, R., Phillips, R. a, Zhang, Y., Khan, D., Crasta, O., and Ahmed, S.A. (2008). Suppression of LPS-induced Interferon-{gamma} and nitric oxide in splenic lymphocytes by select estrogen-regulated microRNAs: A novel mechanism of immune modulation. Blood *112*, 4591–4597.

Dalle-Donne, I., Giustarini, D., Rossi, R., Colombo, R., and Milzani, A. (2003). Reversible S-glutathionylation of Cys374 regulates actin filament formation by inducing structural changes in the actin molecule. Free Radic. Biol. Med. *34*, 23–32.

Dang, P.M.C., Raad, H., Derkawi, R.A., Boussetta, T., Paclet, M.H., Belambri, S.A., Makni-Maalej, K., Kroviarski, Y., Morel, F., Gougerot-Pocidalo, M.A., et al. (2011). The NADPH oxidase cytosolic component p67phox is constitutively phosphorylated in human neutrophils: Regulation by a protein tyrosine kinase, MEK1/2 and phosphatases 1/2A. Biochem. Pharmacol. *82*, 1145–1152.

Dangond, F., Hafler, D. a, Tong, J.K., Randall, J., Kojima, R., Utku, N., and Gullans, S.R. (1998). Differential display cloning of a novel human histone deacetylase (HDAC3) cDNA from PHA-activated immune cells. Biochem. Biophys. Res. Commun. *242*, 648–652.

Dawson, M. a., and Kouzarides, T. (2012). Cancer epigenetics: From mechanism to therapy. Cell *150*, 12–27.

DeNardo, D.G., Brennan, D.J., Rexhepaj, E., Ruffell, B., Shiao, S.L., Madden, S.F., Gallagher, W.M., Wadhwani, N., Keil, S.D., Junaid, S. a, et al. (2011). Leukocyte complexity predicts breast cancer survival and functionally regulates response to chemotherapy. Cancer Discov. *1*, 54–67.

Desmedt, C., Piette, F., Loi, S., Wang, Y., Lallemand, F., Haibe-Kains, B., Viale, G., Delorenzi, M., Zhang, Y., D'Assignies, M.S., et al. (2007). Strong time dependence of the 76-gene prognostic signature for node-negative breast cancer patients in the TRANSBIG multicenter independent validation series. Clin. Cancer Res. *13*, 3207–3214.

DeSmet, C., Lurquin, C., Lethe, B., and Boon, T. (1999). DNA Methylation Is the Primary Silencing Mechanism for a Set of Germ Line- and Tumor-Specific Genes with a CpG-Rich Promoter. Mol. Cell. Biol. *19*, 7327–7335.

Deubzer, H.E., Schier, M.C., Oehme, I., Lodrini, M., Haendler, B., Sommer, A., and Witt, O. (2013). HDAC11 is a novel drug target in carcinomas. Int. J. Cancer *132*, 2200–2208.

Dhalluin, C., Carlson, J.E., Zeng, L., He, C., Aggarwal, a K., and Zhou, M.M. (1999). Structure and ligand of a histone acetyltransferase bromodomain. Nature *399*, 491–496.

Diekmann, D., Abo, a, Johnston, C., Segal, a W., and Hall, a (1994). Interaction of Rac with p67phox and regulation of phagocytic NADPH oxidase activity. Science *265*, 531–533.

Dubik, D., and Shiu, R.P. (1988). Transcriptional regulation of c-myc oncogene expression by estrogen in hormone-responsive human breast cancer cells. J. Biol. Chem. *263*, 12705–12708.

Dutertre, M., Gratadou, L., Dardenne, E., Germann, S., Samaan, S., Lidereau, R., Driouch, K., De La Grange, P., and Auboeuf, D. (2010). Estrogen regulation and physiopathologic significance of alternative promoters in breast cancer. Cancer Res. *70*, 3760–3770.

EBCTCG (2005). Effects of chemotherapy and hormonal therapy for early breast cancer on recurrence and 15-year survival: An overview of the randomised trials. Lancet *365*, 1687–1717.

Eden, A., Gaudet, F., Waghmare, A., and Jaenisch, R. (2003). Chromosomal instability and tumors promoted by DNA hypomethylation. Science *300*, 455.

Ehrlich, M. (2002). DNA methylation in cancer: too much, but also too little. Oncogene *21*, 5400–5413.

Encarnación, C. a, Ciocca, D.R., McGuire, W.L., Clark, G.M., Fuqua, S. a, and Osborne, C.K. (1993). Measurement of steroid hormone receptors in breast cancer patients on tamoxifen. Breast Cancer Res. Treat. *26*, 237–246.

Esserman, L.J., Berry, D. a., Cheang, M.C.U., Yau, C., Perou, C.M., Carey, L., De Michele, A., Gray, J.W., Conway-Dorsey, K., Lenburg, M.E., et al. (2012). Chemotherapy response and recurrence-free survival in Neoadjuvant breast cancer depends on biomarker profiles: Results from the I-SPY 1 TRIAL (CALGB 150007/150012; ACRIN 6657). Breast Cancer Res. Treat. *132*, 1049–1062.

Evangelista, A.M., Thompson, M.D., Bolotina, V.M., Tong, X., and Cohen, R. a. (2012). Nox4- and Nox2-dependent oxidant production is required for VEGF-induced SERCA cysteine-674 S-glutathiolation and endothelial cell migration. Free Radic. Biol. Med. *53*, 2327–2334.

Falahi, F., van Kruchten, M., Martinet, N., Hospers, G. a P., and Rots, M.G. (2014). Current and upcoming approaches to exploit the reversibility of epigenetic mutations in breast cancer. *16*, 1–11.

Feng, W., Lu, Z., Luo, R.Z., Zhang, X., Seto, E., Liao, W.S.L., and Yu, Y. (2007). Multiple histone deacetylases repress tumor suppressor gene ARHI in breast cancer. Int. J. Cancer *120*, 1664–1668.

Ferguson, A.T., Lapidus, R.G., Baylin, S.B., and Davidson, N.E. (1995). Demethylation of the estrogen receptor gene in estrogen receptor-negative breast cancer cells can reactivate estrogen receptor gene expression. Cancer Res. *55*, 2279–2283.

Finn, R.S., Crown, J.P., Lang, I., Boer, K., Bondarenko, I.M., Kulyk, S.O., Ettl, J., Patel, R., Pinter, T., Schmidt, M., et al. (2014). The cyclin-dependent kinase 4/6 inhibitor palbociclib in combination with letrozole versus letrozole alone as first-line treatment of oestrogen receptor-positive, HER2-negative, advanced breast cancer (PALOMA-1/TRIO-18): a randomised phase 2 study. Lancet Oncol. *16*, 25–35.

Fischle, W., Emiliani, S., Hendzel, M.J., Nagase, T., Nomura, N., Voelter, W., and Verdin, E. (1999). A new family of human histone deacetylases related to Saccharomyces cerevisiae HDA1p. J. Biol. Chem. *274*, 11713–11720.

Fischle, W., Dequiedt, F., Fillion, M., Hendzel, M.J., Voelter, W., and Verdin, E. (2001). Human HDAC7 Histone Deacetylase Activity is Associated with HDAC3 in Vivo. J. Biol. Chem. *276*, 35826–35835.

Fiskus, W., Ren, Y., Mohapatra, A., Bali, P., Mandawat, A., Rao, R., Herger, B., Yang, Y., Atadja, P., Wu, J., et al. (2007). Hydroxamic acid analogue histone deacetylase inhibitors attenuate estrogen receptor-alpha levels and transcriptional activity: a result of hyperacetylation and inhibition of chaperone function of heat shock protein 90. Clin. Cancer Res. *13*, 4882–4890.

Fliss, A.E., Benzeno, S., Rao, J., and Caplan, a J. (2000). Control of estrogen receptor ligand binding by Hsp90. J. Steroid Biochem. Mol. Biol. *72*, 223–230.

Fournel, M., Bonfils, C., Hou, Y., Yan, P.T., Trachy-Bourget, M.-C., Kalita, A., Liu, J., Lu, A.-H., Zhou, N.Z., Robert, M.-F., et al. (2008). MGCD0103, a novel isotype-selective histone deacetylase inhibitor, has broad spectrum antitumor activity in vitro and in vivo. Mol. Cancer Ther. *7*, 759–768.

Fraga, M.F., Ballestar, E., Villar-Garea, A., Boix-Chornet, M., Espada, J., Schotta, G., Bonaldi, T., Haydon, C., Ropero, S., Petrie, K., et al. (2005). Loss of acetylation at Lys16 and trimethylation at Lys20 of histone H4 is a common hallmark of human cancer. Nat. Genet. *37*, 391–400.

Frasor, J., Danes, J.M., Komm, B., Chang, K.C.N., Richard Lyttle, C., and Katzenellenbogen, B.S. (2003). Profiling of estrogen up- and down-regulated gene expression in human breast cancer cells: Insights into gene networks and pathways underlying estrogenic control of proliferation and cell phenotype. Endocrinology *144*, 4562–4574.

Fridovich, I. (1970). Quantitative aspects of the production of superoxide anion radical by milk xanthine oxidase. J. Biol. Chem. *245*, 4053–4057.

Frye, R.A. (1999). Characterization of five human cDNAs with homology to the yeast SIR2 gene: Sir2-like proteins (sirtuins) metabolize NAD and may have protein ADP-ribosyltransferase activity. Biochem. Biophys. Res. Commun. *260*, 273–279.

Fu, S., Hou, M.-M., Wheler, J., Hong, D., Naing, A., Tsimberidou, A., Janku, F., Zinner, R., Piha-Paul, S., Falchook, G., et al. (2014). Exploratory study of carboplatin plus the copper-lowering agent trientine in patients with advanced malignancies. Invest. New Drugs *32*, 465–472.

Fuqua, S. a, Chamness, G.C., and McGuire, W.L. (1993). Estrogen receptor mutations in breast cancer. J. Cell. Biochem. *51*, 135–139.

Furumai, R., Matsuyama, A., Kobashi, N., Lee, K.H., Nishiyama, M., Nakajima, H., Tanaka, A., Komatsu, Y., Nishino, N., Yoshida, M., et al. (2002). FK228 (depsipeptide) as a natural prodrug that inhibits class I histone deacetylases. Cancer Res. *62*, 4916–4921.

Gallina, G., Dolcetti, L., Serafini, P., De Santo, C., Marigo, I., Colombo, M.P., Basso, G., Brombacher, F., Borrello, I., Zanovello, P., et al. (2006). Tumors induce a subset of inflammatory monocytes with immunosuppressive activity on CD8+ T cells. J. Clin. Invest. *116*, 2777–2790.

Gao, J., Aksoy, B.A., Dogrusoz, U., Dresdner, G., Gross, B., Sumer, S.O., Sun, Y., Jacobsen, A., Sinha, R., Larsson, E., et al. (2013). Integrative analysis of complex cancer genomics and clinical profiles using the cBioPortal. Sci. Signal. *6*, pl1.

Gao, L., Cueto, M.A., Asselbergs, F., and Atadja, P. (2002). Cloning and functional characterization of HDAC11, a novel member of the human histone deacetylase family. J. Biol. Chem. *277*, 25748–25755.

Gelmetti, V., Zhang, J., Fanelli, M., Minucci, S., Pelicci, P.G., and Lazar, M. a (1998). Aberrant recruitment of the nuclear receptor corepressor-histone deacetylase complex by the acute myeloid leukemia fusion partner ETO. Mol. Cell. Biol. *18*, 7185–7191.

Georgopoulos, K. (2009). From immunity to tolerance through HDAC. Nat. Immunol. *10*, 13–14.

Giampieri, S., Manning, C., Hooper, S., Jones, L., Hill, C.S., and Sahai, E. (2009). Localized and reversible TGFbeta signalling switches breast cancer cells from cohesive to single cell motility. Nat. Cell Biol. *11*, 1287–1296.

Gianni, D., Bohl, B., Courtneidge, S.A., and Bokoch, G.M. (2008). The involvement of the tyrosine kinase c-Src in the regulation of reactive oxygen species generation mediated by NADPH oxidase-1. Mol. Biol. Cell *19*, 2984–2994.

Giannoni, E., Buricchi, F., Raugei, G., Ramponi, G., and Chiarugi, P. (2005). Intracellular reactive oxygen species activate Src tyrosine kinase during cell adhesion and anchorage-dependent cell growth. Mol. Cell. Biol. *25*, 6391–6403.

Gil-Bernabé, A.M., Ferjančič, Š., Tlalka, M., Zhao, L., Allen, P.D., Im, J.H., Watson, K., Hill, S. a., Amirkhosravi, A., Francis, J.L., et al. (2012). Recruitment of monocytes/macrophages by tissue factor-mediated coagulation is essential for metastatic cell survival and premetastatic niche establishment in mice. Blood *119*, 3164–3175.

Ginestier, C., Cervera, N., Finetti, P., Esteyries, S., Esterni, B., Adélaïde, J., Xerri, L., Viens, P., Jacquemier, J., Charafe-Jauffret, E., et al. (2006). Prognosis and gene expression profiling of 20q13-amplified breast cancers. Clin. Cancer Res. *12*, 4533–4544.

Glozak, M.A., and Seto, E. (2009). Acetylation/deacetylation modulates the stability of DNA replication licensing factor Cdt1. J. Biol. Chem. *284*, 11446–11453.

Glück, S., Ross, J.S., Royce, M., McKenna, E.F., Perou, C.M., Avisar, E., and Wu, L. (2012). TP53 genomics predict higher clinical and pathologic tumor response in operable early-stage breast cancer treated with docetaxel-capecitabine ± Trastuzumab. Breast Cancer Res. Treat. *132*, 781–791.

Go, R.-E., Hwang, K.-A., and Choi, K.-C. (2015). Cytochrome P450 1 family and cancers. J. Steroid Biochem. Mol. Biol. *147*, 24–30.

Goelz, S.E., Vogelstein, B., Hamilton, S.R., and Feinberg, A.P. (1985). Hypomethylation of DNA from benign and malignant human colon neoplasms. Science *228*, 187–190.

Gorsky, L.D., Koop, D.R., and Coon, M.J. (1984). On the stoichiometry of the oxidase and monooxygenase reactions catalyzed by liver microsomal cytochrome P-450. Products of oxygen reduction. J. Biol. Chem. *259*, 6812–6817.

Gough, D.R., and Cotter, T.G. (2011). Hydrogen peroxide: a Jekyll and Hyde signalling molecule. Cell Death Dis. *2*, e213.

Graus-Porta, D., Beerli, R.R., and Hynes, N.E. (1995). Single-chain antibody-mediated intracellular retention of ErbB-2 impairs Neu differentiation factor and epidermal growth factor signaling. Mol. Cell. Biol. *15*, 1182–1191.

Greger, V., Passarge, E., Höpping, W., Messmer, E., and Horsthemke, B. (1989). Epigenetic changes may contribute to the formation and spontaneous regression of retinoblastoma. Hum. Genet. *83*, 155–158.

Gregoretti, I. V, Lee, Y.-M., and Goodson, H. V (2004). Molecular evolution of the histone deacetylase family: functional implications of phylogenetic analysis. J. Mol. Biol. *338*, 17–31.

Grozinger, C.M., and Schreiber, S.L. (2000). Regulation of histone deacetylase 4 and 5 and transcriptional activity by 14-3-3-dependent cellular localization. Proc. Natl. Acad. Sci. U. S. A. *97*, 7835–7840.

Grozinger, C.M., Hassig, C. a, and Schreiber, S.L. (1999). Three proteins define a class of human histone deacetylases related to yeast Hda1p. Proc. Natl. Acad. Sci. U. S. A. *96*, 4868–4873.

Grunstein, M. (1997). Histone acetylation in chromatin structure and transcription. Nature *389*, 349–352.

Gruvberger, S., Ringnér, M., Chen, Y., Panavally, S., Saal, L.H., Borg, A., Fernö, M., Peterson, C., and Meltzer, P.S. (2001). Estrogen receptor status in breast cancer is associated with remarkably distinct gene expression patterns. Cancer Res. *61*, 5979–5984.

Guardiola, A.R., and Yao, T.-P. (2002). Molecular cloning and characterization of a novel histone deacetylase HDAC10. J. Biol. Chem. *277*, 3350–3356.

Gui, C.-Y., Ngo, L., Xu, W.S., Richon, V.M., and Marks, P. a (2004). Histone deacetylase (HDAC) inhibitor activation of p21WAF1 involves changes in promoter-associated proteins, including HDAC1. Proc. Natl. Acad. Sci. U. S. A. *101*, 1241–1246.

Gustafson, T., and Wolpert, L. (1999). Studies on the cellular basis of morphogenesis in the sea urchin embryo. Directed movements of primary mesenchyme cells in normal and vegetalized larvae. Exp. Cell Res. *253*, 288–295.

Gutierrez, M.C., Detre, S., Johnston, S., Mohsin, S.K., Shou, J., Allred, D.C., Schiff, R., Osborne, C.K., and Dowsett, M. (2005). Molecular changes in tamoxifen-resistant breast cancer: Relationship between estrogen receptor, HER-2, and p38 mitogen-activated protein kinase. J. Clin. Oncol. *23*, 2469–2476.

Guy, C.T., Webster, M. a, Schaller, M., Parsons, T.J., Cardiff, R.D., and Muller, W.J. (1992). Expression of the neu protooncogene in the mammary epithelium of transgenic mice induces metastatic disease. Proc. Natl. Acad. Sci. U. S. A. *89*, 10578–10582.

Guy, C.T., Cardiff, R.D., and Muller, W.J. (1996). Activated neu induces rapid tumor progression. J. Biol. Chem. *271*, 7673–7678.

Gyorffy, B., Surowiak, P., Budczies, J., and Lánczky, A. (2013). Online survival analysis software to assess the prognostic value of biomarkers using transcriptomic data in non-small-cell lung cancer. PLoS One *8*, e82241.

Haenzi, B., Bonny, O., Masson, R., Lienhard, S., Dey, J.H., Kuro-O, M., and Hynes, N.E. (2014). Loss of Memo, a novel FGFR regulator, results in reduced lifespan. FASEB J. *28*, 327–336.

Haggarty, S.J., Koeller, K.M., Wong, J.C., Grozinger, C.M., and Schreiber, S.L. (2003). Domain-selective small-molecule inhibitor of histone deacetylase 6 (HDAC6)-mediated tubulin deacetylation. Proc. Natl. Acad. Sci. U. S. A. *100*, 4389–4394.

Hannafon, B.N., Sebastiani, P., de las Morenas, A., Lu, J., and Rosenberg, C.L. (2011). Expression of microRNA and their gene targets are dysregulated in preinvasive breast cancer. Breast Cancer Res. *13*, R24.

Hashizume, H., Baluk, P., Morikawa, S., McLean, J.W., Thurston, G., Roberge, S., Jain, R.K., and McDonald, D.M. (2000). Openings between defective endothelial cells explain tumor vessel leakiness. Am. J. Pathol. *156*, 1363–1380.

Hatzis, C., Pusztai, L., Valero, V., Booser, D.J., Esserman, L., Lluch, A., Vidaurre, T., Holmes, F., Souchon, E., Wang, H., et al. (2011). A genomic predictor of response and survival following taxane-anthracycline chemotherapy for invasive breast cancer. JAMA *305*, 1873–1881.

Hayashi, A., Horiuchi, A., Kikuchi, N., Hayashi, T., Fuseya, C., Suzuki, A., Konishi, I., and Shiozawa, T. (2010). Type-specific roles of histone deacetylase (HDAC) overexpression in ovarian carcinoma: HDAC1 enhances cell proliferation and HDAC3 stimulates cell migration with downregulation of E-cadherin. Int. J. Cancer *127*, 1332–1346.

Hayashi, S.I., Hajiro-Nakanishi, K., Makino, Y., Eguchi, H., Yodoi, J., and Tanaka, H. (1997). Functional modulation of estrogen receptor by redox state with reference to thioredoxin as a mediator. Nucleic Acids Res. *25*, 4035–4040.

Heideman, M.R., Wilting, R.H., Yanover, E., Velds, A., de Jong, J., Kerkhoven, R.M., Jacobs, H., Wessels, L.F., and Dannenberg, J.H. (2013). Dosage-dependent tumor suppression by histone deacetylases 1 and 2 through regulation of c-Myc collaborating genes and p53 function. Blood *121*, 2038–2050.

Heinzel, T., Lavinsky, R.M., Mullen, T.M., Söderstrom, M., Laherty, C.D., Torchia, J., Yang, W.M., Brard, G., Ngo, S.D., Davie, J.R., et al. (1997). A complex containing N-CoR, mSin3 and histone deacetylase mediates transcriptional repression. Nature *387*, 43–48.

Heldring, N., Pike, A., Andersson, S., Matthews, J., Cheng, G., Hartman, J., Tujague, M., Ström, A., Treuter, E., Warner, M., et al. (2007). Estrogen receptors: how do they signal and what are their targets. Physiol. Rev. *87*, 905–931.

Herschkowitz, J.I., Simin, K., Weigman, V.J., Mikaelian, I., Usary, J., Hu, Z., Rasmussen, K.E., Jones, L.P., Assefnia, S., Chandrasekharan, S., et al. (2007). Identification of conserved gene expression features between murine mammary carcinoma models and human breast tumors. Genome Biol. *8*, R76.

Holm, C., Kok, M., Michalides, R., Fles, R., Koornstra, R.H.T., Wesseling, J., Hauptmann, M., Neefjes, J., Peterse, J.L., Stål, O., et al. (2009). Phosphorylation of the oestrogen receptor α at serine 305 and prediction of tamoxifen resistance in breast cancer. J. Pathol. *217*, 372–379.

Holmgren, A. (1985). Thioredoxin. Annu. Rev. Biochem. *54*, 237–271.

Hong, L., Schroth, G.P., Matthews, H.R., Yau, P., and Bradbury, E.M. (1993). Studies of the DNA binding properties of histone H4 amino terminus. Thermal denaturation studies reveal that acetylation markedly reduces the binding constant of the H4 "tail" to DNA. J. Biol. Chem. *268*, 305–314.

Huang, Y., Nayak, S., Jankowitz, R., Davidson, N.E., and Oesterreich, S. (2011). Epigenetics in breast cancer: what's new? Breast Cancer Res. *13*, 225.

Hubbert, C., Guardiola, A., Shao, R., Kawaguchi, Y., Ito, A., Nixon, A., Yoshida, M., Wang, X.-F., and Yao, T.-P. (2002). HDAC6 is a microtubule-associated deacetylase. Nature *417*, 455–458.

Hurd, T.R., DeGennaro, M., and Lehmann, R. (2012). Redox regulation of cell migration and adhesion. Trends Cell Biol. *22*, 107–115.

Hynes, N.E., and Watson, C.J. (2010). Mammary Gland Growth Factors: Roles in Normal Development and in Cancer. Cold Spring Harb. Perspect. Biol. *2*, a003186–a003186.

Idziorek, T., Estaquier, J., De Bels, F., and Ameisen, J.C. (1995). YOPRO-1 permits cytofluorometric analysis of programmed cell death (apoptosis) without interfering with cell viability. J. Immunol. Methods *185*, 249–258.

Ikeda, S., Yamaoka-Tojo, M., Hilenski, L., Patrushev, N. a., Anwar, G.M., Quinn, M.T., and Ushio-Fukai, M. (2005). IQGAP1 regulates reactive oxygen species-dependent endothelial cell migration through interacting with Nox2. Arterioscler. Thromb. Vasc. Biol. *25*, 2295–2300.

Inic, Z., Zegarac, M., Inic, M., Markovic, I., Kozomara, Z., Djurisic, I., Inic, I., Pupic, G., and Jancic, S. (2014). Difference between Luminal A and Luminal B Subtypes According to Ki-67, Tumor Size, and Progesterone Receptor Negativity Providing Prognostic Information. Clin. Med. Insights. Oncol. *8*, 107–111.

Inman, J.L., Robertson, C., Mott, J.D., and Bissell, M.J. (2015). Mammary gland development: cell fate specification, stem cells and the microenvironment. Development *142*, 1028–1042.

Insinga, A., Monestiroli, S., Ronzoni, S., Gelmetti, V., Marchesi, F., Viale, A., Altucci, L., Nervi, C., Minucci, S., and Pelicci, P.G. (2005). Inhibitors of histone deacetylases induce tumor-selective apoptosis through activation of the death receptor pathway. Nat. Med. *11*, 71–76.

Ishihama, K., Yamakawa, M., Semba, S., Takeda, H., Kawata, S., Kimura, S., and Kimura, W. (2007). Expression of HDAC1 and CBP/p300 in human colorectal carcinomas. J. Clin. Pathol. *60*, 1205–1210.

Ivshina, A. V., George, J., Senko, O., Mow, B., Putti, T.C., Smeds, J., Lindahl, T., Pawitan, Y., Hall, P., Nordgren, H., et al. (2006). Genetic reclassification of histologic grade delineates new clinical subtypes of breast cancer. Cancer Res. *66*, 10292–10301.

Jackson, T. a, Richer, J.K., Bain, D.L., Takimoto, G.S., Tung, L., and Horwitz, K.B. (1997). The partial agonist activity of antagonist-occupied steroid receptors is controlled by a novel hinge domain-binding coactivator L7/SPA and the corepressors N-CoR or SMRT. Mol. Endocrinol. *11*, 693–705.

Jackson-Fisher, A.J., Bellinger, G., Ramabhadran, R., Morris, J.K., Lee, K.-F., and Stern, D.F. (2004). ErbB2 is required for ductal morphogenesis of the mammary gland. Proc. Natl. Acad. Sci. U. S. A. *101*, 17138–17143.

Jeselsohn, R., Yelensky, R., Buchwalter, G., Frampton, G., Meric-Bernstam, F., Gonzalez-Angulo, A.M., Ferrer-Lozano, J., Perez-Fidalgo, J. a, Cristofanilli, M., Gómez, H., et al. (2014). Emergence of constitutively active estrogen receptor-α mutations in pretreated advanced estrogen receptor-positive breast cancer. Clin. Cancer Res. *20*, 1757–1767.

Jeselsohn, R., Buchwalter, G., De Angelis, C., Brown, M., and Schiff, R. (2015). ESR1 mutations—a mechanism for acquired endocrine resistance in breast cancer. Nat. Rev. Clin. Oncol. *12*, 1–11.

Jiang, K., Yang, Z., Cheng, L., Wang, S., Ning, K., Zhou, L., Lin, J., Zhong, H., Wang, L., Li, Y., et al. (2013). Mediator of ERBB2-driven cell motility (MEMO) promotes extranuclear estrogen receptor signaling involving the growth factor receptors IGF1R and ERBB2. J. Biol. Chem. *288*, 24590–24599.

Johnston, S.R.D. (2010). New strategies in estrogen receptor-positive breast cancer. Clin. Cancer Res. *16*, 1979–1987.

Juarez, J.C., Betancourt, O., Pirie-Shepherd, S.R., Guan, X., Price, M.L., Shaw, D.E., Mazar, A.P., and Doñate, F. (2006). Copper binding by tetrathiomolybdate attenuates angiogenesis and tumor cell proliferation through the inhibition of superoxide dismutase 1. Clin. Cancer Res. *12*, 4974–4982.

Julka, P.K., Chacko, R.T., Nag, S., Parshad, R., Nair, A., Oh, D.S., Hu, Z., Koppiker, C.B., Nair, S., Dawar, R., et al. (2008). A phase II study of sequential neoadjuvant gemcitabine plus doxorubicin followed by gemcitabine plus cisplatin in patients with operable breast cancer: prediction of response using molecular profiling. Br. J. Cancer *98*, 1327–1335.

Kalinina, T., Güngör, C., Thieltges, S., Möller-Krull, M., Penas, E.M.M., Wicklein, D., Streichert, T., Schumacher, U., Kalinin, V., Simon, R., et al. (2010). Establishment and characterization of a new

human pancreatic adenocarcinoma cell line with high metastatic potential to the lung. BMC Cancer *10*, 295.

Kao, H.Y., Downes, M., Ordentlich, P., and Evans, R.M. (2000). Isolation of a novel histone deacetylase reveals that class I and class II deacetylases promote SMRT-mediated repression. Genes Dev. *14*, 55–66.

Kao, K.-J., Chang, K.-M., Hsu, H.-C., and Huang, A.T. (2011). Correlation of microarray-based breast cancer molecular subtypes and clinical outcomes: implications for treatment optimization. BMC Cancer *11*, 143.

Kaplan, R.N., Riba, R.D., Zacharoulis, S., Bramley, A.H., Vincent, L., Costa, C., MacDonald, D.D., Jin, D.K., Shido, K., Kerns, S. a, et al. (2005). VEGFR1-positive haematopoietic bone marrow progenitors initiate the pre-metastatic niche. Nature *438*, 820–827.

Karavitis, J., Hix, L.M., Shi, Y.H., Schultz, R.F., Khazaie, K., and Zhang, M. (2012). Regulation of COX2 Expression in Mouse Mammary Tumor Cells Controls Bone Metastasis and PGE2-Induction of Regulatory T Cell Migration. PLoS One *7*, 1–11.

Kawaguchi, Y., Kovacs, J.J., McLaurin, A., Vance, J.M., Ito, A., and Yao, T.P. (2003). The deacetylase HDAC6 regulates aggresome formation and cell viability in response to misfolded protein stress. Cell *115*, 727–738.

Kawai, H., Li, H., Avraham, S., Jiang, S., and Avraham, H.K. (2003). Overexpression of histone deacetylase HDAC1 modulates breast cancer progression by negative regulation of estrogen receptor alpha. Int. J. Cancer *107*, 353–358.

Kessenbrock, K., Plaks, V., and Werb, Z. (2010). Matrix Metalloproteinases: Regulators of the Tumor Microenvironment. Cell *141*, 52–67.

Khan, N., Jeffers, M., Kumar, S., Hackett, C., Boldog, F., Khramtsov, N., Qian, X., Mills, E., Berghs, S.C., Carey, N., et al. (2008). Determination of the class and isoform selectivity of small-molecule histone deacetylase inhibitors. Biochem. J. *409*, 581–589.

Kim, J.-S., Huang, T.Y., and Bokoch, G.M. (2009). Reactive oxygen species regulate a slingshot-cofilin activation pathway. Mol. Biol. Cell *20*, 2650–2660.

Kim, M.Y., Woo, E.M., Chong, Y.T.E., Homenko, D.R., and Kraus, W.L. (2006). Acetylation of estrogen receptor alpha by p300 at lysines 266 and 268 enhances the deoxyribonucleic acid binding and transactivation activities of the receptor. Mol. Endocrinol. *20*, 1479–1493.

Kim, S.-H., Kang, H.-J., Na, H., and Lee, M.-O. (2010a). Trichostatin A enhances acetylation as well as protein stability of ERalpha through induction of p300 protein. Breast Cancer Res. *12*, R22.

Kim, S.-Y., Lee, J.-G., Cho, W.-S., Cho, K.-H., Sakong, J., Kim, J.-R., Chin, B.-R., and Baek, S.-H. (2010b). Role of NADPH oxidase-2 in lipopolysaccharide-induced matrix metalloproteinase expression and cell migration. Immunol. Cell Biol. *88*, 197–204.

Kirkegaard, T., Witton, C.J., McGlynn, L.M., Tovey, S.M., Dunne, B., Lyon, A., and Bartlett, J.M.S. (2005). AKT activation predicts outcome in breast cancer patients treated with tamoxifen. J. Pathol. *207*, 139–146.

Kisucka, J., Chauhan, A.K., Patten, I.S., Yesilaltay, A., Neumann, C., Van Etten, R. a., Krieger, M., and Wagner, D.D. (2008). Peroxiredoxin1 prevents excessive endothelial activation and early atherosclerosis. Circ. Res. *103*, 598–605.

Kitamura, T., Qian, B.-Z., and Pollard, J.W. (2015). Immune cell promotion of metastasis. Nat. Rev. Immunol. *15*, 73–86.

Kondo, S., Bottos, A., Allegood, J.C., Masson, R., Maurer, F.G., Genoud, C., Kaeser, P., Huwiler, A., Murakami, M., Spiegel, S., et al. (2014). Memo has a novel role in S1P signaling and crucial for vascular development. PLoS One *9*.

Korde, L. a., Lusa, L., McShane, L., Lebowitz, P.F., Lukes, L., Camphausen, K., Parker, J.S., Swain, S.M., Hunter, K., and Zujewski, J.A. (2010). Gene expression pathway analysis to predict response to neoadjuvant docetaxel and capecitabine for breast cancer. Breast Cancer Res. Treat. *119*, 685–699.

Kovacs, J.J., Murphy, P.J.M., Gaillard, S., Zhao, X., Wu, J.-T., Nicchitta, C. V, Yoshida, M., Toft, D.O., Pratt, W.B., and Yao, T.-P. (2005). HDAC6 regulates Hsp90 acetylation and chaperone-dependent activation of glucocorticoid receptor. Mol. Cell *18*, 601–607.

Krusche, C. a., Wülfing, P., Kersting, C., Vloet, A., Böcker, W., Kiesel, L., Beier, H.M., and Alfer, J. (2005). Histone deacetylase-1 and -3 protein expression in human breast cancer: A tissue microarray analysis. Breast Cancer Res. Treat. *90*, 15–23.

Kuiper, J.W.P., Sun, C., Magalhães, M. a O., and Glogauer, M. (2011). Rac regulates PtdInsP 3 signaling and the chemotactic compass through a redox-mediated feedback loop. Blood *118*, 6164–6171.

Kumar, V., and Chambon, P. (1988). The estrogen receptor binds tightly to its responsive element as a ligand-induced homodimer. Cell *55*, 145–156.

Kushner, P.J., Agard, D. a., Greene, G.L., Scanlan, T.S., Shiau, A.K., Uht, R.M., and Webb, P. (2000). Estrogen receptor pathways to AP-1. J. Steroid Biochem. Mol. Biol. *74*, 311–317.

Kuukasjärvi, T., Karhu, R., Tanner, M., Kähkönen, M., Schäffen, A., Nupponen, N., Pennanen, S., Kallioniemi, A., Kallioniemi, O.P., and Isola, J. (1997). Genetic heterogeneity and clonal evolution

underlying development of asynchronous metastasis in human breast cancer. Cancer Res. *57*, 1597–1604.

Lambeth, J.D., and Neish, A.S. (2014). Nox enzymes and new thinking on reactive oxygen: a double-edged sword revisited. Annu. Rev. Pathol. *9*, 119–145.

Lapidus, R.G., Nass, S.J., Butash, K. a, Parl, F.F., Weitzman, S. a, Graff, J.G., Herman, J.G., and Davidson, N.E. (1998). Mapping of ER gene CpG island methylation by methylation-specific polymerase chain reaction. Cancer Res. *58*, 2515–2519.

LeBoeuf, M., Terrell, A., Trivedi, S., Sinha, S., Epstein, J. a., Olson, E.N., Morrisey, E.E., and Millar, S.E. (2010). Hdac1 and Hdac2 Act Redundantly to Control p63 and p53 Functions in Epidermal Progenitor Cells. Dev. Cell *19*, 807–818.

Leder, A., and Leder, P. (1975). Butyric acid, a potent inducer of erythroid differentiation in cultured erythroleukemic cells. Cell *5*, 319–322.

Lee, D.Y., Hayes, J.J., Pruss, D., and Wolffe, A.P. (1993). A positive role for histone acetylation in transcription factor access to nucleosomal DNA. Cell *72*, 73–84.

Lee, S.R., Kwon, K.S., Kim, S.R., and Rhee, S.G. (1998). Reversible inactivation of protein-tyrosine phosphatase 1B in A431 cells stimulated with epidermal growth factor. J. Biol. Chem. *273*, 15366–15372.

Leong, H., Sloan, J.R., Nash, P.D., and Greene, G.L. (2005). Recruitment of histone deacetylase 4 to the N-terminal region of estrogen receptor alpha. Mol. Endocrinol. *19*, 2930–2942.

LeRoy, G., Rickards, B., and Flint, S.J. (2008). The Double Bromodomain Proteins Brd2 and Brd3 Couple Histone Acetylation to Transcription. Mol. Cell *30*, 51–60.

Lin, L., Hou, J., Ma, F., Wang, P., Liu, X., Li, N., Wang, J., Wang, Q., and Cao, X. (2013). Type I IFN inhibits innate IL-10 production in macrophages through histone deacetylase 11 by downregulating microRNA-145. J. Immunol. *191*, 3896–3904.

Lister, R., Pelizzola, M., Dowen, R.H., Hawkins, R.D., Hon, G., Tonti-Filippini, J., Nery, J.R., Lee, L., Ye, Z., Ngo, Q.-M., et al. (2009). Human DNA methylomes at base resolution show widespread epigenomic differences. Nature *462*, 315–322.

Liu, X.F., and Bagchi, M.K. (2004). Recruitment of Distinct Chromatin-modifying Complexes by Tamoxifen-complexed Estrogen Receptor at Natural Target Gene Promoters in Vivo. J. Biol. Chem. *279*, 15050–15058.

Liu, H., Hu, Q., Kaufman, A., D'Ercole, A.J., and Ye, P. (2008). Developmental expression of histone deacetylase 11 in the murine brain. J. Neurosci. Res. *86*, 537–543.

Liu, H., Hu, Q., D'ercole, A.J., and Ye, P. (2009). Histone deacetylase 11 regulates oligodendrocyte-specific gene expression and cell development in OL-1 oligodendroglia cells. Glia *57*, 1–12.

Liu, J., Cui, Z., Luo, Y., Jiang, L., Man, X., and Zhang, X. (2004). Effect of cyclin G2 on proliferative ability of SGC-7901 cell. Tumor Biol. *35*, 3017–3024.

Liu, Z., Zhang, X.-S., and Zhang, S. (2014). Breast tumor subgroups reveal diverse clinical prognostic power. Sci. Rep. *4*, 4002.

Lobera, M., Madauss, K.P., Pohlhaus, D.T., Wright, Q.G., Trocha, M., Schmidt, D.R., Baloglu, E., Trump, R.P., Head, M.S., Hofmann, G. a, et al. (2013). Selective class IIa histone deacetylase inhibition via a nonchelating zinc-binding group. Nat. Chem. Biol. *9*, 319–325.

Lopez-Garcia, J., Periyasamy, M., Thomas, R.S., Christian, M., Leao, M., Jat, P., Kindle, K.B., Heery, D.M., Parker, M.G., Buluwela, L., et al. (2006). ZNF366 is an estrogen receptor corepressor that acts through CtBP and histone deacetylases. Nucleic Acids Res. *34*, 6126–6136.

Los, M., Schenk, H., Hexel, K., Baeuerle, P. a, Dröge, W., and Schulze-Osthoff, K. (1995). IL-2 gene expression and NF-kappa B activation through CD28 requires reactive oxygen production by 5-lipoxygenase. EMBO J. *14*, 3731–3740.

De los Santos, M., Martínez-Iglesias, O., and Aranda, A. (2007). Anti-estrogenic actions of histone deacetylase inhibitors in MCF-7 breast cancer cells. Endocr. Relat. Cancer *14*, 1021–1028.

Loschen, G., Flohé, L., and Chance, B. (1971). Respiratory chain linked H2O2 production in pigeon heart mitochondria. FEBS Lett. *18*, 261–264.

Lu, P., Ewald, A.J., Martin, G.R., and Werb, Z. (2008). Genetic mosaic analysis reveals FGF receptor 2 function in terminal end buds during mammary gland branching morphogenesis. Dev. Biol. *321*, 77–87.

Lu, W.L., Jansen, L., Post, W.J., Bonnema, J., Van De Velde, J.C., and De Bock, G.H. (2009). Impact on survival of early detection of isolated breast recurrences after the primary treatment for breast cancer: A meta-analysis. Breast Cancer Res. Treat. *114*, 403–412.

Lubahn, D.B., Moyer, J.S., Golding, T.S., Couse, J.F., Korach, K.S., and Smithies, O. (1993). Alteration of reproductive function but not prenatal sexual development after insertional disruption of the mouse estrogen receptor gene. Proc. Natl. Acad. Sci. U. S. A. *90*, 11162–11166.

Luger, K., Mäder, a W., Richmond, R.K., Sargent, D.F., and Richmond, T.J. (1997). Crystal structure of the nucleosome core particle at 2.8 A resolution. Nature *389*, 251–260.

Luo, J., Nikolaev, A.Y., Imai, S. ichiro, Chen, D., Su, F., Shiloh, A., Guarente, L., and Gu, W. (2001). Negative control of p53 by Sir2α promotes cell survival under stress. Cell *107*, 137–148.

MacDonald, G., Nalvarte, I., Smirnova, T., Vecchi, M., Aceto, N., Dolemeyer, A., Frei, A., Lienhard, S., Wyckoff, J., Hess, D., et al. (2014). Memo is a copper-dependent redox protein with an essential role in migration and metastasis. Sci. Signal. *7*, ra56.

Machida, Y.J., Hamlin, J.L., and Dutta, A. (2005). Right place, right time, and only once: Replication initiation in metazoans. Cell *123*, 13–24.

Macias, H., and Hinck, L. (2012). Mammary gland development. Wiley Interdiscip. Rev. Dev. Biol. *1*, 533–557.

Maheswaranathan, M., Gole, H.K. a, Fernandez, I., Lassègue, B., Griendling, K.K., and San Martiń, A. (2011). Platelet-derived growth factor (PDGF) regulates slingshot phosphatase activity via Nox1-dependent auto-dephosphorylation of serine 834 in vascular smooth muscle cells. J. Biol. Chem. *286*, 35430–35437.

Mallepell, S., Krust, A., Chambon, P., and Brisken, C. (2006). Paracrine signaling through the epithelial estrogen receptor alpha is required for proliferation and morphogenesis in the mammary gland. Proc. Natl. Acad. Sci. U. S. A. *103*, 2196–2201.

Mann, B.S., Johnson, J.R., Cohen, M.H., Justice, R., and Pazdur, R. (2007). FDA approval summary: vorinostat for treatment of advanced primary cutaneous T-cell lymphoma. Oncologist *12*, 1247–1252.

Marc J. Van De V Ijver (2002). A gene-expression signature as a predictor of survival in breast cancer. Engl. J. *347*, 1999–2009.

Marone, R., Hess, D., Dankort, D., Muller, W.J., Hynes, N.E., and Badache, A. (2004). Memo mediates ErbB2-driven cell motility. Nat. Cell Biol. *6*, 515–522.

Marquard, L., Gjerdrum, L.M., Christensen, I.J., Jensen, P.B., Sehested, M., and Ralfkiaer, E. (2008). Prognostic significance of the therapeutic targets histone deacetylase 1, 2, 6 and acetylated histone H4 in cutaneous T-cell lymphoma. Histopathology *53*, 267–277.

Martínez-Balbás, M. a, Bauer, U.M., Nielsen, S.J., Brehm, a, and Kouzarides, T. (2000). Regulation of E2F1 activity by acetylation. EMBO J. *19*, 662–671.

Meira, M., Masson, R., Stagljar, I., Lienhard, S., Maurer, F., Boulay, A., and Hynes, N.E. (2009). Memo is a cofilin-interacting protein that influences PLCgamma1 and cofilin activities, and is essential for maintaining directionality during ErbB2-induced tumor-cell migration. J. Cell Sci. *122*, 787–797.

Menasce, L.P., White, G.R., Harrison, C.J., and Boyle, J.M. (1993). Localization of the estrogen receptor locus (ESR) to chromosome 6q25.1 by FISH and a simple post-FISH banding technique. Genomics *17*, 263–265.

Meng, T.C., Fukada, T., and Tonks, N.K. (2002). Reversible oxidation and inactivation of protein tyrosine phosphatases in vivo. Mol. Cell *9*, 387–399.

Merenbakh-Lamin, K., Ben-Baruch, N., Yeheskel, A., Dvir, A., Soussan-Gutman, L., Jeselsohn, R., Yelensky, R., Brown, M., Miller, V. a., Sarid, D., et al. (2013). D538G mutation in estrogen receptor-α: A novel mechanism for acquired endocrine resistance in breast cancer. Cancer Res. *73*, 6856–6864.

Métivier, R., Penot, G., Hübner, M.R., Reid, G., Brand, H., Koš, M., and Gannon, F. (2003). Estrogen receptor-α directs ordered, cyclical, and combinatorial recruitment of cofactors on a natural target promoter. Cell *115*, 751–763.

Meyer, D.S., Brinkhaus, H., Müller, U., Müller, M., Cardiff, R.D., and Bentires-Alj, M. (2011). Luminal expression of PIK3CA mutant H1047R in the mammary gland induces heterogeneous tumors. Cancer Res. *71*, 4344–4351.

Minn, A.J., Gupta, G.P., Siegel, P.M., Bos, P.D., Shu, W., Giri, D.D., Viale, A., Olshen, A.B., Gerald, W.L., and Massagué, J. (2005). Genes that mediate breast cancer metastasis to lung. Nature *436*, 518–524.

Miyake, T., Nakayama, T., Naoi, Y., Yamamoto, N., Otani, Y., Kim, S.J., Shimazu, K., Shimomura, A., Maruyama, N., Tamaki, Y., et al. (2012). GSTP1 expression predicts poor pathological complete response to neoadjuvant chemotherapy in ER-negative breast cancer. Cancer Sci. *103*, 913–920.

Moldovan, L., Moldovan, N.I., Sohn, R.H., Parikh, S. a, and Goldschmidt-Clermont, P.J. (2000). Redox changes of cultured endothelial cells and actin dynamics. Circ. Res. *86*, 549–557.

Montgomery, R.L., Davis, C. a., Potthoff, M.J., Haberland, M., Fielitz, J., Qi, X., Hill, J. a., Richardson, J. a., and Olson, E.N. (2007). Histone deacetylases 1 and 2 redundantly regulate cardiac morphogenesis, growth, and contractility. Genes Dev. *21*, 1790–1802.

Moore, K.W., de Waal Malefyt, R., Coffman, R.L., and O'Garra, A. (2001). Interleukin-10 and the interleukin-10 receptor. Annu. Rev. Immunol. *19*, 683–765.

Mootha, V.K., Lindgren, C.M., Eriksson, K.-F., Subramanian, A., Sihag, S., Lehar, J., Puigserver, P., Carlsson, E., Ridderstråle, M., Laurila, E., et al. (2003). PGC-1alpha-responsive genes involved in oxidative phosphorylation are coordinately downregulated in human diabetes. Nat. Genet. *34*, 267–273.

Mottamal, M., Zheng, S., Huang, T.L., and Wang, G. (2015). Histone Deacetylase Inhibitors in Clinical Studies as Templates for New Anticancer Agents. Molecules *20*, 3898–3941.

Müller, B.M., Jana, L., Kasajima, A., Lehmann, A., Prinzler, J., Budczies, J., Winzer, K., Dietel, M., Weichert, W., and Denkert, C. (2013). Differential expression of histone deacetylases HDAC1, 2

and 3 in human breast cancer--overexpression of HDAC2 and HDAC3 is associated with clinicopathological indicators of disease progression. BMC Cancer *13*, 215.

Neve, R.M., Chin, K., Fridlyand, J., Yeh, J., Baehner, F.L., Fevr, T., Clark, L., Bayani, N., Coppe, J.P., Tong, F., et al. (2006). A collection of breast cancer cell lines for the study of functionally distinct cancer subtypes. Cancer Cell *10*, 515–527.

Nguyen, D.X., Bos, P.D., and Massagué, J. (2009). Metastasis: from dissemination to organ-specific colonization. Nat. Rev. Cancer.

Nilsson, S., and Gustafsson, J.-Å. (2011). Estrogen receptors: therapies targeted to receptor subtypes. Clin. Pharmacol. Ther. *89*, 44–55.

Nimnual, A.S., Taylor, L.J., and Bar-Sagi, D. (2003). Redox-dependent downregulation of Rho by Rac. Nat. Cell Biol. *5*, 236–241.

Noda, Y., Nishikawa, S., Shiozuka, K.I., Kadokura, H., Nakajima, H., Yoda, K., Katayama, Y., Morohoshi, N., Haraguchi, T., and Yamasaki, M. (1990). Molecular cloning of the protocatechuate 4,5-dioxygenase genes of Pseudomonas paucimobilis. J. Bacteriol. *172*, 2704–2709.

Novotny-Diermayr, V., Sangthongpitag, K., Hu, C.Y., Wu, X., Sausgruber, N., Yeo, P., Greicius, G., Pettersson, S., Liang, A.L., Loh, Y.K., et al. (2010). SB939, a novel potent and orally active histone deacetylase inhibitor with high tumor exposure and efficacy in mouse models of colorectal cancer. Mol. Cancer Ther. *9*, 642–652.

Osborne, C.K. (1998). Steroid hormone receptors in breast cancer management. Breast Cancer Res. Treat. *51*, 227–238.

Palumbo, J.S., Talmage, K.E., Massari, J. V, La Jeunesse, C.M., Flick, M.J., Kombrinck, K.W., Jirousková, M., and Degen, J.L. (2005). Platelets and fibrin(ogen) increase metastatic potential by impeding natural killer cell-mediated elimination of tumor cells. Blood *105*, 178–185.

Parbin, S., Kar, S., Shilpi, a., Sengupta, D., Deb, M., Rath, S.K., and Patra, S.K. (2013). Histone Deacetylases: A Saga of Perturbed Acetylation Homeostasis in Cancer. J. Histochem. Cytochem. *62*, 11–33.

Parker, J.S., Mullins, M., Cheung, M.C.U., Leung, S., Voduc, D., Vickery, T., Davies, S., Fauron, C., He, X., Hu, Z., et al. (2009). Supervised risk predictor of breast cancer based on intrinsic subtypes. J. Clin. Oncol. *27*, 1160–1167.

Parra, M., Mahmoudi, T., and Verdin, E. (2007). Myosin phosphatase dephosphorylates HDAC7, controls its nucleocytoplasmic shuttling, and inhibits apoptosis in thymocytes. Genes Dev. *21*, 638–643.

Parri, M., and Chiarugi, P. (2010). Rac and Rho GTPases in cancer cell motility control. Cell Commun. Signal. *8*, 23.

Patani, N., Barbashina, V., Lambros, M.B.K., Gauthier, A., Mansour, M., Mackay, A., and Reis-Filho, J.S. (2011). Direct evidence for concurrent morphological and genetic heterogeneity in an invasive ductal carcinoma of triple-negative phenotype. J. Clin. Pathol. *64*, 822–828.

Peart, M.J., Smyth, G.K., van Laar, R.K., Bowtell, D.D., Richon, V.M., Marks, P. a, Holloway, A.J., and Johnstone, R.W. (2005). Identification and functional significance of genes regulated by structurally different histone deacetylase inhibitors. Proc. Natl. Acad. Sci. U. S. A. *102*, 3697–3702.

Perou, C.M., Sørlie, T., Eisen, M.B., van de Rijn, M., Jeffrey, S.S., Rees, C. a, Pollack, J.R., Ross, D.T., Johnsen, H., Akslen, L. a, et al. (2000). Molecular portraits of human breast tumours. Nature *406*, 747–752.

Plath, K., Fang, J., Mlynarczyk-Evans, S.K., Cao, R., Worringer, K.A., Wang, H., de la Cruz, C.C., Otte, A.P., Panning, B., and Zhang, Y. (2003). Role of histone H3 lysine 27 methylation in X inactivation. Science *300*, 131–135.

Prat, A., and Perou, C.M. (2011). Deconstructing the molecular portraits of breast cancer. Mol. Oncol. *5*, 5–23.

Prat, A., Parker, J.S., Karginova, O., Fan, C., Livasy, C., Herschkowitz, J.I., He, X., and Perou, C.M. (2010). Phenotypic and molecular characterization of the claudin-low intrinsic subtype of breast cancer. *12*, R68.

Qiu, C., Lienhard, S., Hynes, N.E., Badache, A., and Leahy, D.J. (2008). Memo is homologous to nonheme iron dioxygenases and binds an ErbB2-derived phosphopeptide in its vestigial active site. J. Biol. Chem. *283*, 2734–2740.

Qiu, Y., Zhao, Y., Becker, M., John, S., Parekh, B.S., Huang, S., Hendarwanto, A., Martinez, E.D., Chen, Y., Lu, H., et al. (2006). HDAC1 Acetylation Is Linked to Progressive Modulation of Steroid Receptor-Induced Gene Transcription. Mol. Cell *22*, 669–679.

Quaedackers, M.E., van den Brink, C.E., van der Saag, P.T., and Tertoolen, L.G.J. (2007). Direct interaction between estrogen receptor alpha and NF-kappaB in the nucleus of living cells. Mol. Cell. Endocrinol. *273*, 42–50.

Rae, J.M., Johnson, M.D., Scheys, J.O., Cordero, K.E., Larios, J.M., and Lippman, M.E. (2005). GREB 1 is a critical regulator of hormone dependent breast cancer growth. Breast Cancer Res. Treat. *92*, 141–149.

Ramsahoye, B.H., Biniszkiewicz, D., Lyko, F., Clark, V., Bird, a P., and Jaenisch, R. (2000). Non-CpG methylation is prevalent in embryonic stem cells and may be mediated by DNA methyltransferase 3a. Proc. Natl. Acad. Sci. U. S. A. *97*, 5237–5242.

Ray, P.D., Huang, B.W., and Tsuji, Y. (2012). Reactive oxygen species (ROS) homeostasis and redox regulation in cellular signaling. Cell. Signal. *24*, 981–990.

Redeuilh, G., Moncharmont, B., Secco, C., and Baulieu, E.E. (1987). Subunit composition of the molybdate-stabilized "8-9 S" nontransformed estradiol receptor purified from calf uterus. J. Biol. Chem. *262*, 6969–6975.

Reichert, N., Choukrallah, M.A., and Matthias, P. (2012). Multiple roles of class i HDACs in proliferation, differentiation, and development. Cell. Mol. Life Sci. *69*, 2173–2187.

Reid, G., Hübner, M.R., Métivier, R., Brand, H., Denger, S., Manu, D., Beaudouin, J., Ellenberg, J., and Gannon, F. (2003). Cyclic, proteasome-mediated turnover of unliganded and liganded ERα on responsive promoters is an integral feature of estrogen signaling. Mol. Cell *11*, 695–707.

Reid, G., Métivier, R., Lin, C.-Y., Denger, S., Ibberson, D., Ivacevic, T., Brand, H., Benes, V., Liu, E.T., and Gannon, F. (2005). Multiple mechanisms induce transcriptional silencing of a subset of genes, including oestrogen receptor alpha, in response to deacetylase inhibition by valproic acid and trichostatin A. Oncogene *24*, 4894–4907.

Reik, W. (2007). Stability and flexibility of epigenetic gene regulation in mammalian development. Nature *447*, 425–432.

Ridley, A.J. (2011). Life at the leading edge. Cell *145*, 1012–1022.

Ridley, A.J., and Hall, A. (1992). The small GTP-binding protein rho regulates the assembly of focal adhesions and actin stress fibers in response to growth factors. Cell *70*, 389–399.

Ridley, A.J., Schwartz, M. a, Burridge, K., Firtel, R. a, Ginsberg, M.H., Borisy, G., Parsons, J.T., and Horwitz, A.R. (2003). Cell migration: integrating signals from front to back. Science *302*, 1704–1709.

Riggs, M.G., Whittaker, R.G., Neumann, J.R., and Ingram, V.M. (1977). n-Butyrate causes histone modification in HeLa and Friend erythroleukaemia cells. Nature *268*, 462–464.

Robinson, D.R., Wu, Y.-M., Vats, P., Su, F., Lonigro, R.J., Cao, X., Kalyana-Sundaram, S., Wang, R., Ning, Y., Hodges, L., et al. (2013). Activating ESR1 mutations in hormone-resistant metastatic breast cancer. Nat. Genet. *45*, 1446–1451.

Roman-Blas, J. a, Castañeda, S., Largo, R., and Herrero-Beaumont, G. (2009). Osteoarthritis associated with estrogen deficiency. Arthritis Res. Ther. *11*, 241.

Le Romancer, M., Poulard, C., Cohen, P., Sentis, S.P., Renoir, J.M., and Corbo, L. (2011). Cracking the estrogen receptor's posttranslational code in breast tumors. Endocr. Rev. *32*, 597–622.

De Ruijter, A.J.M., van Gennip, A.H., Caron, H.N., Kemp, S., and van Kuilenburg, A.B.P. (2003). Histone deacetylases (HDACs): characterization of the classical HDAC family. Biochem. J. *370*, 737–749.

Sabnis, G.J., Goloubeva, O., Chumsri, S., Nguyen, N., Sukumar, S., and Brodie, A.M.H. (2011). Functional activation of the estrogen receptor-α and aromatase by the HDAC inhibitor entinostat sensitizes ER-negative tumors to letrozole. Cancer Res. *71*, 1893–1903.

Sahakian, E., Powers, J.J., Chen, J., Deng, S.L., Cheng, F., Distler, A., Woods, D.M., Rock-Klotz, J., Sodre, A.L., Youn, J.-I., et al. (2014). Histone deacetylase 11: A novel epigenetic regulator of myeloid derived suppressor cell expansion and function. Mol. Immunol. *63*, 579–585.

Saji, S., Kawakami, M., Hayashi, S.-I., Yoshida, N., Hirose, M., Horiguchi, S.-I., Itoh, A., Funata, N., Schreiber, S.L., Yoshida, M., et al. (2005). Significance of HDAC6 regulation via estrogen signaling for cell motility and prognosis in estrogen receptor-positive breast cancer. Oncogene *24*, 4531–4539.

Sakai, J., Li, J., Subramanian, K.K., Mondal, S., Bajrami, B., Hattori, H., Jia, Y., Dickinson, B.C., Zhong, J., Ye, K., et al. (2012). Reactive Oxygen Species-Induced Actin Glutathionylation Controls Actin Dynamics in Neutrophils. Immunity *37*, 1037–1049.

Sandor, V., Senderowicz, a, Mertins, S., Sackett, D., Sausville, E., Blagosklonny, M. V, and Bates, S.E. (2000). P21-dependent g(1)arrest with downregulation of cyclin D1 and upregulation of cyclin E by the histone deacetylase inhibitor FR901228. Br. J. Cancer *83*, 817–825.

San-Miguel, J.F., Hungria, V.T.M., Yoon, S.-S., Beksac, M., Dimopoulos, M.A., Elghandour, A., Jedrzejczak, W.W., Günther, A., Nakorn, T.N., Siritanaratkul, N., et al. (2014). Panobinostat plus bortezomib and dexamethasone versus placebo plus bortezomib and dexamethasone in patients with relapsed or relapsed and refractory multiple myeloma: a multicentre, randomised, double-blind phase 3 trial. Lancet. Oncol. *15*, 1195–1206.

Saville, B., Wormke, M., Wang, F., Nguyen, T., Enmark, E., Kuiper, G., Gustafsson, J.Å., and Safe, S. (2000). Ligand-, cell-, and estrogen receptor subtype (α/β)-dependent activation at GC-rich (Sp1) promoter elements. J. Biol. Chem. *275*, 5379–5387.

Saxena, T., Lee, E., Henderson, K.D., Clarke, C. a., West, D., Marshall, S.F., Deapen, D., Bernstein, L., and Ursin, G. (2010). Menopausal hormone therapy and subsequent risk of specific invasive breast cancer subtypes in the California Teachers Study. Cancer Epidemiol. Biomarkers Prev. *19*, 2366–2378.

Schaefer, T.M., Wright, J. a., Pioli, P. a., and Wira, C.R. (2005). IL-1beta-mediated proinflammatory responses are inhibited by estradiol via down-regulation of IL-1 receptor type I in uterine epithelial cells. J. Immunol. *175*, 6509–6516.

Schlatter, I.D., Meira, M., Ueberschlag, V., Hoepfner, D., Movva, R., and Hynes, N.E. (2012). MHO1, an evolutionarily conserved gene, is synthetic lethal with PLC1; Mho1p has a role in invasive growth. PLoS One *7*, e32501.

Schröder, K., Helmcke, I., Palfi, K., Krause, K.-H., Busse, R., and Brandes, R.P. (2007). Nox1 mediates basic fibroblast growth factor-induced migration of vascular smooth muscle cells. Arterioscler. Thromb. Vasc. Biol. *27*, 1736–1743.

Schroeder, J.A., and Lee, D.C. (1998). Dynamic expression and activation of ERBB receptors in the developing mouse mammary gland. Cell Growth Differ. *9*, 451–464.

Serafini, P., Borrello, I., and Bronte, V. (2006). Myeloid suppressor cells in cancer: Recruitment, phenotype, properties, and mechanisms of immune suppression. Semin. Cancer Biol. *16*, 53–65.

Shimizu, T., LoRusso, P.M., Papadopoulos, K.P., Patnaik, a., Beeram, M., Smith, L.S., Rasco, D.W., Mays, T. a., Chambers, G., Ma, a., et al. (2014). Phase I First-in-Human Study of CUDC-101, a Multitargeted Inhibitor of HDACs, EGFR, and HER2 in Patients with Advanced Solid Tumors. Clin. Cancer Res. *20*, 5032–5040.

Shiozawa, T., Miyamoto, T., Kashima, H., Nakayama, K., Nikaido, T., and Konishi, I. (2004). Estrogen-induced proliferation of normal endometrial glandular cells is initiated by transcriptional activation of cyclin D1 via binding of c-Jun to an AP-1 sequence. Oncogene *23*, 8603–8610.

Singh, B.N., Zhang, G., Hwa, Y.L., Li, J., Dowdy, S.C., and Jiang, S.-W. (2010). Nonhistone protein acetylation as cancer therapy targets. Expert Rev. Anticancer Ther. *10*, 935–954.

Skibinski, A., and Kuperwasser, C. (2015). The origin of breast tumor heterogeneity. Oncogene 1–8.

Slamon, D.J., Clark, G.M., Wong, S.G., Levin, W.J., Ullrich, A., and McGuire, W.L. (1987). Human breast cancer: correlation of relapse and survival with amplification of the HER-2/neu oncogene. Science *235*, 177–182.

Soriano, P. (1999). Generalized lacZ expression with the ROSA26 Cre reporter strain. Nat. Genet. *21*, 70–71.

Sørlie, T., Perou, C.M., Tibshirani, R., Aas, T., Geisler, S., Johnsen, H., Hastie, T., Eisen, M.B., van de Rijn, M., Jeffrey, S.S., et al. (2001). Gene expression patterns of breast carcinomas distinguish tumor subclasses with clinical implications. Proc. Natl. Acad. Sci. U. S. A. *98*, 10869–10874.

Sorokin, a V, and Chen, J. (2013). MEMO1, a new IRS1-interacting protein, induces epithelial-mesenchymal transition in mammary epithelial cells. Oncogene *32*, 3130–3138.

Stanley, A., Thompson, K., Hynes, A., Brakebusch, C., and Quondamatteo, F. (2014). NADPH oxidase complex-derived reactive oxygen species, the actin cytoskeleton, and Rho GTPases in cell migration. Antioxid. Redox Signal. *20*, 2026–2042.

Stoeber, K., Tlsty, T.D., Happerfield, L., Thomas, G. a, Romanov, S., Bobrow, L., Williams, E.D., and Williams, G.H. (2001). DNA replication licensing and human cell proliferation. J. Cell Sci. *114*, 2027–2041.

Subramanian, A., Tamayo, P., Mootha, V.K., Mukherjee, S., Ebert, B.L., Gillette, M.A., Paulovich, A., Pomeroy, S.L., Golub, T.R., Lander, E.S., et al. (2005). Gene set enrichment analysis: a knowledge-based approach for interpreting genome-wide expression profiles. Proc. Natl. Acad. Sci. U. S. A. *102*, 15545–15550.

Sugimoto, K., Senda, T., Aoshima, H., Masai, E., Fukuda, M., and Mitsui, Y. (1999). Crystal structure of an aromatic ring opening dioxygenase LigAB, a protocatechuate 4,5-dioxygenase, under aerobic conditions. Structure *7*, 953–965.

Sun, Y., and Oberley, L.W. (1996). Redox regulation of transcriptional activators. Free Radic. Biol. Med. *21*, 335–348.

Sun, M., Paciga, J.E., Feldman, R.I., Yuan, Z.Q., Coppola, D., Lu, Y.Y., Shelley, S. a., Nicosia, S. V., and Cheng, J.Q. (2001). Phosphatidylinositol-3-OH kinase (PI3K)/AKT2, activated in breast cancer, regulates and is induced by estrogen receptor a (ERa) via interaction between ERa and PI3K. Cancer Res. *61*, 5985–5991.

Szatrowski, T.P., and Nathan, C.F. (1991). Production of Large Amounts of Hydrogen Peroxide by Human Tumor Cells. Cancer Res. *51*, 794–798.

Tamimi, R.M., Colditz, G. a., Hazra, A., Baer, H.J., Hankinson, S.E., Rosner, B., Marotti, J., Connolly, J.L., Schnitt, S.J., and Collins, L.C. (2012). Traditional breast cancer risk factors in relation to molecular subtypes of breast cancer. Breast Cancer Res. Treat. *131*, 159–167.

Tanaka, Y., Tran, P.O.T., Harmon, J., and Robertson, R.P. (2002). A role for glutathione peroxidase in protecting pancreatic beta cells against oxidative stress in a model of glucose toxicity. Proc. Natl. Acad. Sci. U. S. A. *99*, 12363–12368.

Tang, J., Yan, H., and Zhuang, S. (2013). Histone deacetylases as targets for treatment of multiple diseases. Clin. Sci. (Lond). *124*, 651–662.

Tarone, G., Cirillo, D., Giancotti, F.G., Comoglio, P.M., and Marchisio, P.C. (1985). Rous sarcoma virus-transformed fibroblasts adhere primarily at discrete protrusions of the ventral membrane called podosomes. Exp. Cell Res. *159*, 141–157.

Taunton, J., Hassig, C.A., and Schreiber, S.L. (1996). A mammalian histone deacetylase related to the yeast transcriptional regulator Rpd3p. Science *272*, 408–411.

Teyssier, C., Belguise, K., Galtier, F., Cavailles, V., and Chalbos, D. (2003). Receptor-interacting protein 140 binds c-Jun and inhibits estradiol-induced activator protein-1 activity by reversing glucocorticoid receptor-interacting protein 1 effect. Mol. Endocrinol. *17*, 287–299.

The Cancer Genome Atlas Network (2012). Comprehensive molecular portraits of human breast tumours. Nature *490*, 61–70.

Thiagalingam, S., Cheng, K.-H., Lee, H.J., Mineva, N., Thiagalingam, A., and Ponte, J.F. (2003). Histone deacetylases: unique players in shaping the epigenetic histone code. Ann. N. Y. Acad. Sci. *983*, 84–100.

Thomas, C., and Gustafsson, J.-Å. (2011). The different roles of ER subtypes in cancer biology and therapy. Nat. Rev. Cancer *11*, 597–608.

Tiwari, N., Tiwari, V., Waldmeier, L., Balwierz, P., Arnold, P., Pachkov, M., Meyer-Schaller, N., Schübeler, D., vanNimwegen, E., and Christofori, G. (2013). Sox4 Is a Master Regulator of Epithelial-Mesenchymal Transition by Controlling Ezh2 Expression and Epigenetic Reprogramming. Cancer Cell *23*, 768–783.

Todd, P.K., Oh, S.Y., Krans, A., Pandey, U.B., Di Prospero, N. a., Min, K.T., Taylor, J.P., and Paulson, H.L. (2010). Histone deacetylases suppress cgg repeat-induced neurodegeneration via transcriptional silencing in models of Fragile X Tremor Ataxia Syndrome. PLoS Genet. *6*, 1–17.

Tong, J.J., Liu, J., Bertos, N.R., and Yang, X.-J. (2002). Identification of HDAC10, a novel class II human histone deacetylase containing a leucine-rich domain. Nucleic Acids Res. *30*, 1114–1123.

Torre, L. a, Bray, F., Siegel, R.L., Ferlay, J., Lortet-tieulent, J., and Jemal, A. (2015). Global Cancer Statistics, 2012. CA. Cancer J. Clin. *65*, 87–108.

Torres-Arzayus, M.I., Zhao, J., Bronson, R., and Brown, M. (2010). Estrogen-dependent and estrogen-independent mechanisms contribute to AIB1-mediated tumor formation. Cancer Res. *70*, 4102–4111.

Touyz, R.M., Yao, G., Quinn, M.T., Pagano, P.J., and Schiffrin, E.L. (2005). p47phox associates with the cytoskeleton through cortactin in human vascular smooth muscle cells role in NAD(P)H oxidase regulation by angiotensin II. Arterioscler. Thromb. Vasc. Biol. *25*, 512–518.

Toyokuni, S., Okamoto, K., Yodoi, J., and Hiai, H. (1995). Persistent oxidative stress in cancer. FEBS Lett. *358*, 1–3.

Ursini-Siegel, J., Hardy, W.R., Zuo, D., Lam, S.H.L., Sanguin-Gendreau, V., Cardiff, R.D., Pawson, T., and Muller, W.J. (2008). ShcA signalling is essential for tumour progression in mouse models of human breast cancer. EMBO J. *27*, 910–920.

van't Veer, L.J., Dai, H., van de Vijver, M.J., He, Y.D., Hart, A.A.M., Mao, M., Peterse, H.L., van der Kooy, K., Marton, M.J., Witteveen, A.T., et al. (2002). Gene expression profiling predicts clinical outcome of breast cancer. Nature *415*, 530–536.

Ververis, K., Hiong, A., Karagiannis, T.C., and Licciardi, P. V. (2013). Histone deacetylase inhibitors (HDACIS): Multitargeted anticancer agents. Biol. Targets Ther. *7*, 47–60.

Villagra, A., Cheng, F., Wang, H.-W., Suarez, I., Glozak, M., Maurin, M., Nguyen, D., Wright, K.L., Atadja, P.W., Bhalla, K., et al. (2009). The histone deacetylase HDAC11 regulates the expression of interleukin 10 and immune tolerance. Nat. Immunol. *10*, 92–100.

Vo, N., Fjeld, C., and Goodman, R.H. (2001). Acetylation of nuclear hormone receptor-interacting protein RIP140 regulates binding of the transcriptional corepressor CtBP. Mol. Cell. Biol. *21*, 6181–6188.

Waddell, N., Cocciardi, S., Johnson, J., Healey, S., Marsh, A., Riley, J., da Silva, L., Vargas, A.C., Reid, L., Simpson, P.T., et al. (2010). Gene expression profiling of formalin-fixed, paraffin-embedded familial breast tumours using the whole genome-DASL assay. J. Pathol. *221*, 452–461.

Wagner, B., and Gorin, Y. (2014). Src tyrosine kinase mediates platelet-derived growth factor BB-induced and redox-dependent migration in metanephric mesenchymal cells. Am. J. Physiol. Renal Physiol. *306*, F85–F97.

Wagner, K.U., Ward, T., Davis, B., Wiseman, R., and Hennighausen, L. (2001). Spatial and temporal expression of the Cre gene under the control of the MMTV-LTR in different lines of transgenic mice. Transgenic Res. *10*, 545–553.

Wan, L., Pantel, K., and Kang, Y. (2013). Tumor metastasis: moving new biological insights into the clinic. Nat. Med. *19*, 1450–1464.

Wang, C., Fu, M., Angeletti, R.H., Siconolfi-Baez, L., Reutens, a T., Albanese, C., Lisanti, M.P., Katzenellenbogen, B.S., Kato, S., Hopp, T., et al. (2001). Direct acetylation of the estrogen receptor alpha hinge region by p300 regulates transactivation and hormone sensitivity. J. Biol. Chem. *276*, 18375–18383.

Wang, Y., Klijn, J.G.M., Zhang, Y., Sieuwerts, A.M., Look, M.P., Yang, F., Talantov, D., Timmermans, M., Meijer-Van Gelder, M.E., Yu, J., et al. (2005). Gene-expression profiles to predict distant metastasis of lymph-node-negative primary breast cancer. Lancet *365*, 671–679.

Watanabe, T., Noritake, J., and Kaibuchi, K. (2005). Regulation of microtubules in cell migration. Trends Cell Biol. *15*, 76–83.

Weichert, W. (2009). HDAC expression and clinical prognosis in human malignancies. Cancer Lett. *280*, 168–176.

Weichert, W., Röske, A., Gekeler, V., Beckers, T., Stephan, C., Jung, K., Fritzsche, F.R., Niesporek, S., Denkert, C., Dietel, M., et al. (2008). Histone deacetylases 1, 2 and 3 are highly expressed in prostate cancer and HDAC2 expression is associated with shorter PSA relapse time after radical prostatectomy. Br. J. Cancer *98*, 604–610.

West, A.C., and Johnstone, R.W. (2014). New and emerging HDAC inhibitors for cancer treatment. J. Clin. Invest. *124*, 30–39.

Wientjes, F.B., Reeves, E.P., Soskic, V., Furthmayr, H., and Segal, a W. (2001). The NADPH oxidase components p47(phox) and p40(phox) bind to moesin through their PX domain. Biochem. Biophys. Res. Commun. *289*, 382–388.

Wilting, R.H., Yanover, E., Heideman, M.R., Jacobs, H., Horner, J., van der Torre, J., DePinho, R. a, and Dannenberg, J.-H. (2010). Overlapping functions of Hdac1 and Hdac2 in cell cycle regulation and haematopoiesis. EMBO J. *29*, 2586–2597.

Winter, M., Moser, M. a, Meunier, D., Fischer, C., Machat, G., Mattes, K., Lichtenberger, B.M., Brunmeir, R., Weissmann, S., Murko, C., et al. (2013). Divergent roles of HDAC1 and HDAC2 in the regulation of epidermal development and tumorigenesis. EMBO J. *32*, 3176–3191.

Wittmann, T., and Waterman-Storer, C.M. (2005). Spatial regulation of CLASP affinity for microtubules by Rac1 and GSK3b in migrating epithelial cells. J. Cell Biol. *169*, 929–939.

Wong, P.G., Glozak, M. a., Cao, T. V., Vaziri, C., Seto, E., and Alexandrow, M.G. (2014). Chromatin unfolding by Cdt1 regulates MCM loading via opposing functions of HBO1 and HDAC11-geminin. Cell Cycle *9*, 4351–4363.

Wood, W., and Martin, P. (2002). Structures in focus--filopodia. Int. J. Biochem. Cell Biol. *34*, 726–730.

Wu, J.M., Fackler, M.J., Halushka, M.K., Molavi, D.W., Taylor, M.E., Wei, W.T., Griffin, C., Fetting, J., Davidson, N.E., De Marzo, A.M., et al. (2008). Heterogeneity of breast cancer metastases: Comparison of therapeutic target expression and promoter methylation between primary tumors and their multifocal metastases. Clin. Cancer Res. *14*, 1938–1946.

Wu, R.F., Gu, Y., Xu, Y.C., Nwariaku, F.E., and Terada, L.S. (2003). Vascular endothelial growth factor causes translocation of p47 phox to membrane ruffles through WAVE1. J. Biol. Chem. *278*, 36830–36840.

Wu, R.F., Xu, Y.C., Ma, Z., Nwariaku, F.E., Sarosi, G. a., and Terada, L.S. (2005). Subcellular targeting of oxidants during endothelial cell migration. J. Cell Biol. *171*, 893–904.

Yamaguchi, T., Cubizolles, F., Zhang, Y., Reichert, N., Kohler, H., Seiser, C., and Matthias, P. (2010). Histone deacetylases 1 and 2 act in concert to promote the G1-to-S progression. Genes Dev. *24*, 455–469.

Yang, X.-J., and Seto, E. (2008). The Rpd3/Hda1 family of lysine deacetylases: from bacteria and yeast to mice and men. Nat. Rev. Mol. Cell Biol. *9*, 206–218.

Yang, X., Ferguson, A.T., Nass, S.J., Phillips, D.L., Butash, K.A., Wang, S.M., Herman, J.G., and Davidson, N.E. (2000). Transcriptional activation of estrogen receptor alpha in human breast cancer cells by histone deacetylase inhibition. Cancer Res. *60*, 6890–6894.

Yardley, D. a, Ismail-Khan, R.R., Melichar, B., Lichinitser, M., Munster, P.N., Klein, P.M., Cruickshank, S., Miller, K.D., Lee, M.J., and Trepel, J.B. (2013). Randomized phase II, double-blind, placebo-controlled study of exemestane with or without entinostat in postmenopausal women with locally recurrent or metastatic estrogen receptor-positive breast cancer progressing on treatment with a nonsteroidal aromata. J. Clin. Oncol. *31*, 2128–2135.

Yi, X., Wei, W., Wang, S.-Y., Du, Z.-Y., Xu, Y.-J., and Yu, X.-D. (2008). Histone deacetylase inhibitor SAHA induces ERalpha degradation in breast cancer MCF-7 cells by CHIP-mediated ubiquitin pathway and inhibits survival signaling. Biochem. Pharmacol. *75*, 1697–1705.

Zafrani, B., Aubriot, M.H., Mouret, E., De Crémoux, P., De Rycke, Y., Nicolas, a., Boudou, E., Vincent-Salomon, a., Magdelénat, H., and Sastre-Garau, X. (2000). High sensitivity and specificity of immunohistochemistry for the detection of hormone receptors in breast carcinoma: Comparison with biochemical determination in a prospective study of 793 cases. Histopathology *37*, 536–545.

Zaoui, K., Honoré, S., Isnardon, D., Braguer, D., and Badache, A. (2008). Memo-RhoA-mDia1 signaling controls microtubules, the actin network, and adhesion site formation in migrating cells. J. Cell Biol. *183*, 401–408.

Zaoui, K., Benseddik, K., Daou, P., Salaün, D., and Badache, A. (2010). ErbB2 receptor controls microtubule capture by recruiting ACF7 to the plasma membrane of migrating cells. Proc. Natl. Acad. Sci. U. S. A. *107*, 18517–18522.

Zardavas, D., Maetens, M., Irrthum, A., Goulioti, T., Engelen, K., Fumagalli, D., Salgado, R., Aftimos, P., Saini, K.S., Sotiriou, C., et al. (2014). The AURORA initiative for metastatic breast cancer. Br. J. Cancer *111*, 1–7.

Zhang, D., Li, J., Costa, M., Gao, J., and Huang, C. (2010a). JNK1 mediates degradation HIF-1α by a VHL-independent mechanism that involves the chaperones Hsp90/Hsp70. Cancer Res. *70*, 813–823.

Zhang, L., Huang, H., Wu, K., Wang, M., and Wu, B. (2010b). Impact of BTG2 expression on proliferation and invasion of gastric cancer cells in vitro. Mol. Biol. Rep. *37*, 2579–2586.

Zhang, R., Chen, H.Z., Liu, J.J., Jia, Y.Y., Zhang, Z.Q., Yang, R.F., Zhang, Y., Xu, J., Wei, Y.S., Liu, D.P., et al. (2010c). SIRT1 suppresses activator protein-1 transcriptional activity and cyclooxygenase-2 expression in macrophages. J. Biol. Chem. *285*, 7097–7110.

Zhang, X., Yuan, Z., Zhang, Y., Yong, S., Salas-Burgos, A., Koomen, J., Olashaw, N., Parsons, J.T., Yang, X.J., Dent, S.R., et al. (2007a). HDAC6 Modulates Cell Motility by Altering the Acetylation Level of Cortactin. Mol. Cell *27*, 197–213.

Zhang, Y., Adachi, M., Kawamura, R., and Imai, K. (2006). Bmf is a possible mediator in histone deacetylase inhibitors FK228 and CBHA-induced apoptosis. Cell Death Differ. *13*, 129–140.

Zhang, Y., Carr, T., Dimtchev, A., Zaer, N., Dritschilo, A., and Jung, M. (2007b). Attenuated DNA damage repair by trichostatin A through BRCA1 suppression. Radiat. Res. *168*, 115–124.

Zhang, Z., Yamashita, H., Toyama, T., Sugiura, H., Omoto, Y., Ando, Y., Mita, K., Hamaguchi, M., Hayashi, S.I., and Iwase, H. (2004). HDAC6 expression is correlated with better survival in breast cancer. Clin. Cancer Res. *10*, 6962–6968.

Zhang, Z., Yamashita, H., Toyama, T., Sugiura, H., Ando, Y., Mita, K., Hamaguchi, M., Hara, Y., Kobayashi, S., and Iwase, H. (2005). Quantitation of HDAC1 mRNA expression in invasive carcinoma of the breast. Breast Cancer Res. Treat. *94*, 11–16.

Zhao, H., Langerød, A., Ji, Y., Nowels, K.W., Nesland, J.M., Tibshirani, R., Bukholm, I.K., Kåresen, R., Botstein, D., Børresen-Dale, A.-L., et al. (2004). Different gene expression patterns in invasive lobular and ductal carcinomas of the breast. Mol. Biol. Cell *15*, 2523–2536.

Zhao, J.-J., Lin, J., Yang, H., Kong, W., He, L., Ma, X., Coppola, D., and Cheng, J.Q. (2008). MicroRNA-221/222 negatively regulates estrogen receptor alpha and is associated with tamoxifen resistance in breast cancer. J. Biol. Chem. *283*, 31079–31086.

Zhao, Y., Tan, J., Zhuang, L., Jiang, X., Liu, E.T., and Yu, Q. (2005). Inhibitors of histone deacetylases target the Rb-E2F1 pathway for apoptosis induction through activation of proapoptotic protein Bim. Proc. Natl. Acad. Sci. U. S. A. *102*, 16090–16095.

Zumbrunn, J., Kinoshita, K., Hyman, A. a., and Näthke, I.S. (2001). Binding of the adenomatous polyposis coli protein to microtubules increases microtubule stability and is regulated by GSK3β phosphorylation. Curr. Biol. *11*, 44–49.

6. Abbreviations

AP1	activator protein 1
CCND1	cyclin D1
CDK1	cyclin-dependent kinase 1
DMFS	distant metastasis-free survival
DNMT	DNA-methyltransferase
ECM	extra cellular matrix
EGF	epidermal growth factor
EMT	epithelial to mesenchymal transition
ER	estrogen receptor
ERE	estrogen response element
ERK	extracellular-signal-regulated kinase
FDR	false discovery rate
Fulv	fulvestrant
GEF	guanine exchange factor
GSEA	gene set enrichment analysis
HAT	histone acetyltransferase
HDAC	histone deacetylase
HRG	heregulin
Hsp90	heat shock protein 90
IGF1R	insulin-like growth factor 1 receptor
IHC	immunohistochemistry
IL-10	interleukin 10
IRS1	insulin receptor substrate 1
KD	knockdown
KO	knockout
MAPK	mitogen activated protein kinases
MDSC	myeloid derived suppressor cell
Memo	Mediator of ErbB2-driven cell motility
MET	mesenchymal to epithelial transition
MMP	matrix metalloprotease
MMTV	mouse mammary tumor virus
miR	microRNA
NCoR	nuclear receptor corepressor
NeuNT	mutated neuro glioblastoma derived oncogene homolog (V664Q)
NK	natural killer cells
NOX	NADPH oxidase
PDGF	platelet derived growth factor
PI3K	phosphatdidylinositol-3-kinase
PR	progesterone receptor
PTM	post-translational modification
PTP	protein tyrosine phosphatase
RFS	recurrence-free survival
RIP140/NRIP1	receptor interacting protein 140/nuclear receptor-interacting protein 1
ROS	reactive oxygen species
RTK	receptor tyrosine kinase
SSH-1L	slingshot-1L
TAM	tamoxifen
TF	transcription factor
T_{Reg}	regulatory T cells
VEGF	vascular endothelial growth factor

7. Acknowledgement

First I would like to thank Prof. Dr. Nancy Hynes for giving me the opportunity to work in her lab and for her support during my PhD. I also would like to thank my Thesis Committee members Prof. Dr. Gerhard Christofori and Dr. Ulrich Rass for many helpful discussions and suggestions.

I thank Gwen MacDonald, Ivan Nalvarte and Richard Heideman for the great collaboration on different projects, for stimulating scientific discussions and for their catching enthusiasm for science.

I'm especially grateful to Barbara, Gwen, Alessia and Albana for their motivating and encouraging support inside and outside of the lab. It was a pleasure working with you.

A very big thank goes to Barbara for proofreading my thesis.

I would like to thank all the present and former labmembers for the great atmosphere in the lab. I also thank the FMI facilities, especially Tim Roloff for his help with the bioinformatics analyses, Sandrine Bichet for histological stainings, and Steven Bourke and Laurent Gelman for technical assistance in microscopy.

The biggest thank goes to Hannes for his love, patience and constant support. You made it so much easier to go through the hard times during these years.

And finally, I would like to thank my family and friends for their love, encouragement, and many wonderful and energizing moments.